

SYNTHESIS OF NEW DENTAL ADHESIVE MONOMERS AND POLYMERS

by

Aylin Ziylan Albayrak

B.S., Chemistry, Boğaziçi University , 1996

M.S., Chemistry, Boğaziçi University, 1999

Submitted to the Institute for Graduate Studies in
Science and Engineering in partial fulfillment of
the requirements for the degree of
Doctor of Philosophy

Graduate Program in Chemistry

Boğaziçi University

2006

Kızım ve Eşime...

ACKNOWLEDGEMENTS

I would like to express my sincere gratitude to my supervisor Prof. Duygu Avcı Semiz for her guidance and suggestions throughout this study.

I am also grateful to my committee members Prof. Ayşen Önen, Prof. İlknur Doğan, Assist. Prof. Amitav Sanyal, Assist. Prof. Ersin Acar for their careful and constructive review of the final manuscript.

I would especially like to thank my laboratory partners, Burcu Ayfer Sunam, Barış Yağcı, Zeynep Saraylı Bilgici and Görkem Şahin for their help and friendship.

I would like to extend my thanks to Prof. Gürkan Hızal and Prof. Ümit Tunca for GPC analysis, Ayla Türkekul and Burcu Selen Çağlayan for NMR analysis and Gökhan Çaylı for TGA analysis.

I also thank Prof. Lon J. Mathias for his invaluable advice during my study in University of Southern Mississippi and I would like to thank to all members of Boğaziçi University Chemistry Department, my instructors, my friends and especially the secretary of the department Hülya Metiner for their help and friendship. I also would like to express my heartfelt thanks to my dear friends Özge Akdeniz Ünal, Tarık Eren, Sinan Şen and Hüseyin Esen for their encouragement and friendship.

My greatest thank is to my mother, father and brother for their endless love, encouragement and support and I am also very grateful to my mother and father-in-law for all their help. Finally, I would like to thank my husband and my sweet daughter with all my heart for their understanding, help and love.

This study has been supported by Boğaziçi University Scientific Research Project (03HB501D, 02HB501, 04HB501 and 05B502) and DPT (03K120250).

ABSTRACT

SYNTHESIS OF NEW DENTAL ADHESIVE MONOMERS AND POLYMERS

New phosphonate, phosphonic acid, carboxylic acid, iminodiacetate containing adhesive monomers based on alkyl α -hydroxymethyl acrylates and their derivatives were synthesized.

A new phosphonate-containing cyclic monomer was obtained from the reaction of 2-(2-chlorocarbonyl-allyloxymethyl)-acryloyl chloride with diethyl hydroxymethyl phosphonate. This monomer showed high cyclization tendency during homopolymerization and copolymerization with 2-(2-tert-butoxycarbonyl-allyloxymethyl)-acrylic acid tert-butyl ester (TBEED) using initiators 2,2'-azobis(isobutyronitrile) (AIBN) at 75-77 °C. The T_g of the copolymers decreased with increasing amounts of phosphonate-containing monomer whereas the char residues of the copolymers increased. The selective hydrolysis of the phosphonate monomer with trimethylsilyl bromide gave a water soluble phosphonic acid-containing monomer. This monomer could not be homopolymerized but copolymerized with TBEED and its dicarboxylic acid derivative, 2-(2-carboxy-allyloxymethyl)-acrylic acid.

A series of 4,4-disubstituted 1,6-heptadiene monomers were synthesized from the reaction of ethyl- α -bromomethyl acrylate and tert-butyl- α -bromomethyl acrylate with triethylphosphonoacetate and tetraethylmethylenediphosphonate using sodium hydride followed by selective hydrolysis of the ester groups. Photopolymerizations of the monomers were investigated to understand the effect of the cyclic monomer structure on their polymerization reactivity. A strong effect of the substituents at 2, 4 and 6 positions of the monomers on polymerization rate was observed. The polymerizability of the monomers were successfully correlated with the ^{13}C -NMR chemical shifts of the vinyl carbons. Conversion values were consistent with the T_g being a measure of the flexibility

of a monomer. The monomers containing phosphonic acid groups were soluble in water and ethanol. The acidic nature of the aqueous solutions of these monomers is expected to give them etching properties, important for dental applications. The interaction of the acid monomers with hydroxyapatite was investigated using ^{13}C NMR technique. It was found that phosphonic acid-containing monomers demineralized the calcium phosphate in the HAP in preference to the carboxylic acid.

Four new methacrylate monomers containing phosphonic and/or carboxylic acids were synthesized from the reaction of tert-butyl α -bromomethyl acrylate with triethyl phosphite followed by selective hydrolysis of the phosphonate or tert-butyl ester groups using trimethylsilyl bromide and trifluoroacetic acid. The copolymerization of these monomers with 2-hydroxyethyl methacrylate (HEMA) was investigated by photodifferential scanning calorimetry. The reactivities of the monomers increased by decreasing steric hindrance and increasing hydrogen bonding capacity due to hydrolysis of phosphonate or tert-butyl ester groups.

Furthermore, new adhesive monomers with diethyliminodiacetate as a potential chelating group were synthesized from the reaction of ethyl- α -bromomethyl acrylate, 2-chloromethyl-acryloyl chloride and 2-(2-carboxy-allyloxymethyl)-acrylic acid with diethyl iminodiacetate. The monomers were homopolymerized and copolymerized with TBEED and HEMA. Rate of copolymerizations and conversions decreased with an increase in the monomer concentrations. Low polymerizability of these monomers were explained with the steric effect of the N,N-disubstituted methacrylamides and the presence of allyl amine group leading to degradative chain transfer. The monomers were hydrolyzed by potassium hydroxide solution and the salt derivatives were copolymerized with acrylamide in water using 2,2'-azobis(N,N'-amidinopropane) dihydrochloride (V-50). Polymer yields after dialysis were low and decreased with increasing monomer concentrations. The Ni^{+2} chelating ability of the monomers were shown using UV-visible spectroscopy. Thermal stability of the copolymer increased on complexation with Ni^{+2} ions.

ÖZET

YENİ DİŞ YAPIŞTIRICI MONOMER VE POLİMERLERİN SENTEZİ

Yeni fosfonat, fosfonik asit, karboksilit asit, iminodiasetat içeren yapıştırıcı monomerler, alkil α -hidroksi metil akrilatlar ve onların türevlerinden sentezlendi.

Yeni fosfonat içeren siklik monomer, 2-(2-klorokarbonil-aliloksimetil)-akriloil klorür ile dietil hidroksimetil fosfonatin reaksiyonundan elde edildi. Bu monomer 2,2'-azobis(izobütüronitril) (AIBN) kullanılarak, 75-77 °C'de homopolimerleştirildiğinde ve 2-(2-tert-bütoksikarbonil-aliloksimetil)-akrilik asit tert-butil ester (TBEED) ile kopolimer-leştirildiğinde yüksek siklizasyon eğilimi gösterdi. Kopolimerde fosfonat içeren monomer miktarı arttığında T_g değeri azalırken, kömürleşmenin arttığı gözlemlendi. Fosfonat monomerinin trimetilsilil bromür ile seçici hidrolizi sonucunda suda çözülebilen ve fosfonik asit içeren bir monomer elde edildi. Ancak, bu monomer homopolimerleşemez-ken, TBEED ve onun dikarboksilik asit türevi olan 2-(2-karboksialiloksimetil)-akrilik asit ile kopolimerleşti.

Etil- α -bromometil akrilat ve tert-bütül- α -bromometil akrilatin, trietilfosfonoasetat ve tetraetilmetilendifosfonat ile sodyum hidrür kullanarak gerçekleşen reaksiyonundan bir seri 4,4-disübstitüe 1,6-heptadien monomerleri sentezlendi ve bunu takiben ester gruplarının seçici hidrolizi yapıldı. Siklik monomer yapısının polimerleşme reaktifliği üzerindeki etkisini anlamak amacıyla bu monomerlerin fotopolimerizasyonları incelendi. Monomerlerin 2., 4. ve 6. pozisyonlarındaki grupların polimerleşme hızına önemli ölçüde etkisi olduğu gözlemlendi. Vinil karbonlarının ^{13}C -NMR kimyasal kaymaları monomerlerin polimerleşebilme eğilimleri ile ilişkilendirildi. Monomerlerin esnekliğinin göstergesi olan T_g değerleri ile dönüşüm yüzdeleri arasında ilişki kuruldu. Fosfonik asit grupları içeren monomerler suda ve etanolde çözünebilirlik gösterdi. Bu monomerlerin asidik sulu çözeltilerinin aşındırıcılık özelliği olması dişçilik uygulamalarında önemli olduğu için,

asit monomerlerinin hidroksiapatit ile etkileşimi ^{13}C -NMR tekniği kullanılarak incelendi. Fosfonik asit içeren monomerlerin, karboksilik asit içeren monomere oranla kalsiyum fosfat maddesini daha etkili bir şekilde demineralize ettiği bulundu.

Dört yeni fosfonik ve/veya karboksilik asit içeren metakrilat monomerleri tert-bütül α -bromometil akrilatın trietil fosfit ile reaksiyonu ve bunu takiben fosfonat veya tert-bütül gruplarının trimetilsilil bromür veya trifloroasetik asit kullanılarak seçici olarak hidrolizinden sentezlendi. Bu monomerlerin 2-hidroksietil metakrilat (HEMA) ile kopolimerleşmesi foto-differansiyel taramalı kalorimetre kullanılarak incelendi. Monomerlerin reaktivliklerinde, fosfonat veya tert-bütül ester gruplarının hidrolizinden ötürü sterik etkilerin azalması ve hidrojen bağ kapasitelerinin artması sonucu artış görüldü.

Bunlara ek olarak, etil- α -bromometil akrilat, 2-klorometil-akriloil klorür ve 2-(2-karboksi-aliloksümetil)-akrilik asitin dietiliminodiasetat ile reaksiyonlarından potansiyel kelat grubu içeren yeni yapıştırıcı monomerler sentezlendi. Monomerler homopolimerleştirildi, TBEED ve HEMA ile kopolimerleştirildi. Sentezlenen monomerlerin konsantrasyonlarının artmasıyla, kopolimerizasyon hızı ve dönüşüm verimi azaldı. Bu monomerlerin düşük polimerizasyon reaktivlikleri, N,N-disübstitüe metakrilamidin sterik etkisi ve alil amin grubunun zincir transfer etkisi ile açıklandı. Monomerler potasyum hidroksit çözeltisi ile hidroliz edildi ve oluşan tuz türevleri akrilamid ile suda 2,2'-azobis(N,N'-amidinopropan) dihidroklorür (V-50) kullanılarak kopolimerleştirildi. Dializ sonrası polimer verimliliğinin düşük olduğu ve artan monomer konsantrasyonuyla azaldığı görüldü. Ni^{+2} maddesinin bağ kurma kapasitesi UV-görünür spektroskopisi ile gösterildi. Kopolimerin Ni^{+2} iyonu ile kompleksleşmesi ısı kararlılığını arttırdı.

TABLE OF CONTENTS

ACKNOWLEDEMENTS.....	iv
ABSTRACT.....	v
ÖZET	vii
LIST OF FIGURES.....	xv
LIST OF TABLES	xxvi
LIST OF SYMBOLS/ABBREVIATIONS.....	xxix
1. INTRODUCTION.....	1
1.1. Adhesives in Dentistry.....	1
1.1.1. Structure of a Tooth.	1
1.1.2. Role and Categories of Dental Adhesives.....	3
1.1.3. Etch and Rinse Adhesives	4
1.1.4. Self-Etching Adhesives	5
1.1.4.1. Adhesive Monomers in Self-Etching Enamel-Dentin Adhesives	8
1.1.4.2. Monofunctional Co-Monomers in Commercial Adhesives.....	31
1.1.4.3. Cross-Linking Monomers in Commercial Adhesives	32
1.1.4.4. Initiators	33
1.1.4.5. Fillers	34
1.1.4.6. Additives	35
1.1.5. Adhesion to and Decalcification of Hydroxyapatite by Acids.....	36
1.1.6. Bonding Effectiveness.....	38
1.1.7. Effect of Smear Layer on Bonding	41
1.1.8. Effect of Smear Layer on Fluid Movement Across Dentin.....	44
1.2. Alkyl α -Hydroxy Methylacrylates (RHMA)s.....	45
1.2.1. Synthesis of RHMA monomers.....	45
1.2.2. Physical and Chemical Properties of RHMA Monomers and Polymers	49
1.2.3. Derivatives of RHMA monomers.....	52
1.2.3.1. Ether Derivatives of RHMA	55
1.2.3.2. Ester Derivatives of RHMA.....	59
1.2.4. Polymerization Reactivity of α -(Substituted Methyl) Acrylates	61
1.2.5. Ether Dimers of RHMA Monomers.....	64

1.2.6. Cyclopolymerization	65
2. OBJECTIVES	75
3. EXPERIMENTAL	76
3.1. Materials and Apparatus	76
3.1.1. Materials	76
3.1.2. Apparatus	76
3.2. Monomer Synthesis	77
3.2.1. Synthesis of Phosphorus-Containing Cyclopolymerizable Monomers from 2-(2-tert-Butoxycarbonyl-Allyloxymethyl)-Acrylic Acid tert-Butyl Ester (TBEED)	77
3.2.1.1. Synthesis of 2-(2-tert-Butoxycarbonyl-Allyloxymethyl)- Acrylic Acid tert-Butyl Ester (TBEED)	77
3.2.1.2. Synthesis of 2-(2-Chlorocarbonyl-Allyloxymethyl)- Acryloyl Chloride	77
3.2.1.3. Synthesis of 2-(2-Carboxy-Allyloxymethyl)-Acrylic Acid (TBEED-acid)	78
3.2.1.4. Synthesis of 2-[2-(Diethoxy-Phosphorylmethoxycarbonyl)- Allyloxymethyl]-Acrylic Acid Diethoxy-Phosphorylmethyl Ester (PHOSEED)	78
3.2.1.5. Synthesis of 2-(2-Phosphonomethoxycarbonyl- Allyloxymethyl)-Acrylic Acid Phosphonomethyl Ester (PHOSEED-acid)	79
3.2.2. Synthesis of Phosphorus-Containing Cyclopolymerizable Monomers from tert-Butyl α -Hydroxymethyl Acrylate (TBHMA) and Ethyl α - Hydroxymethyl Acrylate (EHMA)	79
3.2.2.1. Synthesis of tert-Butyl- α -Hydroxymethyl Acrylate (TBHMA)	79
3.2.2.2. Synthesis of tert-Butyl- α -Bromomethyl Acrylate (TBBr)	80
3.2.2.3. Synthesis of Ethyl α -Hydroxymethyl Acrylate (EHMA)	80
3.2.2.4. Synthesis of Ethyl- α -Bromomethyl Acrylate (EBBr)	81

3.2.2.5. Synthesis of 4-Diethoxyphosphoryl-4-Ethoxycarbonyl -2,6-bis(tert-Butoxycarbonyl)-1,6-Heptadiene (BC-EPA).....	81
3.2.2.6. Synthesis of 4-Diethoxyphosphoryl-4-Ethoxycarbonyl -2,6-bis(Ethoxycarbonyl)-1,6-Heptadiene (EC-EPA)	82
3.2.2.7. Synthesis of 4-Ethoxycarbonyl-4-Phosphonic Acid -2,6-bis(Carboxylic acid)-1,6-Heptadiene (CA-PA).....	82
3.2.2.8. Synthesis of 4-Diethoxyphosphoryl-4-Ethoxycarbonyl -2,6-bis(Carboxylic acid)-1,6-Heptadiene (CA-EPA).....	83
3.2.2.9. Synthesis of 4-Ethoxycarbonyl-4-Phosphonic Acid -2,6-bis(Ethoxycarbonyl)-1,6-Heptadiene (EC-PA)	83
3.2.2.10. Synthesis of 4,4-Diethoxyphosphoryl-2,6-bis(tert- Butoxycarbonyl)-1,6-Heptadiene (BC-TEP)	84
3.2.2.11. Synthesis of 2-(Diethoxy-Phosphoryl)-4-Methylene- Pentanedioic Acid 5-tert-Butyl Ester 1-Ethyl Ester (MBC-EPA)	84
3.2.3. Synthesis of Phosphorus-Containing Monomers from TBHMA	85
3.2.3.1. Synthesis of 2-(Diethoxy-Phosphorylmethyl)-Acrylic Acid tert-Butyl Ester (TBEP).....	85
3.2.3.2. Synthesis of 2-Phosphonomethyl-Acrylic Acid tert-Butyl Ester (TBPA).....	86
3.2.3.3. Synthesis of 2-Phosphonomethyl-Acrylic Acid (CAPA)	86
3.2.3.4. Synthesis of 2-(Diethoxy-Phosphorylmethyl)-Acrylic Acid (CAEP).....	86
3.2.4. Synthesis of Diethyliminodiacetate-Containing Monomers from EHMA, TBHMA and TBEED.....	87

3.2.4.1. Synthesis of 2-Chloromethyl-Acryloyl Chloride (CMAC)	87
3.2.4.2. Synthesis of ({2-[2-(Bis-Ethoxycarbonylmethyl)- Carbamoyl]-Allyloxymethyl]-Acryloyl}- Ethoxycarbonylmethyl-Amino)-Acetic Acid Ethyl Ester (TBEED-IDA)	87
3.2.4.3. Synthesis of 2-[(Bis-Ethoxycarbonylmethyl-Amino)- Methyl]-Acrylic Acid Ethyl Ester (EBBr-IDA).....	88
3.2.4.4. Synthesis of Potassium Salt of 2-[(Bis-Carboxymethyl- Amino)-Methyl]-Acrylic Acid (EBBr-IDA-K ⁺)	88
3.2.4.5. Synthesis of {2-(Bis-Ethoxycarbonylmethyl-Carbamoyl)- Allyl]-Ethoxycarbonylmethyl-Amino}-Acetic Acid Ethyl Ester (CMAC-IDA)	89
3.2.4.6. Synthesis of Potassium Salt of {[2-(Bis-Carboxymethyl- Carbamoyl)-Allyl]-Carboxymethyl-Amino}-Acetic Acid (CMAC-IDA-K ⁺).....	89
3.3. Photopolymerizations	90
3.3.1. Polymerization Procedure	90
3.3.2. Sample Preparation of the Phosphorus-Containing Cyclopolymerizable Monomers, BC-EPA, EC-EPA, CA-PA, CA-EPA, EC-PA and BC-TEP	91
3.3.3. Sample Preparation of the Phosphorus-Containing Monomers, TBEP, TBPA, CAPA and CAEP	91
3.3.4. Sample Preparation of the Diethyliminodiacetate-Containing Monomers, TBEED-IDA, EBBr-IDA and CMAC-IDA	92
3.4. Bulk or Solution Polymerizations	92
3.4.1. Polymerization Procedure	92
3.4.2. Polymerization of PHOSEED, TBEED and PHOSEED-acid.....	92
3.4.2.1. Polymerization of PHOSEED	92
3.4.2.2. Polymerization of TBEED	93
3.4.2.3. Polymerization of PHOSEED-acid	93
3.4.3. Polymerization of BC-EPA, EC-EPA and CA-EPA	93
3.4.3.1. Polymerization of BC-EPA and EC-EPA.....	93

3.4.3.2. Polymerization of CA-EPA.....	93
3.4.4. Polymerization of EBBr-IDA-K ⁺ and CMAC-IDA-K ⁺	93
3.5. Binding Capacity of Phosphorus-Containing Cyclopolymerizable Monomers, CA-PA and EC-PA	94
3.5.1. Determination of the pH Dependencies of the Chemical Shifts of the Carbonyl Carbon and α -Methylene Carbon in CA-PA	94
3.5.2. Interacted Amounts of Carboxylic Acid and Phosphonic Acid in CA-PA with the Calcium in the HAP.....	94
3.5.3. Determination of the pH Dependency of the Chemical Shifts of α -Methylene Carbon in EC-PA	95
3.5.4. Interacted Amount of Phosphonic Acid in EC-PA with the Calcium in the HAP.....	95
3.6. Chelating Ability of Diethyliminodiacetate-Containing Monomers, EBBr-IDA-K ⁺ and CMAC-IDA-K ⁺	96
4. RESULTS AND DISCUSSION	97
4.1. Synthesis of Phosphorus-Containing Cyclopolymerizable Monomers from 2-(2-tert- Butoxycarbonyl-Allyloxymethyl)-Acrylic Acid tert-Butyl Ester (TBEED)	97
4.1.1. Synthesis of Monomers	97
4.1.2. Polymerization.....	103
4.1.3. GPC Results.....	108
4.1.4. DSC Results.....	109
4.1.5. TGA Results	111
4.2. Synthesis of Phosphorus-Containing Cyclopolymerizable Monomers from tert-Butyl α -Hydroxymethyl Acrylate (TBHMA) and Ethyl α -Hydroxymethyl Acrylate (EHMA)	113
4.2.1. Synthesis of BC-EPA, CA-PA and CA-EPA	113
4.2.2. Synthesis of EC-EPA, EC-PA and BC-TEP	121
4.2.3. Photopolymerizations.....	129
4.2.4. Polymerization in Bulk or Solution	137
4.2.5. Interacted Amounts of Carboxylic and Phosphonic Acids in CA-PA and EC-PA with the Calcium in the HAP.....	138
4.3. Synthesis of Phosphorus-Containing Monomers and Polymers from tert-Butyl α - Hydroxymethyl Acrylate (TBHMA).....	143

4.3.1. Monomer Synthesis.....	143
4.3.2. Photopolymerizations.....	154
4.3.3. Computational Strategy.....	156
4.4. Synthesis of Diethyliminodiacetate-Containing Monomers from AHM, EHMA, TBHMA and TBEED.....	160
4.4.1. Reaction of 3-Acryloyloxy-2-Hydroxypropylmethacrylate (AHM) with Diethyliminodiacetate.....	160
4.4.2. Synthesis of TBEED-IDA.....	161
4.4.3. Synthesis of EBBr-IDA and EBBr-IDA-K ⁺	166
4.4.4. Synthesis of CMAC-IDA and CMAC-IDA-K ⁺	173
4.4.5. Photopolymerizations.....	181
4.4.6. Solution Polymerizations in Water.....	184
4.4.7. TGA Results.....	185
4.4.8. Ultraviolet-Visible Spectrophotometer Results.....	189
5. CONCLUSION.....	191
6. REFERENCES.....	193

LIST OF FIGURES

Figure 1.1. The anatomy of tooth	1
Figure 1.2. SEM images of the treated dentin: The original magnification was x2500 (A) ground dentin surface; surface was covered with smear layer (B) 40 wt % H ₃ PO ₄ for 30 s, water-rinse, air-dried; smear layer was removed and dentin tubules were widely opened.....	4
Figure 1.3. Examples of self-etching primers	6
Figure 1.4. Components of currently available self-etching enamel-dentin primers/adhesives.....	7
Figure 1.5. Design of an self-etching adhesive monomer.....	9
Figure 1.6. Adhesive groups (AD)	9
Figure 1.7. Examples of polymerizable acidic phosphates used in dentin adhesives.....	10
Figure 1.8. Phosphorylation of 10-hydroxydecyl methacrylate with POCl ₃	11
Figure 1.9. Phosphorylation of alkyl α -hydroxy methyl acrylates (RHMA) with diethylchlorophosphate	11
Figure 1.10. Phosphorylation of AHM with diethylchlorophosphate	11
Figure 1.11. Order of hydrolytic stability of the phosphoric esters.....	12
Figure 1.12. Hydrolysis of MEP in the presence of water	12
Figure 1.13. General formula of the polymerizable phosphates of the invention	13

Figure 1.14. Example of a phosphate ester	13
Figure 1.15. Possible polymerizable phosphoric acid ester derivatives of the invention.....	15
Figure 1.16. Examples of 2-(oxa-ethyl) acryl derivatives of polymerizable phosphoric acids.....	15
Figure 1.17. Structure of monomeric phosphonic acids VPA and VBPA.....	16
Figure 1.18. Synthesis of dimethyl(2-methacryloyloxyethyl)phosphonate by Arbuzov reaction	16
Figure 1.19. Synthesis of dimethyl(2-methacryloyloxyethyl)phosphonate by radical addition of dialkyl hydrogenphosphonate	16
Figure 1.20. Synthesis of dimethyl(2-methacryloyloxyethyl)phosphonate by the Micheal addition of methacrylic acid on the dialkyl vinyl phosphonate.....	17
Figure 1.21. Synthesis of dimethyl(2-methacryloyloxyethyl)phosphonate using hydroxyalkylphosphonate precursor	17
Figure 1.22. Hydrolysis of dimethyl(2-methacryloyloxyethyl)phosphonate.....	17
Figure 1.23. Synthetic scheme of phosphonic acid containing monomer	18
Figure 1.24. Synthesis of polymerizable phosphonates.....	19
Figure 1.25. Phosphorus-containing monomer with identical ester and ether group	19
Figure 1.26. Phosphorus-containing monomer with mixed ester and ether groups	20
Figure 1.27. Examples of polymerizable phosphonates	22

Figure 1.28. General acrylphosphonic acid structure of the invention.....	22
Figure 1.29. Synthesis of acrylphosphonic acids	23
Figure 1.30. Examples of acrylphosphonic acids.....	23
Figure 1.31. Synthesis of 2-(meth)acrylamido-2-methyl-propanephosphonic acid.....	24
Figure 1.32. General adhesive monomer structures of the invention	24
Figure 1.33. Two examples of the invention.....	25
Figure 1.34. Monomeric aminomethylphosphonic acids.....	25
Figure 1.35. Suggested structure of the metal ion-monomer complex at different pHs, (a) in basic medium (b) in acidic medium.....	26
Figure 1.36. Structures of monofunctional resins	26
Figure 1.37. Intraligand hydrogen bonds that reduce the affinities of the phosphonoacetate ligand	27
Figure 1.38. Examples of COOH-containig adhesive monomers	28
Figure 1.39. Synthesis of fluoride-releasing dimethacrylate monomer.....	29
Figure 1.40. Monomer that contains metal-chelating functionality	30
Figure 1.41. Structure of GMA-IDA chelating monomer	30
Figure 1.42. Examples of -COOH containing monomers.....	31
Figure 1.43. Structure of HEMA substitutes with improved hydrolytic stability	32

Figure 1.44. Cross-linking dimethacrylates used in dentin adhesives.....	32
Figure 1.45. Structure of bis(acrylamide)s with improved hydrolytic stability.....	33
Figure 1.46. Initiator system for the photopolymerization of VIS-light curing adhesives.....	33
Figure 1.47. Acid-base reaction of an amine/peroxide redox initiator system for radical polymerization.....	34
Figure 1.48. Structure of acylphosphine oxide.....	34
Figure 1.49. A polymerizable antimicrobial agent.....	35
Figure 1.50. Schematic presentation of the adhesion/decalcification concept.....	36
Figure 1.51. The pH dependencies of the chemical shift of the carbonyl carbon peak attributed to the carboxylic acid in the NMGLY.....	38
Figure 1.52. a) SEM image of a self-etching sample showing a thin hybrid layer and b) SEM image of a etch and rinse sample showing a thick hybrid layer.....	39
Figure 1.53. Model of hydrogen bonding between NMGLY and dentinal collagen.....	40
Figure 1.54. Smear layer samples etched with (a) Clearfil SE primer, and different concentrations of phosphoric acid (b) 0.13 % phosphoric acid (pH=2, similar to SE primer) (c) 20 % phosphoric acid (pH=0.21) (d) 35 % phosphoric acid (pH=-0.28).....	43
Figure 1.55 Examples of α -alkyl acrylates (1 and 2) which give low molecular weight polymers and ethyl α -hydroxy methylacrylate (3) which gives high molecular weight polymer.....	45

Figure 1.56. DABCO catalyzed synthesis of RHMA monomers.....	46
Figure 1.57. Radical polymerization of RHMA monomers.....	50
Figure 1.58. Rise in T_g by lactone cyclization	50
Figure 1.59. Polyhydroxypolycarboxylic acid	51
Figure 1.60. Synthesis of an unsaturated polyester	52
Figure 1.61. Synthesis of an unsaturated copolyester.....	52
Figure 1.62. Synthesis of reactive intermediates from RHMA.....	53
Figure 1.63. The addition-fragmentation of methyl α -(bromomethyl)acrylate in methyl methacrylate polymerization	54
Figure 1.64. Synthesis of fluoroalkyl containing monomers based on CMAC	55
Figure 1.65. Synthetic scheme for the synthesis of ether derivatives.....	56
Figure 1.66. Synthesis of difunctional acrylate crosslinking agents	58
Figure 1.67. Synthesis of difunctional acrylate crosslinking agents	58
Figure 1.68. Synthesis of hydroxyl-containing dimethacrylate monomers	59
Figure 1.69. General synthetic schemes for the synthesis of ester derivatives of EHMA	60
Figure 1.70. General scheme for synthesis of benzoate ester monomers	60
Figure 1.71. General synthetic scheme for C-18 monomers.....	61

Figure 1.72. Rate versus time graph of MHMA and EHMA photopolymerizations	63
Figure 1.73. DABCO catalyzed formation of RHMA ether dimers and the proposed mechanism	65
Figure 1.74. Crosslinking reactions with RHMA dimers and the diacid ether	65
Figure 1.75. Possible reaction courses for radical polymerization of α,ω -dienes	66
Figure 1.76. Intramolecular cyclization and intermolecular monomer addition	67
Figure 1.77. The bis-acrylate monomers used in synthetic dental compositions	68
Figure 1.78. Shielding effect of C _b carbon that is linked to the carboxyester carbon	70
Figure 1.79. Synthesis and cyclopolymerization of dicyano-containing diacrylates	71
Figure 1.80. Synthesis of the 4,4-disubstituted 1,6-diene monomers	71
Figure 1.81. General synthetic scheme for amine derivatives	72
Figure 1.82. Quaternization of polymers	72
Figure 1.83. Synthesis of a cyclopolymerizable monomer based on TBBr	73
Figure 1.84. Structures of (a) poly[ethyl α -[(allyloxy)methyl]-acrylate] and (b) poly[allyl α -(hydroxymethyl)acrylate]	73
Figure 1.85. General synthetic scheme for allyl-acrylate quaternary ammonium salts ...	74
Figure 3.1. 2,2-Dimethoxy-2-phenyl acetophenone (Irgacure 651)	90

Figure 3.2. Equation of the rate of polymerization.....	91
Figure 4.1. Synthesis of PHOSEED	98
Figure 4.2. ¹³ C-NMR spectra of PHOSEED and PHOSEED-acid.....	99
Figure 4.3. ¹ H-NMR spectra of PHOSEED and PHOSEED-acid.....	100
Figure 4.4. FT-IR spectrum of PHOSEED	101
Figure 4.5. Synthesis of PHOSEED-acid.....	102
Figure 4.6. Polymerization of PHOSEED.....	103
Figure 4.7. ¹ H-NMR spectrum of poly-PHOSEED.....	104
Figure 4.8. Copolymerization of PHOSEED with TBEED	105
Figure 4.9. Polymerization of TBEED.....	106
Figure 4.10. Copolymerization of PHOSEED-acid with TBEED	108
Figure 4.11. DSC curves of PHOSEED:TBEED copolymers	110
Figure 4.12. TGA curves of PHOSEED:TBEED copolymers.....	112
Figure 4.13. General structures of the monomers	113
Figure 4.14. Synthesis of BC-EPA, CA-PA and CA-EPA	114
Figure 4.15. ¹³ C-NMR spectra of BC-EPA, CA-PA and CA-EPA.....	116
Figure 4.16. ¹ H-NMR spectra of BC-EPA, CA-PA and CA-EPA.....	117

Figure 4.17. FT-IR spectrum of BC-EPA	118
Figure 4.18. FT-IR spectrum of CA-EPA.....	119
Figure 4.19. FT-IR spectrum of CA-PA	120
Figure 4.20. Synthesis of EC-EPA and EC-PA.....	121
Figure 4.21. ¹³ C-NMR spectra of BC-TEP, EC-EPA and EC-PA	122
Figure 4.22. ¹ H-NMR spectra of BC-TEP, EC-EPA and EC-PA	123
Figure 4.23. FT-IR spectrum of EC-EPA	125
Figure 4.24. FT-IR spectrum of EC-PA.....	126
Figure 4.25. Synthesis of BC-TEP	127
Figure 4.26. FT-IR spectrum of BC-TEP	128
Figure 4.27. General formula for cyclopolymerizable diacrylates.....	129
Figure 4.28. Structure of MBC-EPA	130
Figure 4.29. Rate of polymerization versus time graph of BC-EPA, EC-EPA, CA-EPA, EC-PA, BC-TEP and MBC-EPA:BC-EPA (60:40 %) at 40 °C	131
Figure 4.30. Conversion versus time graph of BC-EPA, EC-EPA, CA-EPA, EC-PA, BC-TEP and MBC-EPA:BC-EPA (60:40 %) at 40 °C	131
Figure 4.31. Per cent conversion versus monomeric T _g graph.....	134
Figure 4.32. Rate of polymerization as a function of conversion	135

Figure 4.33. Rate of polymerization versus time graph of all the monomers with HEMA at 40 °C	136
Figure 4.34. Conversion versus time graph of all the monomers with HEMA at 40 °C	136
Figure 4.35. pH Dependencies of the chemical shift of the α -methylene peak to the phosphorus in EC-PA.....	139
Figure 4.36. pH Dependencies of the chemical shift of the α -methylene peak to the phosphorus and carbonyl carbon peak in CA-PA.....	140
Figure 4.37. Synthesis of phosphorus-containing methacrylate monomers	143
Figure 4.38. ^{13}C -NMR spectra of the phosphorus-containing monomers	145
Figure 4.39. FT-IR spectrum of TBEP	146
Figure 4.40. ^1H -NMR spectra of TBPA, CAEP and CAPA	148
Figure 4.41. FT-IR spectrum of TBPA.....	149
Figure 4.42. FT-IR spectrum of CAPA	151
Figure 4.43. FT-IR spectrum of CAEP	153
Figure 4.44. Rate of polymerization versus time graph for the copolymerizations of monomers	155
Figure 4.45. Conversion-time plots for the copolymerizations of monomers	155

Figure 4.46. Model propagation and termination by chain transfer to monomer reactions (X represents the phosphonic acid derivatives and Y represents the carboxylic acid derivatives)	157
Figure 4.47. Micheal addition of diethyliminodiacetate to AHM	161
Figure 4.48. Synthesis of TBEED-IDA	162
Figure 4.49. ^{13}C -NMR spectrum of TBEED-IDA	163
Figure 4.50. ^1H -NMR spectrum of TBEED-IDA	164
Figure 4.51. FT-IR spectrum of TBEED-IDA	165
Figure 4.52. Synthesis of EBBR-IDA and EBBR-IDA- K^+	167
Figure 4.53. ^{13}C -NMR spectra of EBBR-IDA and EBBR-IDA- K^+	168
Figure 4.54. ^1H -NMR spectra of EBBR-IDA and EBBR-IDA- K^+	169
Figure 4.55. FT-IR spectrum of EBBR-IDA	170
Figure 4.56. FT-IR spectrum of EBBR-IDA- K^+	172
Figure 4.57. Synthesis of CMAC-IDA and CMAC-IDA- K^+	174
Figure 4.58. ^{13}C -NMR spectra of CMAC-IDA and CMAC-IDA- K^+	176
Figure 4.59. ^1H -NMR spectra of CMAC-IDA and CMAC-IDA- K^+	177
Figure 4.60. FT-IR spectrum of CMAC-IDA	178
Figure 4.61. FT-IR spectrum of CMAC-IDA- K^+	180

Figure 4.62. Rate of polymerization versus time graph of TBEED-IDA with TBEED	181
Figure 4.63. Rate of polymerization versus time graph of EBBr-IDA with HEMA.....	182
Figure 4.64. Copolymerizations of the chelating monomers with acrylamide	184
Figure 4.65. TGA curves of EBBr-IDA-K ⁺ and the copolymers, acrylamide:EBBr- IDA-K ⁺ (95:5), acrylamide:EBBr-IDA-K ⁺ (90:10)	186
Figure 4.66. TGA curves of CMAC-IDA-K ⁺ and the copolymers, acrylamide:CMAC- IDA-K ⁺ (95:5), acrylamide:CMAC-IDA-K ⁺ (90:10).....	187
Figure 4.67. Weight loss and derivative of the weight loss curves with respect to temperature of acrylamide: EBBr-IDA-K ⁺ (90:10)	188
Figure 4.68. Weight loss and derivative of the weight loss curves with respect to temperature of acrylamide:EBBr-IDA-K ⁺ (90:10) complexed with Ni ⁺² ..	189

LIST OF TABLES

Table 1.1.	Approximate composition of enamel and dentin	2
Table 1.2.	Adhesive categories	3
Table 1.3.	Example of monomer mixture composition in bonding agent and in composite resin	5
Table 1.4.	Adhesive strength of monomers on human tooth	14
Table 1.5.	Photopolymerization results of phosphorus-containing monomers.....	21
Table 1.6.	The chemical shift of the carbonyl carbon peak of the carboxylic acid in the NMGLY, in the absence and in the presence of teeth components and the amount of decalcification.....	38
Table 1.7.	Enamel tensile bond strengths of the self-etching adhesives and the etch and rinse control group.....	41
Table 1.8.	Abrasive and adhesive influence on shear bond strength.....	44
Table 1.9.	Different reaction conditions for Baylis-Hillman reaction.....	48
Table 1.10.	Structures and properties of four RHMA monomers	49
Table 1.11.	Decomposition temperatures of homopolymers	50
Table 1.12.	Per cent water absorption of homopolymers	51

Table 1.13. Homopolymerization of ethyl α -(halomethyl)acrylates ($\text{CH}_2=\text{C}(\text{CH}_2\text{Y})\text{COOEt}$) at 50 °C.....	54
Table 1.14. Polymerization of methyl α -(alkoxymethyl) acrylates in benzene and alkyl α -(fluoroalkoxymethyl) acrylates in dioxane at 60 °C: $[\text{M}] = 2.0 \text{ mol l}^{-1}$, $[\text{AIBN}] = 5.0 \text{ mmol l}^{-1}$	57
Table 1.15. Polymerization of α -(substituted methyl) acrylates ($\text{CH}_2=\text{C}(\text{CH}_2\text{Y})\text{COOR}$).....	62
Table 1.16. The k_p and k_t values of α -(substituted methyl) acrylates ($\text{CH}_2=\text{C}(\text{CH}_2\text{Y})\text{COOR}$).....	64
Table 1.17. Glass transition temperatures of cyclopolymers and the corresponding acrylates and methacrylates.....	67
Table 1.18. Comparison of polymerization shrinkage and conversion results of the diethyl bis-acrylate with that of commercial monomer, TEGDMA.....	68
Table 1.19. Comparison of tensile strength (TS) value.....	68
Table 1.20. Dependence of k_c/k_i values on affective bulkiness.....	70
Table 4.1. Polymer characterization results.....	106
Table 4.2. Maximum rate of polymerizations, conversions and ^{13}C -NMR chemical shifts of the two vinyl carbon peaks of the monomers.....	132
Table 4.3. Comparison of monomeric T_g with % conversion.....	133
Table 4.4. Photopolymerization results.....	136
Table 4.5. Polymer characterization results.....	137

Table 4.6.	Interaction of CA-PA and EC-PA with HAP	141
Table 4.7.	Rate of polymerization and conversion data for the copolymerization of TBEP, TBPA, CAPA and CAEP with HEMA.....	155
Table 4.8.	Calculated activation barriers and reaction enthalpies (kcal/mol).....	156
Table 4.9.	Rate constants for addition (k_p) and chain transfer by hydrogen-abstraction (k_{ct}) compared to experimental rate	157
Table 4.10.	Photopolymerization results	181
Table 4.11.	^{13}C -NMR chemical shifts of the two vinyl carbon peaks of the monomers	182
Table 4.12.	Polymerization conditions and polymer characterization results	184
Table 4.13.	Results of UV-visible spectrophotometer studies.....	189

LIST OF SYMBOLS/ABBREVIATIONS

k_{ct}	Chain transfer by hydrogen abstraction
k_p	Propagation rate constant
R_p	Rate of polymerization
T_g	Glass transition temperature
DSC	Differential Scanning Calorimetry
GPC	Gel Permeation Chromatography
NMR	Nuclear Magnetic Resonance Spectroscopy
TGA	Thermal Gravimetric Analysis
AIBN	2,2'-azobis(isobutyronitrile)
DABCO	1,4-Diazobicyclo [2.2.2] octane
DCC	1,3-Dicyclohexylcarbodiimid
Irgacure 651	2,2'-dimethoxy-2-phenylacetophenone
TMSiBr	Bromotrimethylsilane
V-50	2,2'-azobis(N,N'-amidinopropane) dihydrochloride
BC-EPA	4-Diethoxyphosphoryl-4-Ethoxycarbonyl-2,6-bis(tert-Butoxy-carbonyl)-1,6-Heptadiene
BC-TEP	4,4-Diethoxyphosphoryl-2,6-bis(tert-Butoxycarbonyl)-1,6-Heptadiene
CAEP	2-(Diethoxy-Phosphorylmethyl)-Acrylic Acid
CA-EPA	4-Diethoxyphosphoryl-4-Ethoxycarbonyl-2,6-bis(Carboxylic Acid)-1,6-Heptadiene
CAPA	2-Phosphonomethyl-Acrylic Acid
CA-PA	4-Ethoxycarbonyl-4-Phosphonic Acid-2,6-bis(Carboxylic Acid)-1,6-Heptadiene
CMAC	2-Chloromethyl-Acryloyl Chloride

CMAC-IDA	{[2-(Bis-Ethoxycarbonylmethyl-Carbamoyl)-Allyl]-Ethoxycarbonylmethyl-Amino}-Acetic Acid Ethyl Ester
CMAC-IDA-K ⁺	Potassium Salt of {[2-(Bis-Carboxymethyl-Carbamoyl)-Allyl]-Carboxymethyl-Amino}-Acetic Acid
EBBr	Ethyl- α -Bromomethyl Acrylate
EBBr-IDA	2-[(Bis-Ethoxycarbonylmethyl-Amino)-Methyl]-Acrylic Acid Ethyl Ester
EBBr-IDA-K ⁺	Potassium Salt of 2-[(Bis-Carboxymethyl-Amino)-Methyl]-Acrylic Acid
EC-EPA	4-Diethoxyphosphoryl-4-Ethoxycarbonyl-2,6-bis(Ethoxycarbonyl)-1,6-Heptadiene
EC-PA	4-Ethoxycarbonyl-4-Phosphonic Acid-2,6-bis(Ethoxycarbonyl)-1,6-Heptadiene
EHMA	Ethyl α -Hydroxymethyl Acrylate
MBC-EPA	2-(Diethoxy-Phosphoryl)-4-Methylene-Pentanedioic Acid 5-tert-Butyl Ester 1-Ethyl Ester
PHOSEED	2-[2-(Diethoxy-Phosphorylmethoxycarbonyl)-Allyloxymethyl]-Acrylic Acid Diethoxy-Phosphorylmethyl Ester
PHOSEED-acid	2-(2-Phosphonomethoxycarbonyl-Allyloxymethyl)-Acrylic Acid Phosphonomethyl Ester
TBBr	tert-Butyl- α -Bromomethyl Acrylate
TBEED	2-(2-tert-Butoxycarbonyl-Allyloxymethyl)-Acrylic Acid tert-Butyl Ester
TBEED-acid	2-(2-Carboxy-Allyloxymethyl)-Acrylic Acid
TBEED-IDA	(({2-[2-(Bis-Ethoxycarbonylmethyl-Carbamoyl)-Allyloxymethyl]-Acryloyl} Ethoxycarbonylmethyl-Amino)-Acetic Acid Ethyl Ester
TBEP	2-(Diethoxy-Phosphorylmethyl)-Acrylic Acid tert-Butyl Ester
TBHMA	tert-Butyl- α -Hydroxymethyl Acrylate
TBPA	2-Phosphonomethyl-Acrylic Acid tert-Butyl Ester

1. INTRODUCTION

1.1. Adhesives in Dentistry

1.1.1. Structure of a Tooth

A human tooth has three main parts [1]:

- crown; the visible part of the tooth.
- neck; the region that is at the gum line, between the root and the crown.
- root; the anchor of the tooth that extends into the jawbone (Figure 1.1).

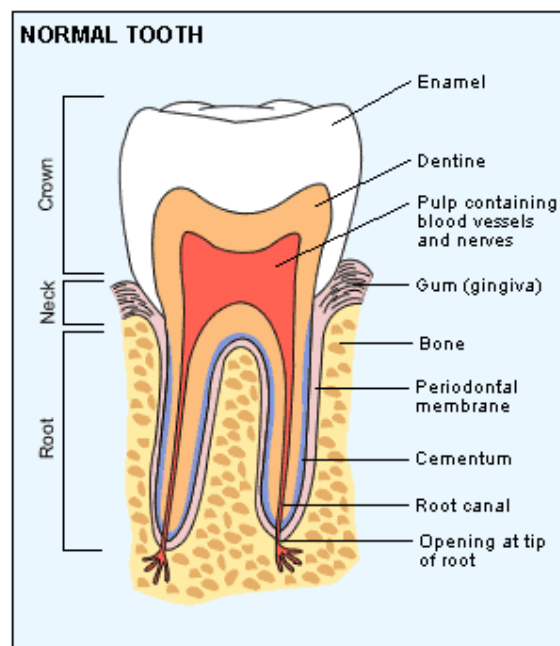


Figure 1.1. The anatomy of tooth

The white and shiny outer surface of the tooth is called *enamel*. It is the hardest substance in the human body, even harder than bone. It gains its hardness from tightly packed rows of calcium and phosphorus crystals within a protein matrix structure. Mature enamel is not considered to be a living tissue [2].

Dentin is the major component of the inside of the tooth and it is located under enamel and cementum. It is yellowish and slightly softer than enamel, with a structure more like bone. It is elastic and compressible in contrast to the brittle nature of enamel. Dentin is sensitive as it contains tiny tubules throughout its structure that connect with the central nerve of the tooth within the pulp. So, dentin is classified as a live tissue [2].

Dentin and enamel are composed of hydroxyapatite, $\text{Ca}_{10}(\text{PO}_4)_6(\text{OH})_2$ and collagen (Table 1.1). The collagen of the dentin provides hydroxyl, carboxyl and amino groups which can be utilized in bonding to this structure [3].

Table 1.1. Approximate composition of enamel and dentin

	Enamel	Dentin
Mineral phase (hydroxyapatite)	97 %	69%
Organic phase (mainly collagen)	1%	20%
Water	2%	11%

When the dentin is cut by a dental instrument, a layer of loosely adhered debris is left covering the dentinal tubules. Because of its appearance, this layer, which contains the components of the ground dentin, is referred to as the *smear layer* [4].

The *pulp* forms the central chamber of the tooth. It is made of soft tissue and contains blood vessels to supply nutrients to the tooth, and nerves to enable the tooth to sense heat and cold. The pulp also contains lymph vessels which carry white blood cells to the tooth to help fight bacteria [2].

Below the gum, the dentin of the root is covered with a thin layer of cementum, rather than enamel. *Cementum* is a hard bone-like substance onto which the periodontal membrane attaches. This membrane bonds the root of the tooth to the bone of the jaw. It contains elastic fibres to allow some movement of the tooth within socket [2].

1.1.2. Role and Categories of Dental Adhesives

Dentistry is concerned with the repair and treatment of the teeth in order to give proper function and secondarily good aesthetics. The main dental treatments that employ adhesives are orthodontics and restoration [3]. Various kinds of metals, organic polymers and ceramics are used for the restoration of teeth. When these restorative materials are placed in the mouth, it is necessary to ensure that they are securely bonded to the teeth, or to each other in a wet condition [5].

In dental treatment in recent years, polymerizable dental filling materials are becoming increasingly used around the world. These materials are supplied in the form of low viscosity liquids or pastes and are readily inserted into the cavity in the tooth. Once in place, a polymerization reaction is commonly initiated by visible light converting the liquid or paste into a hard polymeric solid [6].

Various adhesives and pretreatments of the dentin have been used in order to achieve a strong bond between a dental filling material and the tooth substance (dentin and enamel). Current adhesives may be divided into two major categories based on the number of clinical steps and their interaction with the tooth surface: “etch and rinse” and “self-etch” (Table 1.2) [7].

Table 1.2. Adhesive categories

Adhesive Categories		
Etch and Rinse Adhesives	Self-Etching Adhesives	
<u>Three-step</u> <ul style="list-style-type: none"> • conditioner • primer • bonding agent 	<u>Two-step</u> <ul style="list-style-type: none"> • conditioner + primer • bonding agent 	<u>One-step</u> <ul style="list-style-type: none"> • conditioner + primer + bonding agent

1.1.3. Etch and Rinse Adhesives

“Etch and rinse” adhesives (also known as total-etch) have been around since the early 1990’s. These adhesives require three steps that use an acidic conditioner, primer and bonding agent.

Step one involves the application of the acidic conditioner or etchant whose function is to remove the smear layer by demineralizing the hydroxyapatite (HAP). A significantly roughened surface with cavities is produced which makes the tooth surface more permeable for the next step. The acid etchant is usually a 37 per cent solution of phosphoric acid in water. Also nitric acid or some organic acids such as oxalic, citric, maleic or lactic acid are used as etchants. After it is applied, the tooth surface has to be washed with water and then air dried (Figure 1.2) [4, 8].

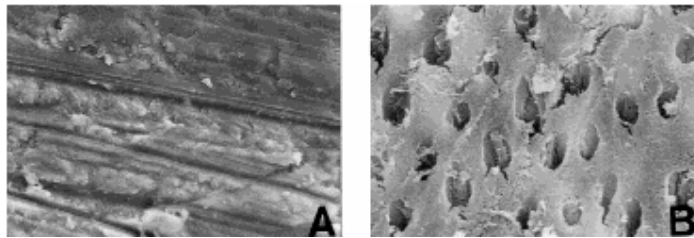


Figure 1.2. SEM images of the treated dentin: The original magnification was x2500. (A) ground dentin surface; surface was covered with smear layer (B) 40 wt per cent H_3PO_4 for 30 s, water-rinse, air-dried; smear layer was removed and dentin tubules were widely opened

Step two involves the application of the primer to the dentin. The primer is usually a hydrophilic monomer such as 2-hydroxy-ethylmethacrylate (HEMA) that serves as an agent to wet and penetrate the etched dentin, preparing it to receive the bonding agent. Because much of the mineral has been removed by the acid, the primer penetrates into a mostly organic material composed of collagen fibrils. HEMA facilitates the restoration of the collagenous layer in which the collagen fiber arrangement had collapsed during air-drying process [4].

The third and final step is to apply the bonding agent. The composition of the bonding agent is similar to the composition of the composite resin except that hydrophilic molecules have been added (Table 1.3) [9]. The bonding agent is brushed onto the prepared dentin surface so that it coats as well as partially penetrates the dentin surface. The bonding agent is then light cured. Once the adhesive monomers become polymerized it bonds to the dentin, mostly by surrounding the exposed collagen fibrils and mechanically locking into the rough dentin surface [4].

Table 1.3. Example of monomer mixture composition in bonding agent and in composite resin

Monomer Composition in Bonding Agent	Monomer Composition in Composite Resin
<ul style="list-style-type: none"> • Bisphenol A glycidyl methacrylate (Bis-GMA) • HEMA • Neopentylglycol dimethacrylate (NPG) • Phosphonic/phosphoric acid containing monomer 	<ul style="list-style-type: none"> • Bis-GMA • Triethylene glycol dimethacrylate (TEGDMA)

Advantages of the etch and rinse adhesives are a good predictable enamel etch and the availability of favorable long-term clinical studies. However, the etch and rinse systems are sensitive to the level of dentin wetness after rinsing off the acidic conditioner. Too little or too much remaining water may lead to reduced adhesion [10].

1.1.4. Self-Etching Adhesives

“Self-etching” adhesives have only recently been introduced to the dental market at a time when dentist desired easier and less technique-sensitive adhesive materials. They are divided into one- and two-step systems.

Two-step self-etching adhesives combine the acidic conditioner with the primer in the initial step. So, in the first step, self-etching primer is applied to the tooth, which consists of an acidic and hydrophilic methacrylate monomer and it both etches and primes the tooth. In the second step, bonding agent is applied to the conditioned surface [7]. The etching potential of the enamel or dentin by the self-etching primer is strongly dependant on the type of acidic group such as phosphoric, phosphonic or carboxylic acid. Examples of self-etching primers are N-methacryloyl glycine (NMGLY) and N-methacryloyl-2-aminoethyl phosphonic acids (NMEP) (Figure 1.3) [11].

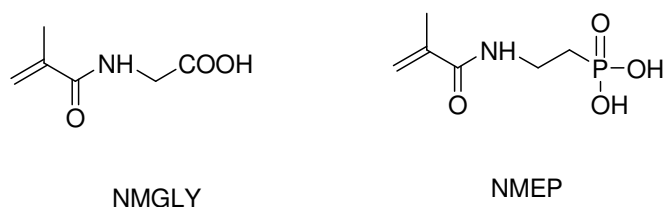


Figure 1.3. Examples of self-etching primers

Even further reduction in the number of steps came with the introduction of one-step self-etching adhesives that combine the conditioner, primer and adhesive. One advantage of the self-etching adhesives is that the conditioner need not be rinsed off. The clinician does not need to be concerned about the level of dentin wetness [12].

The commercial self-etching enamel-dentin adhesives consist of a mixture of self-etching adhesive monomers, crosslinkers, additional monofunctional co-monomers and additives (Figure 1.4) [13].

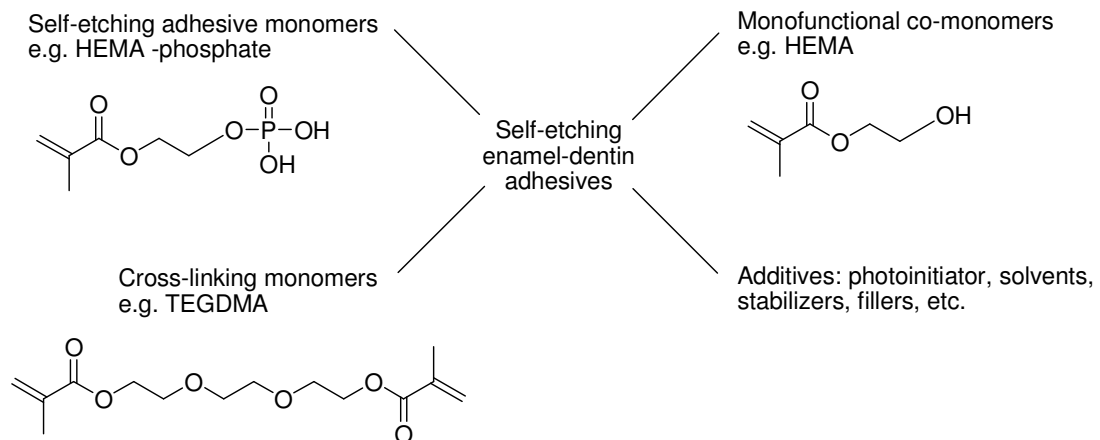


Figure 1.4. Components of currently available self-etching enamel-dentin primers/adhesives

The monomers contained in commercial self-etching enamel-dentin adhesives can be divided into three main groups according to their function:

- adhesive monomers
- cross-linking monomers
- monofunctional co-monomers

All these monomers have to meet the following general requirements:

- High rate of free radical homopolymerization or copolymerization with the other monomers in the adhesive.
- The monomers should be conveniently miscible with aqueous solutions of acetone and ethanol, which are mainly used as solvents in commercial adhesive systems.
- Sufficient stability of both the monomer and the formed polymer against degradation by oxygen, heat, light and of course water during storage.
- Minimal water uptake and low swelling degree of the formed polymer.
- Low polymerization shrinkage or at least contribution of the monomer to reduce shrinkage or thermal stress in the adhesive layer.
- Low oral toxicity and cytotoxicity of the monomers.

Among the various free radically polymerizable groups, methacrylate functions show sufficient reactivity. Acrylates are more reactive but they may increase the toxicological risk of the monomers. Vinyl or styryl monomers are less reactive in the free radical polymerization. (Meth)acrylamides provide hydrolytic stability under acidic conditions. Allyl monomers exhibit a low tendency towards homopolymerization and if mixed with other monomers, show a degradative chain transfer reaction [13].

1.1.4.1. Adhesive Monomers in Self-Etching Enamel-Dentin Adhesives. Self-etching adhesive monomers are responsible for the specific interaction of the adhesive with the dental hard tissue. Therefore, they should meet, beside the above mentioned general requirements for the adhesive monomers, the following additional demands [13]:

- Capability of self-etching the enamel surface in a relatively short time while forming a surface with increased roughness that enables micromechanical bonding of the adhesive on enamel.
- Optimal wetting and film forming behaviour on the tooth surface and the capability of penetrating, for example, into the dental tubules.
- Fast ionic or covalent interaction with components of the dental hard tissue, e.g., the formation of low soluble calcium salts or formation of covalent bonds with collagen.

In general, these bonding agents are bifunctional molecules, containing a polymerizable group P, for example, a methacrylate group, which can react both with the other monomers of the adhesive and the restorative material by copolymerization, an adhesive group AD, such as a strong acidic group capable of both etching the dental hard tissues and interacting with the tooth substance, and a spacer group R, designed to influence the solubility, flexibility and the wetting properties of the adhesive monomer (Figure 1.5) [14].

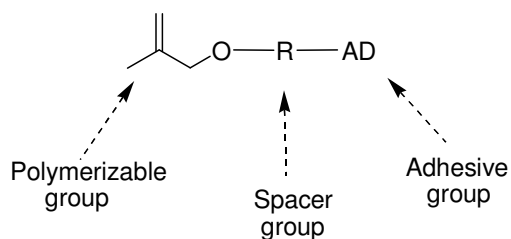
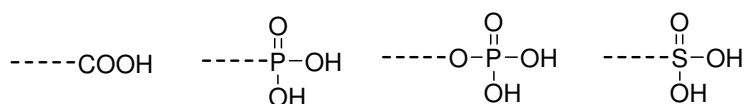


Figure 1.5. Design of an self-etching adhesive monomer

Suitable adhesive groups are shown in Figure 1.6. The general potential of the acidic monomers to etch enamel largely depends on the acidity of the monomers that increases in the following order: carboxylic acids < phosphonic acids < acid phosphates < sulfonic acid. Acid groups can form ionic bonds and chelating groups can form coordinative linkages with the calcium ions of enamel or dentin. Also, as dentinal collagen contains reactive groups such as amino or hydroxyl, the reaction of covalent coupling groups with the dentin can form covalent bonds with the collagen fibers if conditions are mild. Moreover, Van der Waals forces, London dispersion forces, hydrogen bonding or charge-transfer interactions may additionally contribute to the physical adhesion [13].

Acid groups



Chelating groups



Covalent coupling groups

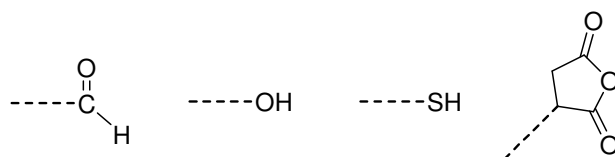


Figure 1.6. Adhesive groups (AD)

In general, phosphorus-containing monomers are capable of etching enamel and dentin and promote monomer diffusion. Among the phosphorus-containing monomers, mainly polymerizable phosphonic acids or phosphoric acids are used.

Polymerizable phosphoric acids: One of the first chemical compounds proposed to improve bonding to human dentin was the glycerol dimethacrylate ester of phosphoric acid (GDMP) [15]. Further examples of commercially available acidic methacrylate phosphates applied to improve bonding on dentin are, methacryloyloxyethyl phenyl hydrogen phosphate (MEP-P), 10-methacryloyloxy methacrylate MDP, and methacryloyloxyethyl dihydrogen phosphate (MEP, HEMA-phosphate) (Figure 1.7) [5, 9].

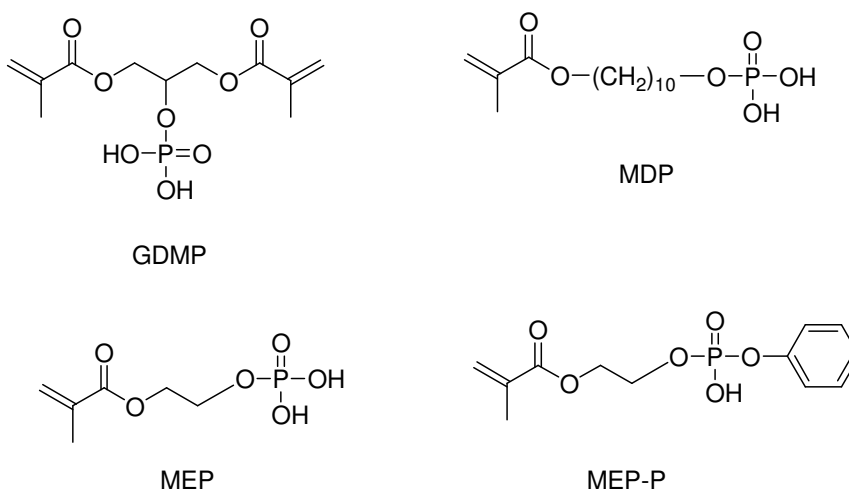


Figure 1.7. Examples of polymerizable acidic phosphates used in dentin adhesives

The polymerizable acidic phosphates are generated by the reaction of phosphorus oxychloride (POCl_3) with the corresponding OH-group containing methacrylate. For example, the reaction of POCl_3 with 10-hydroxydecyl methacrylate in the presence of triethylamine (TEA) at -30 to -40 °C resulted in MDP (Figure 1.8) [16].

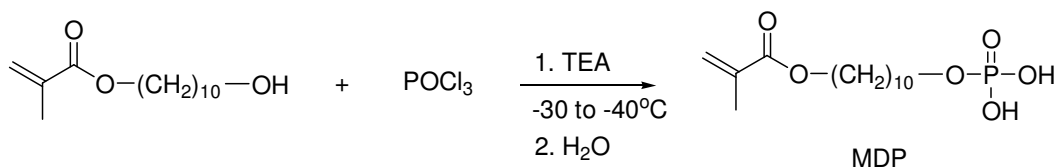


Figure 1.8. Phosphorylation of 10-hydroxydecyl methacrylate with POCl_3

Avci *et al.* synthesized phosphate-containing monomers by reacting diethylchlorophosphate with ethyl α -hydroxy methyl acrylate (EHMA), tert-butyl α -hydroxy methyl acrylate (TBHMA) (Figure 1.9) and 3-acryloyloxy-2-hydroxypropyl methacrylate (AHM) (Figure 1.10). But the attempted hydrolysis of the monomers was unsuccessful because of the loss of diethyl phosphate group [17, 18].

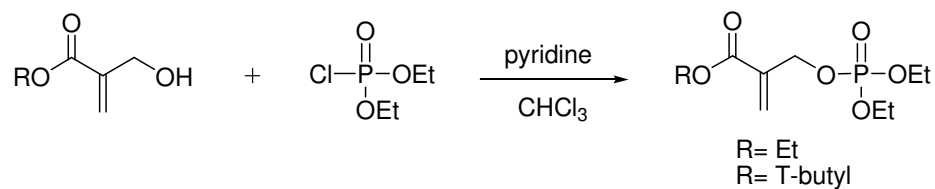


Figure 1.9. Phosphorylation of alkyl α -hydroxy methyl acrylates (RHMA) with diethylchlorophosphate

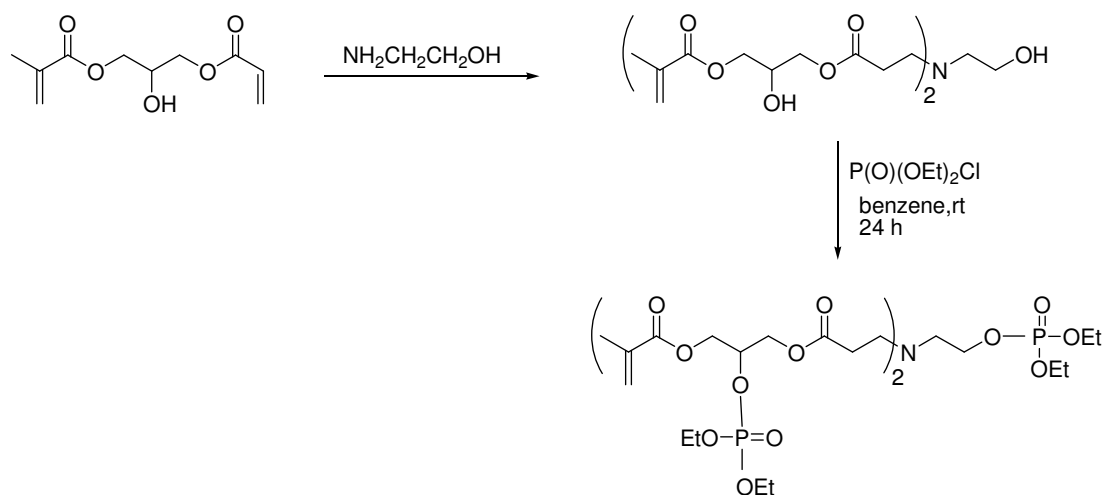


Figure 1.10. Phosphorylation of AHM with diethylchlorophosphate

In general, the hydrolytic stability of the phosphoric acid esters increases in the following order: dialkyl hydrogen phosphate < trialkyl phosphate < monoalkyl dihydrogen phosphate (Figure 1.11).

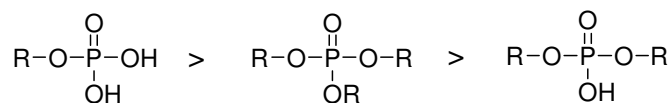


Figure 1.11. Order of hydrolytic stability of the phosphoric esters

In the case of acidic methacrylate phosphates, an additional hydrolytic instability results from the hydrolysis of the methacrylate ester bond. For MEP, even though hydrolysis of the phosphate ester bond was not expected, it was found that the hydrolysis of both the methacrylate and phosphate ester bonds resulted in the formation of methacrylic acid and HEMA (Figure 1.12) [13].

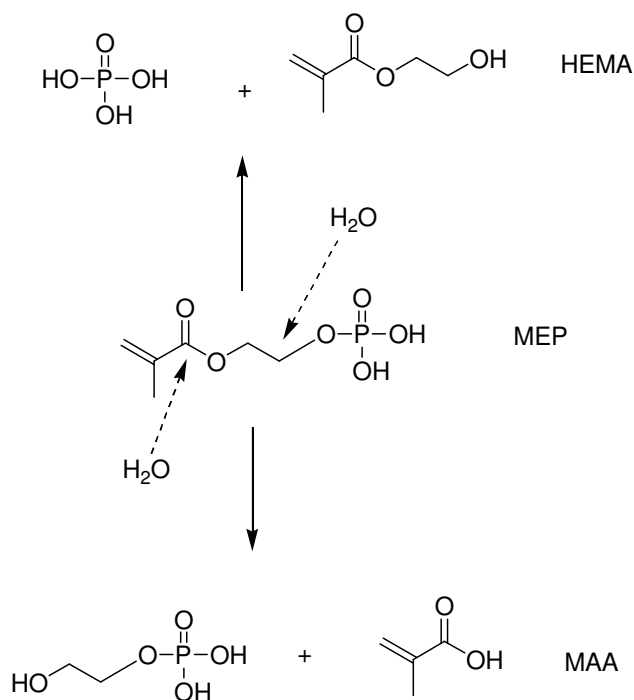
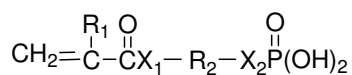
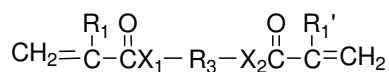


Figure 1.12. Hydrolysis of MEP in the presence of water

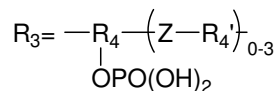
Omura *et al.* proposed dental adhesives from polymerizable phosphate compounds of the formula (I) or (II) as shown in Figure 1.13 [19].



(I)

R₁, R₁'= H or CH₃X₁, X₂= O, S or NHR₂= organic residue of 5-40 C atoms

(II)

R₄= hydrocarbon group of 1-29 C atoms

Z= O, COO, NH

Figure 1.13. General formula of the polymerizable phosphates of the invention

These compounds showed a superior adhesive strength on any of hard tissues in a living body, such as teeth and bones, metals, organic polymers and ceramics. They maintain a high adhesive strength for a long time even they are exposed to moisture or immersed in water. For example, the phosphate ester of the general formula in Figure 1.14, in which $j = 2, 3, 4, 5, 6, 7, 8, 9, 10$ or 12 were tested for adhesive strength in water after one year. It was observed that an improved adhesive strength in water was obtained with an increase in the value of j , particularly when it was 8 or more.

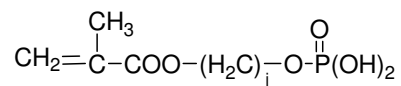


Figure 1.14. Example of a phosphate ester

In Table 1.4, the adhesive strengths of some of the phosphate compounds of the invention on human tooth were compared.

Table 1.4. Adhesive strength of monomers on human tooth

Adhesive vinyl compound	Adhesive strength on human tooth (kg/cm ²)
$\text{CH}_2=\overset{\text{CH}_3}{\text{C}}-\text{COO}(\text{CH}_2)_6\text{OPO}(\text{OH})_2$	110
$\text{CH}_2=\overset{\text{CH}_3}{\text{C}}-\text{COO}(\text{CH}_2)_{10}\text{OPO}(\text{OH})_2$	172
$\text{CH}_2=\overset{\text{CH}_3}{\text{C}}-\text{COO}(\text{CH}_2)_2\text{O}-\text{C}_6\text{H}_4-\text{O}(\text{CH}_2)_2\text{OPO}(\text{OH})_2$	151
$\text{CH}_2=\overset{\text{CH}_3}{\text{C}}-\text{COO}-\text{C}_6\text{H}_4-\text{OPO}(\text{OH})_2$	91
$\text{CH}_2=\overset{\text{CH}_3}{\text{C}}-\text{CONHCH}_2\text{COO}(\text{CH}_2)_5\text{OPO}(\text{OH})_2$	90
$\text{CH}_2=\overset{\text{CH}_3}{\text{C}}-\text{COO}-\text{C}_6\text{H}_4-\text{COO}(\text{CH}_2)_{12}\text{OPO}(\text{OH})_2$	152

It was claimed in EP 1, 548,021 A1 that, self-etching, self-priming dental adhesive composition which contains a polymerizable phosphoric acid ester derivative has some advantages over phosphonic acid containing composition such that; phosphoric acids are more acidic, the intermediates for producing the phosphonic acid derivatives are toxic and phosphonic ester derivatives are more expensive. It was also stated that, the polymerizable phosphoric acid ester derivatives of the invention are resistant against hydrolysis in acidic medium (Figure 1.15) [20].



Z = COOR', COSR'', CON(R')₂, CONHR', CONR'R''

R', R'' = H, C₁₋₁₈ alkyl group optionally substituted by :C₃₋₈ cycloalkyl group,
C₄₋₁₈ aryl or heteroaryl group, C₁₅₋₁₈ alkylaryl or alkylheteroaryl group,

a, b = integer, preferably 1 to 5.

L = organic residue containing 2 to 45 carbon atoms and optionally heteroatoms such as O, N and S.

Figure 1.15. Possible polymerizable phosphoric acid ester derivatives of the invention

The polymerizable phosphoric acid ester derivatives in Figure 1.16 have the advantage that a large number of polymerizable 2-(oxa-ethyl) acryl derivative group which can enhance the bond strength and/or a large number of acidic phosphate groups which can enhance the self-etching feature are linked to one molecule.

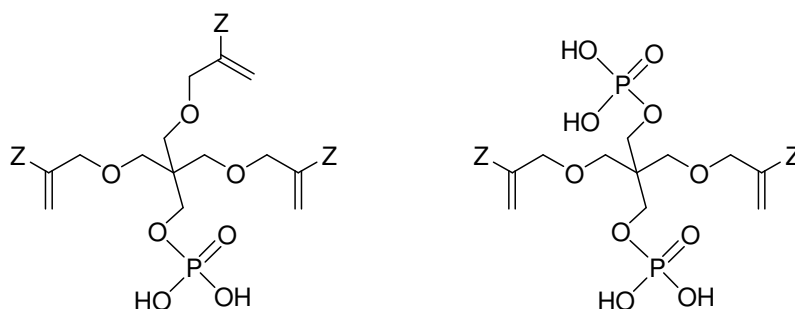


Figure 1.16. Examples of 2-(oxa-ethyl) acryl derivatives of polymerizable phosphoric acids

Polymerizable phosphonic acids: Hydrolytic instability of the methacrylate phosphates was tried to be solved using monomers that contain more hydrolytically stable bonds and by the use of phosphonates.

A first evaluation of polymerizable phosphonates for dental adhesives was carried out by Anbar *et al.* [21, 22]. They proved that vinyl phosphonic acid (VPA) and 4-vinylbenzyl phosphonic acid (VBPA) can improve the adhesion of the filling composites

on etched enamel. Unfortunately, VPA and VBPA are less reactive than methacrylates in radical polymerization. However, hydrogels containing copolymers of VPA and acrylamide supported the adhesion and proliferation behaviour of bone-related cells which suggests potential uses of phosphonate-containing hydrogels in bone tissue engineering [23].

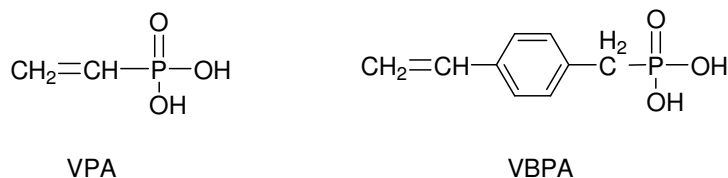


Figure 1.17. Structure of monomeric phosphonic acids VPA and VBPA

The methacrylated phosphonate, dimethyl(2-methacryloyloxyethyl)phosphonate was first employed by d'Alelio *et al.* who carried out the Arbuzov reaction as shown in Figure 1.18 [24].

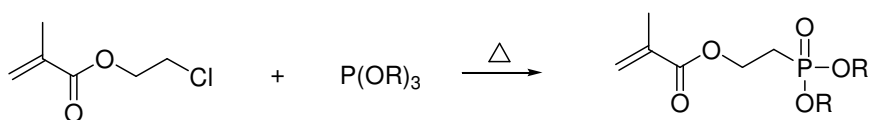


Figure 1.18. Synthesis of dimethyl(2-methacryloyloxyethyl)phosphonate by Arbuzov reaction

Misato *et al.* described the radical addition of dialkyl hydrogenphosphonate on a vinyl methacrylate according to the following reaction as shown in Figure 1.19 [24].

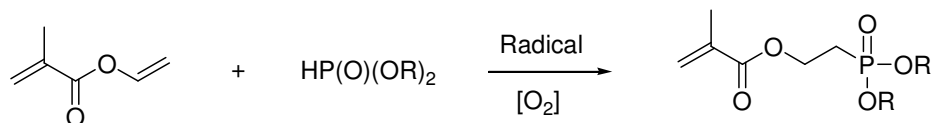


Figure 1.19. Synthesis of dimethyl(2-methacryloyloxyethyl)phosphonate by radical addition of dialkyl hydrogenphosphonate

Nazakin realized the Micheal addition of methacrylic acid on the dialkyl vinyl phosphonate (Figure 1.20) [24].

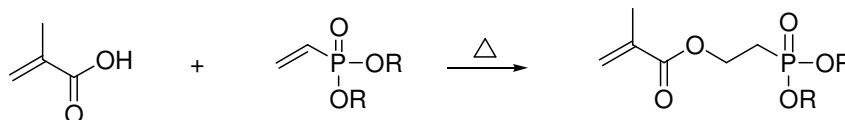


Figure 1.20. Synthesis of dimethyl(2-methacryloyloxyethyl)phosphonate by the Micheal addition of methacrylic acid on the dialkyl vinyl phosphonate

The strategy which remains the most widely used is the methacrylation of a hydroxyalkylphosphonate precursor (Figure 1.21) [25].

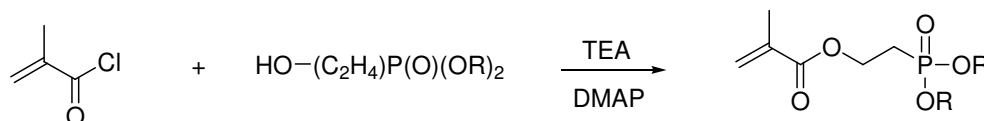


Figure 1.21. Synthesis of dimethyl(2-methacryloyloxyethyl)phosphonate using hydroxyalkylphosphonate precursor

Dimethyl(2-methacryloyloxyethyl)phosphonate can then be converted to the corresponding phosphonic acids by using bromotrimethylsilane followed by the hydrolysis of the silylated intermediate by an excess of methyl alcohol (Figure 1.22) [25, 26].

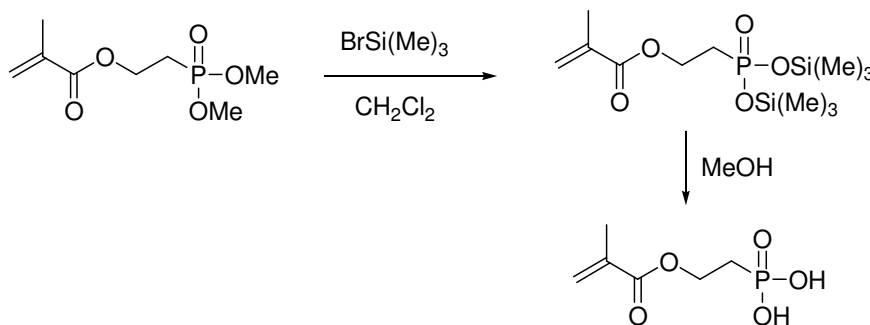


Figure 1.22. Hydrolysis of dimethyl(2-methacryloyloxyethyl)phosphonate

Mou *et al.* synthesized phosphonic acid monomer for use in dental composites by the base-catalyzed rearrangement of the corresponding diethyl aryl phosphonate. They claimed that this aromatic monomer would yield materials with improved mechanical properties (Figure 1.23)[27].

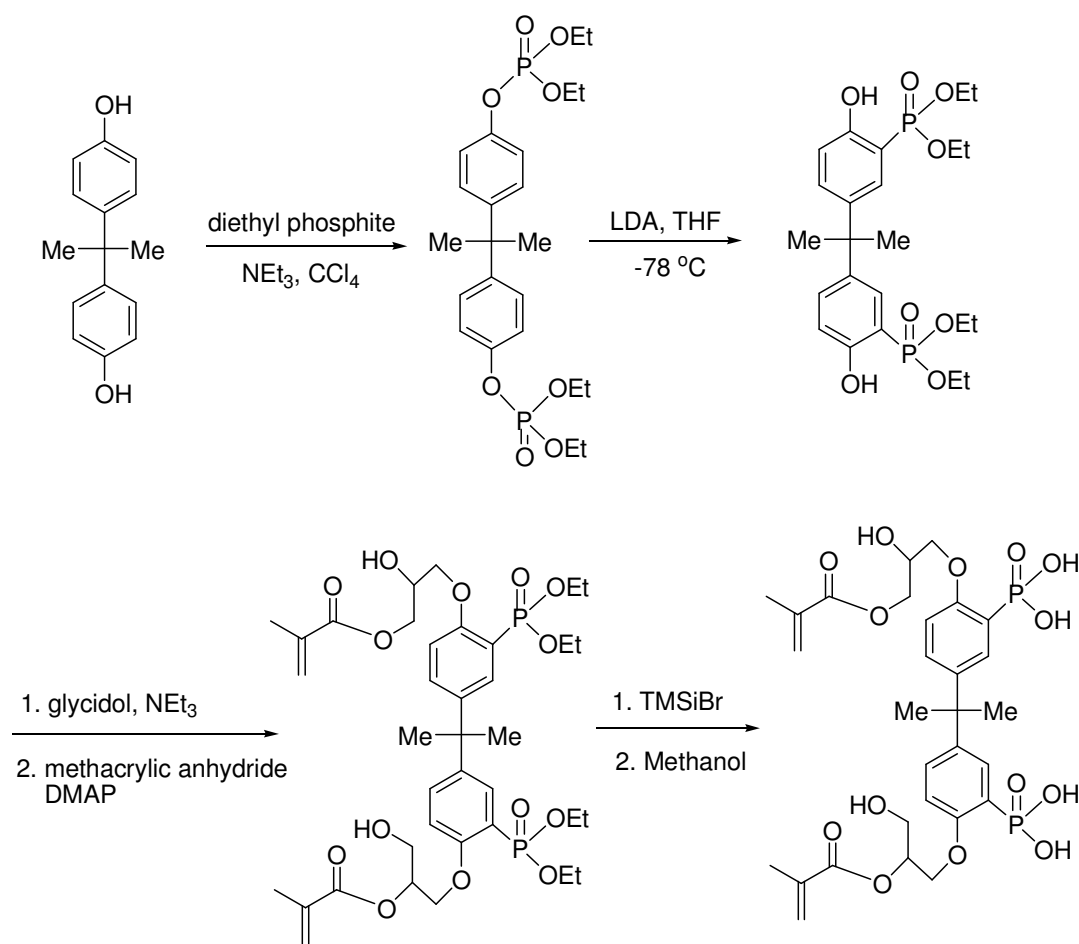


Figure 1.23. Synthetic scheme of phosphonic acid containing monomer

Avcı *et al.* synthesized phosphonic ester monomers by the ester formation of ethyl α -chloromethyl acrylate (ECMA) and tert-butyl α -bromomethyl acrylate (TBBr) with diethylphosphonoacetic acid. The selective hydrolysis of the ethyl ester phosphonic ester compound was carried out with bromotrimethylsilane, producing a phosphonic acid monomer (Figure 1.24) [17].

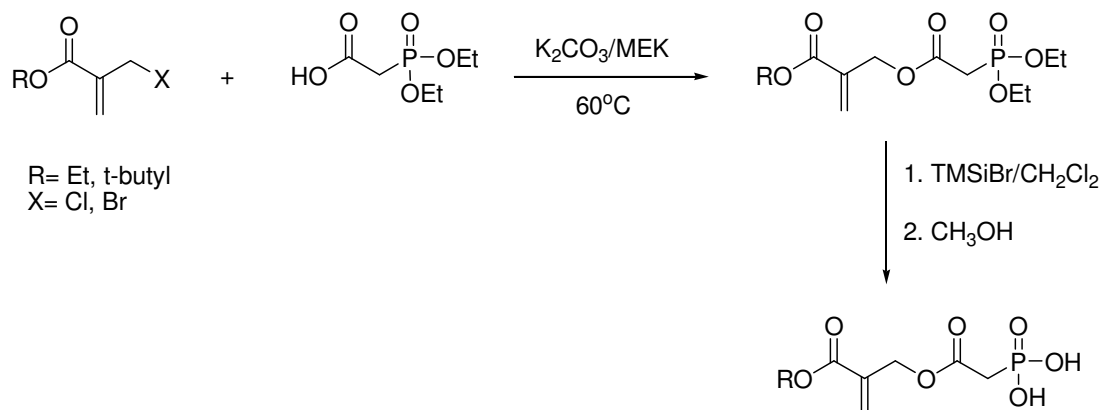


Figure 1.24. Synthesis of polymerizable phosphonates

In another study, TBHMA was converted into a reactive intermediate α -(chloromethyl)acryloyl chloride (CMAC) with thionyl chloride to allow the incorporation of identical ester and ether groups, both phosphorus-containing (Figure 1.25) or mixed ester-ether groups, phosphorus-containing and nonphosphorus-containing (Figure 1.26) [28].

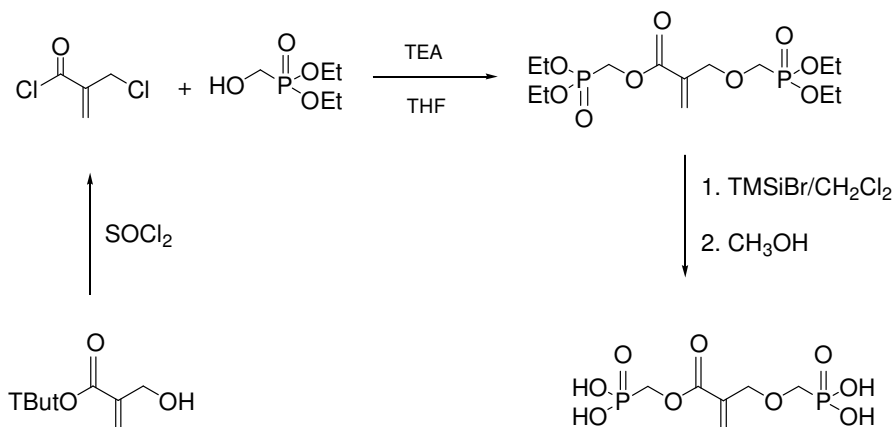


Figure 1.25. Phosphorus-containing monomer with identical ester and ether group

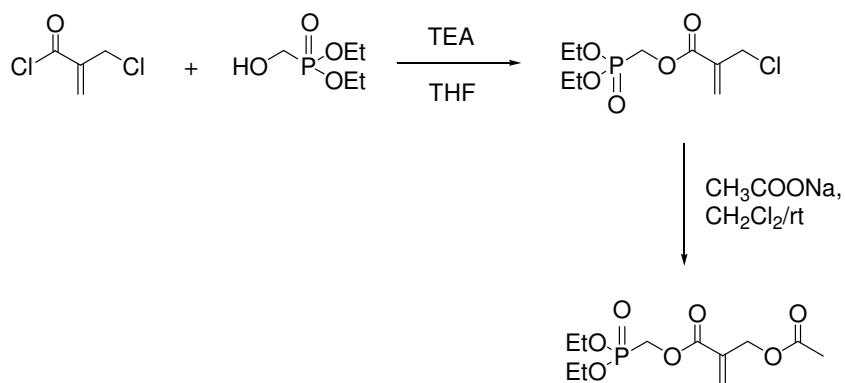
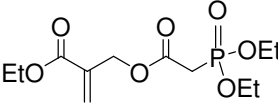
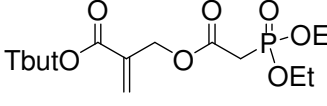
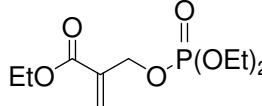
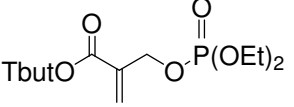
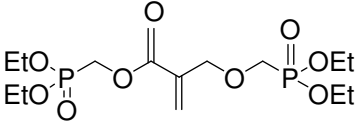
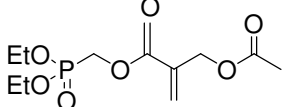


Figure 1.26. Phosphorus-containing monomer with mixed ester and ether groups

The relative reactivities of the synthesized phosphorus-containing monomers in photopolymerizations were compared and it was shown that incorporation of an ester group increased the rate of polymerization. Also, polymerization of monomers with phosphorus atoms close to the double bond were found to be very slow due to steric effects of phosphorus groups (Table 1.5) [28].

Table 1.5. Photopolymerization results of phosphorus-containing monomers

Monomer	temp ($^{\circ}\text{C}$)	R_p ($\text{kJ mol}^{-1} \text{min}^{-1}$)	conv (%)
	28	45	77
	29	7	56
	26	7	36
	28	6	43
	27	8	45
	28	71	90

Moszner *et al.* synthesized a number of phosphonic acid containing monomers with improved hydrolytic stability and reactivity [13, 14, 25, 29, 30]. Among the synthesized monomers, 2-[4-(dihydroxyphosphoryl)-2-oxa butyl] acrylate (EAEPA) and 2,4,6-trimethylphenyl 2-[4-(dihydroxyphosphoryl)-2-oxabutyl] acrylate (MAEPA) show the best dentin adhesive properties, whereas the carboxylic acid and nitrile derivatives, 2-[4-(dihydroxyphosphoryl)-2-oxabutyl]acrylic acid (CAEPA) and 2-[4-(dihydroxyphosphoryl) -2-oxabutyl]acrylonitrile (NAEPA), exhibited less adhesive action. The monomers CAEPA, NAEPA and MAEPA are hydrolytically stable in aqueous solutions at room temperature (Figure 1.27).

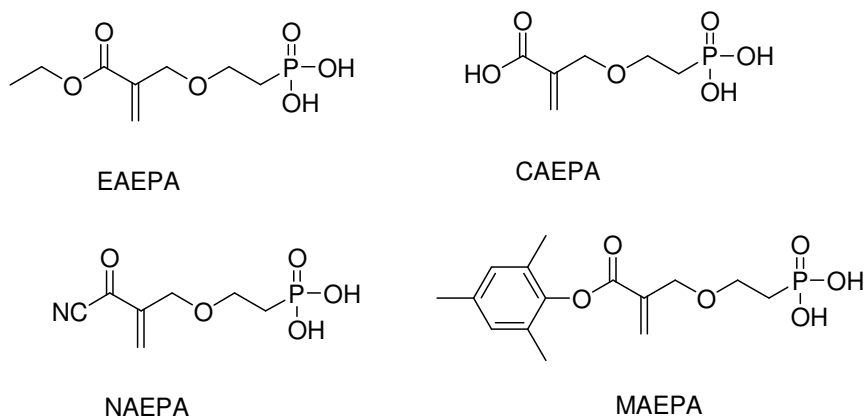


Figure 1.27. Examples of polymerizable phosphonates

In U.S. Patent No. 6,172,131 B1, Moszner *et al.* presents polymerizable acrylphosphonic acids which have a high degree of hydrolytic stability and it is assumed that they form ionic and/or complex compounds with the calcium ions of the tooth dentine or with the metal ions [29].

The acrylphosphonic acids according to the invention are compounds of the following general formula;

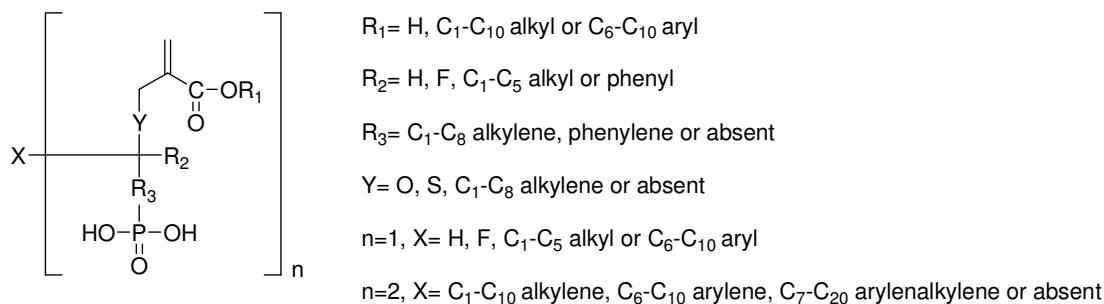


Figure 1.28. General acrylphosphonic acid structure of the invention

The acrylphosphonic acids can be prepared by reaction of α -halomethylacrylic acid esters with protected mono- or difunctional phosphonic acid esters and cleavage of the protecting groups.

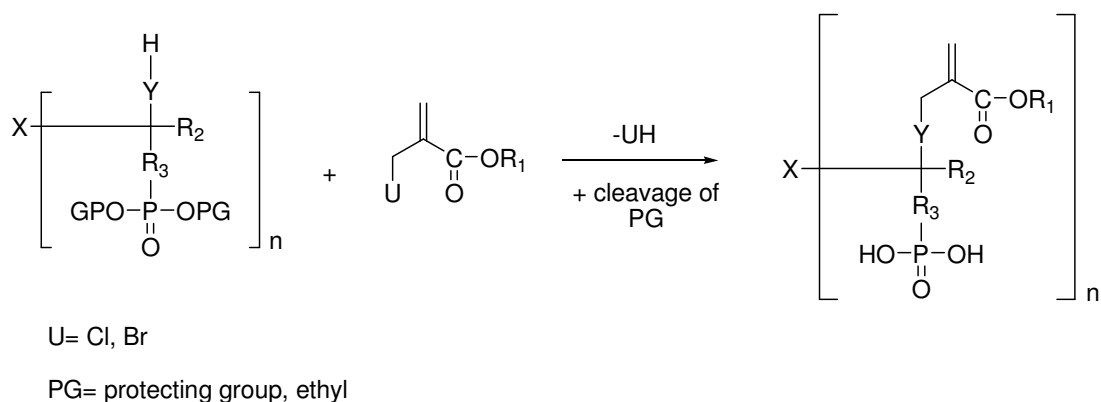


Figure 1.29. Synthesis of acrylphosphonic acids

Some examples of acrylphosphonic acids are given in Figure 1.30.

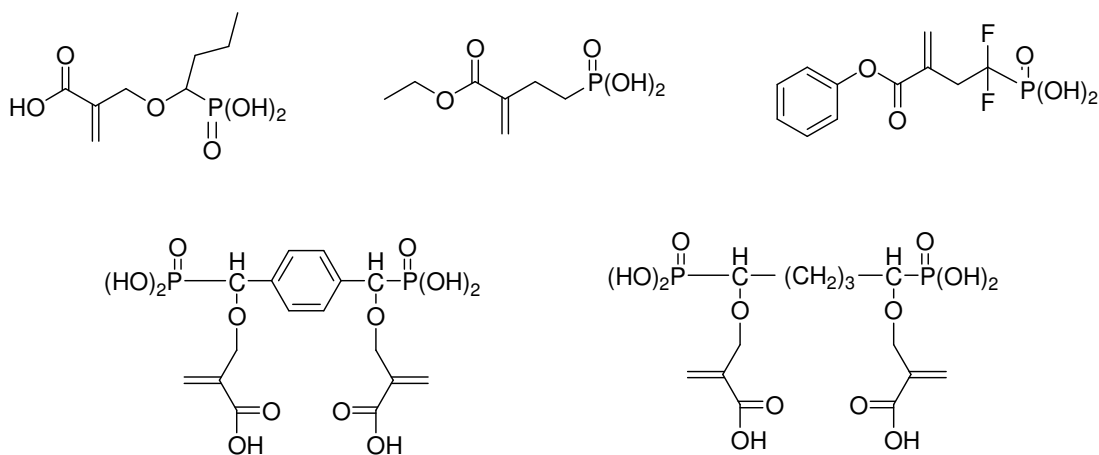


Figure 1.30. Examples of acrylphosphonic acids

Finke *et al.* synthesized 2-(meth)acrylamido-2-methyl-propanephosphonic acid from (meth)acrylonitrile and 2-methyl-prop-1-ene-1-phosphonic acid or 2-methyl-prop-2-ene-1-phosphonic acid in the presence of strong acids such as H_2SO_4 , H_3PO_4 , HClO_4 or HF (Figure 1.31). It was found out that, this compound and its salts are extremely stable to hydrolysis and were valuable monomers for the manufacture of copolymers with acrylamide, acrylic acid and acrylonitrile [31].

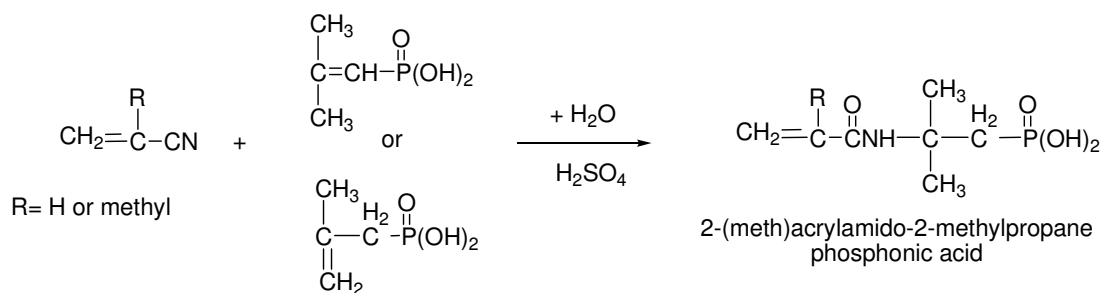


Figure 1.31. Synthesis of 2-(meth)acrylamido-2-methyl-propanephosphonic acid

Recently, U.S. Patent No. 6,902,608 B2 shows the synthesis of new dental materials which have good adhesive properties and high resistance to hydrolysis [32]. The dental materials comprise phosphonic acids with the general structures given below:

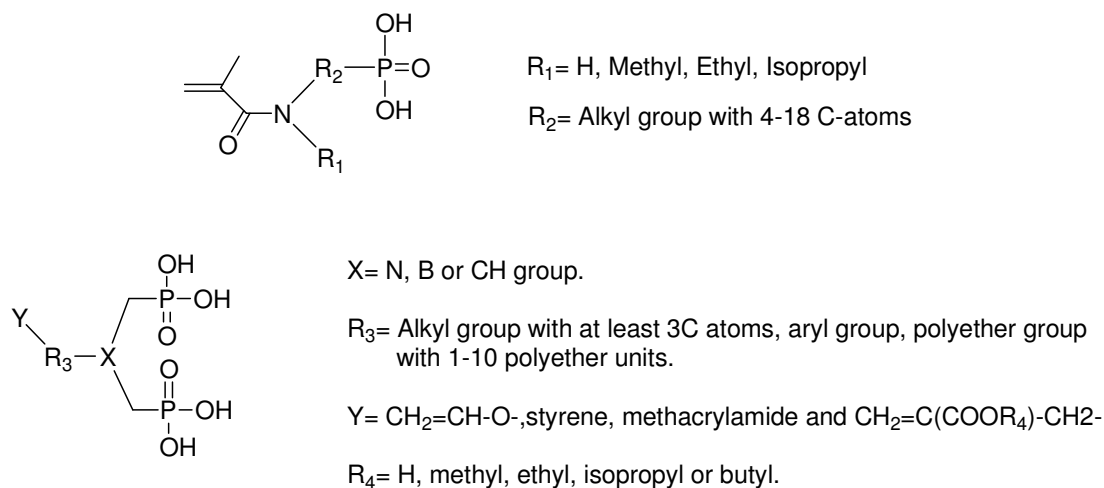


Figure 1.32. General adhesive monomer structures of the invention

Two examples of the invention are given in Figure 1.33.

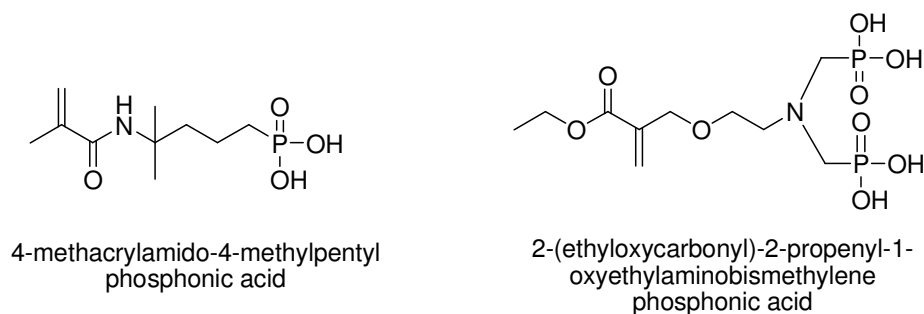


Figure 1.33. Two examples of the invention

Also, the metal binding capability of phosphonic acids has been widely studied with various cations [33, 34, 35]. Riedelsberger and Jaeger showed that monomeric and polymeric aminomethylphosphonic acids exhibit good complexation ability for the transition metal ions Cd^{+2} and Hg^{+2} (Figure 1.34). This selective extraction of the metal ions from aqueous solution can be used as the treatment of wastewater, groundwater and seawater [36].

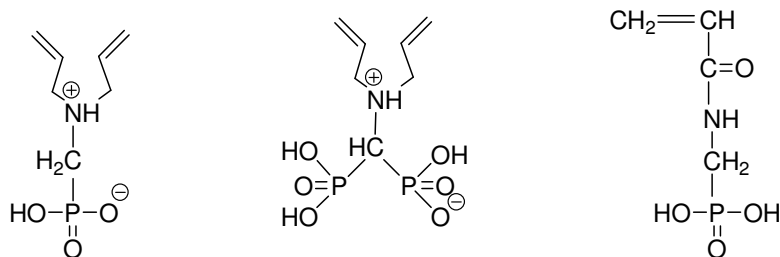


Figure 1.34. Monomeric aminomethylphosphonic acids

The complexation of the metal ions is carried out using the oxygen atoms of the phosphonic acid group. In the acidic pH range, the metal ion is not bound by four oxygen atoms, but only two oxygen atoms of two different phosphonic acid groups are used for complexation, because the second OH group of the phosphonic acid molecule is not dissociated (Figure 1.35) [37].

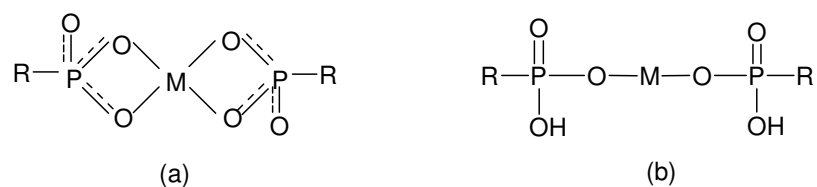


Figure 1.35. Suggested structure of the metal ion-monomer complex at different pH's, (a) in basic medium (b) in acidic medium

Alexandratos and Smith synthesized monofunctional resins including β -ketophosphonic acid (β kPh), phosphonoacetic acid (PhAc) and phosphonic acid (Ph) (Figure 1.36) [38].

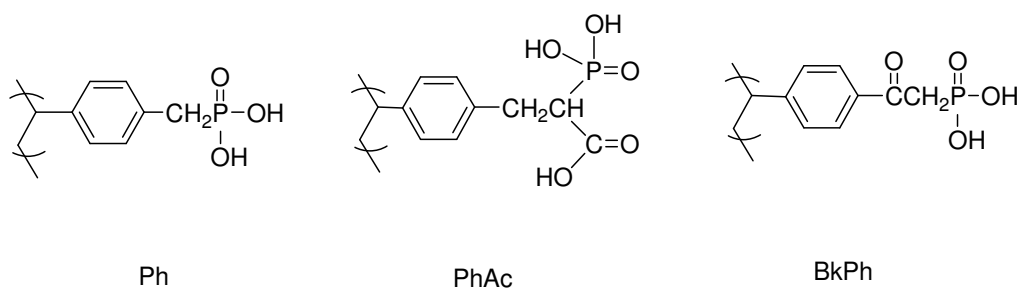


Figure 1.36. Structures of monofunctional resins

They showed that the β -ketophosphonate resin has the highest metal-ion affinities, whereas the phosphonoacetate resin has an affinity similar to that of the phosphonate resin. The reduced affinity of the phosphonoacetate ligand for the metal ions was explained by the formation of intraligand hydrogen bonding which made the carbonyl group unavailable for ion-binding cooperation with the phosphoryl group (Figure 1.37).

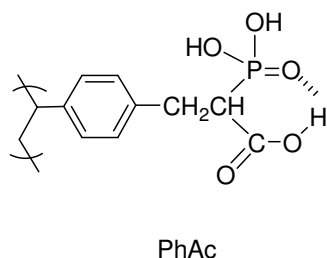


Figure 1.37. Intraligand hydrogen bonds that reduce the affinities of the phosphonoacetate ligand

Polymerizable carboxylic acids: Only a few polymerizable carboxylic acids are used commercially as a self-etching adhesive. Examples are 4-methacryloyloxyethyl trimellitic acid (4-MET), 10- methacryloyloxydecyl malonic acid (MAC-10), N-acryloyl aspartic acid (NAASP), N-methacryloyl-1-aminosalicylic acid (MASA), N-(vinylbenzyl)iminodiacetic acid (NVBIDA) and N-methacryloyl glycine (NMGLY) (Figure 1.38). Aqueous solutions of these acids show a pH value below 2.0 and enable to etch both the dentin and enamel [6, 8, 39].

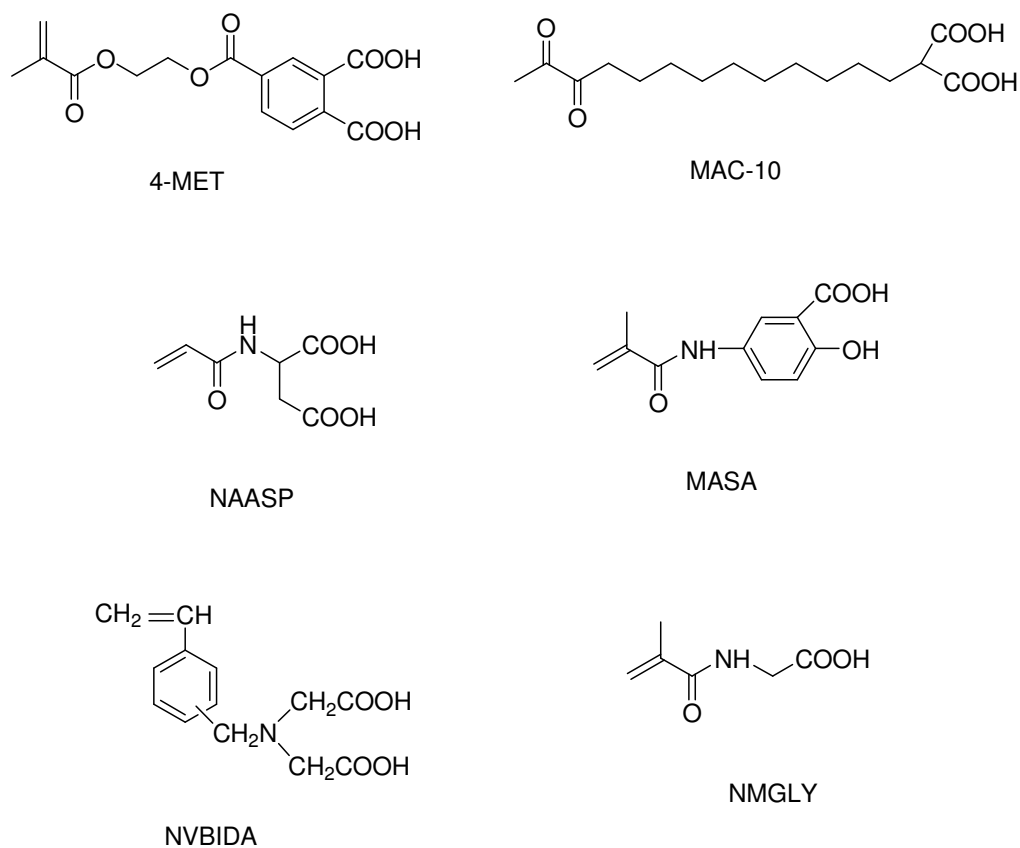


Figure 1.38. Examples of COOH-containing adhesive monomers

Kitoh *et al.* showed that N-(vinylbenzyl)iminodiacetic acid (NVBIDA) could provide strong and durable adhesion for calcium metaphosphate ceramic used in esthetic dentistry when the ceramic surface was etched with alkali [40].

New fluoride-releasing dimethacrylate monomers containing bis(aminodiacetic acid) chelating ligand and its complex with zirconium and fluoride were synthesized (Figure 1.39). It was shown that the experimental composites containing such monomers have increased fluoride release and recharge capacity [41, 42].

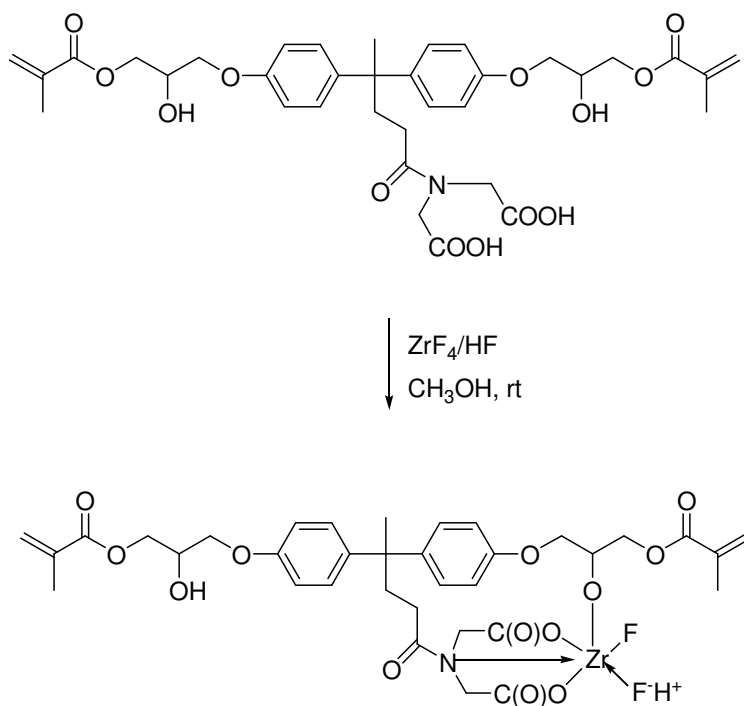


Figure 1.39. Synthesis of fluoride-releasing dimethacrylate monomer

Vanderlaan have prepared metal chelating, hydrogel polymers which can be used in the fabrication of soft contact lenses from 2-hydroxyethyl methacrylate (HEMA) as hydrophilic monomer, EGDMA as crosslinker and a monomer that contains metal chelating functionality which is either an ester or amide of aminopolycarboxylic acids such as ethylenediamine tetraacetic acid (EDTA), diethylenetriamine pentaacetic acid (DTPA) or diethylenetriamine tetraacetic acid. Figure 1.40 shows an example of a monomer that contains metal chelating functionality which was prepared from HEMA and DTPA where HEMA moiety joined through an ester linkage to the DTPA moiety. The invention showed that such lenses which have the ability to chelate metal ions such as iron, calcium, copper, magnesium, molybdenum and zinc and therefore have anti-bacterial properties, as bacteria can not maintain sustained growth in the absence of these ions [43].

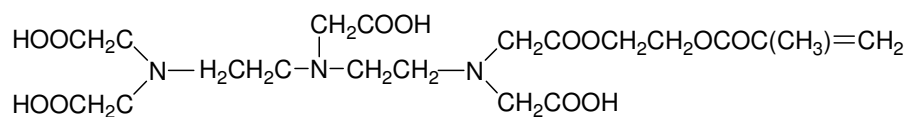


Figure 1.40. Monomer that contains metal-chelating functionality

Chen *et al.* designed a chelating vinyl monomer from glycidyl methacrylate (GMA) and iminodiacetic acid (IDA) (Figure 1.41). Iminodiacetic acid was chosen as a chelating group because it possess one aminopolycarboxylate and provides a reactive secondary amine hydrogen that can be easily introduced to the side chain of a polymer or vinyl monomer [44, 45].

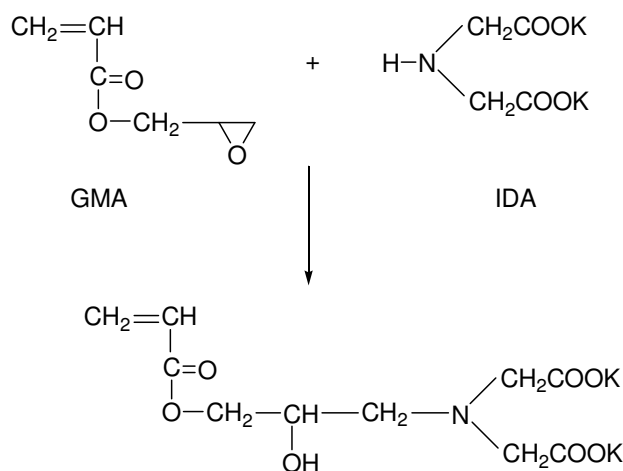


Figure 1.41. Structure of GMA-IDA chelating monomer

In US. Patent No. 5,321,053, Hino *et al.* presents polymerizable vinyl monomers containing at least one COOH group in the molecule that can be used for adhesion to the tooth or metals [9]. Some examples of COOH containing monomers are shown in Figure 1.42.

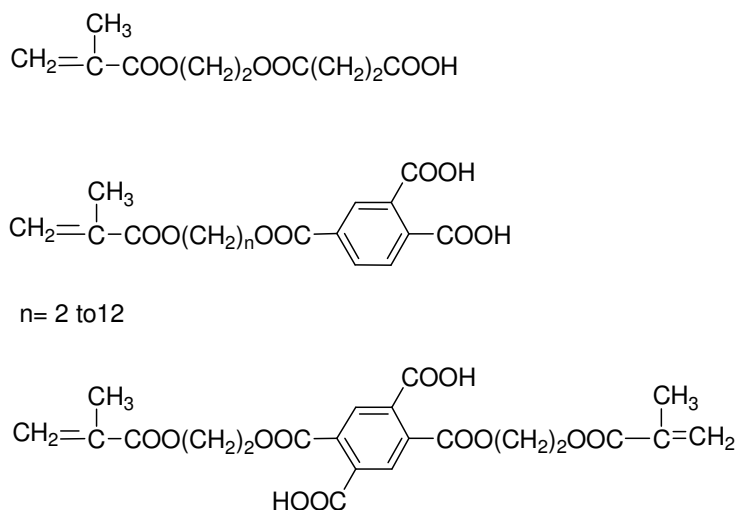


Figure 1.42. Examples of -COOH containing monomers

1.1.4.2. Monofunctional Co-Monomers in Commercial Adhesives. Among the monofunctional monomers HEMA is the most frequently used one. Its hydrophilic nature improves the miscibility and solubility of the adhesive components and the wetting behaviour of the adhesive on the dental hard tissue. In addition HEMA can stabilize the collagen fibril network and it improves the dentinal permeability and monomer diffusion into the dentin structure.

Nishiyama *et al.* showed that, HEMA solution applied to etched dentin resulted in an increase in the bond strength. However, the bond strength was strongly dependent on the pH of the aqueous solution for the HEMA primer as the interaction that exists between the ester carbonyl portion in the HEMA and the undissociated carboxylic acid of the collagen functional group became stronger when the pH was decreased. Conversely, when the pH of the aqueous solution for the HEMA primer was increased, the bond strength was decreased due to the deformation in hydrogen bonding, since most of the carboxylic acids of the collagen functional group dissociated [46, 47].

Also, different substitutes of HEMA, N-(2-hydroxyethyl)-methacrylamide (HEMAM) and N-methyl-N-(2-hydroxyethyl)-acrylamide (MHEAM) were synthesized as they have improved hydrolytic stability and showed very low cytotoxicity [13].

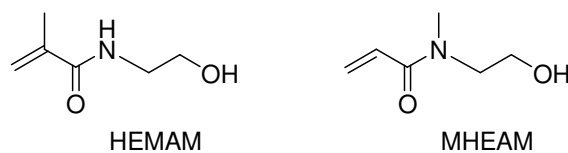


Figure 1.43. Structure of HEMA substitutes with improved hydrolytic stability

1.1.4.3. Cross-Linking Monomers in Commercial Adhesives. Cross-linking dimethacrylates, such as Bis-GMA, TEGDMA, urethane dimethacrylate (UDMA) and glycerol dimethacrylate (GDMA) are used in order to improve the polymerization rate of the adhesive because of the gel effect and the mechanical properties of the adhesive layer formed. Finally, the formed cross-linked layer is not water soluble and the degree of swelling decreases with increasing polymer network density. Bis-GMA shows high reactivity but it has high viscosity and low water solubility. In contrast, TEGDMA and GDMA exhibit low viscosity and better solubility in water (Figure 1.44) [30].

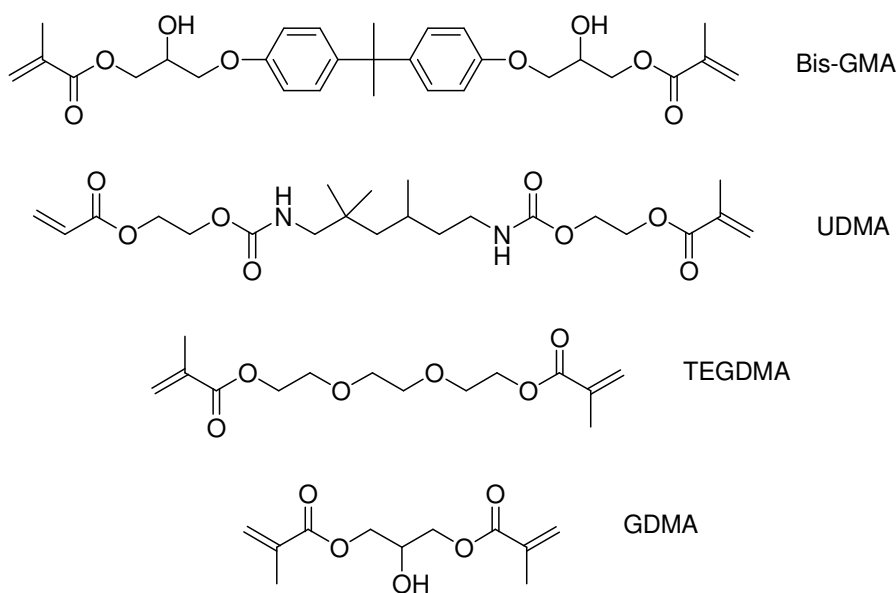


Figure 1.44. Cross-linking dimethacrylates used in dentin adhesives

Unfortunately, all these dimethacrylates are not hydrolytically stable in aqueous acidic solutions and degrade forming the corresponding diols and methacrylic acid. So, new cross-linking bisacrylamides with improved hydrolytical and storage stability were

synthesized (Figure 1.45). The monomer N,N'-diethyl-1,3-bis(acrylamido)-propane (DEBAAP) remained stable in aqueous ethanol in the presence of 20 wt per cent of phosphoric acid after it had been stored at 37 °C for a test period of 4 months whereas GDMA was not stable and methacrylic acid started to build after one day under the same conditions. These bis(acrylamide)s are completely soluble in water and ethanol and show similar reactivity with GDMA. However, bis(methacrylamide)s are less reactive than the corresponding bis(acrylamide)s. Finally, they showed a significantly lower cytotoxicity than commonly used dimethacrylates such as TEGDMA [30].

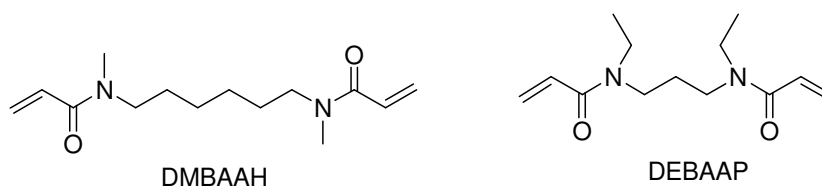


Figure 1.45. Structure of bis(acrylamide)s with improved hydrolytic stability

1.1.4.4. Initiators. As in the case of composite filling materials, adhesives can be photopolymerized or the polymerization can be initiated by a redox initiator system. In visible light curing adhesives, such as the camphorquinone/amine system, visible light causes the camphorquinone to become reactive and amine acts as accelerator of the reaction (Figure 1.46). Whereas, in amine/peroxide system in chemically curing adhesives, amine causes the benzoyl peroxide to become reactive (Figure 1.47) [48, 49].

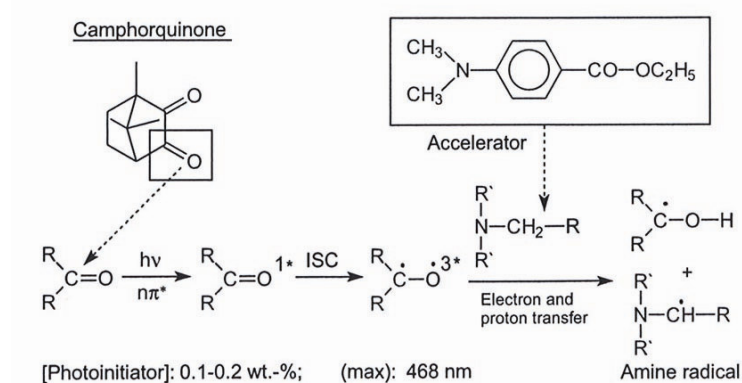


Figure 1.46. Initiator system for the photopolymerization of VIS-light curing adhesives

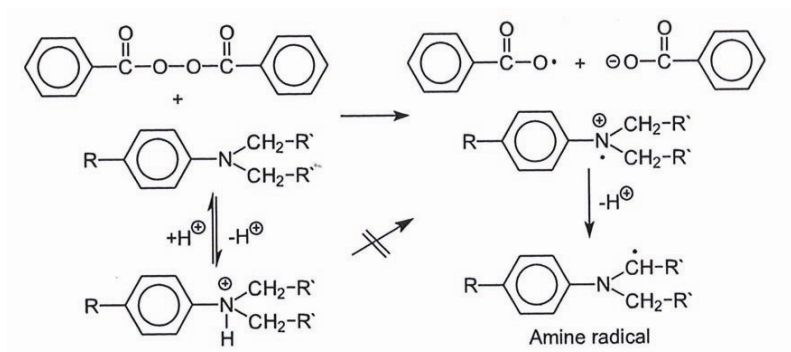


Figure 1.47. Acid-base reaction of an amine/peroxide redox initiator system for radical polymerization

An intrinsic problem of dental adhesives is the acid-base reaction of the acidic monomers with amines used in the initiator systems. In both cases, the concentration of the amine, and therefore, the formed amine radical, which is responsible for the initiation of polymerization decreases.

Acylphosphine oxides were introduced as the new photoinitiators which do not require amine accelerators and absorb light in the wavelength range of 400-500 nm but the carbon-phosphorus bond can be easily cleaved in the presence of nucleophilic compounds such as water or alcohols [13].

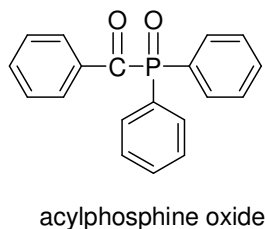


Figure 1.48. Structure of acylphosphine oxide

1.1.4.5. Fillers. Various dental adhesive systems with a significant amount of filler amount are available on the market. Compared to composite filling materials, filler content and composition of dental adhesives play a minor role. Silica, alumina, ceramics, clay minerals, ZrO₂, TiO₂, quartz powder, glass ceramic powder or glass powder etc. are

often used as fillers to increase the mechanical properties [50]. Adhesive systems with fluoroaluminosilicate glass powder continuously release fluoride ions so that an effective reinforcement of the tooth structure and inhibition of secondary caries can be expected [51].

1.1.4.6. Additives. Some manufacturers add different dyes to their adhesive formulations. In two component systems, dyes are used to indicate to the clinician that both components have been properly mixed by featuring a color change. The color is also useful for facilitating the control of homogenous tooth coverage. When the adhesive system is light cured, the colour fades out [13].

During the last years, it was shown that total etch and self etch adhesive systems possess short term inherent antibacterial activity due to their low pH values during the acid etch procedure [52]. But, addition of antibacterial components to the adhesive formulations are manifold to ensure the biological sealing of the restoration as oral bacteria can penetrate through micro gaps in between restoration and tooth generating secondary caries and pulp damage. For many years, glutaraldehyde has been used as a disinfectant, which features antibacterial properties. Due to the fact that glutaraldehyde can not be polymerized into the adhesive matrix, the antibacterial effect persists after polymerization because the molecules are leaching. In contrast, a polymerizable antibacterial monomer 12-methacryloyloxydodecylpyridinium bromide (MDPB) was introduced by Kuraray Company (Figure 1.49). If this monomer is used in the adhesive system, it will provide antibacterial effects before polymerization and polymerized adhesive will have bacteriostatic activity as a contact antimicrobial [53].

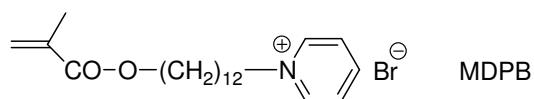


Figure 1.49. A polymerizable antimicrobial agent

1.1.5. Adhesion to and Decalcification of Hydroxyapatite by Acids

In dentistry, acids are generally applied to teeth for two reasons. Some acids adhere or bind to human calcified tissues, while some are used to demineralize the hydroxyapatite (HAP) for the development of a roughened tooth surface. So, it is important to clarify why certain acids adhere to while others decalcify HAP. Yoshida et al. explained the phenomena of adhesion and decalcification resulting from carboxylic acids interacting with hydroxyapatite by an “Adhesion-Decalcification Concept” as shown schematically in Figure 1.50. In the first phase, carboxyl groups of the acids form ionic bonds to calcium at the HAP surface. This step may largely be determined by the pKa of the acids. At the same time, PO_4^{-3} and OH^- are extracted by H_3O^+ from the HAP surface and brought into solution. In the second phase, the acids investigated either remained attached to the HAP surface, with only a limited decalcification step, or debonded with a significant decalcification effect [54]. It was shown that, carboxylic acids, regardless of concentration or pH, either adhere to or decalcify hydroxyapatite, depending on the dissolution rate of the respective calcium salts in the acid solution. The less soluble the calcium salt of the acidic molecule, the more intense and stable the molecular adhesion to a hydroxyapatite-based substrate.

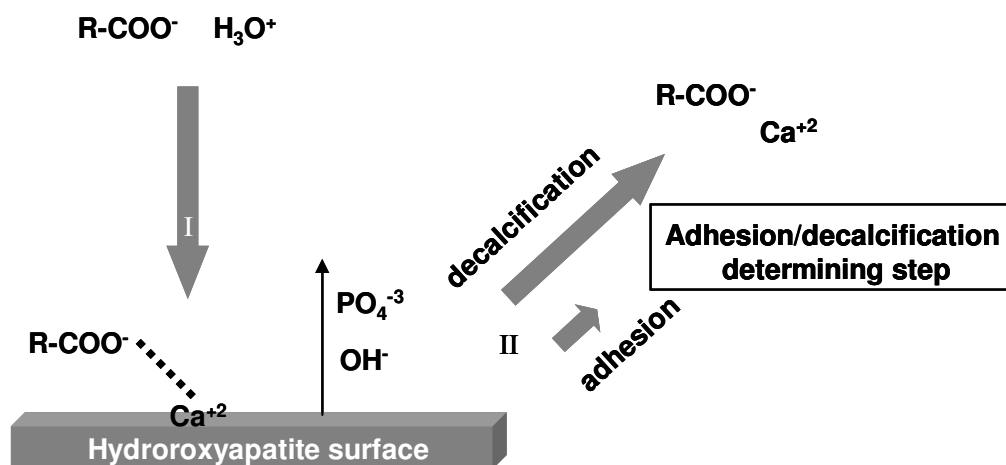


Figure 1.50. Schematic presentation of the adhesion/decalcification concept

Yoshida *et al.* characterized the adhesive interaction of 3 functional monomers, MDP, 4-MET and MEP-P (see Figures 1.7 and 1.38), with synthetic hydroxyapatite, using x-ray photoelectron spectroscopy and atomic absorption spectroscopy (AAS) [55]. It was stated that, MDP has a high chemical bonding potential to hydroxyapatite within a clinically reasonable application time. The chemical bonding capacity of 4-MET is weaker and it is doubtful that 4-MET within a short application time, is capable of chemically bonding to hydroxyapatite. The chemical bonding efficacy of MEP-P is the lowest among the 3 functional monomers investigated. In accordance to the adhesion-decalcification concept (AD), AAS results showed that calcium salt of MDP was hardly soluble, the calcium salt of 4-MET could be dissolved more easily, whereas MEP-P was very soluble in water. These data conform the higher and more stable bonding performance of MDP with respect to that of 4-MET.

Nishiyama *et al.* examined the amount of decalcification of the hydroxyapatite or dentin in NMGLY (see Figure 1.38) as a self-etching primer. The addition of teeth components to the NMGLY solution resulted in a shift of the carbonyl carbon peak of the carboxylic acid which is at 173.60 ppm to a lower field (to 174.46 ppm in the presence of hydroxyapatite and to 174.72 ppm in the presence of dentin) (Table 1.6). This shift was attributed to the formation of an acid-base interaction between the carboxylic acid of NMGLY and the calcium in the tooth component. The amount of decalcification (R) of the hydroxyapatite and dentin by the carboxylic acid in the NMGLY was determined by dividing the shift difference of the carbonyl carbon peak obtained in the presence of hydroxyapatite and dentin (0.86 ppm and 1.12 ppm respectively) by the shift difference of the carbonyl carbon peak attributed to the completely undissociated and dissociated carboxylic acid in the NMGLY (3.20 ppm) (Figure 1.51). The observed higher degree of demineralization of the dentin compared to hydroxyapatite was due to the differences in the crystallinity of the calcium phosphates within the hydroxyapatite and dentin [56].

Table 1.6. The chemical shift of the carbonyl carbon peak of the carboxylic acid in the NMGLY, in the absence and in the presence of teeth components and the amount of decalcification

Self-etching primer		Control		Addition of teeth components					
				Hydroxyapatite			Dentin		
Primer	pKa	pH	Cs	pH	Cs	R (%)	pH	Cs	R (%)
NMGLY	3.5	1.87	173.60	2.98	174.46	27.0	3.30	174.72	35.1

Control: No addition of teeth components.

Cs: Chemical shift of the carbonyl carbon of the carboxylic acid.

R: Ratio of the interacted carboxylic acid with calcium.

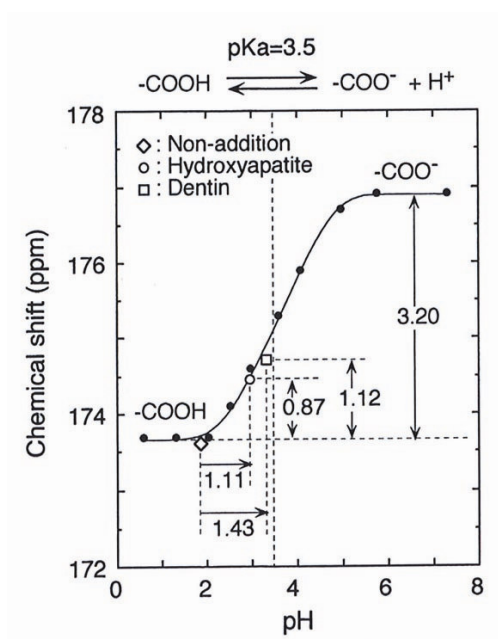


Figure 1.51. The pH dependencies of the chemical shift of the carbonyl carbon peak attributed to the carboxylic acid in the NMGLY

1.1.6. Bonding Effectiveness

It was demonstrated in the literature that acid etchant causes selective demineralization of the hydroxyapatite by removing the smear layer and expose the

collagen tubules, leading to the development of a roughened surface. The surface changes greatly, becoming chalky, due to development of microporosity within the surface. The achievement of the bond between bonding resin and dentin depends on the penetration of the bonding resin into the microporosities of the conditioned dentine surface in order to create a micro-mechanical interlocking between the dentinal collagen and resin to form a hybrid layer [57]. So the extent and the depth of the etching pattern as well as the ionic, covalent or physical interactions between the dentin and the resin should influence the bonding performance of an adhesive.

Strong self-etch adhesives ($\text{pH} < 1$), like etch and rinse adhesives, completely remove smear layer from dentin. Dentinal tubules were opened and devoid of smear plugs. In applying a bonding agent to the dentin surface, several micrometers thick, relatively deep resin-dentin hybrid zone is formed. However, as mild self-etch adhesives (pH around 2 or more) can only partially demineralize the dentin surface, the etching pattern was not deep enough to obtain good penetration of bonding resin and therefore adhesion of the bonding agent is obtained micro-mechanically through shallow hybridization [58].

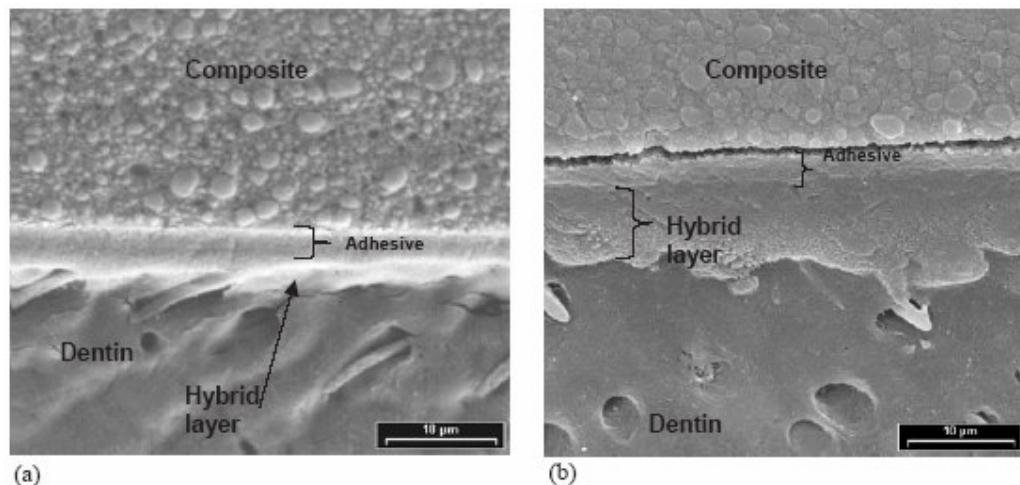


Figure 1.52. a) SEM image of a self-etching sample showing a thin hybrid layer and b) SEM image of an etch and rinse sample showing a thick hybrid layer

Nishiyama *et al.* proposed an adhesion mechanism of the resin to the acid-etched dentin treated with NMGLY primer. The application of the primer facilitated the restoration of the dentinal collagen which had collapsed during the air-drying process. Further, the amide group and/or the carboxylic acid group in the NMGLY molecule hydrogen bonded with the dentinal collagen (Figure 1.53). Since the interaction of the NMGLY molecule promoted the hybridization of the resin to the dentinal collagen molecule at the interface, it enhanced the bonding of the resin to the dentinal collagen fiber and provided a noticeably higher bond strength [59, 60, 61].

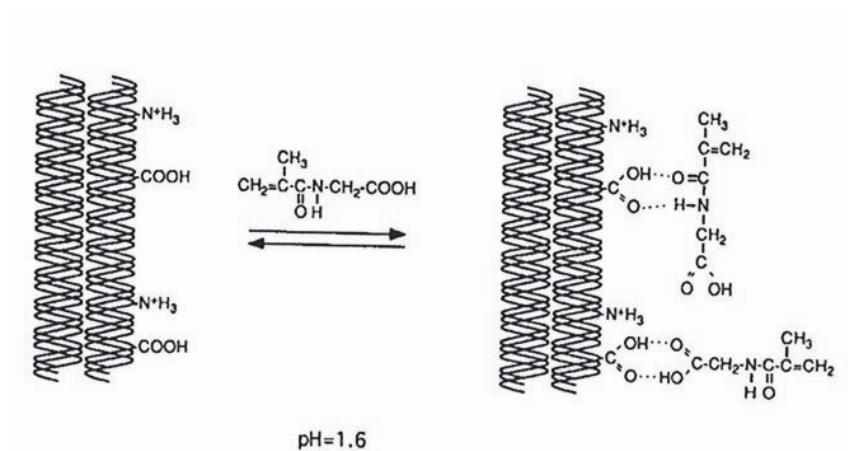


Figure 1.53. Model of hydrogen bonding between NMGLY and dentinal collagen

The application of NMGLY to both the enamel and dentin resulted in an increase in the bond strength of the resin. However, the bond strength to the enamel was only 16 MPa, whereas, the bond strength to dentin was 23.6 MPa. This difference was probably due to different composition of the two tooth substrates that favored different enamel and dentin adhesion mechanisms. Enamel is composed of hydroxyapatite (97 per cent), water (two per cent) and organic component (one per cent). Dentine contains much more organic material (20 per cent) and water (11 per cent). It was stated that, the principle adhesion mechanism of resin to enamel is of a micro-mechanical interlocking type. But for dentin adhesion, the formation of hydrogen bonding interactions between the dentinal collagen and the primer enhanced the bonding of the resin as well as the micro-mechanical interlocking between the dentinal collagen and resin [56, 62, 63].

1.1.7. Effect of Smear Layer on Bonding

Mild self-etch adhesives demineralize dentin only partially, leaving hydroxyapatite around collagen within a hybrid layer. Since hydroxyapatite remains available for interaction, it was hypothesized that this residual hydroxyapatite may serve as a receptor for chemical interaction with the functional monomer and subsequently, contribute to adhesive performance in addition to micro-mechanical hybridization.

Tay and Pashley, compared the tensile bond strengths (TBS) of the three commercially used self-etching adhesives with varying aggressiveness with the tensile bond strength of the etch and rinse control group. The results showed that, tensile bond strengths of the three experimental groups on enamel were lower than the control group, but not very different from one another. On the other hand, when enamel was etched only with the self-etching adhesives but the bonding resins were replaced with the control adhesive after etching, tensile bond strengths of NCR/Prime&Bond NT and Prompt L-Pop were not very different from that of the control group [64].

Table 1.7. Enamel tensile bond strengths of the self-etching adhesives and the etch and rinse control group

Group	Agressiveness	TBS ^a (MPa)	TBS ^b (MPa)
Clearfill Mega Bond	mild-self-etching	11.6	20.6
NCR/Prime&Bond NT	moderate-self-etching	10.3	27.4
Prompt L-Pop	agressive-self-etching	13.9	25.9
32 % H ₃ PO ₄ /All-Bond 2 (control adhesive)	etch and rinse	27.0	27.0

^aTBS of the self-etching adhesives as well as the control group

^b TBS of enamel that were etched only with the self-etching adhesives but the resins were replaced with the All-Bond 2 primers and resins

Koibuchi *et al.* investigated the effect of retained smear layer on bonding to human dentin in determining the feasibility for clinical use of a self-etching primer. They

showed that bonding results are directly related to the manner of smear preparation. A smooth smear layer which was prepared with #600 abrasive paper yielded a tensile bond strength of 28.5 MPa whereas a coarse smear layer which was prepared with #180 abrasive paper yielded a bond strength of 10.0 MPa only. It was concluded that it might be better to remove the “course” smear layers in order to achieve a stable dentin adhesion [65].

Oliveira *et al.* determined the effect of dentin smear layers created by various abrasives on the adhesion of a self-etching primer (SE) and etch and rinse (SB) bonding systems [66]. For the SB system, the shear bond strength was not sensitive to the method used to prepare the smear layer as it was removed completely during acid-etching (Figure 1.54). This was not true for the SE system that the method used to prepare the smear layer affects the bond strength of this system. However, the shear bond strength was lower when SB was used than SE. This challenges the general consensus that it is necessary to remove the smear layer in order to achieve a high bond strength. But they stated that, self-etching primers should be used in vivo with a surface preparation method that creates a thin smear layer (Table 1.8).

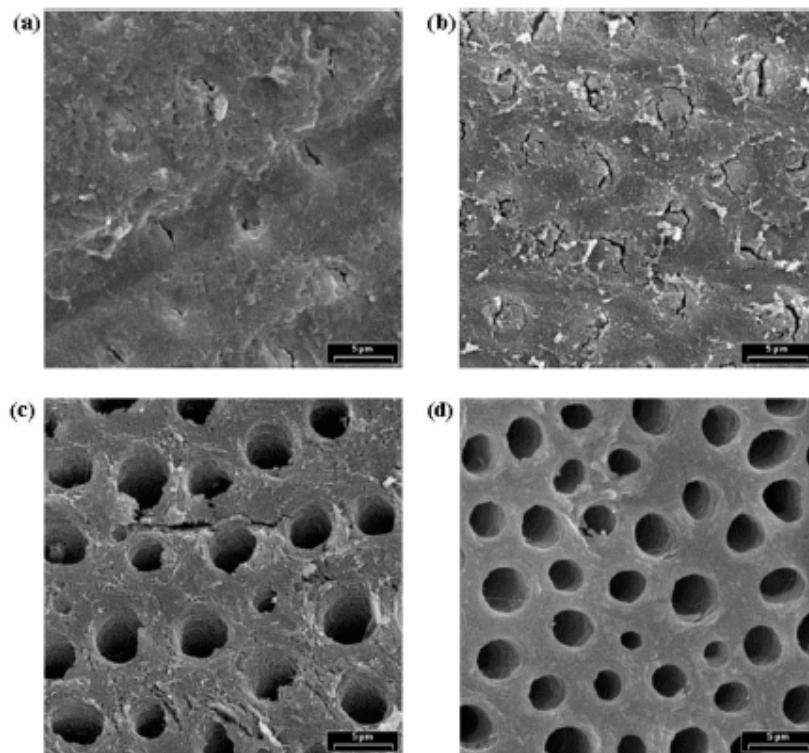


Figure 1.54. Smear layer samples etched with (a) Clearfil SE primer, and different concentrations of phosphoric acid (b) 0.13 % phosphoric acid (pH=2, similar to SE primer) (c) 20 % phosphoric acid (pH=0.21) (d) 35 % phosphoric acid (pH=-0.28)

Table 1.8. Abrasive and adhesive influence on shear bond strength

Adhesive System	Composition	Abrasive paper used	Shear Bond Strength (MPa)
SB (Single bond) Etch and Rinse	35 % phosphoric acid, Bisphenol A diglycidyl ether dimethacrylate, HEMA, dimethacrylate, solvent, water	#600 grit	25.4
		#240 grit	22.4
SE (Clearfil SE bond) Self-etch	<u>Primer</u> 10-MDP, HEMA, hydrophilic dimethacrylate, water...	#600 grit	42.0
	<u>Adhesive</u> 10-MDP, Bis-GMA, HEMA, hydrophilic dimethacrylate...	#240 grit	35.7

Several papers on bonding effectiveness of self-etch adhesives compared to etch-and-rinse adhesives have been submitted. As can be seen from the previous examples, no consensus exists upon the use of self-etch adhesives instead of etch and rinse ones.

1.1.8. Effect of Smear Layer on Fluid Movement Across Dentin

The finding that the self-etching primer did not totally remove the smear layer or open all the tubules may be important from the clinical standpoint. Pashley at al. showed that, fluid flow across dentin bonded with self-etching adhesive systems was lower than that of total-etch adhesives. Because, the smear layer provides a sealing cap for the dentinal tubule, removing this barrier would produce an outward dentinal fluid movement from the pulp toward the dentin surface which could interfere with dentin adhesion and dilute the adhesive agents. Also, this fluid flow causes adjacent nerve fibers to be stimulated resulting a post-operative pain [67].

1.2. Alkyl α -Hydroxymethyl Acrylates (RHMA)s

Acrylates and methacrylates possess a number of attractive properties for commercial and academic applications. They are readily available and inexpensive. A wide variety of derivatives can be obtained through several synthetic methods. The polymers possess good thermal and photochemical resistance along with excellent hardness and clarity. These combine to make them suitable for coatings, optical devices and medical/dental applications [68].

The reactivities of acrylic monomers depend on the polar, resonance and steric effects of the substituents. For example, acrylate monomers having α -alkyl substituents greater than methyl (first and second monomers in Figure 1.55) show poor or no polymerizability under free radical polymerization conditions due to steric effects. However, substitution of an oxygen atom β to the double bond (monomer **3** in Figure 1.55) increases the reactivity of these monomers to the point of totally overcoming steric effects [69, 70].

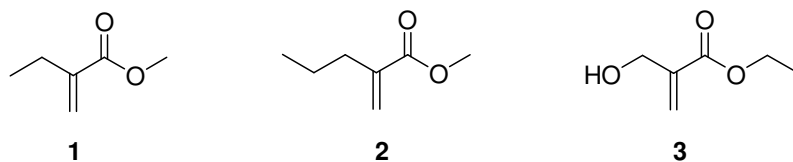


Figure 1.55 Examples of α -alkyl acrylates (1 and 2) which give low molecular weight polymers and ethyl α -hydroxymethyl acrylate (3) which gives high molecular weight polymer

1.2.1. Synthesis of RHMA Monomers

Several groups have been exploring the chemistry of 1,1-disubstituted vinyl monomers based on esters of α -hydroxymethyl acrylate. General procedures have been published for the synthesis of alkyl α -hydroxymethyl acrylates (RHMA)s via Baylis-Hilman reaction, involving the 1,4-diazobicyclo [2.2.2] octane (DABCO) catalyzed

insertion of paraformaldehyde at the α -position of acrylic esters to produce alkyl α -hydroxymethyl acrylates [71] (Figure 1.56).

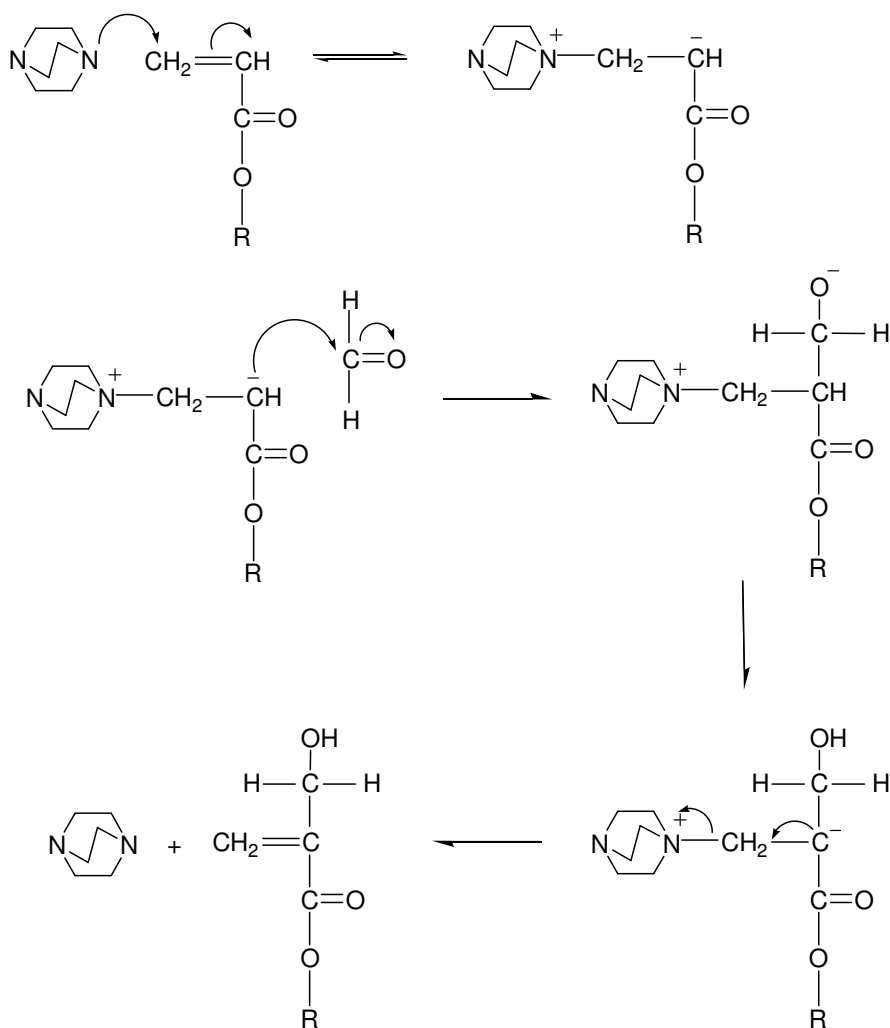


Figure 1.56. DABCO catalyzed synthesis of RHMA monomers

However, it should be mentioned that the Baylis-Hilman reaction has considerable shortcomings such as low reaction yields and long reaction time. Efforts to accelerate the reaction include low temperature techniques, variation of Lewis base catalysts such as DABCO, DMAP, 1,8-diazobicyclo[5.4.0]undec-7-ene (DBU), PPh_3 , PBu_3 or PPh_2Me and Lewis acid catalysts such as $\text{La}(\text{OTf})$ or LiClO_4 , solvents, the use of high pressure or microwave technique [72]. For example, addition of methyl acrylate to propionaldehyde required 10 days to reach 84 per cent completion at room temperature in dichloromethane

in the presence of DABCO (entry one in Table 1.9) [73]. Yu *et al.* developed a practical set of conditions using a base catalyst (DABCO) and an aqueous medium (1:1 mixture of 1,4-dioxane and water) to overcome the problems associated with the Baylis-Hilman reaction. They stated that selection of the environmentally friendly water as a solvent was critical for achieving the fast rate of reaction and the high yield of the product as water could stabilize the charged transition states and intermediates through intermolecular charge-dipole interactions as well as hydrogen-bonding interactions (entry two in Table 1.9) [71]. Aggarwal *et al.* used formamide in the presence of Yb(OTf)₃ and achieved a rate acceleration. When compared to water, formamide has higher dielectric constant and therefore can stabilize the charged intermediate better without the possibility of ester hydrolysis. It also coordinates to Yb(OTf)₃, which results in even more polarized NH bonds leading to increased hydrogen bond donor ability and therefore increased rates (entry three in Table 1.9) [74]. In their another work, with the help of triethanolamine, the Lewis acid and Lewis base could promote the reaction without interference from each other as the lanthanide no longer associates with DABCO and prefers oxygen-rich triethanolamine (entry four in Table 1.9) [75]. Yang *et al.* used camphor-derived chiral ligand with La(OTf)₃ in order to have high enantioselectivity (entry five in Table 1.9) [76]. Pereira *et al.* and He *et al.* used derivatives of trialkylphosphine organocatalyst for the Baylis-Hilman reaction as the nucleophilicity of trialkylphosphines is the strongest among their amine analogues. However, trialkylphosphines are air-sensitive. So, they used ferrocenyldialkyl phosphine and 1,3,5-triaza-7-phosphaadamantane derivatives as they have increased air stability (entries six and seven in Table 1.9) [77, 78]. Caumul and Hailes performed Baylis Hilman reaction under aqueous acidic conditions at pH one, where protonation of the acrylate and aldehyde moieties enhanced the reaction (entry eight in Table 1.9) [79]. Among them we used the conditions of entry 11 in order to synthesize ethyl or tert-butyl α -hydroxymethyl acrylate [80].

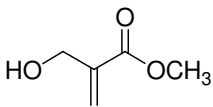
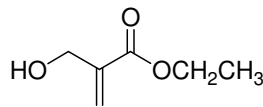
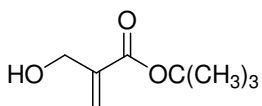
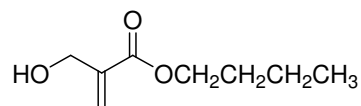
Table 1.9. Different reaction conditions for Baylis-Hillman reaction

	Aldehyde	Acrylate	Catalyst	Solvent	Time	Temp.	Yield
1	propionaldehyde	methylacrylate	DABCO	CH ₂ Cl ₂	10 d	rt	84 %
2	p-nitrobenzaldehyde	methylacrylate	DABCO	1,4-dioxane-water (1:1)	3 h	rt	83 %
3	benzaldehyde	methylacrylate	3-hydroxyquinuclidine + Yb(OTf) ₃	formamide	6 h	rt	74 %
4	p-nitrobenzaldehyde	methylacrylate	DABCO + La(OTf) ₃ + triethanolamine	-	3 h	rt	90 %
5	benzaldehyde	methylacrylate	DABCO + ligand.La(OTf) ₃ complex	CH ₃ CN	10 h	rt	75 %
6	p-nitrobenzaldehyde	benzylacrylate	Ferrocenyldialkyl phosphines	THF	1 h	rt	98 %
7	p-nitrobenzaldehyde	ethylacrylate	1,3,5-triaza-7-phosphaadamantane	-	5 h	rt	91 %
8	2-nitrobenzaldehyde	methylacrylate	Me ₃ N	H ₂ O, pH=1	72 h	0 °C	74 %
9	benzaldehyde	methylacrylate	DABCO	CH ₃ CN	48 h	rt	62 %
10	p-nitrobenzaldehyde	methylacrylate	trimethylamine	H ₂ O	5 h	60 °C	56 %
11	formaldehyde	ethylacrylate	DABCO	DMSO-water (3:1)	0.5 h	100 °C	50 %

1.2.2. Physical and Chemical Properties of RHMA Monomers and Polymers

Table 1.10 summarizes the four RHMA monomers with some indication of their physical and chemical properties [81].

Table 1.10. Structures and properties of four RHMA monomers

<div style="text-align: center;">  <p>MHMA</p> </div> <p>Organic and water soluble Fast polymerization Excellent copolymerization Superb physical properties BUT Vesicant, possibly toxic</p>	<div style="text-align: center;">  <p>EHMA</p> </div> <p>Organic soluble Low water solubility Good polymerizability Good physical properties AND No sign of irritancy or toxicity</p>
<div style="text-align: center;">  <p>TBHMA</p> </div> <p>Organic soluble Good polymerizability Good physical properties AND No sign of irritancy or toxicity</p>	<div style="text-align: center;">  <p>BHMA</p> </div> <p>Organic soluble Good polymerizability Good physical properties AND No sign of irritancy or toxicity</p>

RHMA monomers can polymerize in the two following ways, giving rise to polymers with properties depending on the type of polymerization [82]:

1. RHMA polymers synthesized by radical polymerization:

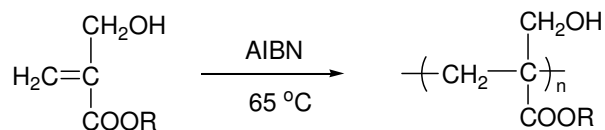
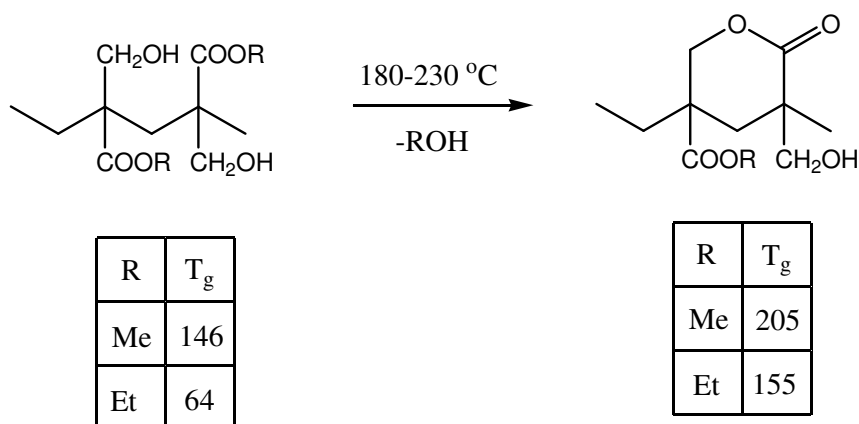


Figure 1.57. Radical polymerization of RHMA monomers

- Lactone cyclization: RHMA polymers can undergo lactone cyclization by heat. In consequence, glass transition temperature (T_g) and heat resistance of the polymers increase (Figure 1.58) [82, 83].

Figure 1.58. Rise in T_g by lactone cyclization

- Thermal decomposition temperature: RHMA polymers have a thermal decomposition temperature higher than that of the (meth)acrylic-based polymers (Table 1.11) [82].

Table 1.11. Decomposition temperatures of homopolymers

Homopolymers	EHMA	BHMA	HEMA	MMA
Air	340 °C	350 °C	240 °C	300 °C >

- Adhesion: RHMA polymers have excellent adhesion with glass, steel plate, copper plate and aluminum plate.
- Surface hardness: A film having a surface hardness can be obtained by UV-hardening of the RHMA so it is useful as a row material for photosensitive resins.
- Optical characteristics: A homopolymer of the RHMA has excellent transparency and thus used as a lens material.
- Water absorbing ability: The MHMA and EHMA polymers are surprisingly resistant to solvation and swelling by water.

Table 1.12. Per cent water absorption of homopolymers

Water absorption				
Homopolymers	MHMA	EHMA	HEMA	MMA
Percentage	11	10	46	0.1

- Chelate capacity: A water soluble polymer having excellent chelate capacity can be obtained by the hydrolysis of a RHMA polymer, turning it into polyhydroxypolycarboxylic acid (Figure 1.59) [82].

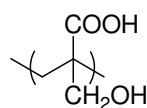


Figure 1.59. Polyhydroxypolycarboxylic acid

- Affinity to cellulose: The RHMA monomers can be easily impregnated into wood due to the affinity of the methylol group to the hydroxyl group of cellulose and can polymerize inside. This treatment increases the water resistance and dimensional stability of wood [68].

2. RHMA polymers synthesized by condensation polymerization.

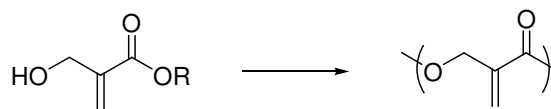


Figure 1.60. Synthesis of an unsaturated polyester

- Thermosetting property: Condensation polymerization of RHMA monomers gives unsaturated polyesters having excellent thermosetting properties.

Mathias and Küsefoğlu prepared a low molecular weight copolyesters in a one step synthesis by reacting bromoacetic acid with 2-(bromomethyl)acrylic acid and triethylamine in diethyl ether (Figure 1.61). 2-(Bromomethyl)acrylic acid is more reactive than the haloacetic acids leading to higher copolymer incorporation. Unsaturation in the copolymers provided a site for crosslinking with vinyl monomers such as styrene and methyl methacrylate [84].

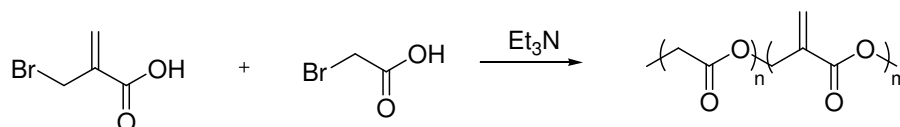


Figure 1.61. Synthesis of an unsaturated copolyester

1.2.3. Derivatives of RHMA Monomers

Monomers based on alkyl α -hydroxymethyl acrylate offer great versatility for obtaining functionalized monomers and polymers [85]. Reaction of the hydroxymethyl group using SOCl_2 and PBr_3 gives excellent yields of reactive allyl halides capable of conversion to a variety of derivatives through nucleophilic displacement [70, 86, 87, 88, 89] (Figure 1.62).

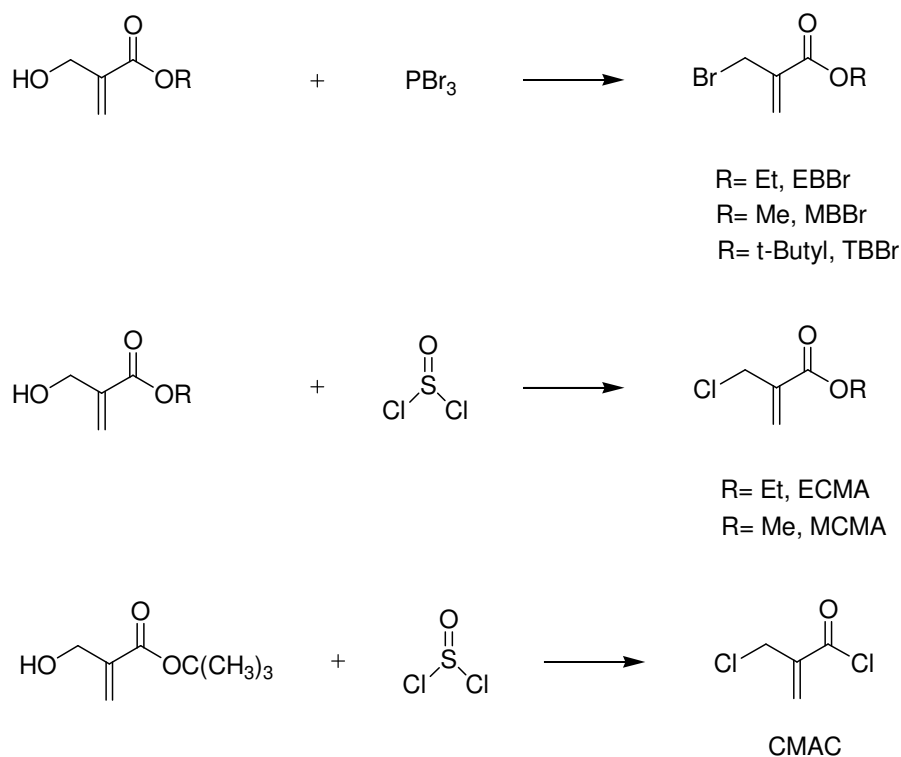


Figure 1.62. Synthesis of reactive intermediates from RHMA

For example, TBHMA when reacted with PBr_3 gives tert-butyl α -bromomethyl acrylate (TBBr) which contains a reactive bromomethyl group as well as a cleavable tert-butyl group [70]. Also, TBHMA can be reacted with SOCl_2 to obtain an intermediate α -chloromethyl acryloyl chloride (CMAC), which contains reactive acid chloride and allyl chloride groups. Therefore, CMAC allows incorporation of identical ester and ether groups or mixed ester and ether groups [86].

Among the α -(halomethyl) acrylates, as the size of the halogen atom increases homopolymerizability decreases as shown in Table 1.13 [90]. Difficulty in homopolymerization of α -(bromomethyl) acrylates (MBBr and EBBr) was explained by steric hinderence and fast addition-fragmentation. It was found that the polymerization of methyl methacrylate in the presence of methyl (or ethyl) α -(bromomethyl) acrylate resulted in a considerable reduction in molecular weight of the consequent polymer due to the addition-fragmentation of MBBr (or EBBr) (Figure 1.63). Addition-fragmentation consists of addition of a propagating radical to the double bond of the α -(bromomethyl) acrylate

and a fast β -fragmentation of the resulting radical followed by reinitiation by the expelled radical [91, 92].

Table 1.13. Homopolymerization of ethyl α -(halomethyl) acrylates
($\text{CH}_2=\text{C}(\text{CH}_2\text{Y})\text{COOEt}$) at 50 °C

Y	[M]	[AVN]	Time	Conversion	M_n
Br	6.25	4.4	40	0	-
Cl	6.51	4.4	14	9.5	9,700
F	7.24	14	1.7	52.4	26,000
I	4.86	6.4	24	0	-

AVN, 2,2-azobis-2,4-dimethylvaleronitrile

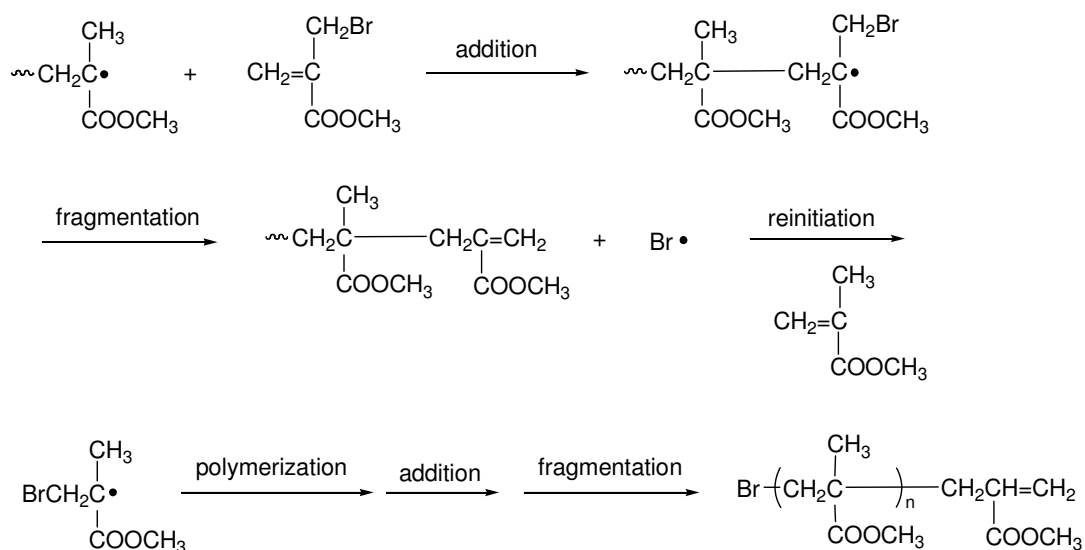


Figure 1.63. The addition-fragmentation of methyl α -(bromomethyl) acrylate in methyl methacrylate polymerization

Polymerization of MCMA also involved addition-fragmentation. As this monomer can give a homopolymer, propagation and fragmentation occur simultaneously. It was observed that, polymerization of ECMA at elevated temperatures yielded low molecular weight polymers however, spontaneous low temperature bulk polymerization gave high

molecular weight polymers due to the fact that fragmentation was facilitated more than propagation by raising the temperature [93, 94].

1.2.3.1 Ether Derivatives of RHMA. Jariwala and Mathias studied the synthesis and polymerization of fluoroalkyl containing monomers based on CMAC [86]. Since preferential substitution at the acid chloride group was desired, alcohol was first reacted with the acid chloride group to give the corresponding esters. The second step involved the substitution of the allylic chloride by the alcohol group (Figure 1.64).

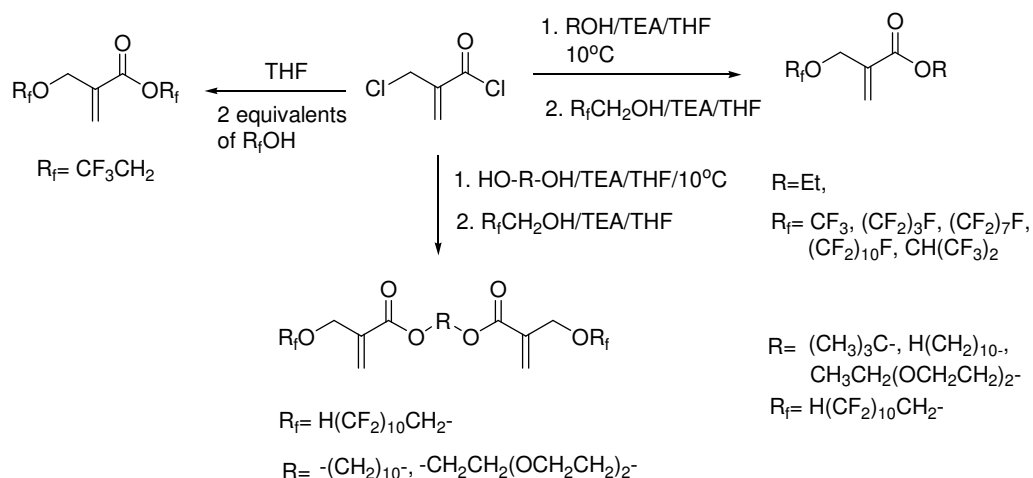
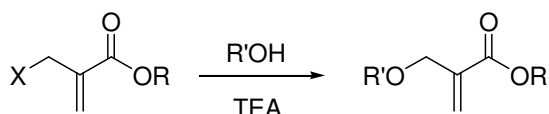


Figure 1.64. Synthesis of fluoroalkyl containing monomers based on CMAC

Homopolymerization of monofunctional monomers with substitution in the α -methyl position by large fluoroalkyl ether groups gave high conversions and high molecular weight polymers. However, polymerization of monomers containing larger alkyl ester groups gave low molecular weight polymers possibly due to a greater sterically induced decrease in propagation rate. Cross-linked polymers were obtained from bulk polymerization of the difunctional monomers.

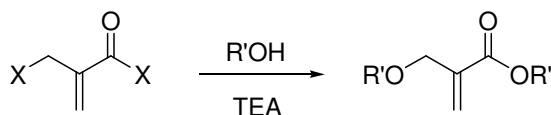
Thompson *et al.* also synthesized various ether derivatives of RHMA monomers using ECMA, EBBR, TBBR and CMAC (Figure 1.65) [70]. Of the ethyl ester monomers synthesized, methyl, ethyl and benzyl ethers polymerized relatively rapidly, giving high conversions in short times. Morpholine and pyrrolidinone derivatives as well as tert-butyl

ester derivative gave polymers with intrinsic viscosity lower for the higher polymerization temperature. This indicated a low polymerization ceiling temperature. Of the symmetrically-substituted monomers from CMAC, the effect of larger substituents was demonstrated by the lower molecular weight. It was stated that, in comparison to α -(n-alkyl)-substituted acrylic monomers, these monomers polymerize well indicating that the ether oxygen might be helping to overcome the combined electronic and steric effects of the alkyl side chains. Also, electronic factors due to the β -functional group showed to play a role in enhancing monomer reactivities even to the extent of overcoming steric inhibition in the propagation step and in reducing chain transfer processes in the polymerization.



X= Br or Cl; R= Et; R'= Me, Benzyl, Propionitrile, N-(2-Hydroxyethyl)pyrrolidinone, N-(2-Hydroxyethyl)morpholine, N-(2-Hydroxyethyl)phthalimide

X= Br; R= t-Butyl; R'= Me



X= Cl; R'= Benzyl, Stearyl, 2-Phenoxyethyl

Figure 1.65. Synthetic scheme for the synthesis of ether derivatives

Yamada and Kobatake summarized the results for the polymerization of some methyl α -(alkoxymethyl) acrylates and alkyl α -(fluoroalkoxymethyl) acrylates (Table 1.14) [90].

Table 1.14. Polymerization of methyl α -(alkoxymethyl) acrylates in benzene and alkyl α -(fluoroalkoxymethyl) acrylates in dioxane at 60 °C: $[M]= 2.0 \text{ mol l}^{-1}$, $[AIBN]= 5.0 \text{ mmol/l}$

Monomer	$R_p \cdot 10^5$ ($\text{mol l}^{-1} \cdot \text{s}^{-1}$)	$M_n \cdot 10^{-4}$ (GPC)
MC ₁ MA	13.6	6.1
MC ₂ MA	9.4	4.2
MC ₃ MA	8.3	3.7
MC ₄ MA	5.6	3.3
M(EO) ₁ MA	15.9	2.6
M(EO) ₂ MA	12.4	2.9
M(EO) ₃ MA	7.5	1.0
DC ₂ F ₃ MA	7.6	5.1
DC ₃ F ₄ MA	5.4	2.0
MC ₂ F ₃ MA	9.2	11.0
MC ₃ F ₄ MA	10.1	6.3
MC ₉ F ₁₆ MA	13.2	3.9
Methyl methacrylate	4.6	9.6

MC_nMA: $\text{CH}_2=\text{C}(\text{CH}_2\text{OC}_n\text{H}_{2n+1})\text{COOCH}_3$,

M(OE)_nMA: $\text{CH}_2=\text{C}[\text{CH}_2\text{O}(\text{CH}_2\text{CH}_2\text{O})_n\text{CH}_3]-\text{COOCH}_3$,

DCFMA: $\text{CH}_2=\text{C}(\text{CH}_2\text{ORf})\text{COORf}$ (see Figure 1.63)

MCFMA: $\text{CH}_2=\text{C}(\text{CH}_2\text{ORf})\text{COOCH}_3$,

C₂F₃: CH_2CF_3 , C₃F₄: $\text{CH}_2\text{CF}_2\text{CF}_2\text{H}$, C₉F₁₆: $\text{CH}_2(\text{CF}_2)_8\text{H}$.

Mathias *et al.* synthesized difunctional acrylate crosslinking agents. Figure 1.66 shows the reaction of EHMA with bisglycidyl ether of bisphenol-A. The reaction product is used in impregnation of wood to give wood-polymer composites [95].

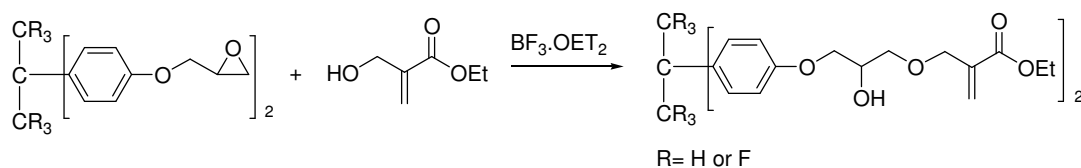


Figure 1.66. Synthesis of difunctional acrylate crosslinking agents

Also, ECMA was reacted with bisphenol-A (BPA) in the presence of base to give the ether compound as shown in Figure 1.67. Application of this procedure to the hexafluoro-derivative of BPA gave a product with thermal stability and surface properties [95].

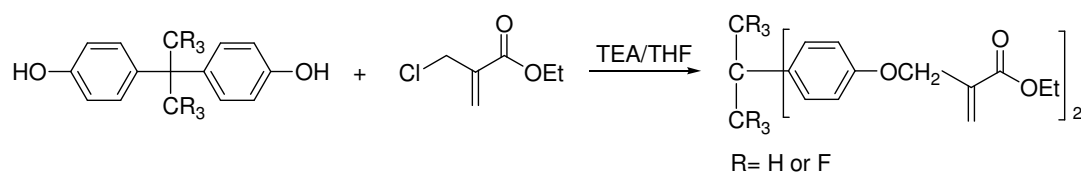


Figure 1.67. Synthesis of difunctional acrylate crosslinking agents

Two hydroxyl-containing dimethacrylate monomers were synthesized from the reaction of MCMA and ECMA with glycerol. It was observed that these monomers polymerized faster and to higher conversion than the trimethacrylate monomers (Figure 1.68). Actually, ECMA-glycerol trimethacrylate was expected to have higher rates of polymerization than the dimethacrylate monomers as when monomer functionality increases, the rate of polymerization increases while the conversion decreases. But the higher rates of polymerizations for hydroxyl-containing dimethacrylate monomers explained in terms of their hydrogen bonding capability which could bring the double bonds close to each other and enhanced the rate of polymerization [96].

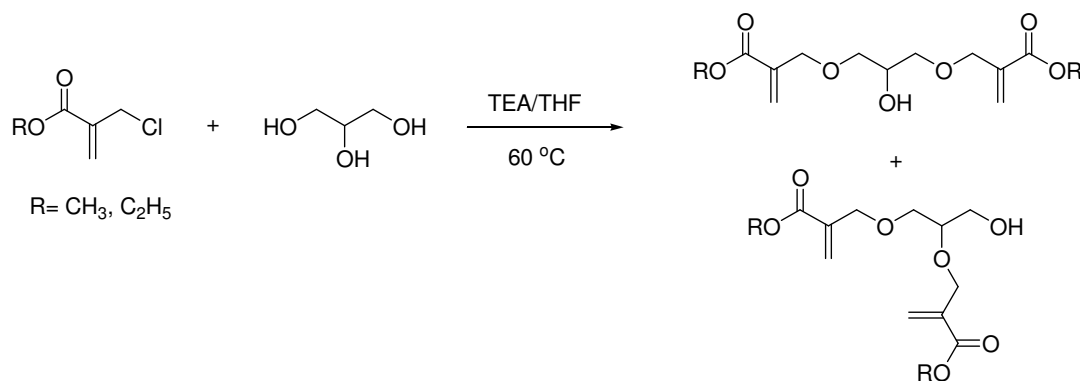


Figure 1.68. Synthesis of hydroxyl-containing dimethacrylate monomers

1.2.3.2. Ester Derivatives of RHMA. Two routes were used for the synthesis of ester derivatives of EHMA. The first involved the reaction of alcohol group of EHMA with acid chlorides with or without added base (pyridine or triethylamine). The second involved the reaction of ECMA with sodium salts of a variety of organic acids in the presence of Aliquat 336, a quaternary ammonium chloride phase transfer catalyst (Figure 1.69). The phase transfer procedure is especially useful resulting in high yields of easily purified products [89].

Bulk polymerizations of the ester derivatives with AIBN gave high molecular weight polymers (112,000-708,000) in comparison to ether derivatives (<100,000). For example, tert-butyl α -alkyloxymethylacrylates did not give high molecular weight polymers whereas tert-butyl α -acetoxyethyl acrylate gave a molecular weight of 255,000. So, the electronic effect of the ester group is clearly important in facilitating polymerization. Comparison of ethyl α -acetoacetoxyethyl acrylate with methyl methacrylate showed that the k_p for this monomer was 82 per cent that of MMA while k_t was only five per cent of the MMA value [89].

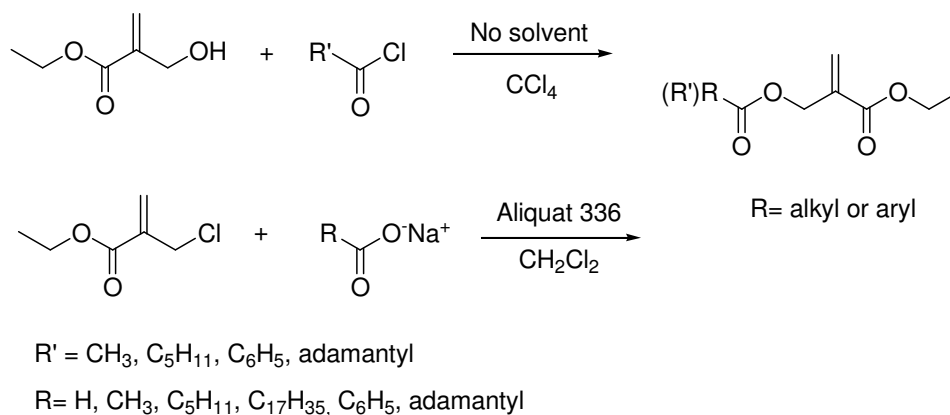


Figure 1.69. General synthetic schemes for the synthesis of ester derivatives of EHMA

Photopolymerization of the various ester derivatives of EHMA showed higher rates of polymerization for benzoate derivatives compared to alkyl ester derivatives (Figure 1.70). For example, rate of polymerization of 3,4,5-trimethoxybenzoate was ten times greater than the alkyl ester monomers and eight times greater than MMA. But, it was not clear how the electronic nature of the substituents effects polymerizability of the monomers and why the aryl ester monomer is more reactive. The presence of the aromatic ring may be the answer of the reactivity, although benzoate derivative is also more reactive than aryl containing ether derivatives, such as methyl α -benzoyloxymethylacrylate [69, 88].

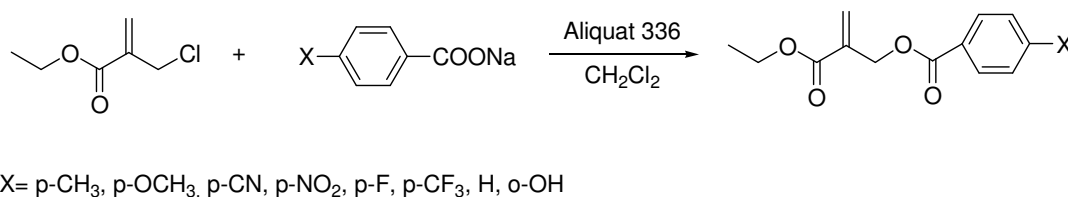


Figure 1.70. General scheme for synthesis of benzoate ester monomers

The reactivity of the benzoate ester was compared to other α -(substituted)-methyl acrylates. Based on their k_p and k_t values obtained from solution polymerization data, benzoate ester is more reactive than itaconates, and the ester and ether derivatives of both ethyl α -hydroxymethylacrylate and methyl α -hydroxymethylacrylate. Also, a comparison

bond or radical center and the functional group. Therefore, the polymerizability of α -(substituted methyl) acrylates are influenced by [90];

1. ceiling temperature
2. steric hinderence to propagation
3. stabilization of propagating radicals
4. balance of propagation and termination rates
5. competition with addition-fragmentation reaction.

Table 1.15 compares the homopolymerization tendency of some α -(substituted methyl) acrylates.

Table 1.15. Polymerization of α -(substituted methyl) acrylates ($\text{CH}_2=\text{C}(\text{CH}_2\text{Y})\text{COOR}$)

Y	Polymerization	Y	Polymerization
H	H	COOR	H
OC ₂ H ₅	H	CN	N
OCOCH ₃	H	NO ₂	N
OC ₆ H ₅	H	OH	H
Br	N	CH ₃	N
Cl	H	C ₆ H ₅	L
I	N	CH ₂ CH(CH ₃)COOCH ₃	L
F	H	CH(COOR) ₂	H

H: High polymer formation. L: Low molecular weight polymer. N: No polymer formation.

Monreal *et al.* studied the polymerization of EHMA and compared the result with that of MMA. It was found that the ratio $k_p/k_t^{1/2}$ for homopolymerization of EHMA is higher than the free radical polymerization of MMA ($18.6 \cdot 10^{-5}$ and $3.9 \cdot 10^{-5} \text{ molL}^{-1}\text{s}^{-1}$) respectively. This could indicate a lower termination rate constant for EHMA than for MMA since the termination rate constant may be higher for the more flexible chains [98].

When the two RHMA derivatives, MHMA and EHMA are compared in terms of their photopolymerization rates, they were found to have fast photopolymerization rates. EHMA has a plateau region (which is not as severe for MHMA) before the onset of autoacceleration. This may be due to the lower density (1.24 g/cm^3) and T_g of poly(EHMA) ($64 \text{ }^\circ\text{C}$) which slows the onset of autoacceleration as autoacceleration results from a decrease in mobility of polymer radicals with an increase in viscosity, which causes a reduced termination rate. Poly(MHMA) has a density of 1.39 g/cm^3 and T_g of $146 \text{ }^\circ\text{C}$. Although different rate profiles were observed for MHMA and EHMA, overall conversions are high for both, 81 per cent (± 2) and 79 per cent (± 2) [99].

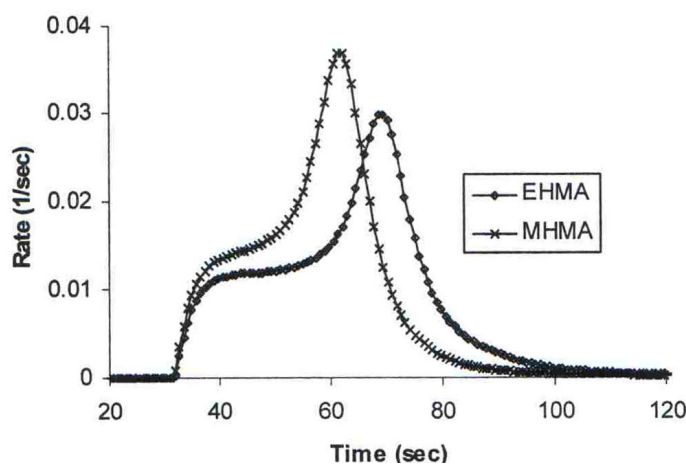


Figure 1.72. Rate versus time graph of MHMA and EHMA photopolymerizations

During the polymerization of α -(substituted methyl) acrylates, k_p and k_t values can be determined based on quantification of propagating radicals via the ESR method (Table 1.16). The k_p values, except that for α -(benzoyloxymethyl)acrylate, are all less than that for methyl methacrylate. Because of the presence of the methylene group that is interpositioned between the double bond and the functional group, the change in k_p can not be ascribed only to a steric effect. On the other hand, all of the k_t values are less than those of methyl methacrylate, indicating that steric suppression of bimolecular termination facilitates their polymerization. Therefore, the polymerization of the α -(substituted methyl) acrylates can be termed “steric hinderence-assisted polymerization”. It should be noted that the magnitude of individual k_p values is not always a good measure of polymerizability [90].

Table 1.16. The k_p and k_t values of α -(substituted methyl) acrylates
($\text{CH}_2=\text{C}(\text{CH}_2\text{Y})\text{COOR}$)

Y	R	Solvent	k_p ($\text{l mol}^{-1}.\text{s}^{-1}$)	k_t ($\text{l mol}^{-1}.\text{s}^{-1}$)
H	CH_3	Bulk	510	42
OC_4H_9	CH_3	Benzene	298	8.0
OCOCH_3	CH_3	Benzene	350	2.1
$\text{OCH}_2\text{C}_6\text{H}_5$	CH_3	Benzene	182	1.6
OCOC_6H_5	C_2H_5	Benzene	990	2.9
$\text{OCOCH}_2\text{COCH}_3$	C_2H_5	Benzene	300	1.0
COOCH_3	CH_3	Benzene	5.2	0.36
CONHC_6H_5	CH_3	Benzene	15	0.29

1.2.5. Ether Dimers of RHMA Monomers

During the synthesis of RHMA monomers, ether dimers are forming spontaneously in the reaction mixtures. If the ethers are the desired product, prolonged heating of the reaction mixture gives excellent yields. An ene-type mechanism for the ether formation was proposed involving six-membered ring transition state with essentially simultaneous transfer of a proton, loss of water, and ether bond formation. It was determined that base is needed to catalyze the ether forming reaction (Figure 1.73) [100].

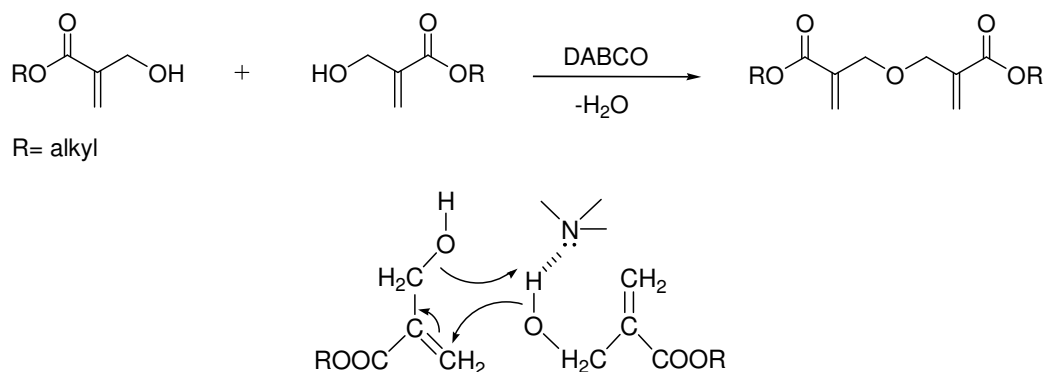


Figure 1.73. DABCO catalyzed formation of RHMA ether dimers and the proposed mechanism

It was reported that the bis ether can be used as crosslinking agents for organic soluble monomers while hydrolyzed diacid of the same compound can be used as crosslinkers for water soluble monomers (Figure 1.74). The ether linkages are not readily susceptible to hydrolysis like esters and therefore present a clear improvement over other crosslinking agents of the bis acrylate type [81].

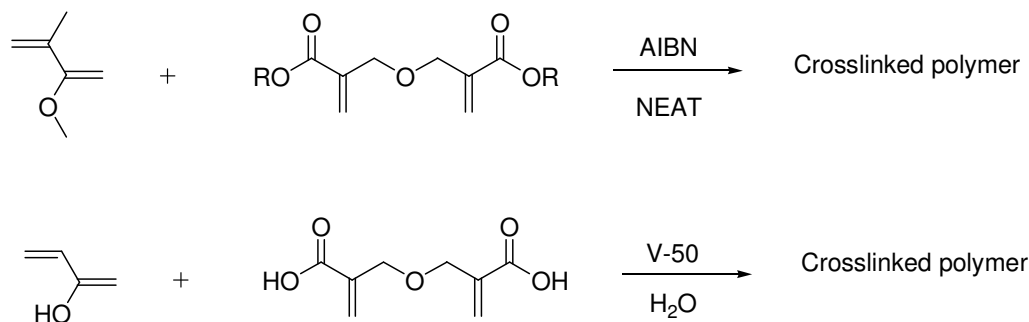


Figure 1.74. Crosslinking reactions with RHMA dimers and the diacid ether

1.2.6. Cyclopolymerization

The polymerization of multifunctional monomers often leads to cross-linked, insoluble polymers. However, some of these monomers yield soluble polymers. Figure 1.75 shows schematically the possible reaction courses for the free radical polymerization of α,ω -dienes. In the case of reaction 1 and/or reaction 2 where

intramolecular cyclization is favored to intermolecular propagation (reaction 5), linear polymers that have cyclic structures (five and/or six-membered rings) in the backbone chain are formed. On the other hand, intermolecular addition leads to a polymer with pendant vinyl groups, which can react with other growing chains to give a crosslinked network. The investigations showed that the proportion of reactions 1, 2 and 5 changes significantly depending on the monomers and polymerization conditions used. So, the formation of cyclized polymers can be achieved by suppressing the intermolecular reaction (reaction 5). For example, polymerizations in highly dilute solutions increase cyclization efficiency [101].

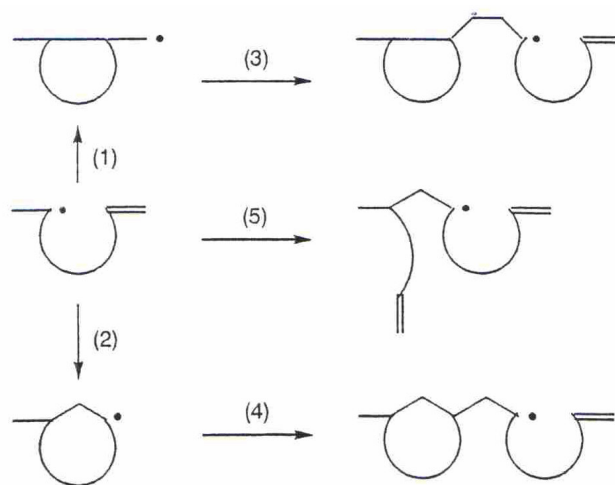


Figure 1.75. Possible reaction courses for radical polymerization of α,ω -dienes

1,6-Dienes have the possibility to form five- and six-membered rings as repeat cyclic units. A six membered ring and its radical are considered to be more stable than the five-membered ring and its radical. However, five-membered rings are often formed. Thus, the formation of the five-membered ring could be explained by the kinetic factor and six-membered ring formation by steric and stabilization factors [101].

It was shown that, bis ether compounds form cyclopolymers by the following reaction (Figure 1.76). High efficiency of cyclization can be attributed to the presence of bulky groups on or near the vinyl groups which favors intramolecular cyclization, inhibiting intermolecular reaction. The cyclopolymers are known to possess many

advantageous properties such as high glass transition temperatures, excellent thermal stabilities and less shrinkage during polymerization than non-cyclic linear polymers (Table 1.17) [102, 103, 104].

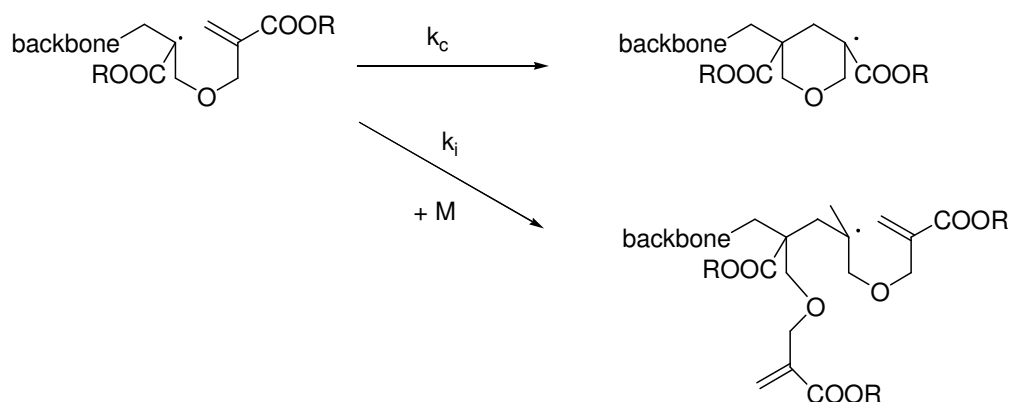


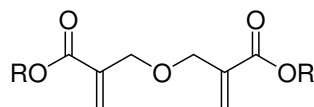
Figure 1.76. Intramolecular cyclization and intermolecular monomer addition

Table 1.17. Glass transition temperatures of cyclopolymers and the corresponding acrylates and methacrylates

Substituent R	T_g °C		
	Acrylate	Methacrylate	Cyclopolymer
Methyl	10	104	165
Ethyl	-24	65	70-90
t-butyl	43-107	113	138
Isobornyl	94	110	230
Adamantyl	153	254	260

Stansbury studied the synthetic dental compositions composed of an inorganic filler and a resin formed by polymerization of at least one bis acrylate monomer (Figure 1.77). Among the bis-acrylate monomers, ether dimers of alkyl α -hydroxymethylacrylates when used in synthetic dental compositions exhibit relatively low volume shrinkage and reduced residual unsaturation as compared with commercial monomers used in dental materials such as triethylene glycol dimethacrylate (Table 1.18). The low volume shrinkage allows the formation of stronger and more durable bonds between the dental compositions and

various substrates (Table 1.19). Also, bis-acrylates lead to high degrees of conversion at or near ambient reaction conditions which results in resins having relatively high glass transition temperatures [105].



R= methyl, ethyl, isobutyl and phenethyl

Figure 1.77. The bis-acrylate monomers used in synthetic dental compositions

Table 1.18. Comparison of polymerization shrinkage and conversion results of the diethyl bis-acrylate with that of commercial monomer, TEGDMA

Monomer	Polymerization Temperature °C (bulk)	Conversion %	Volume Shrinkage %
Diethyl bis-acrylate	60	95	11.6
	23	89	11.2
TEGDMA	60	91	19.9
	37	68	12.5

Table 1.19. Comparison of tensile strength (TS) value

Monomer (wt ratio)	TS, MPa
Bis-GMA / Diethyl bis-acrylate (75:25)	52.5
Diphenethyl bis acrylate / TEGDMA (50:50)	48.3
Bis-GMA / Diphenethyl bis acrylate / TEGDMA (60:27:13)	51.7
Diphenethyl bis acrylate / Diethyl bis-acrylate (70:30)	29.8
Bis-GMA / TEGDMA (70:30)	50.5

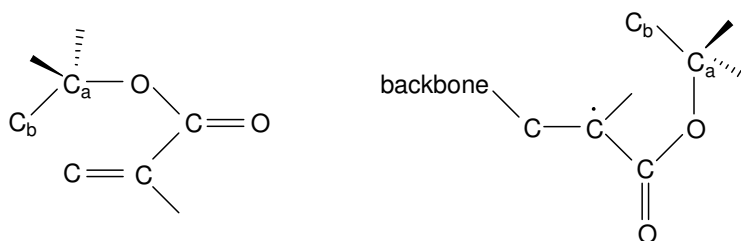
This work also comprises methods for adhesively bonding a substrate to a tooth wherein the adhesive composition is formed by the hydrolysis of the ester group of the bis-acrylate monomer to provide a dicarboxylic acid wherein R is H or a dicarboxylate salt wherein R is a metal cation, for example Na⁺ or K⁺ [105].

Mathias *et al.* investigated the free radical cyclopolymerization of ether dimers of α -hydroxymethylacrylates and evaluated the factors that control the cyclopolymerizability [106].

- They believed that both the cyclization efficiency and the formation of only six-membered rings are related to the flexible sp³ connecting groups between reactive vinyl moieties as rigid connecting groups do not allow molecular flexibility for adopting an appropriate conformation for intramolecular reaction leading to cyclic structures.
- A strong effect of ester substituent on cyclopolymerizability was observed and cyclization efficiency at 80 °C increased in the following order: methyl, ethyl, isobornyl, t-butyl and adamantyl esters. That is, cyclization efficiency is found to be effected by the number of carbons linked to the central ester carbon (which defines the effective bulkiness) rather than the apparent bulkiness (Table 1.20). Increasing the size of the ester moiety decreases the rate constants for both propagation and termination but k_t decreases faster than k_p and k_i decreases faster than k_c, allowing propagation to yield cyclic polymer to a greater extent before termination takes place. So, as shown in Figure 1.78, C_b carbon plays an important role in the substituent effect on cyclization efficiency. Vinyl carbons of monomer or propagating radical are considered to be sterically shielded mainly by C_b carbons. On the other hand, the ether dimer of α -hydroxymethylacrylic acid showed unexpectedly high cyclization efficiency (intermediate between secondary and tertiary esters) despite having the lowest substituent bulkiness. This result was attributed to the capability of hydrogen bond formation between acid groups, which causes a favorable conformation for cyclization [107].

Table 1.20. Dependence of k_c/k_i values on effective bulkiness

Substituent R	k_c/k_i at 80 °C (mol/l)
Methyl	16.7
Ethyl	19.0
Isobornyl	50.0
T-butyl and adamantyl	87.0
H	70.5

Figure 1.78. Shielding effect of C_b carbon that is linked to the carboxyester carbon

- They showed that cyclization efficiencies increased with temperature for all of the monomers studied. Since the entropy term has a temperature factor and since the entropy change is less favored for cyclization than for the intermolecular addition, increasing temperature disfavors the latter more than cyclization, that is, cyclization is favored by default [106].
- Mathias also stated that gem-disubstitution on the sp^3 linkage carbon facilitates cyclization as geminal substitution makes gauche conformations less energetically disfavored, facilitating intra- over intermolecular reactions whereas the unsubstituted compound prefers trans conformation for the methylene connecting segments. Tsuda and Mathias synthesized geminal dicyano-containing diacrylates from methyl or ethyl α -(chloromethyl)acrylate and malononitrile in H_2O/CH_2Cl_2 with a phase transfer catalyst and KOH (Figure 1.79). The two cyano groups enhanced the conformation needed for cyclization so well that, even under bulk polymerization, only cyclopolymer was obtained. Also, electron-withdrawing effect of the dicyano group should enhance radical

cyclopolymerizability because it decreases degradative chain transfer by polarizing and strengthening the α -CH₂ bonds. It was observed that, the cyclopolymers derived from dicyano-containing diacrylates contained six-membered ring structures whereas five-membered ring formation dominates for diallyl malononitrile. This is in good agreement with the results reported for non-substituted 1,6-heptadienes in which kinetically preferred five-membered ring formation dominates over thermodynamically preferred six-membered ring generation [108, 109].

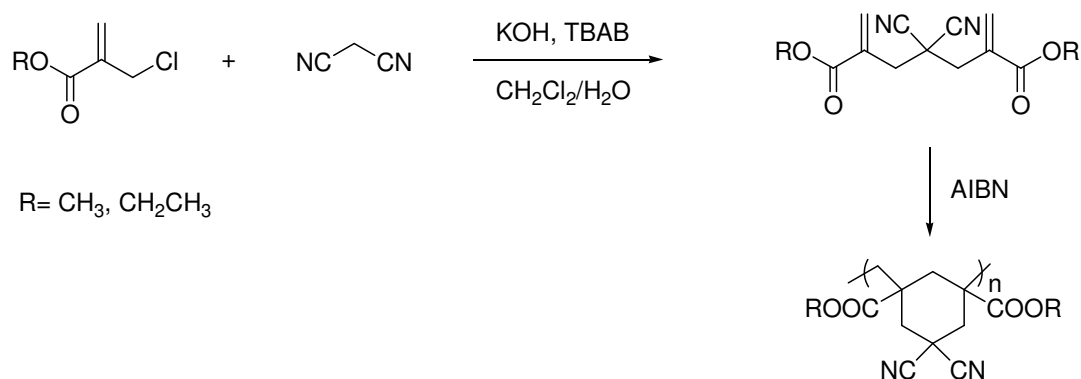


Figure 1.79. Synthesis and cyclopolymerization of dicyano-containing diacrylates

Thang *et al.* patented the synthesis and characterization of 4,4-disubstituted 1,6-diene monomers which are capable of undergoing polymerizations via an alternating intramolecular-intermolecular chain propagation (Figure 1.80) [110].

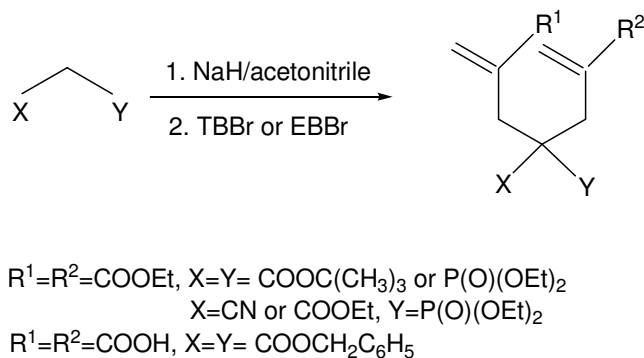


Figure 1.80. Synthesis of the 4,4-disubstituted 1,6-diene monomers

Avci *et al.* synthesized amine derivatives of ECMA and TBBr (Figure 1.81). Only ECMA-cyanamide derivative gave crosslinked polymer. All the other monomers displayed high polymerization and cyclization tendencies. The t-butyl ester monomers showed higher polymerization rates compared to ethyl ester monomers of the same amine derivatives [111].

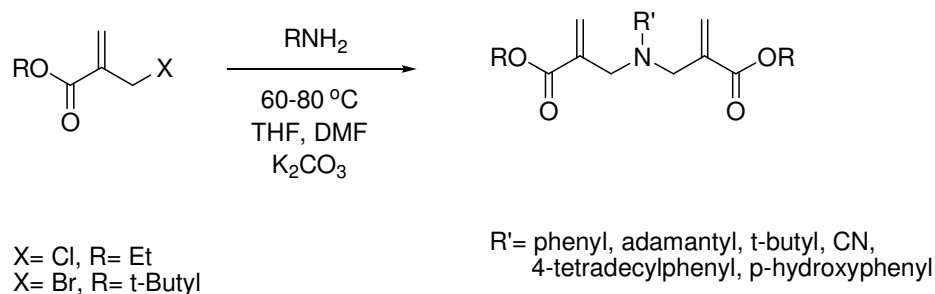


Figure 1.81. General synthetic scheme for amine derivatives

They also synthesized diacrylate monomers with hydrophobic R' groups where R' = C₉H₁₉ or C₁₈H₃₇ (Figure 1.82). High cyclization tendencies were observed. Then the polymers of amine derivatives were quaternized using dimethyl sulfate in THF at 50 °C. Thermal stabilities of the polymers after quaternization increased [112].

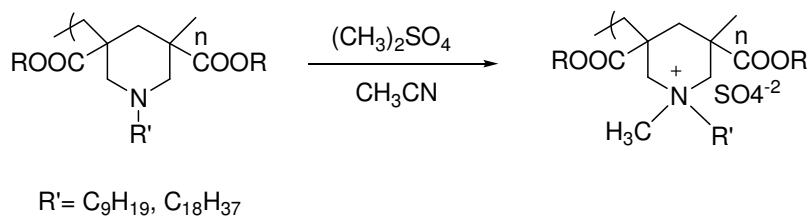


Figure 1.82. Quaternization of polymers

Michalovic *et al.* synthesized t-butyl α -(N-vinylformamidomethyl)acrylate (tBVFA) from TBBr and N-vinyl formamide and found that tBVFA undergoes cyclopolymerization to give soluble products. However, at lower solvent monomer ratio (1:1) and at lower temperature, crosslinking occurred. Also, deprotection of p(tBVFA) to

give the free acid polymer was easily carried out by treatment with trifluoroacetic acid (Figure 1.83) [113].

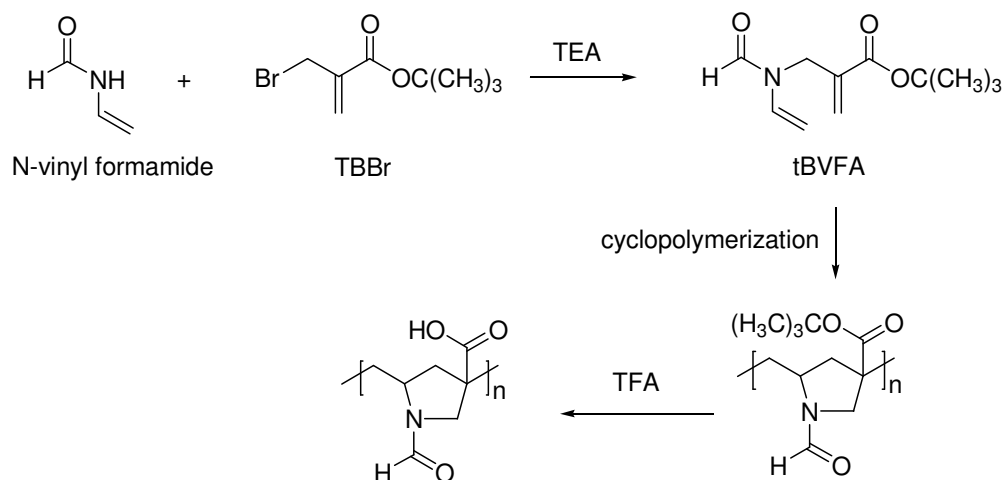


Figure 1.83. Synthesis of a cyclopolymerizable monomer based on TBBr

Thompson *et al.* synthesized poly[ethyl α -[(allyloxy)methyl]-acrylate] (referred to as allyl ether polymer) and poly[allyl α -(hydroxymethyl)acrylate] (referred to as allyl ester polymer) (Figure 1.84). The allyl ether showed a difference in polymerization behaviour in comparison to the allyl ester and it was found to undergo complete cyclopolymerization in solution and in bulk. They stated that, a helical conformation is preferred for ether-linked molecules such as crown ethers and a similar conformation brought the allyl double bond into position for radical addition from the stabilized acrylate radical [114].

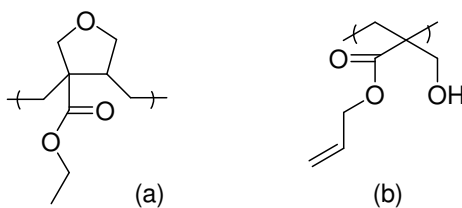
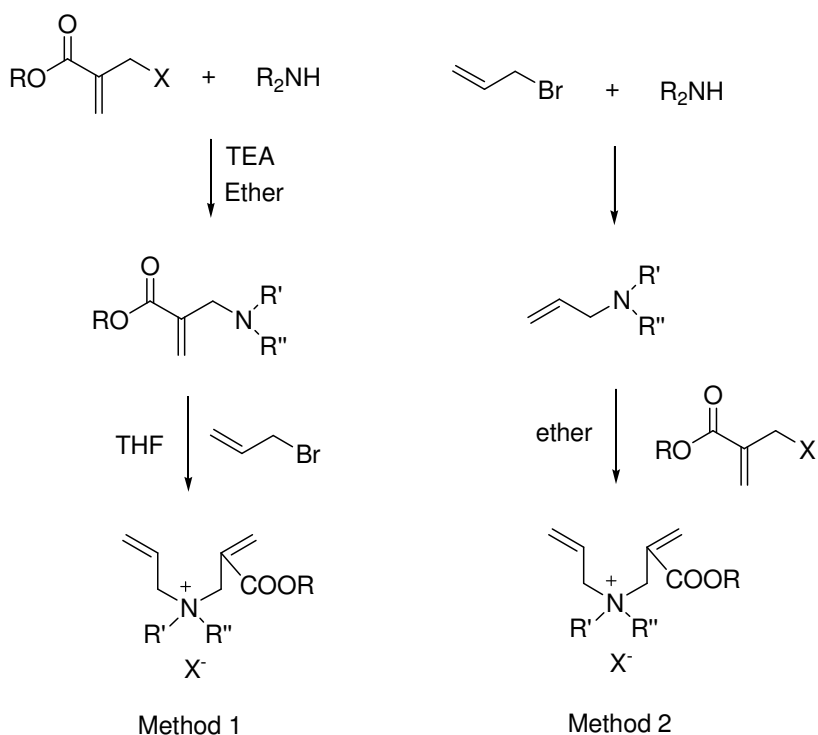


Figure 1.84. Structures of (a) poly[ethyl α -[(allyloxy)methyl]-acrylate] and (b) poly[allyl α -(hydroxymethyl)acrylate]

Avci *et al.* studied the synthesis of allyl-acrylate quaternary ammonium salts using two different methods [115, 116]. In the first method, dialkylamine derivatives of ECMA

and TBBr were prepared in the presence of TEA, then allyl bromide was used to form the corresponding quaternary salts. In the second method, N, N-dialkyl allylamine was prepared first and then reacted with ECMA or TBBr (Figure 1.85). Higher purity monomers were obtained with the method 2. They stated that, the reactivity of allyl-acrylate quaternary ammonium salts could be controlled by changes in the ester group and/or substituent on the nitrogen atom. On the other hand, allyl-acrylate monomers were much more reactive than diallyldimethylammonium salts.



X= Cl, R= methyl R',R''= piperidine(a)

X= Cl, R= ethyl R',R''= piperidine (b), butyl (c), morpholine (d), ethyl

R'=methyl, R''= butyl (e)

X= Br, R= t-butyl R',R''= piperidine (f), butyl, morpholine (g), ethyl

Figure 1.85. General synthetic scheme for allyl-acrylate quaternary ammonium salts

2. OBJECTIVES

Enamel-dentin adhesives are used to achieve a strong bond between a filling composite and dental tissues. The enamel-dentin adhesives contain adhesive monomers particularly acidic monomers containing phosphonic, mono- or dihydrogenphosphate or carboxylic acid groups. These acidic monomers remove the smear layer, demineralize the dentin and enamel, diffuse into collagen fibrils to form a hybrid layer which facilitates binding of dental resins.

The purpose of this study was to develop new monomers aiming all the desired properties of a dental adhesive. These properties include a) rigid structure leading to good mechanical properties and low volume shrinkage, b) ability to form bonds with dental tissue, c) hydrolytic and storage stability, d) high rate of polymerizability and copolymerizability with common monomers used in dental composites e) solubility in water and ethanol f) biocompatibility.

New phosphonic, carboxylic acid and iminodiacetate containing monomers based on alkyl α -hydroxymethyl acrylates were synthesized and characterized. The effect of monomer structure on the homo- and copolymerization reactivity was investigated using photodifferential scanning calorimeter. Bulk and solution polymerization of the monomers were carried out. Properties of the monomers and polymers (solubilities, T_g , molecular weight, thermal stabilities, metal binding capacities) were evaluated. The interaction of the acid monomers with hydroxyapatite (a tooth tissue substitute) was investigated using ^{13}C -NMR technique.

3. EXPERIMENTAL

3.1. Materials and Apparatus

3.1.1. Materials

Tert-butyl acrylate (Aldrich, 98 per cent), paraformaldehyde (Merck), 1,4-diazobicyclo [2.2.2] octane DABCO (Aldrich), N,N-dimethyl formamide (BDH, 99 per cent), thionyl chloride (Acros, 99.5 per cent), diethyl hydroxymethyl phosphonate (Aldrich), bromotrimethylsilane (TMSBr) (Aldrich, 97 per cent), sodium hydride (Fluka, 55-65 per cent dispersion in oil), triethyl phosphonoacetate (Aldrich, 98 per cent), trifluoroacetic acid (Aldrich, 99 per cent), tetraethyl methylenediphosphonate (Aldrich, 97 per cent), NH₄Cl (Merck), Na₂SO₄ (Merck), CaCl₂ (Merck), triethyl phosphite (Fluka, 97 per cent), 1,3-dicyclohexylcarbodiimid (DCC) (Aldrich, 99 per cent), diethyliminodiacetate (Aldrich, 98 per cent), triethylamine (Aldrich, 99 per cent) were used as received without purification.

The photoinitiator, 2,2'-dimethoxy-2-phenylacetophenone (Irgacure 651 or DMPA from Ciba-Geigy), was recrystallized from hexanes before use. The thermal initiators 2,2'-azobis(isobutyronitrile) (AIBN) and 2,2'-azobis(N,N'-amidinopropane) dihydrochloride (V-50) were used as received.

THF used for the synthesis of 4,4-disubstituted dimers was dried over Na and freshly distilled before use. Ethyl acetate and dichloromethane used for column chromatography were received from Akkimya and distilled before use. All other solvents were obtained from Aldrich, Merck or J.T. Baker and used as received.

3.1.2. Apparatus

¹H-NMR and ¹³C-NMR spectra were recorded using Varian Gemini 400 MHz spectrometer. Infrared analysis was performed on a Perkin Elmer 1600 FT-IR spectrometer using NaCl windows or KBr discs. The chelating ability of some monomers

was measured with an ultraviolet-visible spectrophotometer (UNICAM-UV2). Gel permeation chromatography (GPC) analysis were done using an Agilent 1100 series GPC-SEC analysis system with polymethyl methacrylate standards. Thermogravimetric analysis were done with TA Instruments (Q50). Photopolymerizations were carried out by TA Instruments differential photocalorimeter (DPC) (Q100) containing a high pressure mercury lamp.

3.2. Monomer Synthesis

3.2.1. Synthesis of Phosphorus-Containing Cyclopolymerizable Monomers from 2-(2-tert-Butoxycarbonyl-Allyloxymethyl)-Acrylic Acid tert-Butyl Ester (TBEED)

3.2.1.1. Synthesis of 2-(2-tert-Butoxycarbonyl-Allyloxymethyl)-Acrylic Acid tert-Butyl Ester (TBEED). Tert-butyl acrylate (68.85 g, 0.54 mol), paraformaldehyde (16.15 g, 0.54 mol), DABCO (2.69 g, 2.9 wt per cent) and tert-butyl alcohol (4.31 g, 4.7 wt per cent) were added to a 250 ml three-necked round bottom flask. The mixture was stirred at 95 °C for four days. 100 ml of CH₂Cl₂ was added and then mixture was washed three times with 50 ml of three per cent HCl and with 50 ml of water. The organic layer was separated and evaporated under reduced pressure to give crude product. Vacuum distillation in the presence of free radical inhibitor, CuCl₂, gave pure product as a white solid in 28.5 per cent. But it was hard to avoid polymerization during vacuum distillation.

¹H-NMR (CDCl₃): δ= 1.5 (s, 18H, CH₃), 4.2 (s, 4H, CH₂-O), 5.8 (d, 2H, CH₂=C), 6.2 (d, 2H, CH₂=C) ppm.

¹³C-NMR (CDCl₃): δ= 28.37 (CH₃), 69.25 (CH₂-O), 81.00 [(CH₃)₃C], 124.47 (C=CH₂), 138.82 (C=CH₂), 164.97 (C=O) ppm.

FT-IR (neat): 2978 (C-H), 1710 (C=O), 1638 (C=C), 1152 (C-O-C) cm⁻¹.

3.2.1.2. Synthesis of 2-(2-Chlorocarbonyl-Allyloxymethyl)-Acryloyl Chloride. To a mixture of TBEED (9.08 g, 0.03 mol) and one drop of N, N-dimethyl formamide in an ice bath, thionyl chloride (32 ml, 0.44 mol) was added dropwise and the mixture was stirred at 0 °C for one hour. The solution was then heated to 40 °C and allowed to stir for two days.

After evaporation of excess thionyl chloride, the mixture was distilled under reduced pressure using CuCl_2 to give a yellow colored liquid in 38.4 per cent yield.

$^1\text{H-NMR}$ (CDCl_3): δ = 4.3 (s, 4H, $\text{CH}_2\text{-O}$), 6.3 (d, 2H, $\text{CH}_2\text{=C}$), 6.7 (d, 2H, $\text{CH}_2\text{=C}$) ppm.

$^{13}\text{C-NMR}$ (CDCl_3): δ = 69.18 ($\text{CH}_2\text{-O}$), 134.42 (C=CH_2), 141.35 (C=CH_2), 167.23 (C=O) ppm.

FT-IR (neat): 2874 (C-H), 1750 (C=O), 1637 (C=C), 1130 (C-O-C) cm^{-1} .

3.2.1.3. Synthesis of 2-(2-Carboxy-Allyloxymethyl)-Acrylic Acid (TBEEED-acid). To TBEEED (10.83 g, 36.3 mmol), CF_3COOH (12.12 g, 106.3 mmol) was added dropwise on ice, under nitrogen. After mixing at room temperature for 24 h, the precipitate formed was filtered and washed with diethyl ether. The white solid product was dried in vacuo. Yield: 94.2 per cent.

$^1\text{H-NMR}$ (DMSO): δ = 4.17 (s, 4H, $\text{CH}_2\text{-O}$), 5.85 (d, 2H, $\text{CH}_2\text{=C}$), 6.18 (d, 2H, $\text{CH}_2\text{=C}$) ppm.

$^{13}\text{C-NMR}$ (DMSO): δ = 68.3 ($\text{CH}_2\text{-O}$), 124.8 (C=CH_2), 137.9 (C=CH_2), 166.7 (C=O) ppm.

FT-IR (neat): 2880 (C-H), 1683 (C=O), 1628 (C=C), 1131 (C-O-C) cm^{-1} .

3.2.1.4. Synthesis of 2-[2-(Diethoxy-Phosphorylmethoxycarbonyl)-Allyloxymethyl]-Acrylic Acid Diethoxy-Phosphorylmethyl Ester (PHOSEED). To a mixture of diethyl hydroxymethyl phosphonate (2.88 g, 17.10 mmol) and TEA (1.74 g, 17.19 mmol) in 8 ml of THF, 2-(2-chlorocarbonyl-allyloxymethyl)-acryloyl chloride (1.73 g, 7.76 mmol) was added dropwise in an ice bath under nitrogen. The mixture was stirred at room temperature for two days. The reaction mixture was diluted with nine ml of CH_2Cl_2 and then it was extracted three times with 4.5 ml of H_2O . The organic layer was separated and dried with CaCl_2 . Evaporation of CH_2Cl_2 gave the product as a yellow viscous liquid in 91 per cent yield.

$^1\text{H-NMR}$ (CDCl_3): δ = 1.12 (m, 12H, CH_3), 3.95 (m, 8H, $\text{O-CH}_2\text{CH}_3$), 4.03 (s, 4H, $\text{CH}_2\text{-O}$), 4.24 (d, 4H, $\text{CH}_2\text{-P}$), 5.76 (s, 2H, $\text{CH}_2\text{=C}$), 6.15 (s, 2H, $\text{CH}_2\text{=C}$) ppm.

$^{13}\text{C-NMR}$ (CDCl_3): δ = 16.76 (CH_3), 56.41, 58.08 ($\text{CH}_2\text{-P}$), 63.03 ($\text{O-CH}_2\text{CH}_3$), 69.98 ($\text{CH}_2\text{-O}$), 127.52 (C=CH_2), 136.12 (C=CH_2), 164.54 (C=O) ppm.

FT-IR (neat): 2984 (C-H), 1722 (C=O), 1637 (C=C), 1248 (P=O), 1023 (P-O-Et) cm^{-1} .

3.2.1.5. Synthesis of 2-(2-Phosphonomethoxycarbonyl-Allyloxymethyl)-Acrylic Acid Phosphonomethyl Ester (PHOSEED-acid). To a solution of PHOSEED (0.83 g, 1.7 mmol) in 1.7 ml of CH_2Cl_2 , bromotrimethylsilane (TMSBr) (1.04 g, 6.8 mmol) was added under nitrogen in the same manner as discussed in the literature [25]. Then the solution was refluxed for four hours. After evaporation of the solvent, nine ml of methanol was added and the mixture was stirred at room temperature for 24 hours. Then the solvent was evaporated under reduced pressure. The residue was washed with ether to remove any unreacted PHOSEED and dried under reduced pressure to give the product as a viscous liquid in 72 per cent yield.

$^1\text{H-NMR}$ (DMSO): δ = 4.10 (s, 4H, $\text{CH}_2\text{-O}$), 4.3 (d, 4H, $\text{CH}_2\text{-P}$), 5.90 (s, 2H, $\text{CH}_2\text{=C}$), 6.30 (s, 2H, $\text{CH}_2\text{=C}$) ppm.

$^{13}\text{C-NMR}$ (DMSO): δ = 58.67, 60.27 ($\text{CH}_2\text{-P}$), 68.95 ($\text{CH}_2\text{-O}$), 127.38 (C=CH_2), 137.08 (C=CH_2), 165.03 (C=O) ppm.

FTIR (neat): 3500-2300 (OH), 1724 (C=O), 1632 (C=C), 1251 (P=O) cm^{-1} .

3.2.2. Synthesis of Phosphorus-Containing Cyclopolymerizable Monomers from tert-Butyl α -Hydroxymethyl Acrylate (TBHMA) and Ethyl α -Hydroxymethyl Acrylate (EHMA)

3.2.2.1. Synthesis of tert-Butyl- α -Hydroxymethyl Acrylate (TBHMA). tert-Butyl acrylate (128.17 g, 1.0 mol), paraformaldehyde (30 g, 1.0 mol) and 1,4-diazobicyclo [2.2.2] octane (DABCO) (14 g, 0.12 mol) were added to a mixture of DMSO (227 ml) and H_2O (85 ml). The mixture was heated at 100 °C for 30 minutes under N_2 . Then it was cooled and aqueous phase was separated. The organic phase was washed with one wt per cent HCl (2x100 ml), dried with anhydrous CaCl_2 and filtered. The solution was distilled under reduced pressure and pure TBHMA was collected as a colorless liquid in 30-50 per cent yield.

$^1\text{H-NMR}$ (CDCl_3): δ = 1.49 (s, 9H, CH_3), 2.68 (s, 1H, O-H), 4.25 (s, 2H, $\text{CH}_2\text{-O}$), 5.72, 6.12 (d, 2H, $\text{CH}_2\text{=C}$) ppm.

$^{13}\text{C-NMR}$ (CDCl_3): δ = 28.1 (CH_3), 62.4 ($\text{CH}_2\text{-O}$), 81.2 [$\text{C-(CH}_3)_3$], 124.4 (C=CH_2), 140.6 (C=CH_2), 165.4 (C=O) ppm.

FT-IR (neat): 3500-3000 (OH), 2978 (C-H), 1709 (C=O), 1639 (C=C) cm^{-1} .

3.2.2.2. Synthesis of tert-Butyl- α -Bromomethyl Acrylate (TBBr). PBr_3 (5.32 ml, 0.056 mol) was added to a solution of TBHMA (19.16 g, 0.12 mol) in 115 ml of ether on ice, under nitrogen. After three hours of mixing at room temperature, 69 ml of H_2O was added dropwise in an ice bath and the aqueous phase was separated. Then it was extracted with hexane (3x23 ml). The organic phases were combined, washed with saturated NaCl solution (2x23 ml) and dried with anhydrous CaCl_2 . After removal of ether by rotary evaporator, distillation was done under reduced pressure to obtain pure product as a colorless liquid in 70.3 per cent yield.

$^1\text{H-NMR}$ (CDCl_3): δ = 1.47 (s, 9H, CH_3), 4.09 (s, 2H, $\text{CH}_2\text{-Br}$), 5.79, 6.16 (d, 2H, $\text{CH}_2\text{=C}$) ppm.

$^{13}\text{C-NMR}$ (CDCl_3): δ = 28.40 (CH_3), 30.20 ($\text{CH}_2\text{-Br}$), 81.96 [$\text{C-(CH}_3)_3$], 128.12 (C=CH_2), 139.04 (C=CH_2), 164.06 (C=O) ppm.

FT-IR (neat): 2978 (C-H), 1717 (C=O), 1632 (C=C), 720 (C-Br) cm^{-1} .

3.2.2.3. Synthesis of Ethyl α -Hydroxymethyl Acrylate (EHMA). Synthesis is similar to the synthesis of TBHMA. Ethyl acrylate (66.8 g, 0.66 mol), paraformaldehyde (20 g, 0.66 mol) and 1,4-diazobicyclo [2.2.2] octane (DABCO) (9.33 g, 0.08 mol) were added to a mixture of DMSO (151 ml) and H_2O (57 ml). The mixture was heated at 60 $^\circ\text{C}$ for 30 minutes under N_2 . Then it was cooled and extracted with diethyl ether (2x70 ml). The combined organic phases were washed with one wt per cent HCl (3x35 ml), dried with anhydrous CaCl_2 and filtered. After the removal of ether by rotary evaporator, the solution was distilled under reduced pressure and pure EHMA was collected as a colorless liquid in 40-50 per cent yield.

$^1\text{H-NMR}$ (CDCl_3): δ =1.24 (t, 3H, CH_3), 2.94 (s, 1H, O-H), 4.15 [q, 2H, $\text{CH}_2\text{-C(O)}$], 4.24 (s, 2H, $\text{CH}_2\text{-O}$), 5.78, 6.18 (d, 2H, $\text{CH}_2\text{=C}$) ppm.

$^{13}\text{C-NMR}$ (CDCl_3): δ = 14.53 (CH_3), 61.16 ($\text{CH}_2\text{-O}$), 62.25 ($\text{CH}_2\text{-OH}$), 125.40 (C=CH_2), 139.76 (C=CH_2), 166.40 (C=O) ppm.

FT-IR (neat): 3500-3000 (OH), 2983 (C-H), 1710 (C=O), 1637 (C=C) cm^{-1} .

3.2.2.4. Synthesis of Ethyl- α -Bromomethyl Acrylate (EBBr). 2.5 ml of PBr₃ (26.3 mmol) was added to a solution of EHMA (7.25 g, 55.8 mmol) in 50 ml of ether on ice, under nitrogen. After three hours of mixing at room temperature, 30 ml of H₂O was added in an ice bath and the aqueous phase was separated. Then it was extracted with hexane (3x10 ml). The organic phases were combined, washed with saturated NaCl solution (2x10 ml) and dried with anhydrous CaCl₂. After the removal of ether by rotary evaporator, distillation was done under reduced pressure to obtain pure product as a colorless liquid in 74.9 per cent yield.

¹H-NMR (CDCl₃): δ = 1.30 (t, 3H, CH₃), 4.16 (s, 2H, CH₂-Br), 4.25 [q, 2H, CH₂-C(O)], 5.91, 6.30 (d, 2H, CH₂=C) ppm.

¹³C-NMR (CDCl₃): δ = 14.14 (CH₃), 29.31 (CH₂-Br), 61.10 (CH₂-O), 128.48 (C=CH₂), 137.39 (C=CH₂), 164.36 (C=O) ppm.

FT-IR (neat): 2978 (C-H), 1723 (C=O), 1629 (C=C), 721 (C-Br) cm⁻¹.

3.2.2.5. Synthesis of 4-Diethoxyphosphoryl-4-Ethoxycarbonyl-2,6-bis(tert-Butoxycarbonyl)-1,6-Heptadiene (BC-EPA). To a cooled suspension of sodium hydride (1.04 g, 55 per cent dispersion in oil) in dry THF (70 ml), triethyl phosphonoacetate (2.48 g, 11 mmol) was added and allowed to stir at 0 °C for one hour before the addition of TBBr (5.27 g, 24 mmol). Then the reaction mixture was allowed to warm to room temperature and stirred further at this temperature overnight under nitrogen. The reaction mixture was quenched with aq. NH₄Cl (70 ml), and extracted three times with diethyl ether (total 75 ml). The organic phase was then washed with brine and dried over anhydrous CaCl₂. After removal of the solvent under reduced pressure and purification by column chromatography on a silica gel column using CH₂Cl₂ initially and gradually changing to three per cent isopropanol in CH₂Cl₂ as eluent, the pure product (4.89 g, 89.6 per cent) was obtained as a very pale yellow liquid.

¹H-NMR (CDCl₃): δ = 1.28 (m, 9H, CH₂-CH₃), 1.44 (s, 18H, [C(CH₃)₃]), 2.80 (dd, 2H, allylic-CH₂), 3.01 (dd, 2H, allylic-CH₂), 4.10 (m, 6H, O-CH₂), 5.57 (s, 2H, CH₂=), 6.12 (s, 2H, CH₂=) ppm.

^{13}C -NMR (CDCl_3): δ = 14.36 ($\text{CH}_3\text{CH}_2\text{OC}$), 16.79 ($\text{CH}_3\text{CH}_2\text{OP}$), 28.39 [$\text{C}(\text{CH}_3)_3$], 34.34 (CH_2), 52.36, 53.76 (C-P), 61.87 (CH_2OC), 62.88 (CH_2OP), 80.78 [$\text{C}(\text{CH}_3)_3$], 127.37 ($\text{CH}_2=\text{C}$), 137.71 ($\text{CH}_2=\text{C}$), 166.40 (C=O), 170.24 ($\text{CH}_2\text{OC}=\text{O}$) ppm.

FT-IR (neat): 2977 (C-H), 1725 (C=O, ethyl ester), 1710 (C=O, t-butyl ester), 1627 (C=C), 1253 (P=O), 1054 (P-O-Et) cm^{-1} .

3.2.2.6. Synthesis of 4-Diethoxyphosphoryl-4-Ethoxycarbonyl-2,6-bis(Ethoxycarbonyl)-1,6-Heptadiene (EC-EPA). To a cooled suspension of sodium hydride (0.64 g, 55 per cent dispersion in oil) in dry THF (50 ml), triethyl phosphonoacetate (1.53 g, 6.7 mmol) was added and allowed to stir at 0 °C for one hour before the addition of EBBR (2.83 g, 14.7 mmol). Then the reaction mixture was allowed to warm to room temperature and stirred further at this temperature overnight under nitrogen. The reaction mixture was quenched with aq. NH_4Cl (50 ml), and extracted three times with diethyl ether (total 60 ml). The organic phase was then washed with brine and dried over anhydrous CaCl_2 . After removal of the solvent under reduced pressure and purification by column chromatography on a silica gel column using CH_2Cl_2 initially and gradually changing to three per cent isopropanol in CH_2Cl_2 as eluent, the pure product (1.90 g, 63.5 per cent) was obtained as a colorless liquid.

^1H -NMR (CDCl_3): δ = 1.26 (m, 15H, CH_3), 2.86 (dd, 2H, allylic- CH_2), 3.05 (dd, 2H, allylic- CH_2), 4.13 (m, 10H, O- CH_2), 5.65 (s, 2H, $\text{CH}_2=$), 6.22 (s, 2H, $\text{CH}_2=$) ppm.

^{13}C -NMR (CDCl_3): δ = 14.37 ($\text{CH}_3\text{CH}_2\text{OC}$), 16.58 ($\text{CH}_3\text{CH}_2\text{OP}$), 34.41 (CH_2), 52.28, 53.68 (C-P), 60.96, 61.73 (CH_2OC), 62.74 (CH_2OP), 128.22 ($\text{CH}_2=\text{C}$), 136.68 ($\text{CH}_2=\text{C}$), 167.37, 170.41 (C=O) ppm.

FT-IR (neat): 2983 (C-H), 1714-1738 (C=O, ethyl ester), 1626 (C=C), 1246 (P=O), 1058 (P-O-Et) cm^{-1} .

3.2.2.7. Synthesis of 4-Ethoxycarbonyl-4-Phosphonic Acid-2,6-bis(Carboxylic Acid)-1,6-Heptadiene (CA-PA). TMSBr (0.32 g, 2.1 mmol) was added dropwise to a solution of BC-EPA (0.47 g, 0.94 mmol) in 0.6 ml of CH_2Cl_2 under nitrogen and then the solution was refluxed for three hours. After the evaporation of the solvent, five ml of MeOH was added and the mixture was allowed to stir at room temperature overnight. Then the solvent was evaporated and CF_3COOH (0.80 g, 7.0 mmol) was added dropwise in an ice-bath under

nitrogen for further hydrolysis. The solution was mixed at room temperature overnight. After the addition of diethyl ether, the solution was filtered. The white solid product was washed with diethyl ether to remove residual trifluoroacetic acid. Then it was dried in vacuo. Yield: 36.1 per cent.

$^1\text{H-NMR}$ (CD_3OD): δ = 1.26 (t, 3H, CH_3), 2.91 (dd, 2H, allylic- CH_2), 3.04 (dd, 2H, allylic- CH_2), 4.13 (q, 2H, O- CH_2), 5.77 (s, 2H, CH_2 =), 6.27 (s, 2H, CH_2 =) ppm.

$^{13}\text{C-NMR}$ ($\text{D}_2\text{O-DMSO}$): δ = 11.03 (CH_3), 32.16 (CH_2), 49.28, 50.62 (C-P), 60.44 (CH_2OC), 127.62 ($\text{CH}_2=\text{C}$), 134.33 ($\text{CH}_2=\text{C}$), 169.40 (C=O, acid), 170.61 (C=O, ethyl ester) ppm.

FT-IR (neat): 3500-2000 (OH), 2983 (C-H), 1705 (C=O), 1625 (C=C), 1221 (P=O) cm^{-1} .

3.2.2.8. Synthesis of 4-Diethoxyphosphoryl-4-Ethoxycarbonyl-2,6-bis(Carboxylic Acid)-1,6-Heptadiene (CA-EPA). CF_3COOH (1.00 g, 8.8 mmol) was added dropwise to BC-EPA (0.61 g, 1.2 mmol) on ice, under nitrogen. After mixing at room temperature for 24 hours, excess CF_3COOH was removed on a rotary evaporator. Then the product was washed with n-hexane and dried in vacuo to give a very viscous liquid in 62.2 per cent yield.

$^1\text{H-NMR}$ (CD_3OD): δ = 1.21 (m, 9H, CH_3), 2.76 (dd, 2H, allylic- CH_2), 2.98 (dd, 2H, allylic- CH_2), 4.05 (m, 6H, O- CH_2), 5.61 (s, 2H, CH_2 =), 6.16 (s, 2H, CH_2 =) ppm.

$^{13}\text{C-NMR}$ (CD_3OD): δ = 13.97 ($\text{CH}_3\text{CH}_2\text{OC}$), 16.27 ($\text{CH}_3\text{CH}_2\text{OP}$), 34.46 (CH_2), 52.40, 53.85 (C-P), 62.30 (CH_2OC), 63.96 (CH_2OP), 131.10 ($\text{CH}_2=\text{C}$), 135.74 ($\text{CH}_2=\text{C}$), 169.94 (C=O), 172.37 ($\text{CH}_2\text{OC}=\text{O}$) ppm.

FT-IR (neat): 3500-2000 (OH), 2987 (C-H), 1719 (C=O, ethyl ester), 1700 (C=O, acid), 1624 (C=C), 1228 (P=O), 1052 (P-O-Et) cm^{-1} .

3.2.2.9. Synthesis of 4-Ethoxycarbonyl-4-Phosphonic Acid-2,6-bis(Ethoxycarbonyl)-1,6-Heptadiene (EC-PA). TMSBr (0.65 g, 4.2 mmol) was added dropwise to a solution of EC-EPA (0.80 g, 1.8 mmol) in 1.6 ml of CH_2Cl_2 under nitrogen and then the solution was refluxed for three hours. After evaporation of the solvent, 10 ml of MeOH was added and the mixture was allowed to stir at room temperature overnight. The solvent was

evaporated, and the product was obtained as a yellowish brown viscous liquid in 83.8 per cent yield.

^1H NMR (CD_3OD): δ = 1.19 (m, 9H, CH_3), 2.83 (dd, 2H, allylic- CH_2), 2.98 (dd, 2H, allylic- CH_2), 4.06 (m, 6H, O- CH_2), 5.64 (s, 2H, $\text{CH}_2=$), 6.12 (s, 2H, $\text{CH}_2=$) ppm.

^{13}C -NMR (CD_3OD): δ = 13.05, 13.28 ($\text{CH}_3\text{CH}_2\text{OC}$), 33.42 (CH_2), 51.69, 53.03 (C-P), 60.86, 61.35 (CH_2OC), 127.66 ($\text{CH}_2=\text{C}$), 137.09 ($\text{CH}_2=\text{C}$), 167.88, 171.02 (C=O) ppm.

FT-IR (neat): 3500-2000 (OH), 2982 (C-H), 1719 (C=O), 1625 (C=C), 1217 (P=O) cm^{-1} .

3.2.2.10. Synthesis of 4,4-Diethoxyphosphoryl-2,6-bis(tert-Butoxycarbonyl)-1,6-Heptadiene (BC-TEP). To a suspension of sodium hydride (1.11 g, 55 per cent dispersion in oil) in dry THF (20 ml), tetraethyl methylenediphosphonate (2.45 g, 85 mmol) was added and allowed to stir at room temperature for one hour before the addition of TBBr (4.68 gr, 21.2 mmol). Then the reaction mixture was refluxed at 60 °C for two days under nitrogen. After quenching the mixture with aq. NH_4Cl (60 ml), it was extracted three times with ethyl acetate (total 60 ml). The organic phase was then washed with brine and dried over anhydrous Na_2SO_4 . After removal of the solvent under reduced pressure and purification by column chromatography on a silica gel column using ethyl acetate initially and gradually changing to four per cent methanol in ethyl acetate as eluent, the pure product (60.0 per cent) was obtained as a colorless liquid.

^1H -NMR (CDCl_3): δ = 1.25 (t, 12H, $\text{CH}_2\text{-CH}_3$), 1.43 (s, 18H, $[\text{C}(\text{CH}_3)_3]$), 2.93 (t, 4H, allylic- CH_2), 4.09 (m, 8H, O- CH_2), 5.76 (s, 2H, $\text{CH}_2=$), 6.12 (s, 2H, $\text{CH}_2=$) ppm.

^{13}C -NMR (CDCl_3): δ = 15.34 ($\text{CH}_3\text{CH}_2\text{OP}$), 27.02 $[\text{C}(\text{CH}_3)_3]$, 31.04 (CH_2), 45.62, 46.93, 48.24 (C-P), 61.62 (CH_2OP), 79.19 ($\text{C}(\text{CH}_3)_3$), 127.38 ($\text{CH}_2=\text{C}$), 136.82 ($\text{CH}_2=\text{C}$), 165.85 (C=O) ppm.

FTIR (neat): 2978 (C-H), 1715 (C=O), 1627(C=C), 1246 (P=O), 1028 (P-O-Et) cm^{-1} .

3.2.2.11. Synthesis of 2-(Diethoxy-Phosphoryl)-4-Methylene-Pentanedioic Acid 5-tert-Butyl Ester 1-Ethyl Ester (MBC-EPA). To a cooled suspension of sodium hydride (0.4089 g, 55 per cent dispersion in oil) in dry THF (30 ml), triethyl phosphonoacetate (1.9098 g, 8.52 mmol) was added and allowed to stir at 0 °C for one hour before the addition of TBBr (1.8832 g, 8.52 mmol). Then the reaction mixture was allowed to warm to room

temperature and stirred further at this temperature overnight under nitrogen. The reaction mixture was quenched with aq. NH_4Cl (30 ml), and extracted three times with diethyl ether (total 30 ml). The organic phase was then washed with brine and dried over anhydrous CaCl_2 . After removal of the solvent under reduced pressure and purification by column chromatography on a silica gel column using CH_2Cl_2 initially and gradually changing to seven per cent methanol in CH_2Cl_2 as eluent, the product (2.5886 g, 83.4 per cent) was obtained as a colorless liquid with 40 per cent of BC-EPA in it.

$^1\text{H-NMR}$ (CDCl_3): δ = 1.24 (m, 9H, $\text{CH}_2\text{-CH}_3$), 1.42 (s, 9H, $[\text{C}(\text{CH}_3)_3]$), 2.77 (t, 2H, allylic- CH_2), 3.31 (m, 1H, CH-P), 4.10 (m, 6H, O- CH_2), 5.49 (s, 1H, $\text{CH}_2=$), 6.05 (s, 1H, $\text{CH}_2=$) ppm.

$^{13}\text{C-NMR}$ (CDCl_3): δ = 14.28 ($\text{CH}_3\text{CH}_2\text{OC}$), 16.48 ($\text{CH}_3\text{CH}_2\text{OP}$), 28.18 $[\text{C}(\text{CH}_3)_3]$, 30.11 (CH_2), 44.13, 45.44 (C-P), 61.48 (CH_2OC), 62.80 (CH_2OP), 81.14 $[\text{C}(\text{CH}_3)_3]$, 126.62 ($\text{CH}_2=\text{C}$), 138.67 ($\text{CH}_2=\text{C}$), 165.45 (C=O, t-butyl ester), 168.68 (C=O, ethyl ester) ppm.

FT-IR (neat): 2982 (C-H), 1730 (C=O, t-butyl ester), 1634 (C=C), 1251 (P=O), 1021 (P-O-Et) cm^{-1} .

3.2.3. Synthesis of Phosphorus-Containing Monomers from TBHMA

3.2.3.1. Synthesis of 2-(Diethoxy-Phosphorylmethyl)-Acrylic Acid tert-Butyl Ester (TBEP). TBEP was synthesized by the Arbuzov reaction of TBBr (3.91 g, 17.7 mmol) with triethyl phosphite (20.8 g, 125 mmol) at 85 °C for two hours. The mixture was distilled under reduced pressure and the pure product was obtained as a colorless liquid in 84 per cent yield.

$^1\text{H-NMR}$ (CDCl_3): δ = 1.0 (t, 6H, $\text{CH}_3\text{-CH}_2$), 1.2 (s, 9H, $\text{CH}_3\text{-C}$), 2.6 (d, 2H, $\text{CH}_2\text{-P}$), 3.8 (m, 4H, $\text{CH}_2\text{-O}$), 5.5 (d, 1H, $\text{CH}_2=\text{C}$), 5.9 (d, 1H, $\text{CH}_2=\text{C}$) ppm.

$^{13}\text{C-NMR}$ (CDCl_3): δ = 16.7 (CH_3), 27.5, 30.0 ($\text{CH}_2\text{-P}$), 28.0 ($\text{CH}_3\text{-C}$), 62.0 ($\text{CH}_2\text{-O}$), 81.3 (C- CH_3), 128.0 ($\text{CH}_2=\text{C}$), 133.2 ($\text{CH}_2=\text{C}$), 165.2 (C=O) ppm.

FT-IR (neat): 2979 (C-H), 1712 (C=O), 1631 (C=C), 1255 (P=O), 1159 (C-O), 1029 (P-O-Et) cm^{-1} .

3.2.3.2. Synthesis of 2-Phosphonomethyl-Acrylic Acid tert-Butyl Ester (TBPA). TMSBr (1.49 g, 9.69 mmol) was added to a solution of TBEP (1.35 g, 4.84 mmol) in 6.5 ml of

dichloromethane under nitrogen. Then the solution was heated at 45 °C for 3.5 h. After evaporation of the solvent, 15 ml of methanol was added and the mixture was stirred at room temperature for 24 hours. Then, the solvent was evaporated under reduced pressure and the product was obtained as a colorless, viscous liquid in 77.1 per cent yield.

$^1\text{H-NMR}$ (CD_3OD): δ = 1.39 (s, 9H, $\text{CH}_3\text{-C}$), 2.77 (d, 2H, $\text{CH}_2\text{-P}$), 5.64 (d, 1H, $\text{CH}_2\text{=C}$), 6.07 (d, 1H, $\text{CH}_2\text{=C}$) ppm.

$^{13}\text{C-NMR}$ (CD_3OD): δ = 28.4 ($\text{CH}_3\text{-C}$), 30.5, 31.8 ($\text{CH}_2\text{-P}$), 80.9 (C-CH_3), 126.7 ($\text{CH}_2\text{=C}$), 135.0 ($\text{CH}_2\text{=C}$), 165.6 (C=O) ppm.

FT-IR (neat): 2000-3500 (OH), 2974 (C-H), 1708 (C=O), 1624 (C=C), 1244 (P=O), 1151 (C-O) cm^{-1} .

3.2.3.3. Synthesis of 2-Phosphonomethyl-Acrylic Acid (CAPA). CF_3COOH (0.37 g, 3.27 mmol) was added dropwise to TBPA (0.52 g, 2.34 mmol) under nitrogen. The mixture was stirred at room temperature for 18 h. After the addition of diethyl ether, the solution was filtered. The white solid product was washed with diethyl ether to remove residual trifluoroacetic acid. Yield: 59 per cent. Melting point: 157 °C.

$^1\text{H-NMR}$ (CD_3OD): δ = 2.87 (d, 2H, $\text{CH}_2\text{-P}$), 5.86 (d, 1H, $\text{CH}_2\text{=C}$), 6.32 (d, 1H, $\text{CH}_2\text{=C}$) ppm.

$^{13}\text{C-NMR}$ (CD_3OD): δ = 29.1, 30.5 ($\text{CH}_2\text{-P}$), 127.6 ($\text{CH}_2\text{=C}$), 133.1 ($\text{CH}_2\text{=C}$), 168.2 (C=O) ppm.

FT-IR (neat): 3500-2000 (OH), 2983 (C-H), 1702 (C=O), 1628 (C=C), 1247 (P=O) cm^{-1} .

3.2.3.4. Synthesis of 2-(Diethoxy-Phosphorylmethyl)-Acrylic Acid (CAEP). To TBPA (3.68 g, 13.25 mmol), CF_3COOH (4.5 g, 39.4 mmol) was added dropwise under nitrogen. The mixture was stirred at room temperature for 24 h. Then excess CF_3COOH was evaporated under reduced pressure to give a yellow colored viscous liquid.

$^1\text{H-NMR}$ (CD_3OD): δ = 1.21 (s, 9H, $\text{CH}_3\text{-C}$), 2.87, 2.93 (d, 2H, $\text{CH}_2\text{-P}$), 4.00 (m, 4H, $\text{CH}_2\text{-O}$), 5.76 (d, 1H, $\text{CH}_2\text{=C}$), 6.24 (d, 1H, $\text{CH}_2\text{=C}$) ppm.

$^{13}\text{C-NMR}$ (CD_3OD): δ = 16.0 (CH_3), 27.3, 29.0 ($\text{CH}_2\text{-P}$), 62.7 ($\text{CH}_2\text{-O}$), 128.3 ($\text{CH}_2\text{=C}$), 132.2 ($\text{CH}_2\text{=C}$), 167.5 (C=O) ppm.

FT-IR (neat): 3500-2000 (OH), 2983 (C-H), 1713 (C=O), 1631 (C=C), 1238 (P=O), 1177 (C-O), 1030 (P-O-Et) cm^{-1} .

3.2.4. Synthesis of Diethyliminodiacetate-Containing Monomers from EHMA, TBHMA and TBEED

3.2.4.1. Synthesis of 2-Chloromethyl-Acryloyl Chloride (CMAC). To TBHMA (20 g, 0.13 mol), excess thionyl chloride (67 ml, 0.92 mol) was added dropwise in an ice-bath, under nitrogen. The mixture was stirred at room temperature for 24 h. Most of the thionyl chloride was evaporated in the rotary evaporator and vacuum distillation of the residue gave the pure product as a clear liquid in 34.0 per cent yield.

$^1\text{H-NMR}$ (CDCl_3): δ = 4.26 (s, 2H, $\text{CH}_2\text{-Cl}$), 6.41 and 6.74 (2H, $\text{CH}_2\text{=C}$) ppm.

$^{13}\text{C-NMR}$ (CDCl_3): δ = 41.99 ($\text{CH}_2\text{-Cl}$), 136.21 (C=CH_2), 141.44 (C=CH_2), 166.90 (C=O) ppm.

FT-IR (neat): 2966 (C-H), 1747 (C=O), 1640 (C=C), 896 (C-Cl) cm^{-1} .

3.2.4.2. Synthesis of ({2-[2-(Bis-Ethoxycarbonylmethyl-Carbamoyl)-Allyloxymethyl]-Acryloyl} Ethoxycarbonylmethyl-Amino)-Acetic Acid Ethyl Ester (TBEED-IDA). To a mixture of TBEED-acid (0.10 g, 0.54 mmol) and 4-dimethylaminopyridine (DMAP) (4.1 mg) in two ml dichloromethane, diethyliminodiacetate (0.21 g, 1.09 mmol) was added dropwise in an ice bath under nitrogen. 1,3-Dicyclohexylcarbodiimid (DCC) (0.24 g, 1.16 mmol) was then added to this solution. The solution was stirred at room temperature for one day. After dilution with 10 ml of chloroform, the solution was cooled to $-20\text{ }^\circ\text{C}$ and the precipitate was filtered off. Then it was extracted three times with water. The organic layer was separated and dried over CaCl_2 . The evaporation of the solvents gave the product as a yellow oil in a 84.8 per cent yield.

$^1\text{H-NMR}$ (CDCl_3): δ = 1.27 (s, 12 H, CH_3), 4.19 (s, 12 H, $\text{O-CH}_2\text{CH}_3$ and N-CH_2), 4.31 (s, 4H, $\text{CH}_2\text{-O}$), 5.31 (s, 2H, $\text{CH}_2\text{=C}$), 5.52 (s, 2H, $\text{CH}_2\text{=C}$) ppm.

$^{13}\text{C-NMR}$ (CDCl_3): δ =14.13 (CH_3), 47.11, 51.06 ($\text{CH}_2\text{-N}$), 61.09, 61.40 ($\text{O-CH}_2\text{CH}_3$), 71.09 ($\text{CH}_2\text{-O}$), 116.97 (C=CH_2), 140.06 (C=CH_2), 168.32, 168.91 (C=O), 171.71 (N-C=O) ppm.

FT-IR (neat): 2982 (C-H), 1745 (C=O, ester), 1654 (C=O, amide), 1629 (C=C), 1459 (C-N), 1184 [C-C(=O)-O] cm^{-1} .

3.2.4.3. Synthesis of 2-[(Bis-Ethoxycarbonylmethyl-Amino)-Methyl]-Acrylic Acid Ethyl Ester (EBBr-IDA). To a solution of EBBr (0.52 g, 2.69 mmol) in diethylether (3.5 ml) in an ice bath, triethylamine (0.28 g, 2.79 mmol) was added dropwise followed by diethyliminodiacetate (0.51 g, 2.71 mmol). After stirring at room temperature for one day, the mixture was extracted with one wt per cent of HCl (3×10 ml) and the aqueous layer was back-extracted with dichloromethane. The organic layers were combined and dried with CaCl_2 . The evaporation of dichloromethane gave the product as a light yellow oil in a 90.8 per cent yield.

$^1\text{H-NMR}$ (CDCl_3): δ = 1.18 (m, 9 H, CH_3), 3.48 (s, 4 H, $\text{N-CH}_2\text{-C=O}$), 3.54 (s, 2H, $\text{CH}_2\text{-N}$), 4.07 (m, 6 H, $\text{O-CH}_2\text{CH}_3$), 5.74 (s, 1H, $\text{CH}_2\text{=C}$), 6.15 (s, 1H, $\text{CH}_2\text{=C}$) ppm.

$^{13}\text{C-NMR}$ (CDCl_3): δ =14.21 (CH_3), 54.82 ($\text{CH}_2\text{-N}$), 60.30 ($\text{O-CH}_2\text{CH}_3$), 126.52 (C=CH_2), 137.53 (C=CH_2), 166,19 (C=O), 170.84 ($\text{CH}_2\text{-C=O}$) ppm.

FT-IR (neat): 2981 (C-H), 1739 (C=O, ester), 1632 (C=C), 1189 [C-C(=O)-O] cm^{-1} .

3.2.4.4. Synthesis of Potassium Salt of 2-[(Bis-Carboxymethyl-Amino)-Methyl]-Acrylic Acid (EBBr-IDA- K^+). To EBBr-IDA (0.57 g 1.89 mmol), equimolar amount of KOH (3.0 ml, 5.66 mmol) was added in an ice bath. The solution was stirred at room temperature for 12 hours. After removal of water, the solid product was purified by dissolving in warm methanol and precipitating into acetone. Yield: 76.62 per cent.

$^1\text{H-NMR}$ (D_2O): δ = 3.10 (s, 4 H, $\text{N-CH}_2\text{-C=O}$), 3.34 (s, 2H, $\text{CH}_2\text{-N}$), 5.39 (s, 1H, $\text{CH}_2\text{=C}$), 5.73 (s, 1H, $\text{CH}_2\text{=C}$) ppm.

$^{13}\text{C-NMR}$ (D_2O): δ =56.11 ($\text{CH}_2\text{-N}$), 58.08 ($\text{CH}_2\text{-C=O}$), 122.47 (C=CH_2), 143.30 (C=CH_2), 176.84 (C=O), 179.78 ($\text{CH}_2\text{-C=O}$) ppm.

FT-IR (neat): 1577 (asymmetrical stretching of carboxylate anion), 1408 (symmetrical stretching of carboxylate anion) cm^{-1} .

3.2.4.5. Synthesis of {[2-(Bis-Ethoxycarbonylmethyl-Carbamoyl)-Allyl]-Ethoxycarbonylmethyl-Amino}-Acetic Acid Ethyl Ester (CMAC-IDA). To a mixture of CMAC (1.66 g,

11.9 mmol) and triethylamine (4.53 g, 44.7 mmol) in 16 ml of THF, diethyliminodiacetate was added dropwise in an ice bath under nitrogen. The mixture was stirred at room temperature for one day. The formed precipitate was filtered off and the solvent was evaporated. The residue was dissolved in 10 ml of dichloromethane and washed twice with 10 ml of water. After the organic phase was dried with CaCl₂, the solvent was removed to obtain the product as a yellow oil in 91.1 per cent yield.

¹H-NMR (CDCl₃): δ= 1.28 (m, 12 H, CH₃), 3.56 (s, 4 H, N-CH₂-C=O), 3.59 (s, 2H, CH₂-N), 4.18 (m, 12 H, O-CH₂CH₃ and N-CH₂), 5.28 (s, 1H, CH₂=C), 5.51 (s, 1H, CH₂=C) ppm.

¹³C-NMR (CDCl₃): δ= 14.22 (CH₃), 47.21, 51.10 (CH₂-N-C=O), 54.68 (N-CH₂), 56.97 (CH₂-N), 60.31, 61.05, 61.36 (O-CH₂CH₃), 116.78 (C=CH₂), 140.71 (C=CH₂), 168.37, 168.95, 170.64 (C=O), 171.62 (N-C=O) ppm.

FT-IR (neat): 2982 (C-H), 1743 (C=O, ester), 1655 (C=O, amide), 1623 (C=C), 1448 (C-N), 1186 [C-C(=O)-O] cm⁻¹.

3.2.4.6. Synthesis of Potassium Salt of {[2-(Bis-Carboxymethyl-Carbamoyl)-Allyl]-Carboxymethyl-Amino}-Acetic Acid (CMAC-IDA-K⁺). To CMAC-IDA (0.75 g, 1.68 mmol), equimolar amount of KOH (3.6 ml, 6.73 mmol) was added in an ice bath and the reaction mixture was stirred at room temperature for 12 hours. After removal of water, the solid product was purified by dissolving in warm methanol and precipitating into acetone. Yield: 58.49 per cent.

¹H-NMR (D₂O): δ= 3.26 (s, 4 H, N-CH₂-C=O), 3.45 (s, 2H, CH₂-N), 3.98, 4.07 (d, 4 H, CH₂-N-C=O), 5.44 (s, 1H, CH₂=C), 5.63 (s, 1H, CH₂=C) ppm.

¹³C-NMR (D₂O): δ=50.77, 54.29 (CH₂-N-C=O), 56.58 (CH₂-N), 58.08 (N-CH₂), 119.15 (C=CH₂), 140.45 (C=CH₂), 173.85 (N-C=O), 175.85, 176.40, 179.46 (C=O), ppm.

FT-IR (neat): 1594 (asymmetrical stretching of carboxylate anion), 1397 (symmetrical stretching of carboxylate anion) cm⁻¹.

3.3 Photopolymerizations

3.3.1. Polymerization Procedure

All the photopolymerizations were carried out by TA Instruments Q 100 Photo-DSC using Irgacure 651 as the photoinitiator (Figure 3.1).

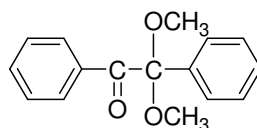


Figure 3.1. 2,2-Dimethoxy-2-phenyl acetophenone (Irgacure 651)

Three to four mg of sample was placed in an uncovered aluminum DSC pan. Then, the photoinitiator which was dissolved in CH_2Cl_2 was added with a micro-syringe to give a final concentration in the monomer of 2.0 mol per cent after evaporation of the solvent. After placing the sample and reference pans to sample compartment, the DSC chamber was purged with nitrogen for 10 min to remove air and CH_2Cl_2 before polymerization and purging was continued during polymerization. The samples were irradiated for 10 minutes at 40 °C or 60 °C with an incident light intensity of 15 mW/cm^2 . The heat flux as a function of time was monitored using DSC under isothermal conditions and both the rates of polymerization (R_p) and conversions were calculated as a function of time. The heat of reaction values, $\Delta H_p = 64.5, 54.5, 57.5, 50$ and 55 kJ/mol , were used as the theoretical heat evolved for methacrylic acid, tert-butyl ester, ethyl ester, 2-hydroxyethyl ester and methyl ester of methacrylic acid double bonds respectively [117]. The rates of polymerizations were calculated according to the following formula:

$$R_p = \frac{(Q/s)M}{n\Delta H_p m}$$

Figure 3.2. Equation of the rate of polymerization

where Q/s is the heat flow per second during reaction, M is the molar mass of the monomer, n is the number of double bonds per monomer molecule, ΔH_p is the heat

released per mole of double bonds reacted and m is the mass of the monomer in the sample [118].

3.3.2. Sample Preparation of the Phosphorus-Containing Cyclopolymerizable Monomers, BC-EPA, EC-EPA, CA-PA, CA-EPA, EC-PA and BC-TEP

First, monomers BC-EPA, EC-EPA, CA-EPA, EC-PA and BC-TEP were homopolymerized at 40 °C but the solid monomer CA-PA could not be photopolymerized at 40 °C due to its high melting point. Monofunctional counterpart of BC-EPA, MBC-EPA containing 40 per cent of BC-EPA was also homopolymerized under the same conditions. Next, all the monomers were copolymerized with HEMA which is the most frequently used monomer in dentistry. The samples were prepared by adding two mole per cent of monomer to HEMA.

3.3.3. Sample Preparation of the Phosphorus-Containing Monomers, TBEP, TBPA, CAPA and CAEP

In this group, copolymerization of the monomers with HEMA was investigated. Bulk photopolymerization of the solid monomer CAPA was not possible at 40 °C due to its high melting point (157 °C). The samples were again prepared by adding two mole per cent of monomer to HEMA.

3.3.4. Sample Preparation of the Diethyliminodiacetate-Containing Monomers, TBEED-IDA, EBBR-IDA and CMAC-IDA

Monomers TBEED-IDA, EBBR-IDA and CMAC-IDA were homopolymerized at 40 °C whereas the solid monomers EBBR-IDA-K⁺ and CMAC-IDA-K⁺ could not be photopolymerized. Also, copolymerization of TBEED-IDA (5, 20 and 50 mol per cent) with TBEED and copolymerization of EBBR-IDA (20 and 50 mol per cent) with HEMA was investigated.

3.4. Bulk or Solution Polymerizations

3.4.1. Polymerization Procedure

For the solution polymerization, the monomers, solvent and the initiator were added in a septum sealed tube, whereas in bulk polymerization no solvent was used. Then the sealed tubes were degassed by means of freeze-thaw cycles before they were placed in a constant temperature bath. After a selected period of time, the viscous polymer solutions were precipitated into nonsolvents. The polymers were filtered and dried under vacuum.

3.4.2. Polymerization of PHOSEED, TBEED and PHOSEED-acid

3.4.2.1. Polymerization of PHOSEED. Homopolymerization of PHOSEED was carried out in bulk at 75-77 °C with 0.5 wt per cent AIBN as an initiator. The purification of the polymer was performed by dissolving in CH₂Cl₂ and precipitating into diethyl ether.

Also, 10, 20 and 50 mole per cent of PHOSEED was copolymerized with TBEED in toluene at 75-77 °C with 0.015 M AIBN. The copolymers TBEED:PHOSEED (70:30) and (50:50) were purified by precipitating into diethyl ether, whereas copolymer TBEED:PHOSEED (90:10) was soluble in ether and was purified by precipitating first into hexane to remove residual TBEED and then into MeOH:H₂O (90:10) to remove PHOSEED.

3.4.2.2. Polymerization of TBEED. TBEED was first polymerized in bulk at 75-77 °C with 0.5 wt per cent AIBN. A crosslinked polymer was obtained in 5 min. Therefore, this monomer was polymerized in toluene at 75-77 °C with 0.015 M AIBN and the polymer was purified by precipitating into hexane in which TBEED was soluble.

3.4.2.3. Polymerization of PHOSEED-acid. The homopolymerization of 2.5 M PHOSEED-acid in DMSO at 70-75 °C with 0.015 M AIBN was unsuccessful. Therefore, PHOSEED-acid was copolymerized with TBEED and carboxylic acid derivative of TBEED (TBEED-acid) in DMSO at 75-77 °C using 0.015 M AIBN. The copolymer of TBEED:PHOSEED-acid (95:5) was purified by precipitating first into hexane, in which

TBEED was soluble, and then into MeOH:H₂O (1:2) to remove the residual acid monomer. The copolymer of TBEED-acid:PHOSEED-acid (95:5) was dissolved in methanol and precipitated into acetone.

3.4.3. Polymerization of BC-EPA, EC-EPA and CA-EPA

3.4.3.1. Polymerization of BC-EPA and EC-EPA. BC-EPA and EC-EPA were polymerized in bulk at 76-78 °C with 0.5 wt per cent AIBN. Also, 2.5 M of these monomers were polymerized in toluene at 76-78 °C with 0.015 M AIBN. The viscous polymers formed were dissolved in dichloromethane and precipitated into hexane to remove the residual monomers.

3.4.3.2. Polymerization of CA-EPA. 1.1 M of CA-EPA was polymerized in toluene at 76-78 °C with 0.015 M AIBN. The purification of the polymer was performed by dissolving in methanol and precipitating into diethyl ether.

3.4.4. Polymerization of EBBR-IDA-K⁺ and CMAC-IDA-K⁺

The solution polymerization of EBBR-IDA-K⁺ and CMAC-IDA-K⁺ with acrylamide (5:95 and 10:90) was run in water in the presence of a water soluble azo initiator (V-50) at 65-67 °C. The total monomer and initiator concentrations were 8.33 M and 0.042 M respectively. The polymer solutions were precipitated into acetone and dried over P₂O₅. Then, purification of the copolymer was performed by dissolution in water and dialysis against water with tubing with a molecular cutoff of 6000-8000. The polymer was recovered by freeze drying.

3.5. Binding Capacity of Phosphorus-Containing Cyclopolymerizable Monomers, CA-PA and EC-PA

The binding capacity of the acidic monomers CA-PA and EC-PA was evaluated first by determining the pH dependencies of the chemical shifts of the corresponding groups in the monomers and then calculating the interacted amount of acidic groups in the monomers with the calcium ion in the HAP.

3.5.1. Determination of the pH Dependencies of the Chemical Shifts of the Carbonyl Carbon and α -Methylene Carbon in CA-PA

0.1913 g of CA-PA (0.569 mmol) was dissolved into 2.5 g of 20 mass per cent of deuterium oxide aqueous solution. Deuterated DMSO was used as an external standart. After the pH value of the solution was measured, the ^{13}C -NMR spectrum was observed. Then, the solution was titrated with 1.77 M sodium hydroxide. After each addition of sodium hydroxide, pH values were measured and the ^{13}C -NMR spectra were obtained. The pH dependencies of the chemical shifts of the carbonyl carbon and α -methylene carbon were plotted to obtain a titration curve for CA-PA. The chemical shift differences corresponding to complete dissociations of the acid groups were determined.

3.5.2. Interacted Amounts of Carboxylic Acid and Phosphonic Acid in CA-PA with the Calcium in the HAP

0.100 g of CA-PA (0.298 mmol) was dissolved into 1.25 g of 20 mass per cent of deuterium oxide aqueous solution. Deuterated DMSO was used as an external standart. The pH value of the solution was measured and ^{13}C -NMR spectrum was obtained. The hydroxyapatite (25 and 50 mg) was then added to this solution. After the suspensions were kept at an ultrasonic bath at 37 °C for one hour, the pH values were measured and the ^{13}C -NMR spectra were obtained. The chemical shift values of the α -methylene carbon assigned to the phosphonic acid and carbonyl carbon assigned to carboxylic acid were determined. The interacted amounts of the carboxylic acid and phosphonic acid with the calcium ion in the HAP were calculated by dividing each shift differences by the corresponding shift differences of total dissociation, as determined by the procedure in section 3.5.1.

3.5.3. Determination of the pH Dependency of the Chemical Shifts of α -Methylene Carbon in EC-PA

0.212 g of EC-PA (0.540 mmol) was dissolved into 2.5 g of 20 mass per cent of deuterium oxide aqueous solution. After the pH value of the solution was measured, the ^{13}C -NMR spectrum was observed. Then, the solution was titrated with 1.65 M sodium hydroxide. After each addition of sodium hydroxide, pH values were measured and the ^{13}C -NMR spectra were obtained. The pH dependencies of the chemical shifts of the α -methylene carbon were plotted to obtain a titration curve for EC-PA. The chemical shift differences corresponding to complete dissociations of the phosphonic acid groups were determined.

3.5.4. Interacted Amount of Phosphonic Acid in EC-PA with the Calcium in the HAP

0.100 gr of EC-PA (0.255 mmol) was dissolved into 1.25 g of 20 mass per cent of deuterium oxide aqueous solution. Deuteriated DMSO was used as an external standart. The pH value of the solution was measured and ^{13}C -NMR spectrum was obtained. The hydroxyapatite (25 and 50 mg) was then added to this solution. After the suspensions were kept at an ultrasonic bath at 37 °C for one hour, the pH values were measured and the ^{13}C NMR spectra were obtained. The chemical shift values of the α -methylene carbon assigned to the phosphonic acid were determined. The interacted amounts phosphonic acid with the calcium in the HAP were calculated by dividing each shift differences by the corresponding shift differences of total dissociation, as determined by the procedure in section 3.5.3.

3.6. Chelating Ability of Diethyliminodiacetate-Containing Monomers, EBBr-IDA- K^+ and CMAC-IDA- K^+

The chelating ability of EBBr-IDA-K⁺ and CMAC-IDA-K⁺ was investigated using UV-visible spectroscopy at 500-900 nm where the monomer has no absorption. First 9.6*10⁻³ M of NiCl₂ and 9.6*10⁻³ M of EBBr-IDA-K⁺ stock solutions were prepared and maximum absorption value for Ni⁺² was obtained. Then, EBBr-IDA-K⁺ stock solution was diluted to 2.4*10⁻³, 4.8*10⁻³ and 7.2*10⁻³ M and mixed with NiCl₂ stock solution in a 1:1 ratio. Also, 6.16*10⁻³ M of CMAC-IDA-K⁺ stock solution was prepared, diluted to 4.62*10⁻³, 3.08*10⁻³ and 1.54*10⁻³ M and mixed with 6.16*10⁻³ M of NiCl₂ stock solution in a 1:1 ratio. As EBBr-IDA-K⁺ or CMAC-IDA-K⁺ was added to the Ni⁺² solution, the maximum absorption values and the corresponding wavelengths were recorded.

4. RESULTS AND DISCUSSION

4.1. Synthesis of Phosphorus-Containing Cyclopolymerizable Monomers from 2-(2-tert-Butoxycarbonyl-Allyloxymethyl)-Acrylic Acid tert-Butyl Ester (TBEED)

In this part, the synthesis and characterization of two new phosphorus-containing 2,6-disubstituted 1,6-heptadiene monomers, their cyclopolymerization and copolymerization behaviour were described. In addition, thermal properties, molecular weights and glass transition temperatures of cyclic homo- and copolymers were investigated. We have chosen cyclopolymers because they have certain advantages like high glass transition temperatures, excellent thermal stabilities and less shrinkage during polymerization. These properties are also important for dental materials, so the purpose was to combine the advantageous properties of cyclopolymers with the adhesion properties of phosphorus compounds.

4.1.1. Synthesis of Monomers

The ether dimer of tert-butyl α -hydroxymethyl acrylate (TBEED), its carboxylic acid and acid chloride derivatives were successfully synthesized using the procedures described in the literature [34]. The acid chloride derivative of TBEED was reacted with diethyl hydroxymethyl phosphonate in the presence of TEA as catalyst in THF at 60 °C (Figure 1). The phosphonate ester derivative (PHOSEED) was obtained as a yellow oily liquid in 91 per cent yield. This procedure gave a very small amount of the hydrolyzed phosphonate ester monomer which was removed by precipitation into diethyl ether.

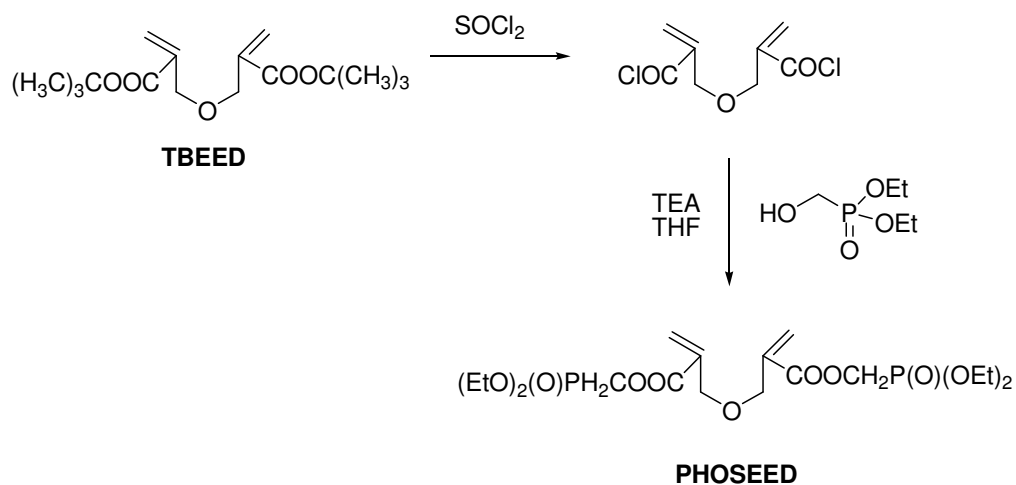


Figure 4.1. Synthesis of PHOSEED

The ^{13}C -NMR spectrum of the monomer showed characteristic peaks for a methyl carbon at 16.8 ppm, methylene carbons of ethyl ester at 63.1 ppm, methylene carbons attached to phosphorus atom at 56.4 and 58.1 (doublet) ppm, methylene carbons attached to double bond carbons at 69.0 ppm, double bond carbons at 127.5 and 136.1 ppm, and a carbonyl carbon at 164.5 ppm (Figure 4.2).

In the ^1H -NMR spectrum, methyl protons at 1.12 ppm, methylenes of ethyl ester at 3.95 ppm, ether methylenes at 4.03 ppm, methylene protons attached to phosphorus atom at 4.24 ppm and double bond protons at 5.76 and 6.15 ppm were characterized (Figure 4.3).

The FT-IR spectrum showed characteristic peaks for carbonyl, double bond, $\text{P}=\text{O}$ and $\text{P}-\text{O}-\text{C}$ at 1722, 1637, 1248 and 1023 cm^{-1} (Figure 4.4).

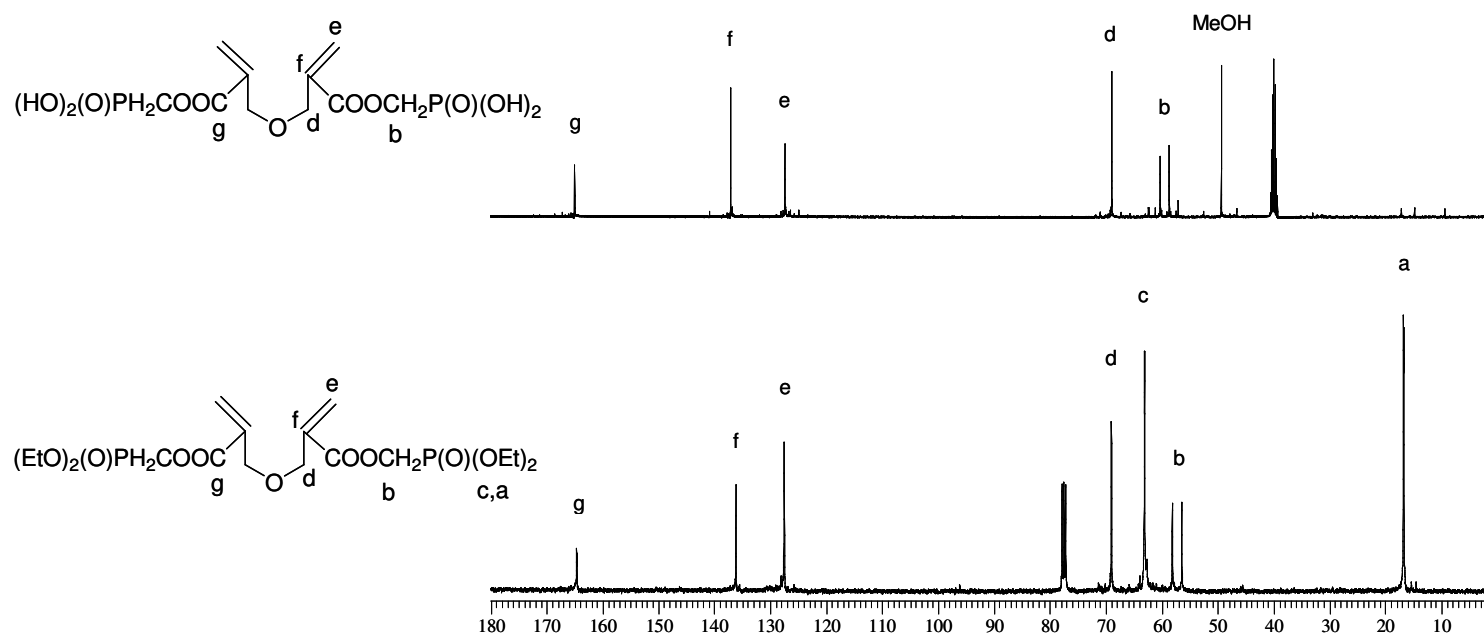
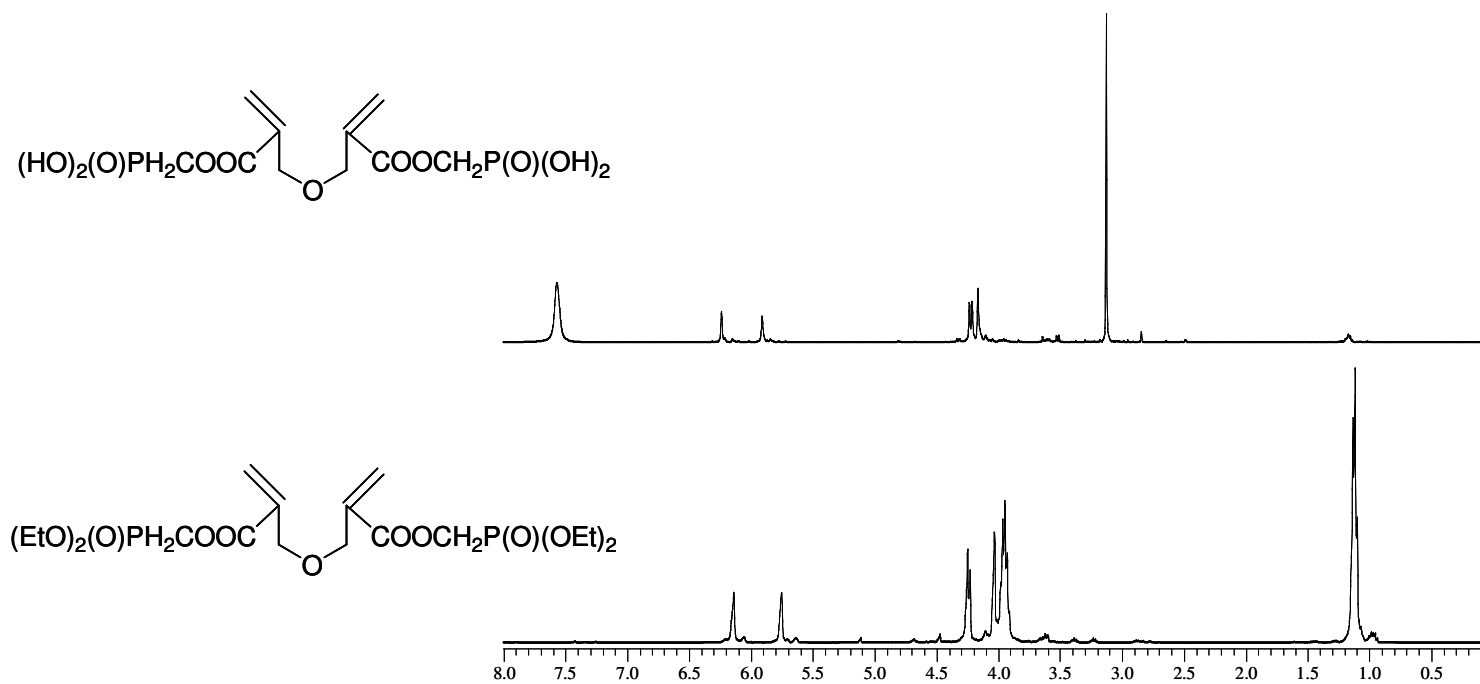


Figure 4.2. ^{13}C -NMR spectra of PHOSEED and PHOSEED-acid

Figure 4.3. $^1\text{H-NMR}$ spectra of PHOSEED and PHOSEED-acid

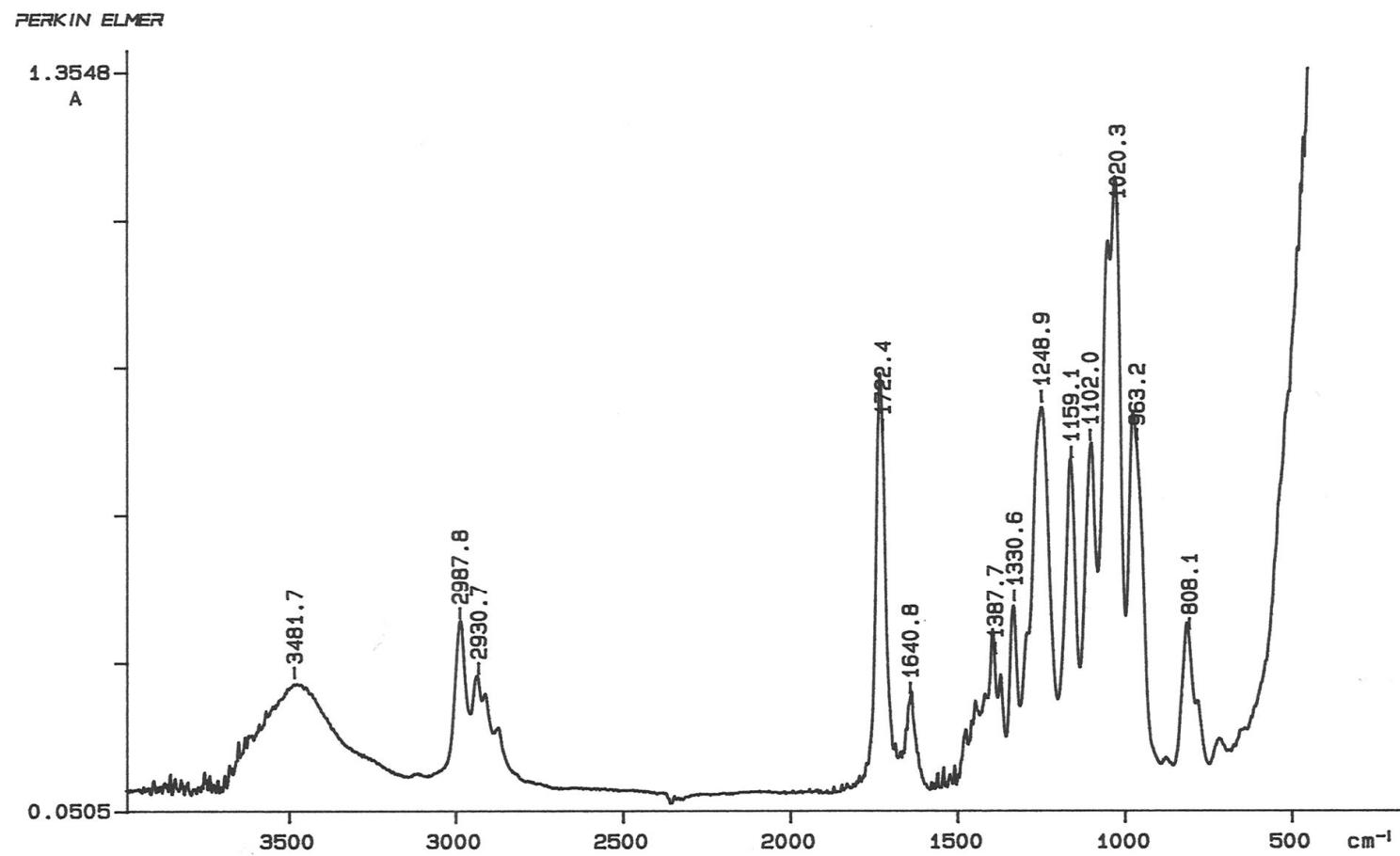


Figure4.4. FT-IR spectrum of PHOSED

The silylation of the phosphonate monomer with TMSiBr, followed by methanolysis of the silyl derivative, gave a phosphonic acid monomer (PHOSEED-acid) as a dark yellow very viscous liquid in 72 per cent yield (Figure 4.5). This monomer was soluble in water, methanol and DMSO but insoluble in ether, acetone, CHCl₃, THF and hexane.

Solubility in water is very important for dental applications. This acidic monomer has the potential to remove the smear layer and demineralize dentin and enamel. However, phosphonic acid groups attached to the double bonds through ester links may undergo hydrolysis in water.

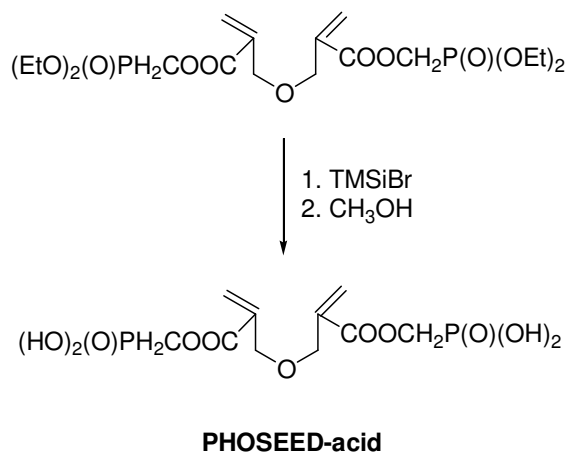


Figure 4.5. Synthesis of PHOSEED-acid

Both ¹³C-NMR and ¹H-NMR spectra showed a complete disappearance of the ethyl groups of the phosphonate ester (Figures 4.2 and 4.3).

The FT-IR spectrum showed a broad peak between 3500 and 2300 cm⁻¹ due to phosphonic acid group of the hydrolyzed monomer, ester carbonyl at 1724 cm⁻¹, C=C stretching peak at 1632 cm⁻¹, and P=O vibrations at 1251 cm⁻¹.

4.1.2. Polymerization

In the cyclopolymerization of the ether dimers of α -hydroxymethyl acrylates, the bulky ester substituents were found to increase the cyclization efficiency [34]. For example, TBEED gives soluble cyclopolymer containing six-membered rings in the polymer backbone. Bulk polymerization of PHOSEED in the presence of 0.5 wt per cent AIBN at 75-77 °C gave soluble polymers (Figure 4.6). This monomer showed high homopolymerization rate with yield of 28 per cent in 90 min (Table 4.1). Polymerization yield had to be lower than 30 per cent or there had to be crosslinking. The polymer was soluble in acetone, THF, CHCl_3 , CH_2Cl_2 and insoluble in diethyl ether and water. The purification of the polymer was performed by dissolving in CH_2Cl_2 and precipitation into diethyl ether. Solubility of the homopolymer in common solvents indicated the formation of highly cyclized polymers. The high cyclization efficiency of this monomer was probably due to the presence of bulky phosphonate group near the double bond which sterically inhibits intermolecular reaction and favoring intramolecular cyclization.

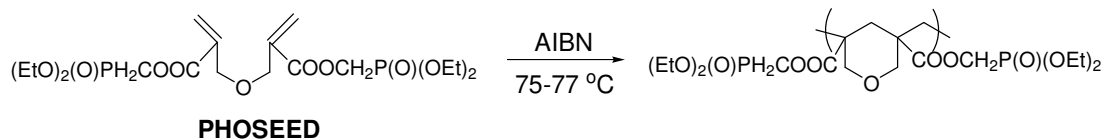


Figure 4.6. Polymerization of PHOSEED

The $^1\text{H-NMR}$ spectrum of the polymer showed methyl hydrogens at 1.37 ppm, methylene hydrogens of the backbone at 1.75 ppm and all other methylene hydrogens overlap around 4.0-4.5 ppm (Figure 4.7). No pendant double bond could be detected. The $^1\text{H-NMR}$ spectrum of the homopolymer did not provide sufficient data to determine if the repeating units consist of five or six-membered rings. It was assumed that the polymers contain six membered ring units similar to poly-TBEED.

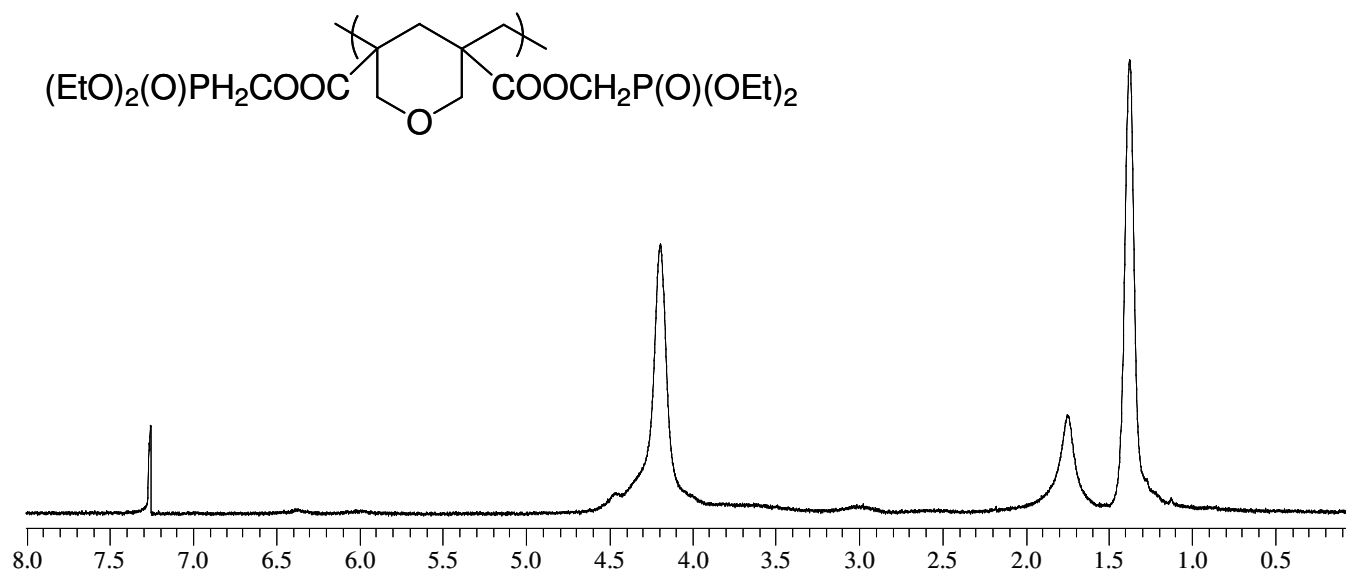
Figure 4.7. ^1H -NMR spectrum of poly-PHOSEED

Table 4.1. Polymer characterization results

Monomers	PHOSEED in the Feed (mol %)	PHOSEED in the Copolymer (mol %)	Solvent	Yield (%)	Time (min)	M_n	M_w
TBEED ^a	-	-	toluene	19.7	15	286,360	1,280,720
TBEED ^b	-	-	-	crosslinked	5	-	-
PHOSEED ^b	100	100	-	28	90	-	-
PHOSEED ^b	100	100	-	20.0	70	9,770	12,440
TBEED:PHOSEED ^a	10	9.0	toluene	15.0	15	130,300	352,160
TBEED:PHOSEED ^a	30	22.0	toluene	16.5	30	131,960	198,400
TBEED:PHOSEED ^a	50	35.0	toluene	20.0	40	34,370	56,200
TBEED:PHOSEED-acid ^a	5	4.0	DMSO	15.5	100	37,690	76,950
TBEED-acid: PHOSEED-acid ^a	5	-	DMSO	9.0	60	crosslinked	-

^a[M]= 2.5 M; [AIBN]= 0.015 M

^b bulk polymerization [AIBN]= 0.5 wt per cent

Temperature= 75-77 °C

The phosphonate monomer (PHOSEED) was also copolymerized with TBEED at different ratios in toluene at 75 °C with 0.5 wt per cent AIBN (Figure 4.8). The copolymers TBEED/PHOSEED (70:30) and (50:50) were isolated by precipitation into diethyl ether, whereas copolymer TBEED/PHOSEED (90:10) was soluble in ether and was purified by precipitation first into hexane to remove residual TBEED and then into MeOH/H₂O (90:10) to remove PHOSEED. The yields were 15, 16,5 and 20 per cent for the copolymers of TBEED/PHOSEED (90:10, 70:30 and 50:50). Table 4.1 shows the copolymerization conditions and characteristics of the resulting polymers. The copolymer compositions were determined from integrated ¹H-NMR spectra with the ratio of peak areas of tert-butyl protons (1.37 ppm) of the TBEED to the peak areas of methylene protons of PHOSEED around 3.8-4.5 ppm. The results shown in Table 4.1 confirm the incorporation of PHOSEED in the copolymers.

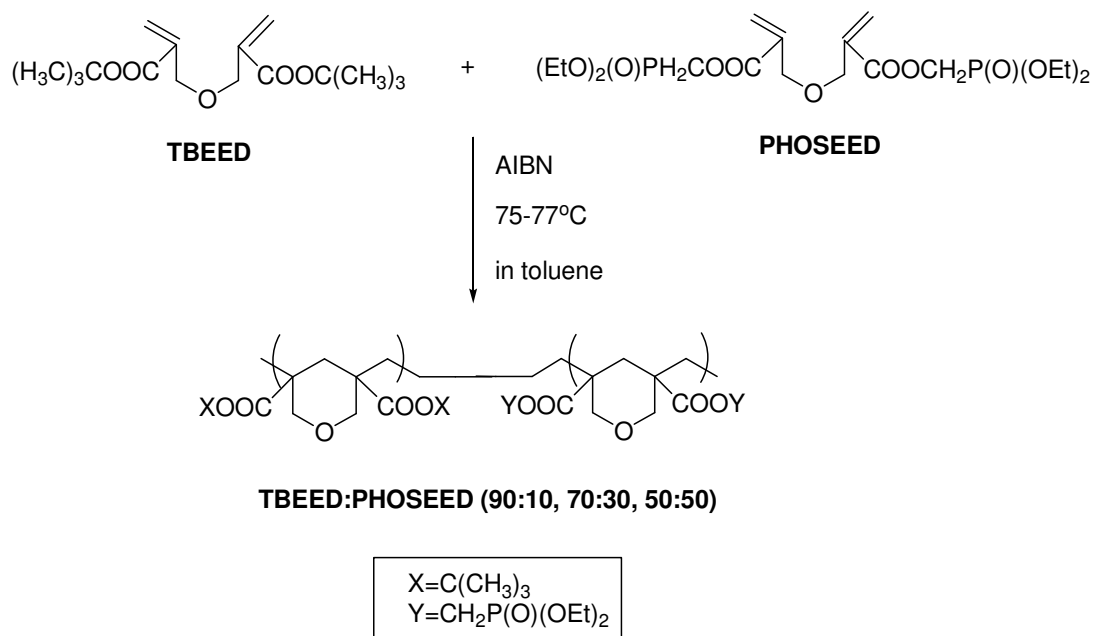


Figure 4.8. Copolymerization of PHOSEED with TBEED

For comparison, TBEED was also homopolymerized under the same conditions (Figure 4.9). Rate of polymerization for this monomer was higher than PHOSEED and gave crosslinked polymers in 5 min. Therefore, this monomer was polymerized in toluene and conversions were kept below 30 per cent to prevent crosslinked polymer formation

(Table 4.1). This polymer was soluble in THF, CH_2Cl_2 and acetone and insoluble in hexane and methanol and purified by precipitation into hexane in which TBEED was soluble.

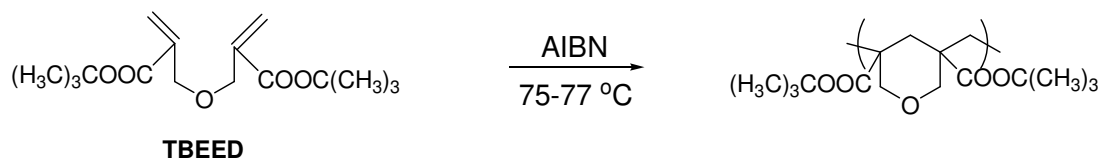


Figure 4.9. Polymerization of TBEED

The $^1\text{H-NMR}$ of the homopolymer showed tert-butyl hydrogens, backbone methylene hydrogens and methylenes attached to ether oxygens at 1.5, 1.93 and 3.66 ppm.

The polymerization of the PHOSEED-acid at 70-75 °C with AIBN was unsuccessful probably due to chain transfer. Therefore, PHOSEED-acid was copolymerized with the TBEED (Figure 4.10) and carboxylic acid derivative of TBEED (TBEED-acid) in DMSO using AIBN. The copolymer of TBEED/PHOSEED-acid (95:5) was purified by precipitation first into hexane, in which TBEED was soluble, and then into methanol/water (1:2) to remove the residual acid monomer. Conversion of 15.5 per cent was obtained in 100 min (Table 4.1). The $^1\text{H-NMR}$ spectrum of the copolymer TBEED/PHOSEED-acid (95:5) showed tert-butyl hydrogens of TBEED, backbone methylenes and methylenes attached to ether oxygens of PHOSEED at 1.45, 1.65, and 4.0-4.3 ppm.

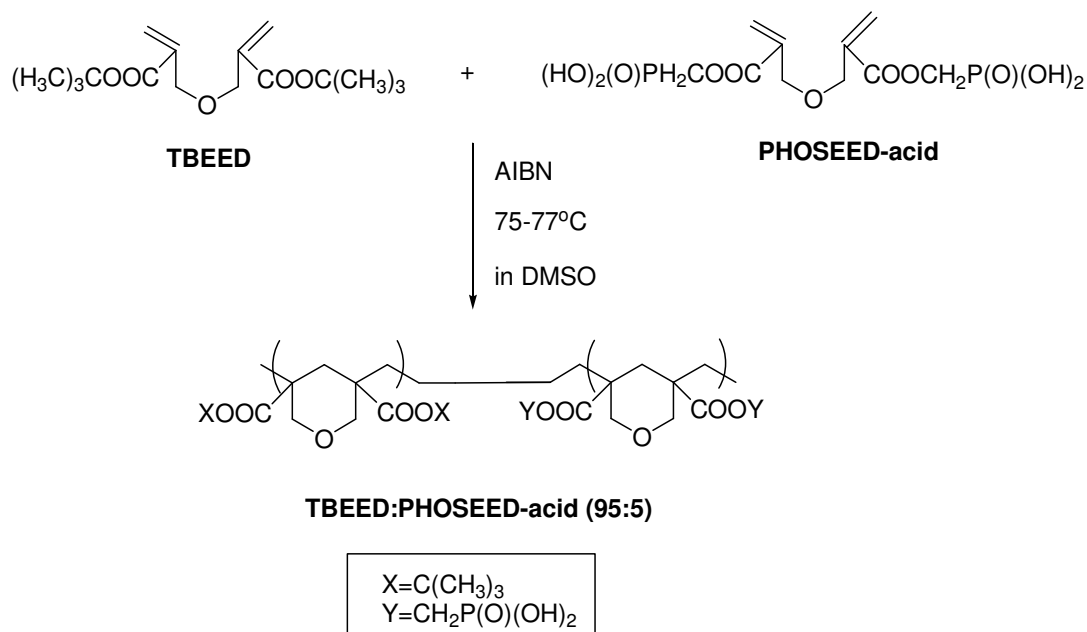


Figure 4.10. Copolymerization of PHOSEED-acid with TBEED

The copolymerization of the carboxylic acid derivative of TBEED with PHOSEED-acid resulted in soluble polymers with 9 per cent yield in 60 min. after first precipitation. However, this copolymer became insoluble on storage. This may be due to residual pendant double bonds or anhydride formation which led to formation of crosslinked polymer.

4.1.3. GPC Results

The number average molecular weight (M_n) and the weight average molecular weight (M_w) for the homopolymer of PHOSEED were 9800 and 12440, as estimated by size exclusion chromatography (Table 4.1). These values were much lower than those of the homopolymer of TBEED ($M_n=286000$, $M_w=1280000$). This difference in molecular weight was probably due to chain transfer to the CH_2 group attached to the phosphonate ester. In our previous work, bulk polymerization of a similar monomer diethyl hydroxymethyl phosphonate derivative of α -(chloromethyl)acryloyl chloride with 0.5 wt per cent AIBN at 60 °C gave a polymer with number average molecular weight of around 12000.

The molecular weights of the copolymers were lower than the homopolymer of TBEED but higher than that of the homopolymer of PHOSEED. For, example, M_n vales of TBEED/PHOSEED (90:10), TBEED/PHOSEED (70:30) and TBEED/PHOSEED (50:50) copolymers were 130300, 131900 and 34400, respectively.

4.1.4. DSC Results

The DSC analysis of the homopolymer of TBEED showed a T_g value of 155 °C (Figure 4.11). The incorporation of phosphorus resulted in a decrease of T_g and gave a value of 44 °C for the homopolymer of PHOSEED. The T_g values of the copolymers were between the T_g values of the two homopolymers: 93, 105 and 148 °C for TBEED/PHOSEED (50:50), TBEED/PHOSEED (70:30) and TBEED/PHOSEED (90:10), respectively.

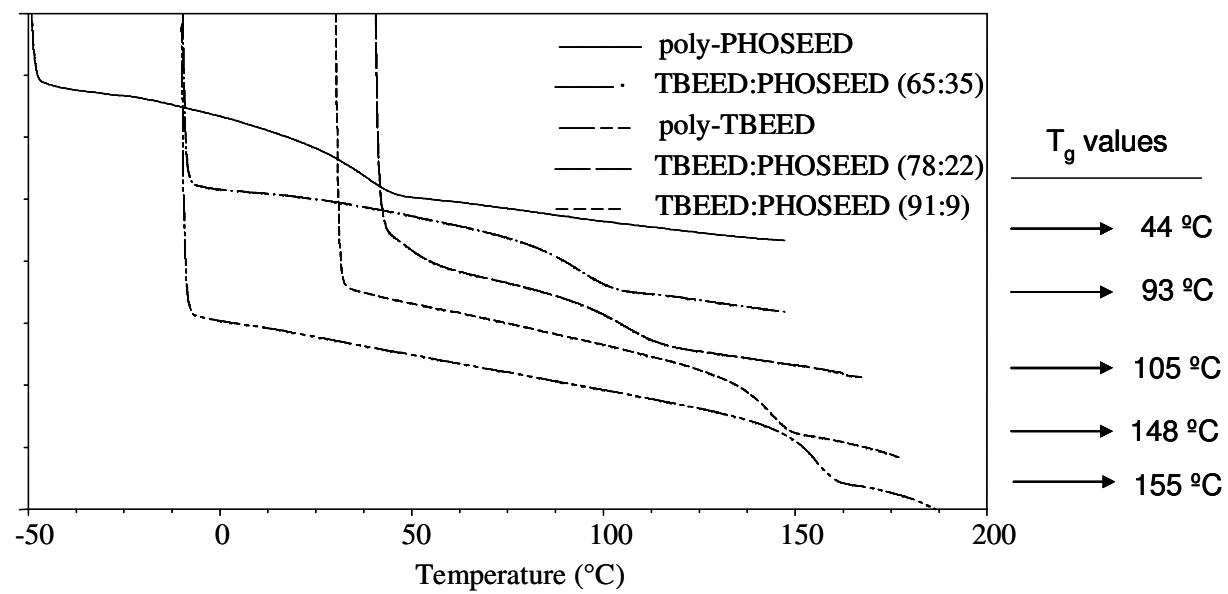


Figure 4.11. DSC curves of PHOSEED:TBEED copolymers

4.1.5. TGA Results

The thermal stabilities and thermal degradation behaviour of the homopolymers and copolymers were investigated by TGA under nitrogen (Figure 4.12).

TBEED homopolymer and its copolymers started to lose weight around 200 °C due to decomposition of the tert-butyl ester group. The char residues increased on the incorporation of PHOSEED. For example, the copolymer TBEED/PHOSEED (70:30) gave a char residue of 31 per cent, whereas the char residue for the copolymer TBEED/PHOSEED (50:50) was 35 per cent, respectively. The homopolymer of PHOSEED was stable until 275 °C and gave the highest amount of residue (36 per cent) at 580 °C.

The TGA of the copolymer TBEED/PHOSEED-acid (95:5) resulted in two step weight loss at 200 and 400 °C and a char yield of 26 per cent at 580 °C.

In general, phosphorus-containing flame retardants promote the production of a thermally stable char layer and thus prevent heat and oxygen transfer. Therefore, the char produced during decomposition of phosphorus-containing compounds improves the thermal stability and increases the decomposition activation energy. This prevents further polymer degradation and combustion of the material. So, the increased char yields on the incorporation of PHOSEED, provided evidence of the likely improvement in the fire performance of the polymers.

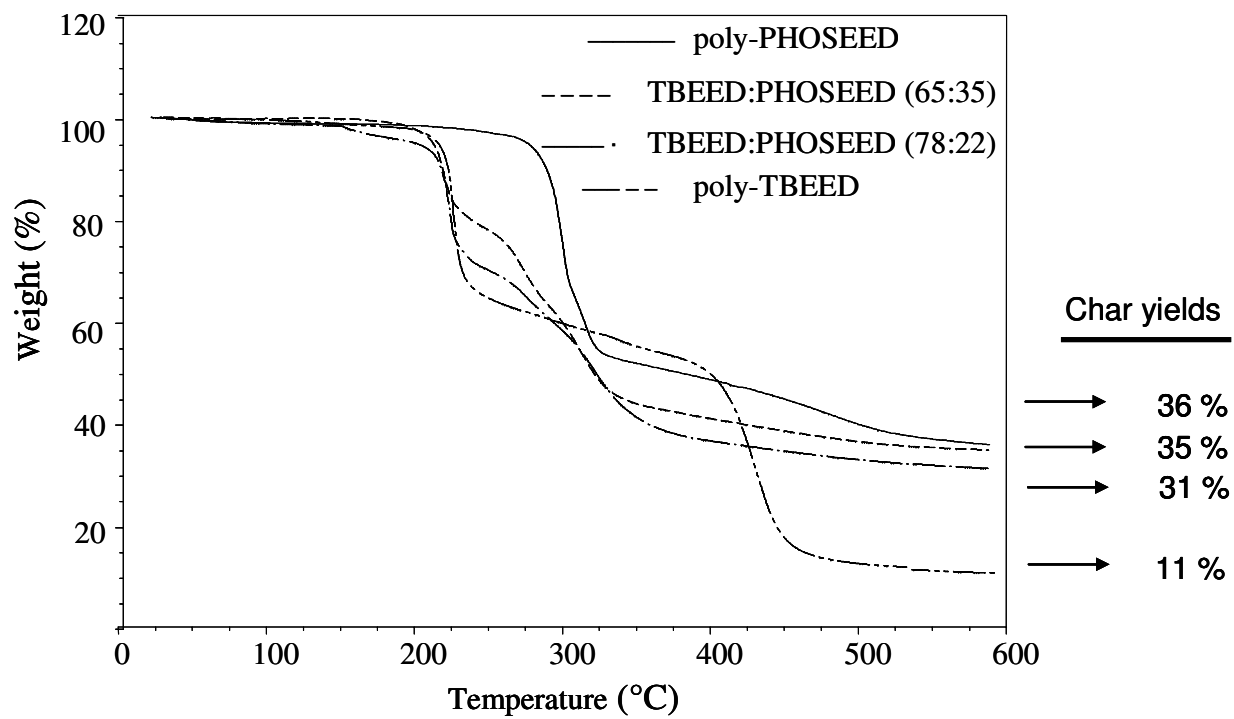


Figure. 4.12. TGA curves of PHOSEED:TBEED copolymers

4.2. Synthesis of Phosphorus-Containing Cyclopolymerizable Monomers from *tert*-Butyl α -Hydroxymethyl Acrylate (TBHMA) and Ethyl α -Hydroxymethyl Acrylate (EHMA)

In this part, we investigated (i) the effect of monomer structure on the homo- and copolymerizability (ii) interaction with the tooth component, HAP, of some cyclic monomers which are expected to have properties desired for self-etching dental adhesives such as high rate of polymerization and copolymerization, stability, low polymerization shrinkage, solubility in water and ethanol, biocompatibility, ability to etch the enamel surface and interact with dental tissues (Figure 4.13).

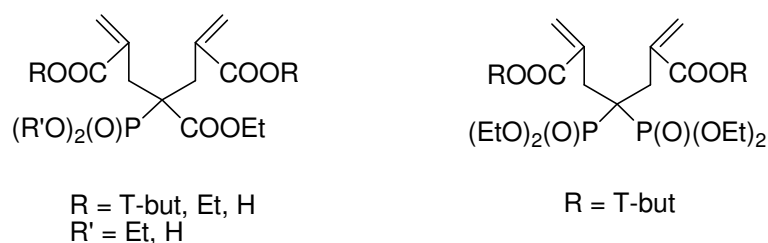


Figure 4.13. General structures of the monomers

4.2.1. Synthesis of BC-EPA, CA-PA and CA-EPA

Triethyl phosphonoacetate was first converted to its carbanion with NaH in dry THF on ice, then alkylation was done with TBBr. After purification of the final product by column chromatography a very pale yellow liquid was obtained in 89.6 % yield. The synthesis of BC-EPA and its two derivatives, CA-PA and CA-EPA were shown in Figure 4.14.

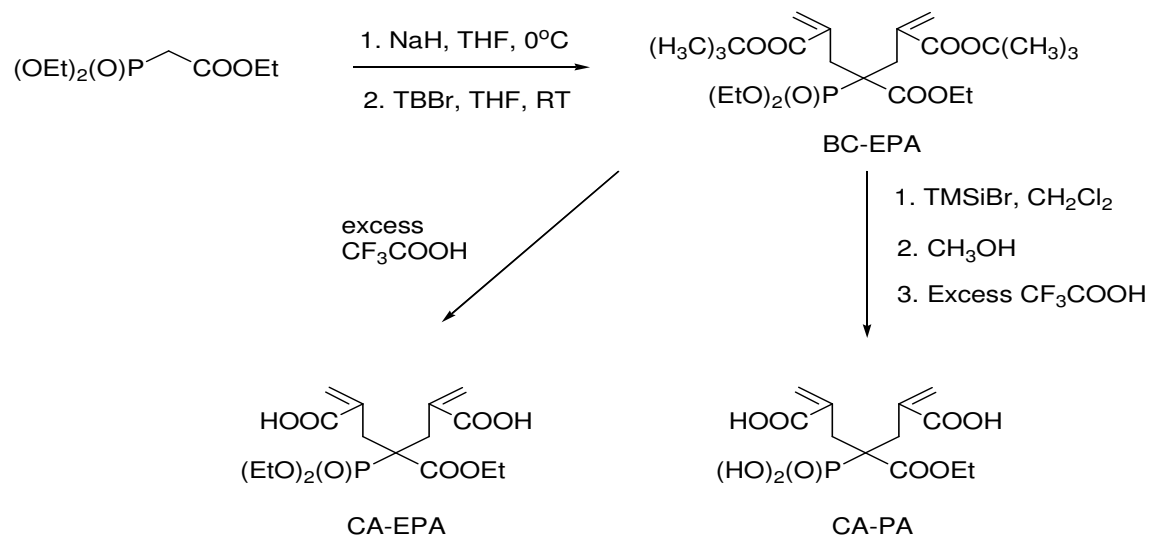


Figure 4.14. Synthesis of BC-EPA, CA-PA and CA-EPA

The ^{13}C -NMR spectrum of BC-EPA showed characteristic peaks for methyl carbons of ethyl ester, phosphonate ester and t-butyl ester at 14.36, 16.79 and 28.39 ppm respectively, methylene carbons attached to double bond carbons at 34.34 ppm, methylene carbon attached to phosphorus atom at 52.36 and 53.76 ppm (doublet), methylene carbons of ethyl ester and phosphonate ester at 61.87 and 62.88 ppm respectively, tertiary carbon of t-butyl ester at 80.78 ppm, double bond carbons at 127.37 and 137.71 ppm and carbonyl carbons of t-butyl ester and ethyl ester at 166.40 and 170.24 ppm (Figure 4.15).

In the ^1H -NMR spectrum of BC-EPA, methyl protons of ethyl ester and phosphonate ester at 1.28 ppm, methyl protons of t-butyl ester at 1.44 ppm, allylic protons at 2.80 and 3.01 ppm, methylenes of ethyl ester and phosphonate ester at 4.10 ppm, double bond protons at 5.57 and 6.12 ppm were characterized (Figure 4.16).

The FT-IR spectrum of BC-EPA showed characteristic peaks for C-H, C=O of ethyl ester, C=O of t-butyl ester, double bond, P=O and P-O-C at 2977, 1725, 1710, 1627, 1253 and 1054 cm^{-1} (Figure 4.17).

Hydrolysis of the t-butyl ester groups of BC-EPA with trifluoroacetic acid gave CA-EPA as a very viscous liquid in 62.2 % yield (Figure 4.14). The ^{13}C -NMR spectrum showed that tert-butyl ester carbons at 28.39 ppm and 80.78 ppm in BC-EPA disappeared in CA-EPA (Figure 4.15). In the ^1H -NMR spectrum, methyl protons of the tert-butyl ester group at 1.44 ppm disappeared in CA-EPA (Figure 4.16). The FT-IR spectrum of CA-EPA showed a broad peak between 3500 and 2000 cm^{-1} due to carboxylic acid group (Figure 4.18).

CA-PA derivative can be obtained by first, silylation of BC-EPA with TMSiBr, followed by methanolysis of the silyl derivative and then hydrolysis of the tert-butyl ester group by mixing with trifluoroacetic acid (Figure 4.14). CA-PA containing both phosphonic acid and carboxylic acid functionalities was obtained as a white solid in 36.1 % yield. The product started to decompose at 192 °C before melting. Both ^{13}C -NMR and ^1H -NMR spectra of CA-PA showed that, peaks due to the phosphonate ester in CA-EPA disappeared (Figure 4.15 and 4.16). In the FT-IR spectrum a broad peak between 3500 and 2000 cm^{-1} was present due to acid groups (Figure 4.19).

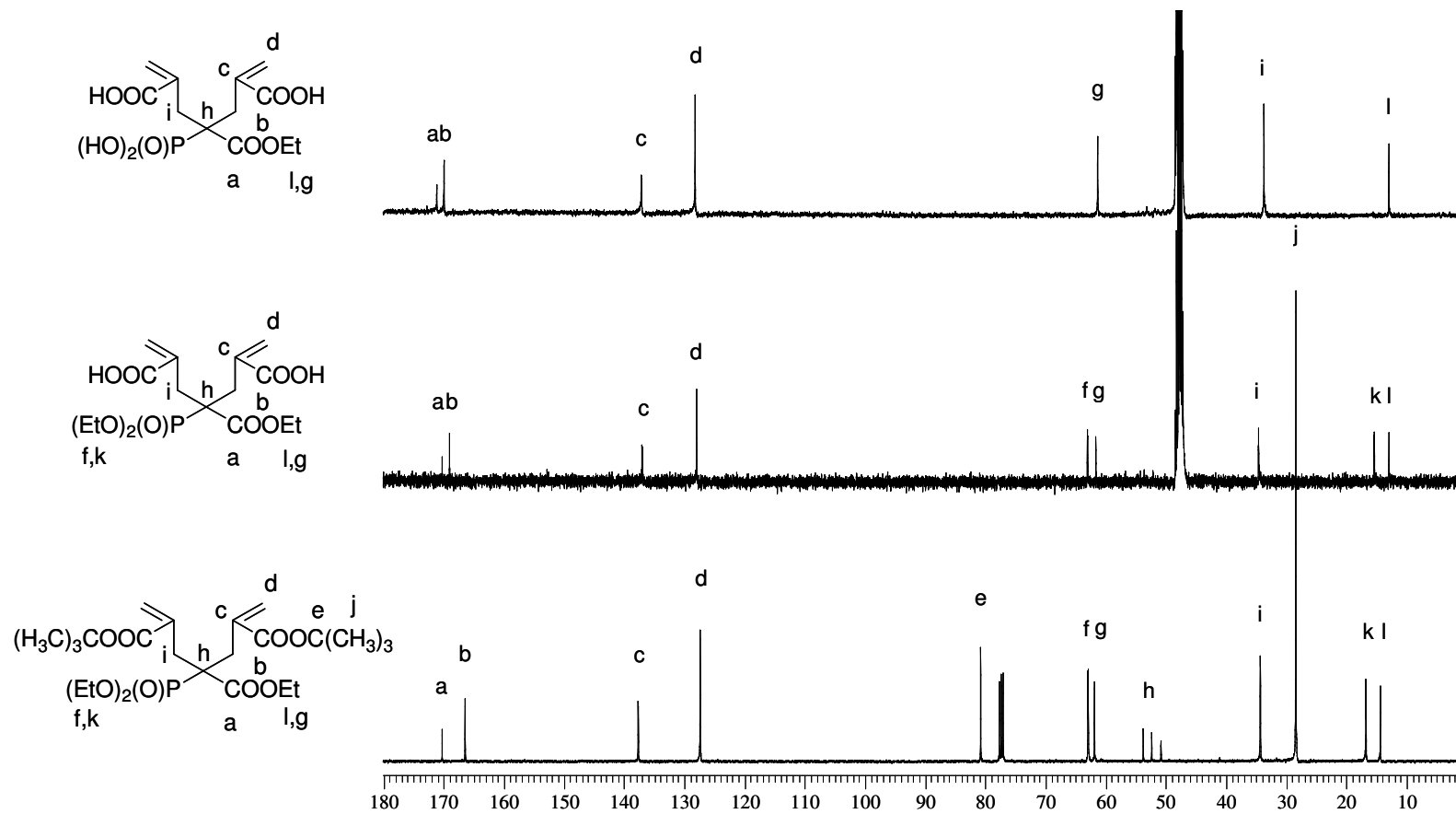


Figure. 4.15. ^{13}C -NMR spectra of BC-EPA, CA-PA and CA-EPA

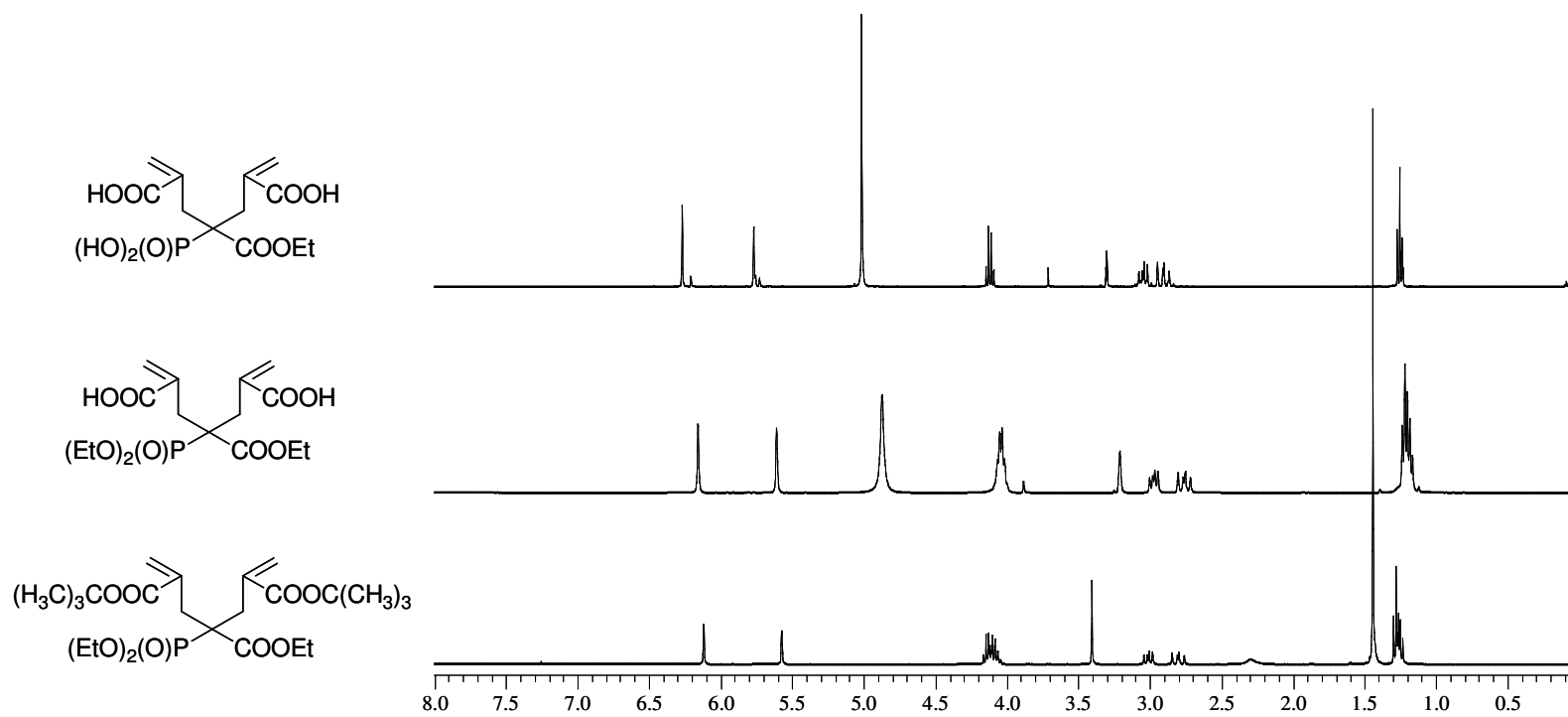


Figure 4.16. $^1\text{H-NMR}$ spectra of BC-EPA (bottom), CA-PA (middle) and CA-EPA (top)

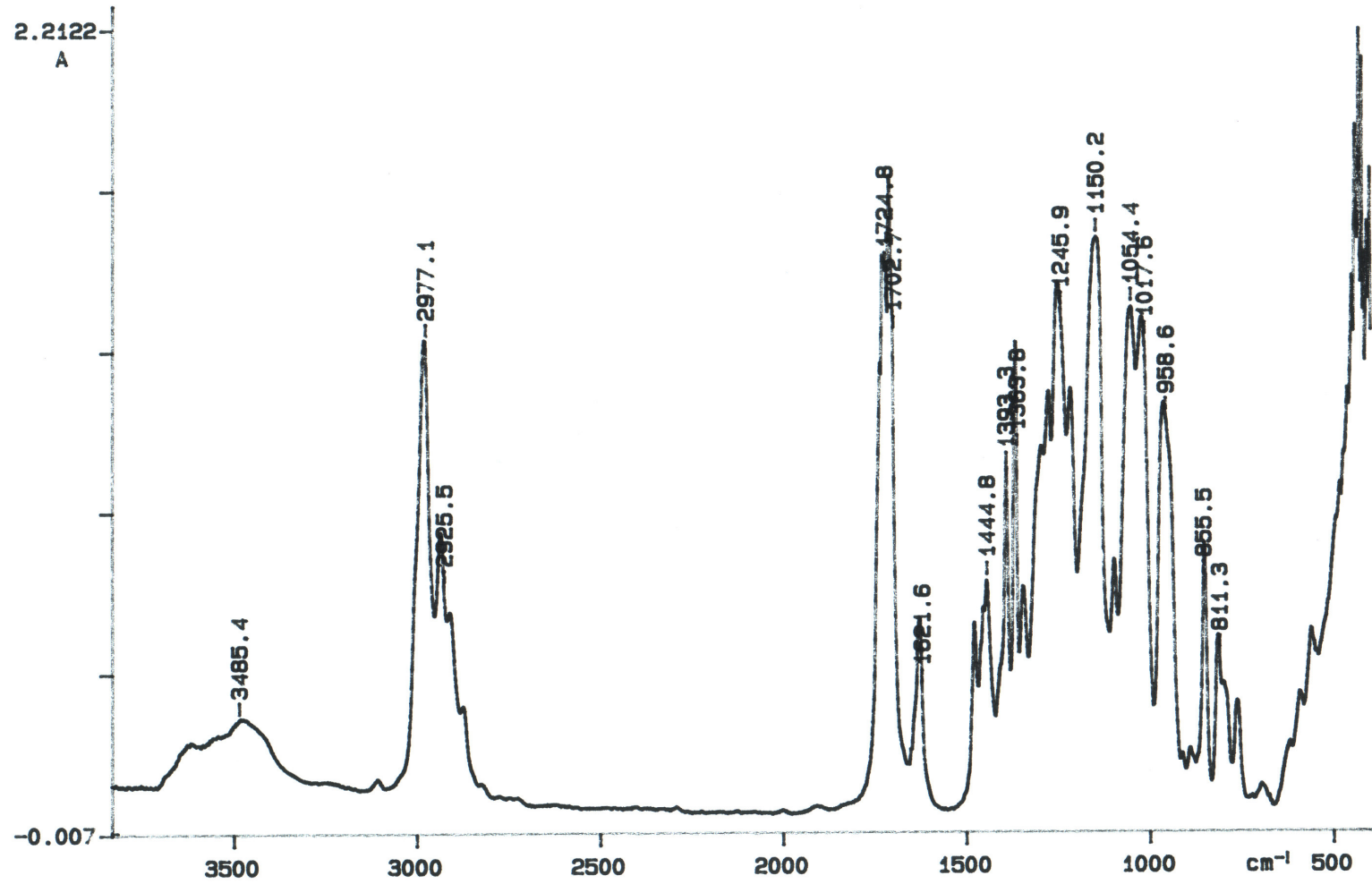


Figure 4.17. FT-IR spectrum of BC-EPA

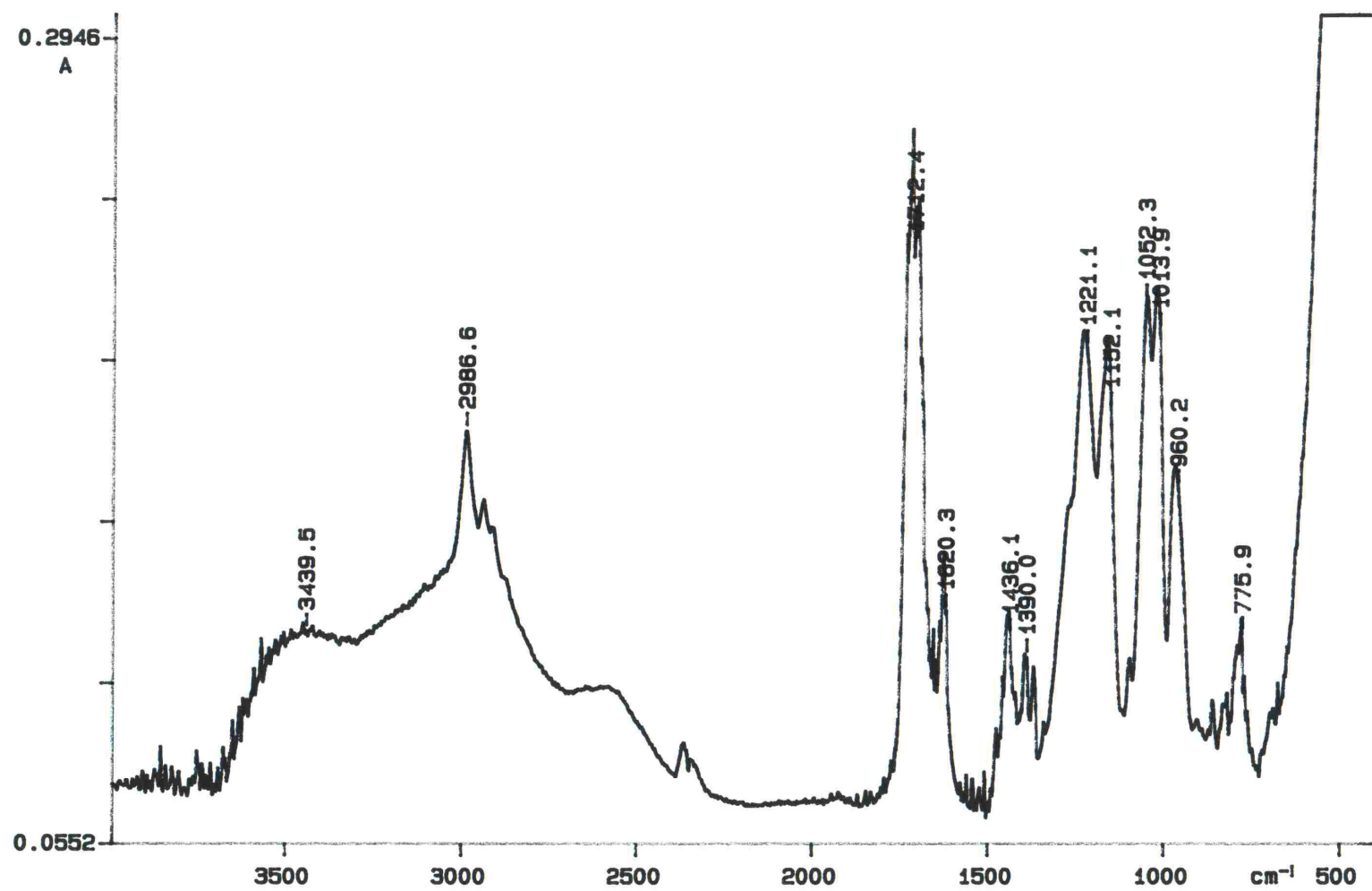


Figure 4.18. FT-IR spectrum of CA-EPA

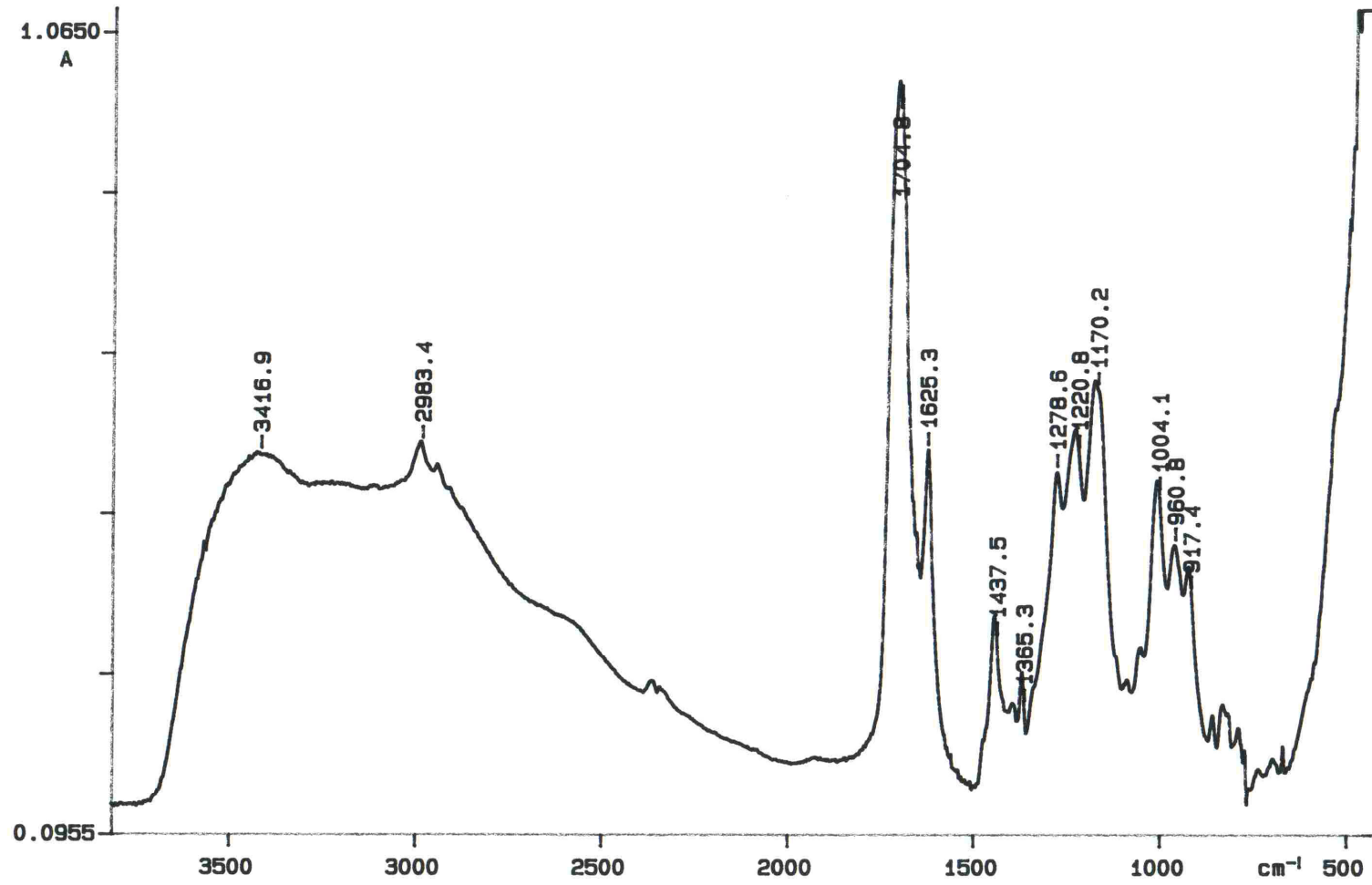


Figure 4.19. FT-IR spectrum of CA-PA

4.2.2. Synthesis of EC-EPA, EC-PA and BC-TEP

EC-EPA was synthesized using the same procedure for BC-EPA using EBBBr instead of TBBBr. The final product was purified by column chromatography to give a colorless liquid in 63.5 % yield. The synthesis of EC-EPA and its derivative, EC-PA were shown in Figure 4.20.

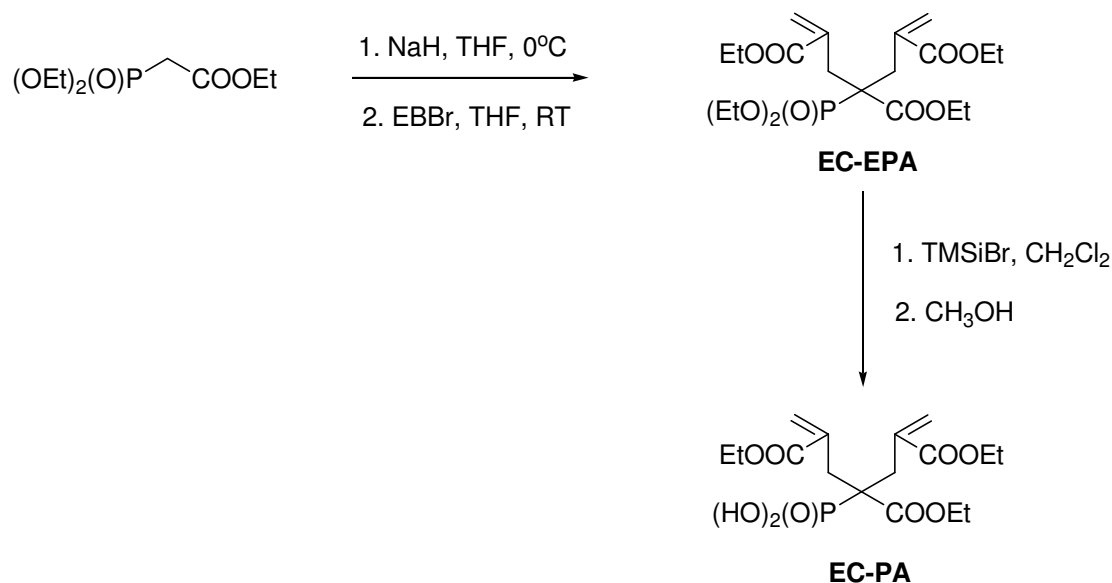


Figure 4.20. Synthesis of EC-EPA and EC-PA

The ^{13}C -NMR spectrum of the monomer showed characteristic peaks for methyl carbons of ethyl ester and phosphonate ester at 14.37 and 16.58 ppm respectively, methylene carbons attached to double bond carbons at 34.41 ppm, methylene carbon attached to phosphorus atom at 52.28 and 53.68 ppm (doublet), methylene carbons of ethyl esters and phosphonate ester at 60.96, 61.73 and 62.74 ppm, double bond carbons at 128.22 and 136.68 ppm and carbonyl carbons at 167.37 and 170.41 ppm (Figure 4.21).

In the ^1H -NMR spectrum, methyl protons at 1.26 ppm, allylic protons at 2.86 and 3.05 ppm, methylenes of ethyl ester and phosphonate ester at 4.13 ppm, double bond protons at 5.65 and 6.22 ppm were characterized (Figure 4.22).

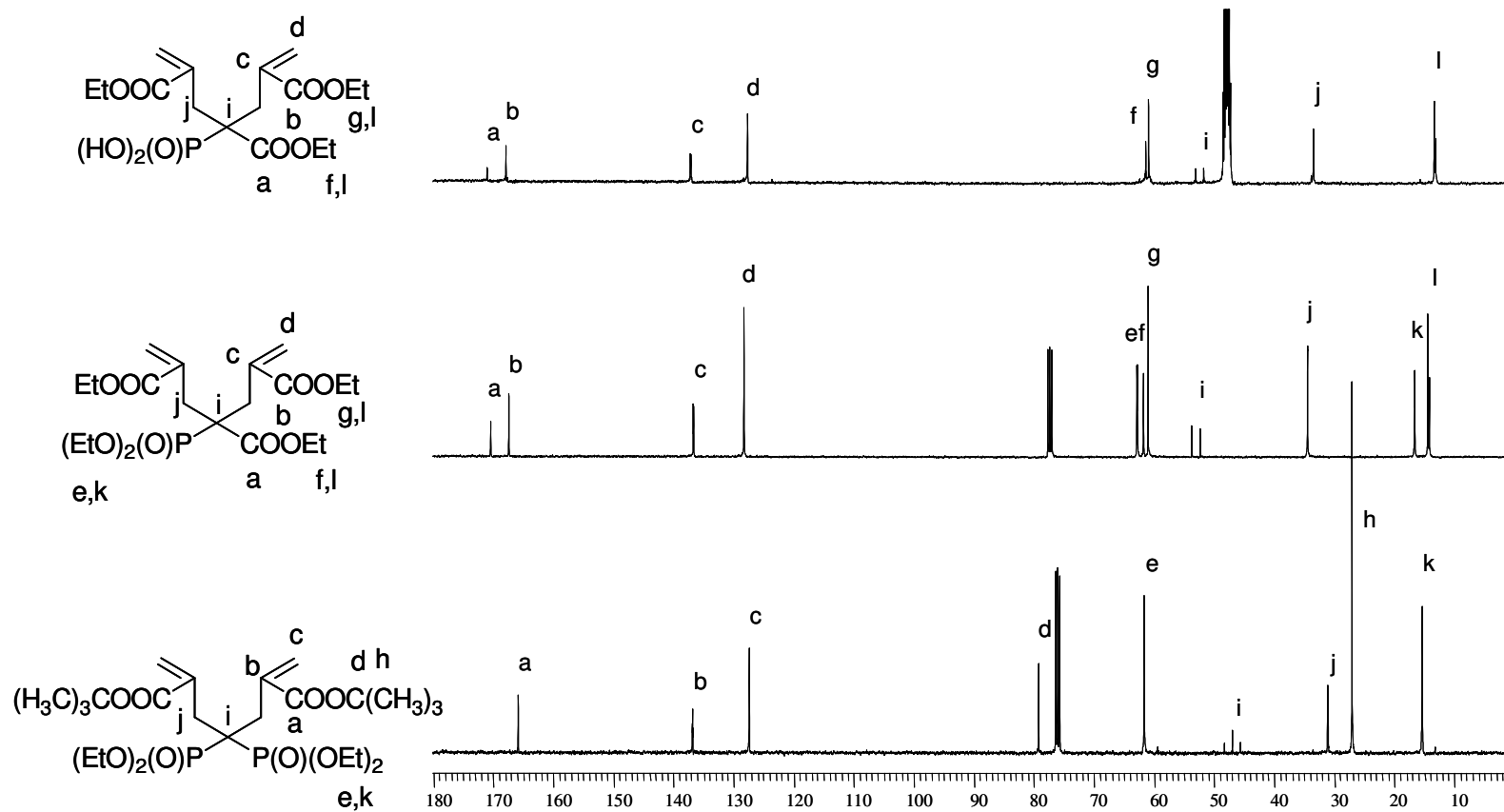


Figure 4.21. ^{13}C -NMR spectra of BC-TEP, EC-EPA and EC-PA

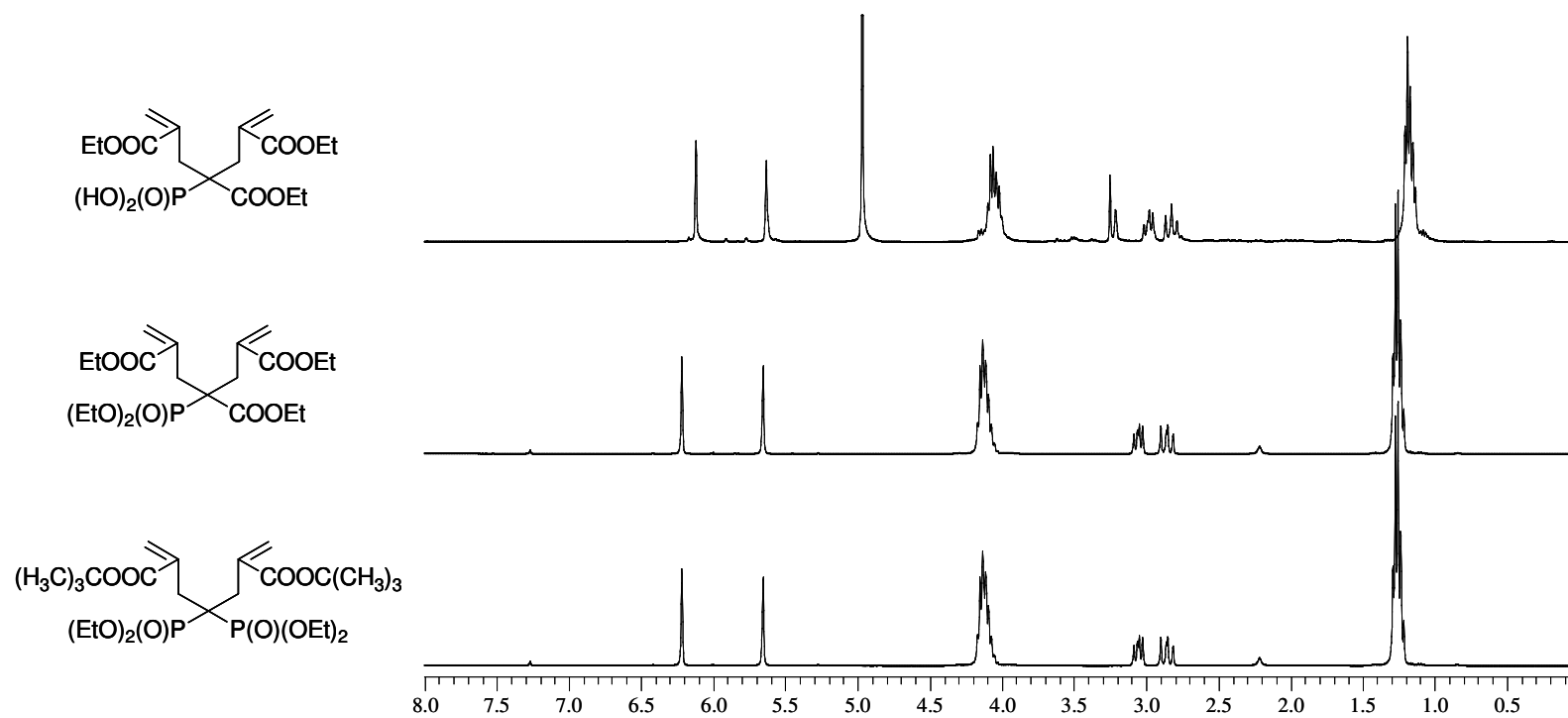


Figure 4.22. $^1\text{H-NMR}$ spectra of BC-TEP (bottom), EC-EPA (middle) and EC-PA (top)

The FT-IR spectrum of EC-EPA showed characteristic peaks for C-H, C=O, double bond, P=O and P-O-C at 2983, 1738-1714, 1626, 1246 and 1058 cm^{-1} (Figure 4.23).

The silylation of EC-EPA with TMSiBr, followed by methanolysis of the silyl derivative, gave a phosphonic acid containing monomer EC-PA as a yellowish brown viscous liquid in 83.8 % yield. Both ^{13}C -NMR and ^1H -NMR spectra of EC-PA showed the disappearance of the peaks due to phosphonate ester in EC-EPA (Figure 4.21 and 4.22). The FT-IR spectrum showed a broad peak between 3500 and 2000 cm^{-1} due to phosphonic acid group (Figure 4.24).

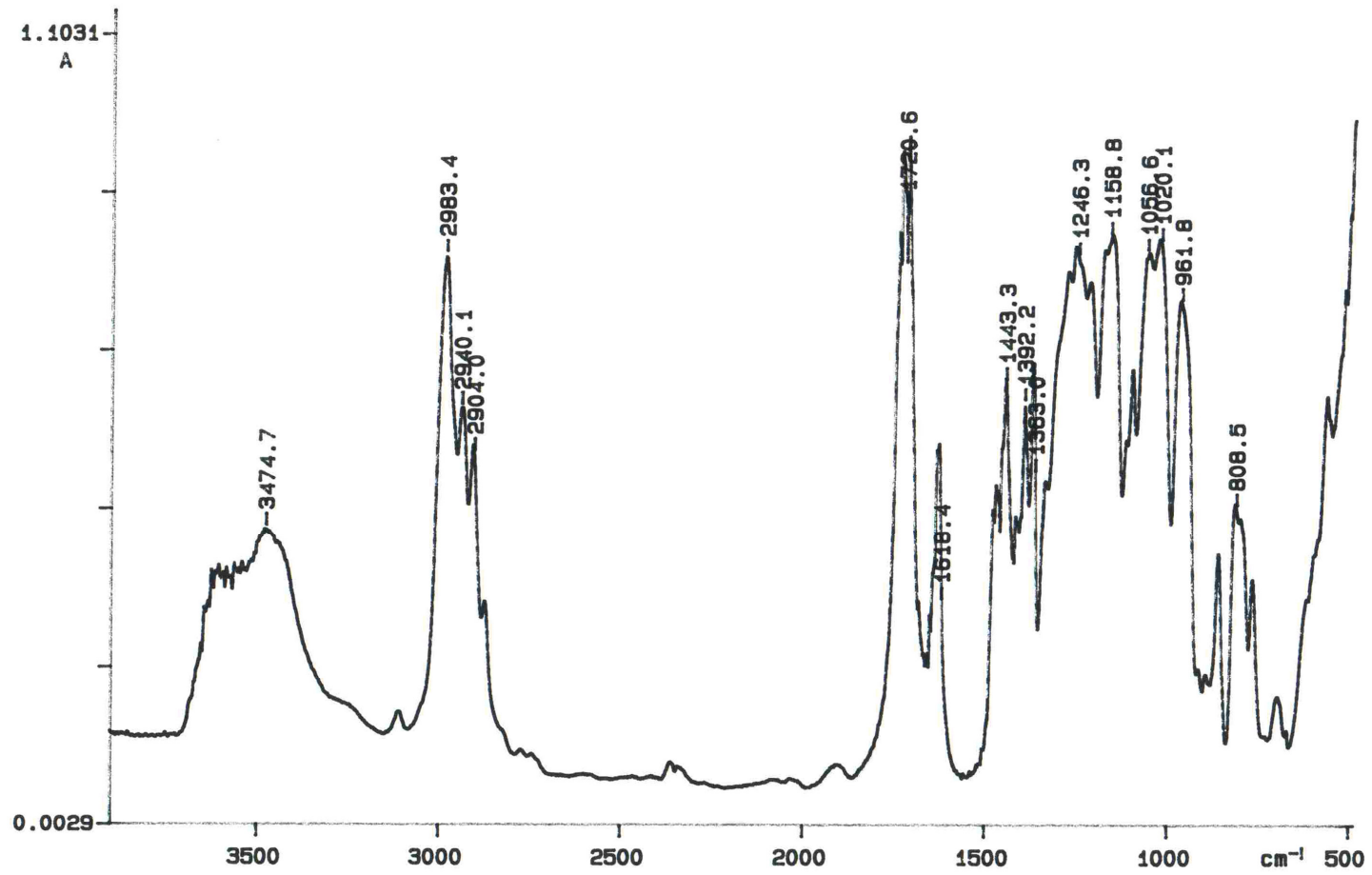


Figure 4.23. FT-IR spectrum of EC-EPA

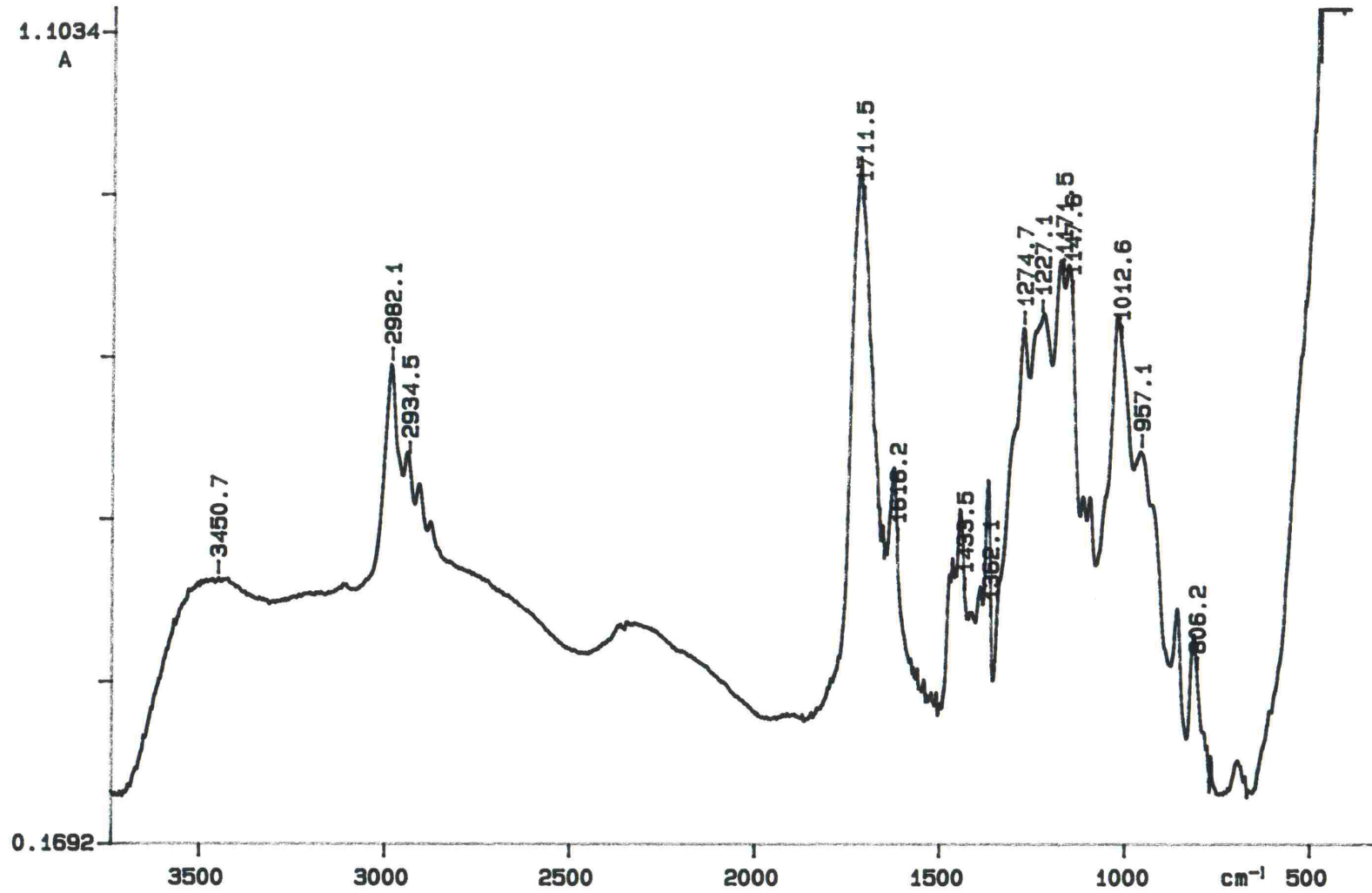


Figure 4.24. FT-IR spectrum of EC-PA

BC-TEP was synthesized similar to BC-EPA, except that tetraethyl methylenephosphonate was used instead of triethyl phosphonoacetate (Figure 4.25). Purification was done by column chromatography and a colorless liquid was obtained as a pure product in 60.0 % yield.

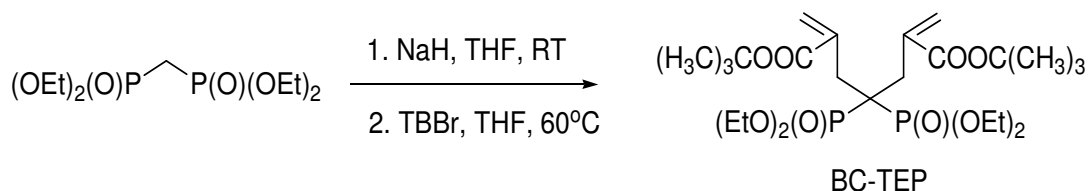


Figure 4.25. Synthesis of BC-TEP

The ^{13}C -NMR spectrum of the monomer showed peaks for methyl carbons of phosphonate ester and t-butyl ester at 15.34 and 27.02 ppm respectively, methylene carbons attached to double bond carbons at 31.04 ppm, methylene carbon attached to phosphorus atom at 45.62, 46.93 and 48.24 ppm (triplet), methylene carbons of phosphonate ester at 61.62 ppm, tertiary carbon of t-butyl ester at 79.19 ppm, double bond carbons at 127.38 and 136.82 ppm and carbonyl carbons at 165.85 ppm (Figure 4.21).

In the ^1H -NMR spectrum, methyl protons of phosphonate ester at 1.25 ppm, methyl protons of t-butyl ester at 1.43 ppm, allylic protons at 2.93 ppm, methylenes of phosphonate ester at 4.09 ppm, double bond protons at 5.76 and 6.12 ppm were characterized (Figure 4.22)

The FT-IR spectrum showed characteristic peaks for C-H, C=O, double bond, P=O and P-O-C at 2978, 1715, 1247, 1028 cm^{-1} respectively (Figure 4.26).

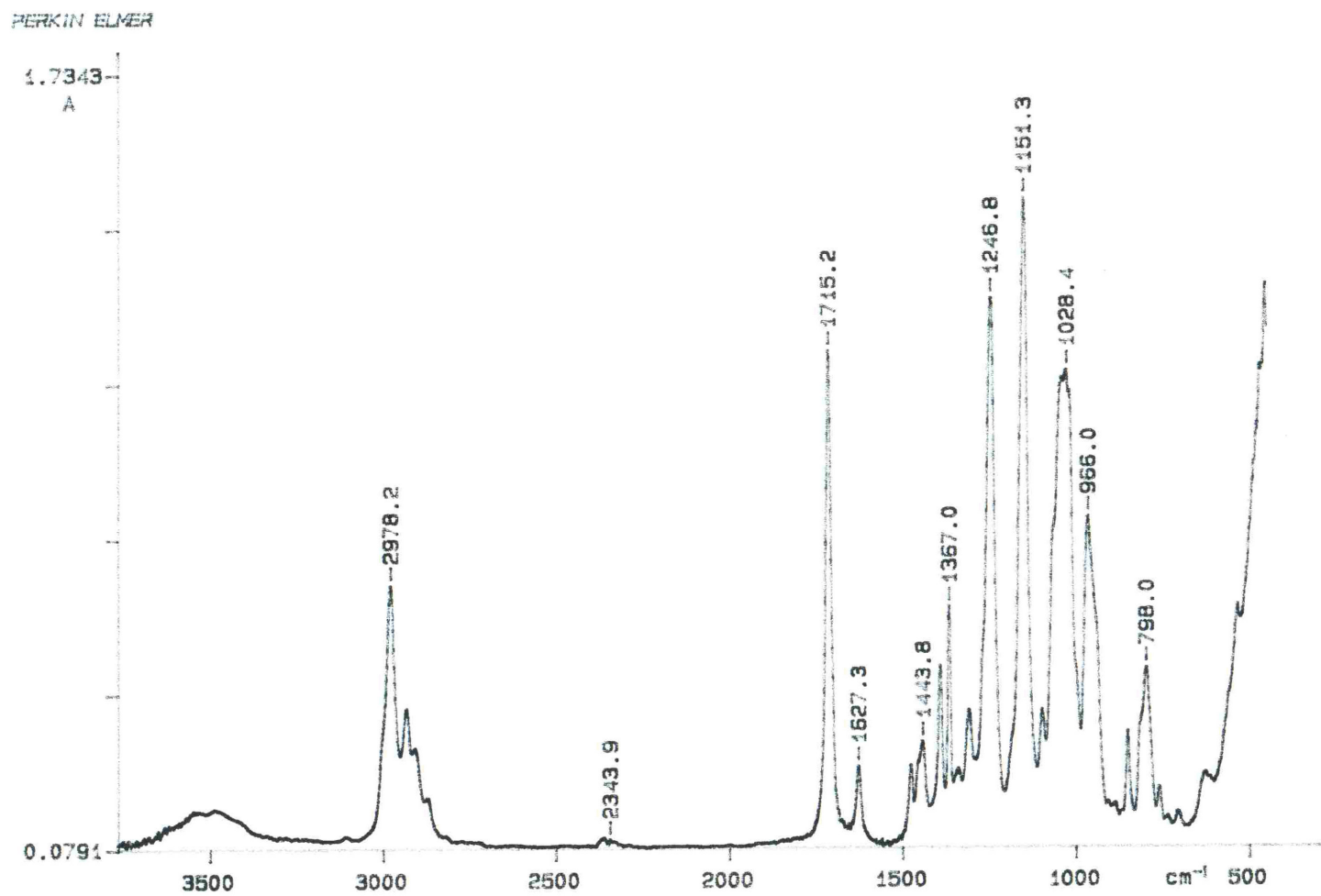


Figure 4.26. FT-IR spectrum of BC-TEP

4.2.7 Photopolymerizations

Earlier study on cyclopolymerization of α,α' -dimethylenepimelates **7**, ether dimer of RHMAAs **8** and dimethacrylmalononitrile **9** having the general formula shown in Figure 4.27, showed that these monomers are excellent cyclomonomers, giving high polymerization rates, high cyclization efficiencies, low polymerization shrinkages, and high thermal stabilities for the resulting cyclopolymers [107, 109].

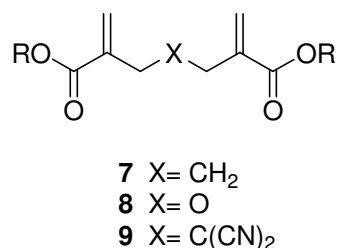


Figure 4.27. General formula for cyclopolymerizable diacrylates

In this study, we investigated the effect of ester groups where R= H, ethyl or t-butyl and the effect of substituents that are on the same central carbon (X= C(COOEt)(PO(OEt)₂), C(COOEt)(PO(OH)₂), C(PO(OEt)₂)(PO(OEt)₂)) on the reactivities of the synthesized monomers in photopolymerization with photo-DSC.

We can attempt to predict the polymerization behavior of our monomers based on the studies done by Kodaïre and Mathias et al [101, 106]. There, it is proposed that unconjugated dienes with both high cyclization tendency and high polymerizability can be obtained by the use of functional groups with no homopolymerization tendency along with a highly conjugative nature. For example 1,6-heptadienes with conjugated C=C and C=O bonds from α -substituted acrylates will have high polymerizabilities even though their monofunctional counterparts do not polymerize due to steric effects. The steric effects at 2,6-positions will inhibit the intermolecular propagation reaction to favor intramolecular reaction and will therefore give rise to highly cyclized polymers. Also, the conjugation between the C=C and C=O bonds of α -substituted acrylates will make them reactive toward radical attacks. Thus, the electron withdrawing substituents will enhance the polymerizability by increasing

conjugation. Furthermore, the inductive and steric effect of the substituents at 4-position of 1,6-dienes are important for the polymerizability of these monomers. For instance, the bulky substituents will decrease the polymerizability due to steric effect. Also, electron withdrawing allyl substituent will increase polymerizability decreasing the degradative chain transfer by strengthening α -CH₂ bonds. The monofunctional counterpart of our monomers will have no homopolymerization tendencies, because acrylates with α -substituents greater than methyl are not polymerizable.

In order to confirm this last behavior we also tried to synthesize the monofunctional counterpart of BC-EPA from the same reaction using 1:1 ratio of TBBr to triethyl phosphonoacetate. MBC-EPA containing 40 % of BC-EPA was obtained as a colorless liquid after the column chromatography on silica gel using CH₂Cl₂ initially and gradually changing to 7% methanol in CH₂Cl₂ as eluent.

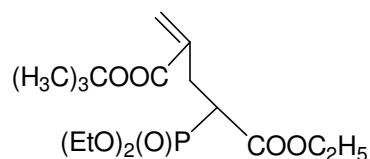


Figure 4.28. Structure of MBC-EPA

Photopolymerizations of the monomers were followed by DPC. All the polymerizations were performed under identical conditions of initiator concentration (2.0 mol%), UV light intensity (15 mW/cm²) and temperature (40 °C). Figure 4.29 and Figure 4.30 show the rate versus time and conversion versus time plots for monomers BC-EPA, EC-EPA, CA-EPA, EC-PA, BC-TEP and MBC-EPA:BC-EPA (60:40 %) mixture. Bulk polymerization of CA-PA was not possible due to its decomposition before melting at 192 °C.

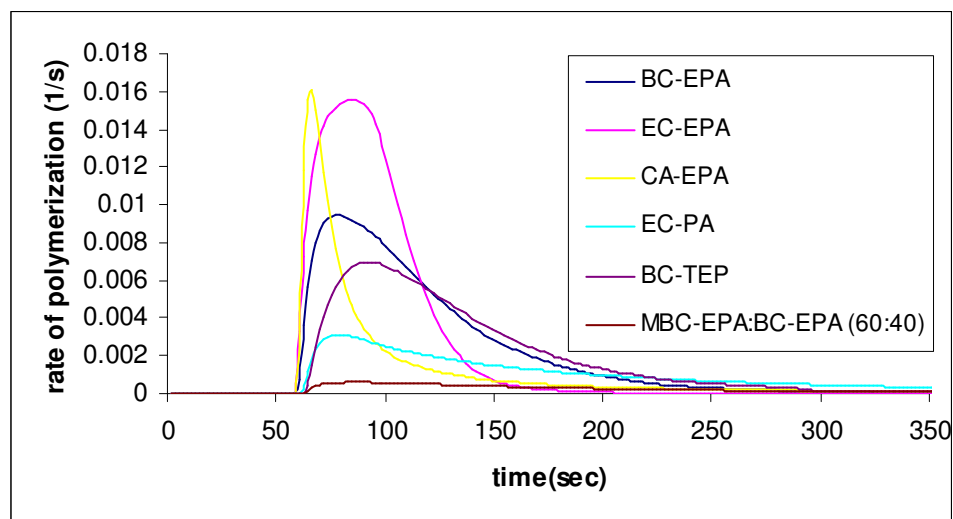


Figure 4.29. Rate of polymerization versus time graph of BC-EPA, EC-EPA, CA-EPA, EC-PA, BC-TEP and MBC-EPA:BC-EPA (60:40 %) at 40 °C

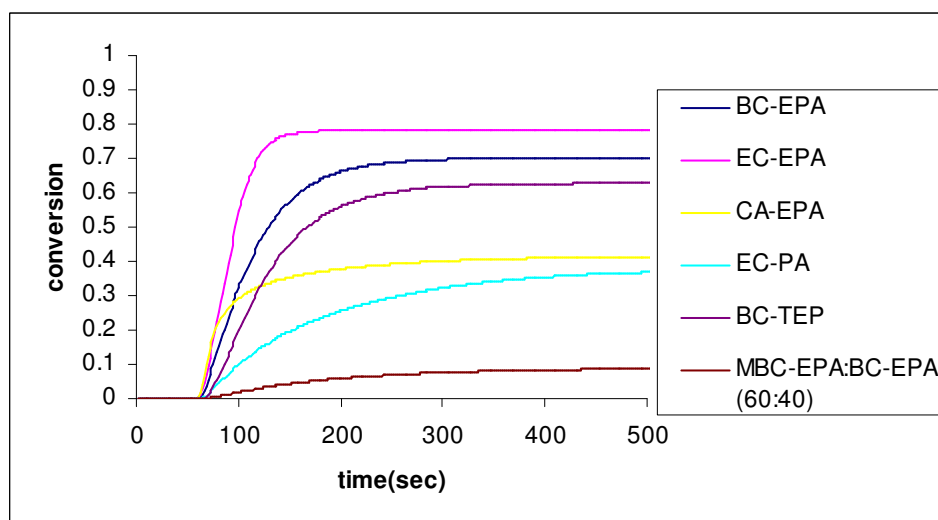


Figure 4.30. Conversion versus time graph of BC-EPA, EC-EPA, CA-EPA, EC-PA, BC-TEP and MBC-EPA:BC-EPA (60:40 %) at 40 °C

The maximum rate of polymerizations clearly increased with a decrease in the size of the ester substituent. BC-EPA with bulky *t*-butyl ester group showed lower rate of polymerization than EC-EPA and CA-EPA with ethyl ester and carboxylic acid substituents.

BC-TEP with the same ester group as BC-EPA showed lower polymerization rate, which we attribute to the presence of the two bulky phosphonate groups compared to one in BC-EPA as well as the electronic effect of P=O group with respect to C=O, the latter being more electron-withdrawing than the former. Comparison of rate of polymerizations of EC-EPA and EC-PA indicates the inductive effect of the substituents. The inhibiting effect (referred to above) on the polymerization rate of the less electron-withdrawing phosphonic acid group in EC-PA overcomes the enhancing steric effect due to its smaller size with respect to the phosphonate ester group in EC-EPA. Low polymerizability of MBC-EPA (containing 40% BC-EPA), the monofunctional counterpart of BC-EPA, supports the principle proposed by Kodaira [101].

The ^{13}C -NMR chemical shift differences ($\Delta\delta$) of the C=C double bonds of allyl monomers ($\text{C}_\beta\text{H}_2=\text{C}_\alpha$) were correlated with the radical polymerizability in the literature []. One proposed explanation is that electron withdrawing substituents cause downfield shifts of the β -carbon peak while the α carbon is shifted upfield. The net result is a decrease in the chemical shift difference between the two double bond peaks with electron-withdrawing substituents on the α carbon [101, 119]. The smaller the $\Delta\delta$ value is, the higher is the polymerizability of the monomer. Also, steric effects of the substituents which reduce the conjugation between C=C and C=O cause an increase in $\Delta\delta$ value and decrease polymerizability. For example lower polymerization reactivity of N,N-disubstituted methacrylamides were explained by the twisted conformation between double bonds reducing conjugation.

Table 4.2 shows the ^{13}C NMR chemical shifts differences $\Delta\delta$ of the C=C double bond carbons of the synthesized monomers. When we compare $\Delta\delta$ values of BC-EPA, EC-EPA and CA-EPA, it is observed that they increase with the size of the alkyl (R) group. CA-EPA with R=H showed the smallest $\Delta\delta$ of 4.64, while BC-EPA and EC-EPA with t-butyl and ethyl groups gave $\Delta\delta$ of 10.34 and 8.46, respectively. The bulkiness of the alkyl group decreases the conjugation between the C=C and C=O groups due to steric effect and increases $\Delta\delta$. The $\Delta\delta$ values correlate well with the polymerizability trend of these monomers. Maximum rate of polymerizations for BC-EPA, EC-EPA and CA-EPA were found to be 0.00943, 0.01555 and

0.01607 s⁻¹, respectively. When we compare EC-EPA and EC-PA, we see that the $\Delta\delta$ values conform to our expectation that the less electron-withdrawing groups should increase the chemical shift. The comparison of CA-PA and CA-EPA is similar. The $\Delta\delta$ values do not correlate with the polymerizability trend of the BC-EPA and BC-TEP, but better polarization of the α -CH₂ bonds in BC-EPA, even though it is less conjugated was expected. MBC-EPA with the largest $\Delta\delta$ of 12.05 was the slowest among all.

Table 4.2. Maximum rate of polymerizations, conversions, T_g values and ¹³C-NMR chemical shifts of the two vinyl carbon peaks of the monomers

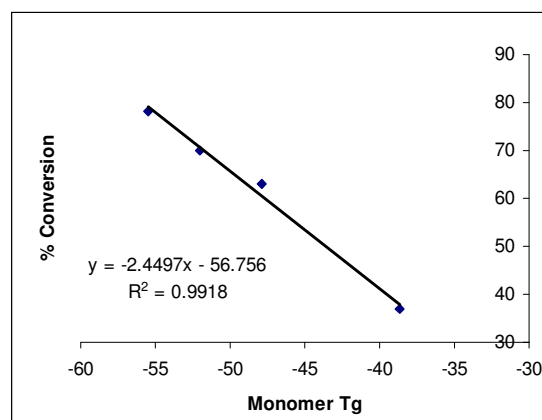
Monomer	R _p (s ⁻¹)	Conversion (%)	C _α =	=C _β H ₂	Δδ
BC-EPA	0.0094	70.0	137.71	127.37	10.34
EC-EPA	0.0156	78.3	136.68	128.22	8.46
CA-PA	-	-	134.33	127.62	6.71
CA-EPA	0.0161	41.3	135.74	131.10	4.64
EC-PA	0.0031	37.1	137.09	127.66	9.43
BC-TEP	0.0069	63.0	136.82	127.38	9.44
MBC-EPA	0.0006	8.9	138.67	126.62	12.05

The T_g value of a monomer is a measure of the flexibility of the monomer and mobility of the polymerizing system; a correlation between the conversion data and the monomeric T_g values was reported [120]. The T_g values of the monomers were determined by using DSC, at a scanning rate of 10 °C/min (Table 4.3). It was observed that the monomer expected to be most flexible (EC-EPA) also gives the highest conversion (78.3 %). BC-EPA has bulky t-butyl groups instead of the ethyl groups of EC-EPA, and showed higher T_g (-52) and lower conversion (70.0 %). BC-TEP has bulkier PO(OEt)₂ groups instead of the COOEt groups of BC-EPA, and its T_g is still higher and conversion still lower. The H-bonding in EC-PA increases T_g and decreases conversion with respect to EC-EPA. CA-EPA with two H-bonding COOH groups has the highest T_g and low conversion (but not the lowest).

Table 4.3. Comparison of monomeric T_g with % conversion

Monomers	T_g values of the monomers	% conversion after photo-polymerization
BC-EPA	-52	70.0
EC-EPA	-55	78.3
CA-EPA	-28	41.2
EC-PA	-39	37.1
BC-TEP	-48	63.0

It was interesting to see a linear relationship with a R-squared value of 0.9918 between per cent conversion and monomeric T_g values of BC-EPA, EC-EPA, EC-PA and BC-TEP (Figure 4.31). It means that the effect of changing the two R groups from ethyl to t-butyl is the same with the changing of COOEt group on the central carbon with the PO(OEt)₂ group in terms of rigidity and conversion. Also, changing the phosphonic ester group on the central carbon in EC-EPA to phosphonic acid in EC-PA has a drastic effect in terms of flexibility and conversion. This might be the other reason of the lowest reactivity of EC-PA among the group. However, this trend is not followed by the most rigid CA-EPA with the conversion of 41.2 %.

Figure 4.31. Per cent conversion versus monomeric T_g graph

The rate of polymerization as a function of double bond conversion for BC-EPA, EC-EPA, CA-EPA, EC-PA and BC-TEP was shown in Figure 4.32. It was observed that as the mobility of the system is increased, autoacceleration was delayed and conversions reached at the point of maximum rate both increased. But CA-EPA with limiting double bond conversion has higher polymerization rates. This can be explained by the hydrogen bonding capability between acid groups that could bring the double bonds close to each other and enhanced the rate.

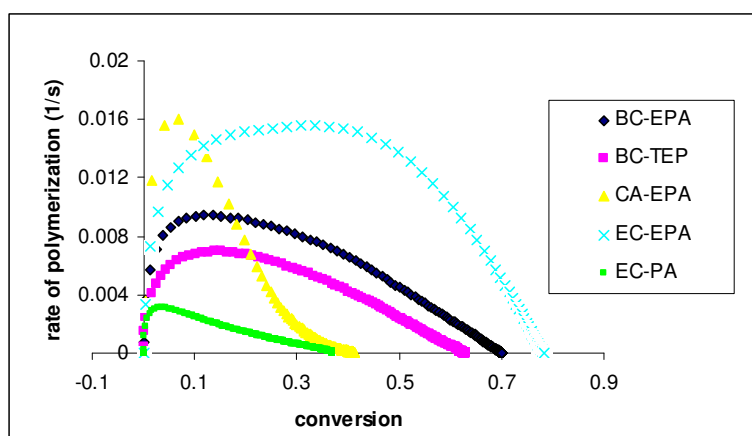


Figure 4.32. Rate of polymerization as a function of conversion

In this study, we also investigated photopolymerization behavior of the resins formed by addition of the synthesized monomers (2 mol %) to a commercial monomer, 2-hydroxyethylmethacrylate (HEMA), which was widely used in dentistry. Since monomers have very different solubility in HEMA, (the presence of carboxylic and phosphonic acids in CA-PA reduces solubility) it was not possible to prepare HEMA solutions with monomer concentrations of greater than 2 %. Figure 4.33 and Figure 4.34 show the rate versus time and conversion versus time plots of the mixtures. In Figure 4.33, a shoulder appears in all mixtures on the rate curve prior to the maximum. The shoulder is probably due to the Trommsdorf effect for the early stages of polymerization. The termination mechanism is reaction diffusion limited as the mobility of the terminated radicals is restricted [121]. The maximum rate of polymerization and conversion of HEMA (0.036 s^{-1} , 93.4 %) were higher

than its mixtures. Incorporation of bulkier BC-EPA and BC-TEP showed lower rates of polymerizations of 0.01653 and 0.01370 s^{-1} respectively whereas EC-EPA, CA-PA, CA-EPA and EC-PA showed similar rates. Surprisingly, 2 % incorporation of the lowest reactive EC-PA to HEMA has the highest polymerization rate of 0.01838 s^{-1} which could be either due to less incorporation of the slower monomer into the copolymer or favourable interaction between the monomer and HEMA. Finally, per cent conversions of the monomer incorporated HEMA mixtures were nearly the same for all compositions (46.8-52.0 %) (Table 4.4).

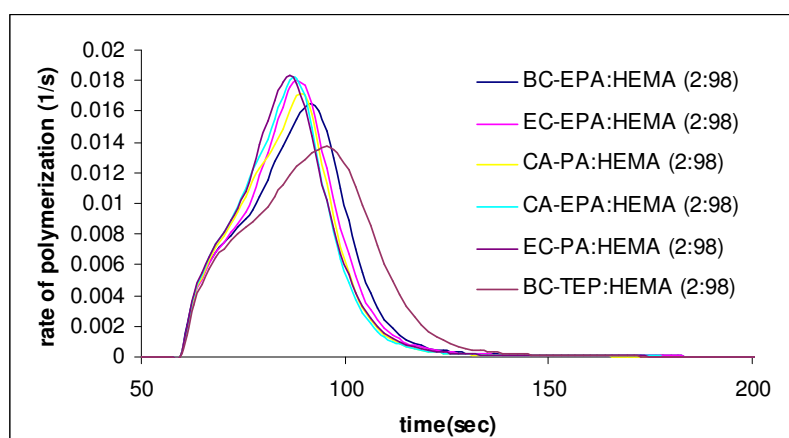


Figure 4.33. Rate of polymerization versus time graph of all the monomers with HEMA at $40 \text{ }^{\circ}\text{C}$

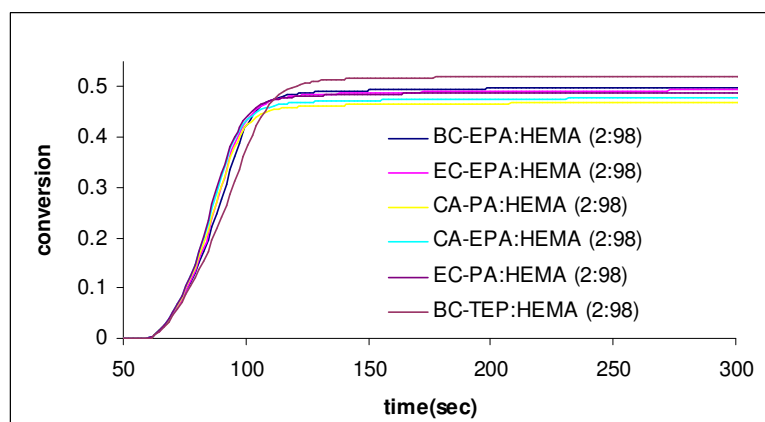


Figure 4.34. Conversion versus time graph of all the monomers with HEMA at $40 \text{ }^{\circ}\text{C}$

Table 4.4. Photopolymerization results

Composition	R_p (s⁻¹)	Conversion (%)
HEMA	0.033	97.3
BC-EPA:HEMA (2:98)	0.0165	49.8
EC-EPA:HEMA (2:98)	0.0180	49.4
CA-PA:HEMA (2:98)	0.0170	46.8
CA-EPA:HEMA (2:98)	0.0181	47.8
EC-PA:HEMA (2:98)	0.0184	49.0
BC-TEP:HEMA (2:98)	0.0137	52.0

4.2.8. Polymerization in Bulk or Solution

Bulk polymerization of BC-EPA and EC-EPA in the presence of 0.5 wt % AIBN at 76-78 °C gave soluble polymers. The purification of the polymers were performed by dissolving in CH₂Cl₂ and precipitating into hexane. Solubility of the homopolymers in common solvents indicated the formation of highly cyclized polymers. EC-EPA showed high homopolymerization rate with a yield of 27.2 % in 10 minutes whereas BC-EPA polymerized with a yield of 19.9 % in 40 minutes. The acidic CA-EPA was polymerized in DMSO using AIBN. The polymer was purified by dissolving in methanol and precipitating into diethyl ether. Conversion of 20.8 % was obtained in 180 min. Table 4.5 shows the polymerization conditions and characteristics of the resulting polymers. Polymer CA-EPA was not soluble in THF therefore its molecular weight could not be determined by GPC. Also, it did not show T_g between 0-160 °C. High cyclization efficiency of these monomers can be explained by the Kodaira's principle as monofunctional counterparts of these monomers do not polymerize due to steric hinderence. CA-EPA showed unexpectedly high cyclization tendency which was attributed to the capability of hydrogen-bond formation between acid groups that causes a favorable conformation for cyclization.

Table 4.5 Polymer characterization results

Monomers	Solvent	Yield (%)	Time (min)	T _g (°C)	M _n	M _w
BC-EPA ^a	Toluene	24.5	90	54	11,740	15,690
BC-EPA ^b	–	19.9	40	-	17,760	29,680
EC-EPA ^a	Toluene	36.8	48	94	56,000	79,780
EC-EPA ^b	–	27.2	10	-	67,570	94,300
CA-EPA ^c	DMSO	20.8	180	-	–	–

^a[M]= 2.5 M;[AIBN]= 0.015 M

^bbulk polymerization [AIBN]= 0.5 wt %

^c[M]= 1.1 M;[AIBN]= 0.015 M

Temperature= 76-78 °C

4.2.9. Interacted Amounts of Carboxylic and Phosphonic Acids in CA-PA and EC-PA with the Calcium in the HAP

Among the acid monomers, CA-PA and EC-PA were soluble in ethanol and water, which is a very important property for dental applications. However, CA-EPA was soluble only in methanol but not in ethanol and water. The aqueous solutions of CA-PA and EC-PA are acidic with a pH values of 1.18 and 1.34 (8 wt %). These values were higher than pH of 8 wt % aqueous phosphoric acid solution (pH=0.86). These monomers enable to etch enamel and dentin. Furthermore, in these monomers the phosphonic acid group is connected to the double bond via a hydrolytically stable bond. In water these monomers may tend to undergo further hydrolysis due to the remaining –COOEt groups. But this will not reduce the adhesive properties of the monomers. Therefore CA-PA and EC-PA can be used in dental adhesives. Based on water solubility, hydrolytic stability, polymerizability and low pH values, CA-PA and EC-PA are expected to have potentials as self-etching adhesive monomers. For example, phosphonic acid group of CA-PA can remove the smear layer, demineralize the dentin and

enamel, and diffuses into collagen fibrils where the carboxylic acid groups of CA-PA can form H-bonds with the hydroxyl and amino groups of the collagen molecule. This process forms a hybrid layer which facilitates binding of the composite resins.

The interaction of CA-PA and EC-PA with hydroxyapatite, as a model compound for dentin and enamel, was investigated using the ^{13}C NMR technique [11, 59, 61]. First the pH dependencies on the chemical shifts of the carbonyl carbon and the α -methylene carbon to the phosphorus (right peak, higher field) were examined (Figures 4.35 and 4.36). When EC-PA was titrated with NaOH, α -methylene carbon peaks were shifted to a lower field reflecting the formation of an acid-base interaction. The titration curve showed two jumps in the chemical shift difference of the α -methylene carbon. These two jumps, 0.64 ppm and 0.62 ppm respectively, correspond to dissociation of the two hydroxyl groups of phosphonic acid, one after the other.

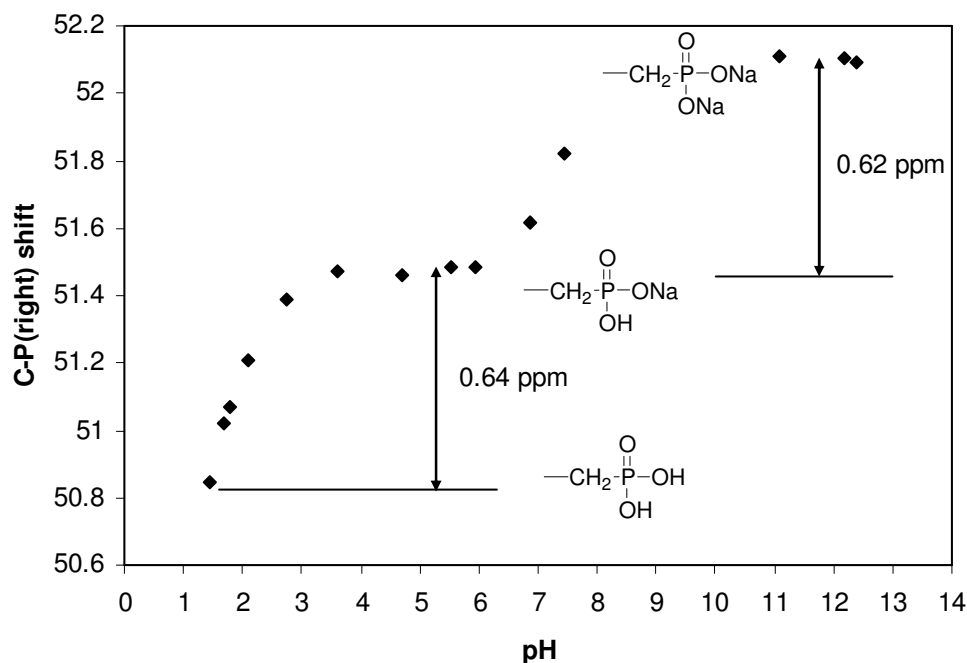


Figure 4.35. pH dependencies of the chemical shift of the α -methylene peak to the phosphorus in EC-PA

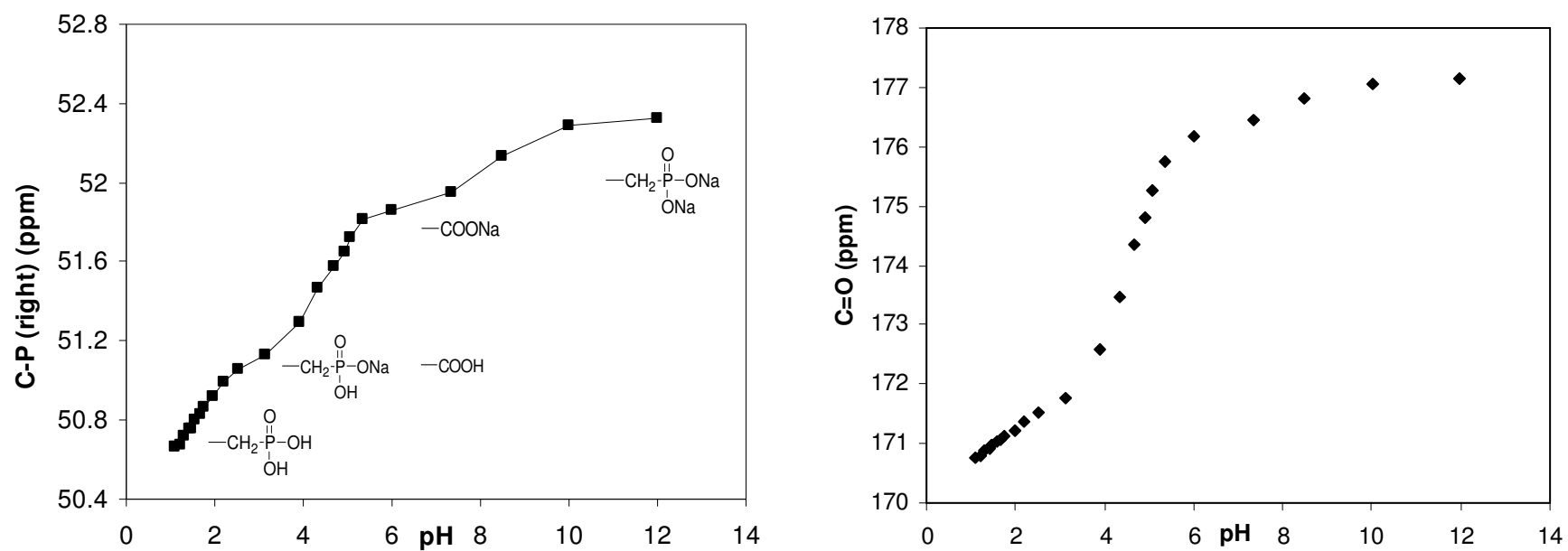


Figure 4.36. pH dependencies of the chemical shift of the α -methylene peak to the phosphorus and carbonyl carbon peak in CA-PA

The titration curves (Figure 4.45) of CA-PA with respect to α -methylene carbon and carbonyl carbon show three such jumps. First, one hydroxyl group of phosphonic acid dissociates (0.46 ppm), then carboxylic acid (0.73 ppm), and finally the remaining hydroxyl group of phosphonic acid (0.47 ppm) dissociates according to the chemical shifts of α -methylene carbon. The shift differences of the 1st, 2nd and 3th proton dissociations with respect to carbonyl carbon are 0.99 ppm, 4.42 ppm and 0.98 ppm respectively. The second dissociation starts before the first one is completely finished, therefore the corresponding jumps in the titration curve almost merge. This causes a difficulty in calculating the shift differences of the first and second proton dissociations for CA-PA.

In order to evaluate interactions of CA-PA and EC-PA with the calcium in the tooth, two different amounts of HAP (as a model compound for enamel and dentin) were added to the aqueous solutions of the monomers. The addition of 25 mg of HAP to the solution of EC-PA resulted in an increase in the pH value from 1.34 to 3.57 and shifted the α -methylene carbon peak to a lower field. Then, the interacted amounts of phosphonic acid with the calcium in the HAP were determined by dividing the shift difference of the α -methylene carbon peak (0.53 ppm) by the value obtained for complete dissociation of the first hydroxyl group of phosphonic acid (0.64 ppm). The interacted amount of EC-PA containing 25 and 50 mg of HAP were found to be 82.3% and 89.5% (Table 4.6).

The chemical shift differences of CA-PA with 25 mg HAP (0.37 ppm for the α -methylene carbon and 0.80 ppm for the carbonyl carbon) are below the value for the start of the second dissociation due to the carboxylic acid group. Interacted amount of the first OH group of the phosphonic acid was 78.7 % when calculated with respect to the α -methylene carbon shifts and 80.6 % when calculated with respect to the carbonyl carbon shifts. When the HAP amount is doubled, the chemical shift differences increase such that, all the first OH group of the phosphonic acid was interacted and 11.7 % of the two carboxylic acids started to interact when calculated with respect to the carbonyl carbon shifts. But, interacted amount of carboxylic acid was turned out to be 5.2 % when calculated with respect to the α -methylene carbon shifts (Table 4.6). This result showed that, phosphonic acid group demineralized the calcium phosphate in the HAP in preference to the carboxylic acid. So both CA-PA and EC-PA were expected to enhance bonding of

the resin to enamel. On the other hand, decalcification by the carboxylic acid group in CA-PA on the hydroxyapatite was limited, so most of the carboxylic acid was left undissociated in the solution. But, as the undissociated carboxylic acid had a priming efficiency to the exposed collagen, the bond strength to the dentin was expected to increase as dentin contains 20 % organic material whereas enamel contains 1 %. As a result, CA-PA could exhibit a priming capacity as well as an etching efficiency.

Table 4.6. Interaction of CA-PA and EC-PA with HAP

Monomer	HAP ^a (mg)	pH	In the presence of HAP			
			<u>α-CH₂ (right)</u>		<u>-COOH</u>	
			S.D. ^b	I.A.(%) ^c	S.D. ^d	I.A.(%) ^e
EC-PA	25	3.57	0.526	82.3	-	-
EC-PA	50	3.96	0.572	89.5	-	-
CA-PA	25	2.63	0.366	78.7	0.800	0
CA-PA	50	3.39	0.503	100	1.509	5.2-11.7

^aAmount of HAP added to monomer solution

^bChemical shift difference for the α -CH₂ peak in CA-PA and EC-PA after addition of HAP

^cInteracted amounts of the phosphonic acid groups in CA-PA and EC-PA with HAP

^dChemical shift difference for the carbonyl carbon of the carboxylic acid in CA-PA and EC-PA after addition of HAP

^eInteracted amounts of the carboxylic acid groups in CA-PA and EC-PA with HAP

4.3. Synthesis of Phosphorus-Containing Monomers and Polymers from *tert*-Butyl α -Hydroxymethyl Acrylate (TBHMA)

In this part, new monomers containing phosphonic acid or both phosphonic and carboxylic acids were synthesized for dental adhesives. The copolymerization behaviour of these monomers with 2-hydroxy-ethylmethacrylate (HEMA) and the effect of the monomer structure on the polymerization reactivity were studied using photodifferential scanning calorimetry. Also, these monomers were modelled by Seyhan Salman using computational tools. The synthesized monomers contain hydrolytically stable bonds between polymerizable methacrylic group and the phosphorus group, so they can be used as dental adhesives in wet condition.

4.3.1. Monomer Synthesis

A carboxylate and phosphonate-containing monomer (TBEP) was synthesized by the Arbuzov reaction of TBBr with triethyl phosphite at 85 °C. The synthesized monomer was easily purified by distillation under reduced pressure giving a colorless liquid in 84 per cent yield (Figure 4.37).

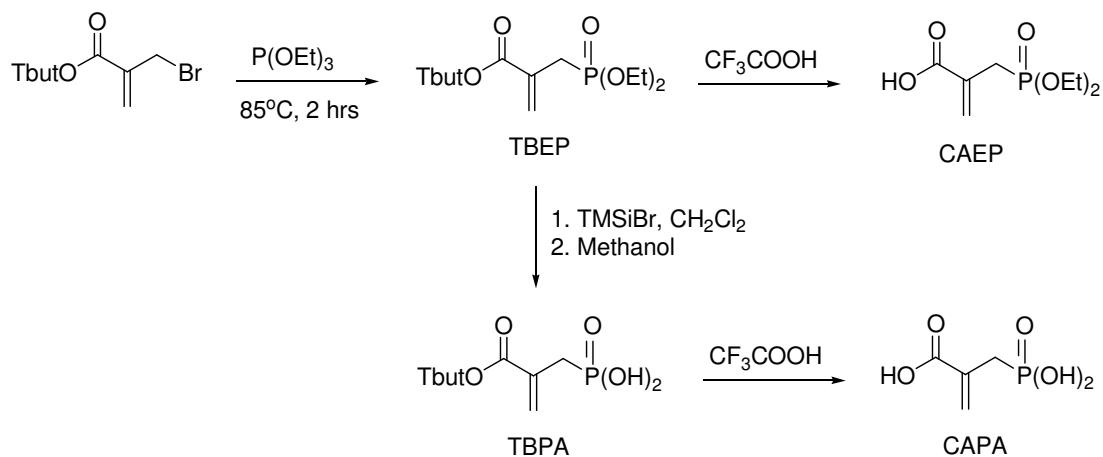
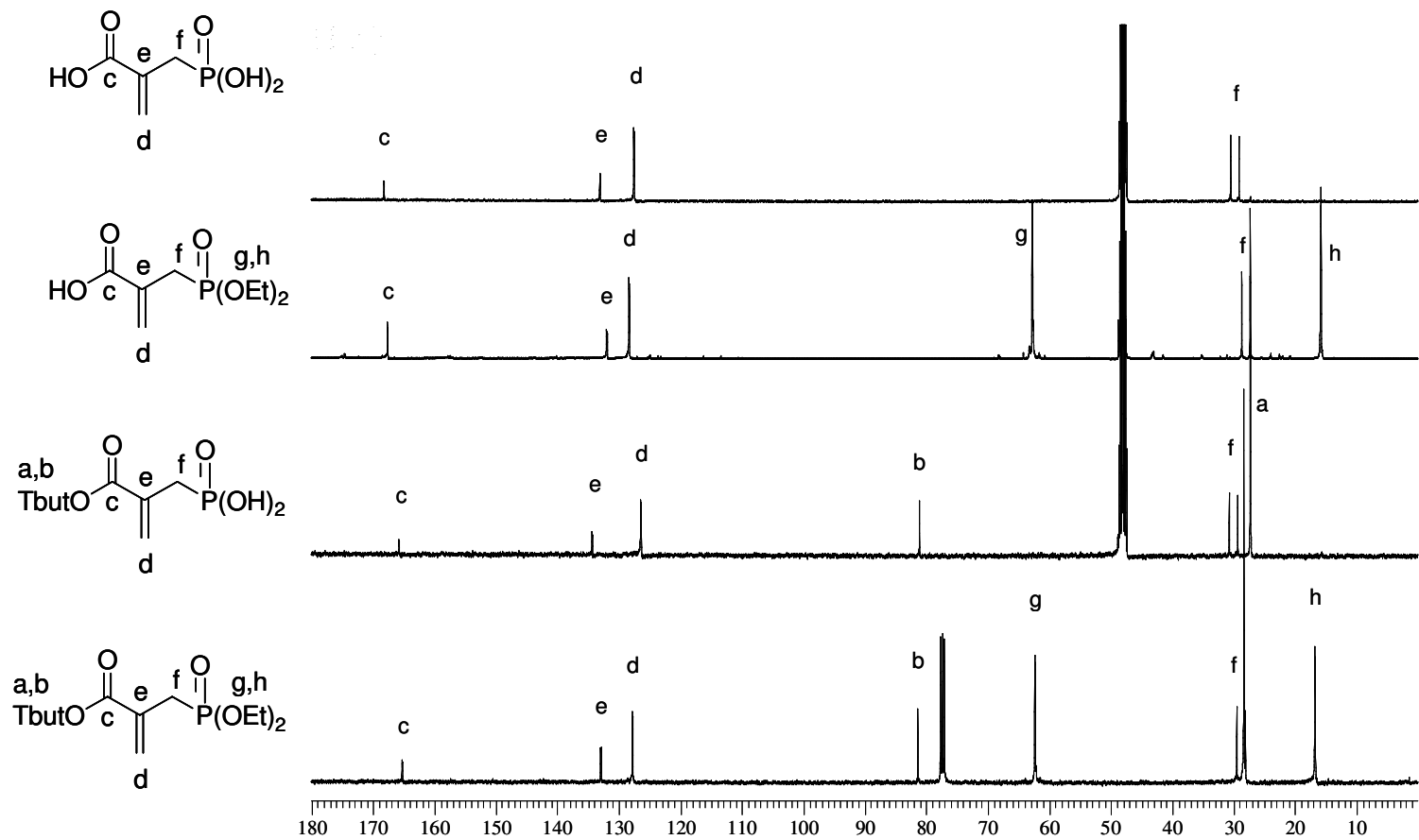


Figure 4.37. Synthesis of phosphorus-containing methacrylate monomers

The ^{13}C -NMR spectrum of the TBEP showed characteristic peaks for a methyl carbon of the ethyl ester at 16.7 ppm, methylene carbon attached to phosphorus atom at 27.5 and 30 (doublet) ppm, tert-butyl ester carbons at 28.0 and 81.3 ppm, methylene carbons of ethyl ester at 62.0 ppm, double bond carbons at 128.0 and 133.2 ppm, and a carbonyl carbon at 165.2 ppm (Figure 4.38).

In the ^1H -NMR spectrum, methyl protons of the ethyl and tert-butyl ester at 1.0 and 1.2 ppm, methylene protons attached to phosphorus atom at 2.6 ppm, methylene of ethyl ester at 3.8 ppm and double bond protons at 5.5 and 5.9 ppm were characterized.

The FT-IR spectrum showed characteristic peaks for carbonyl, double bond, P=O and P-O-C at 1712, 1631, 1255 and 1029 cm^{-1} (Figure 4.39)

Figure 4.38. ^{13}C -NMR spectra of the phosphorus-containing monomers

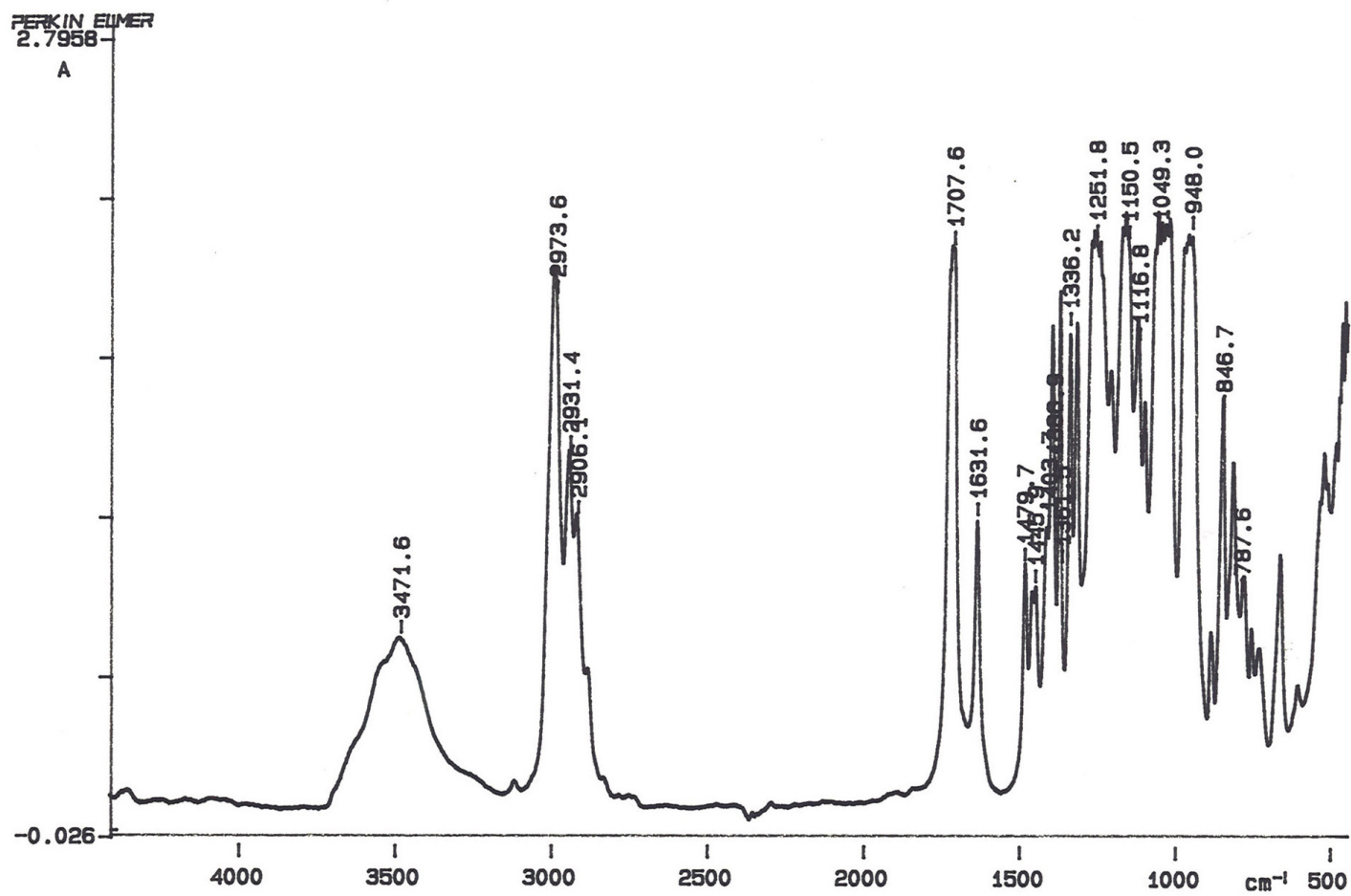
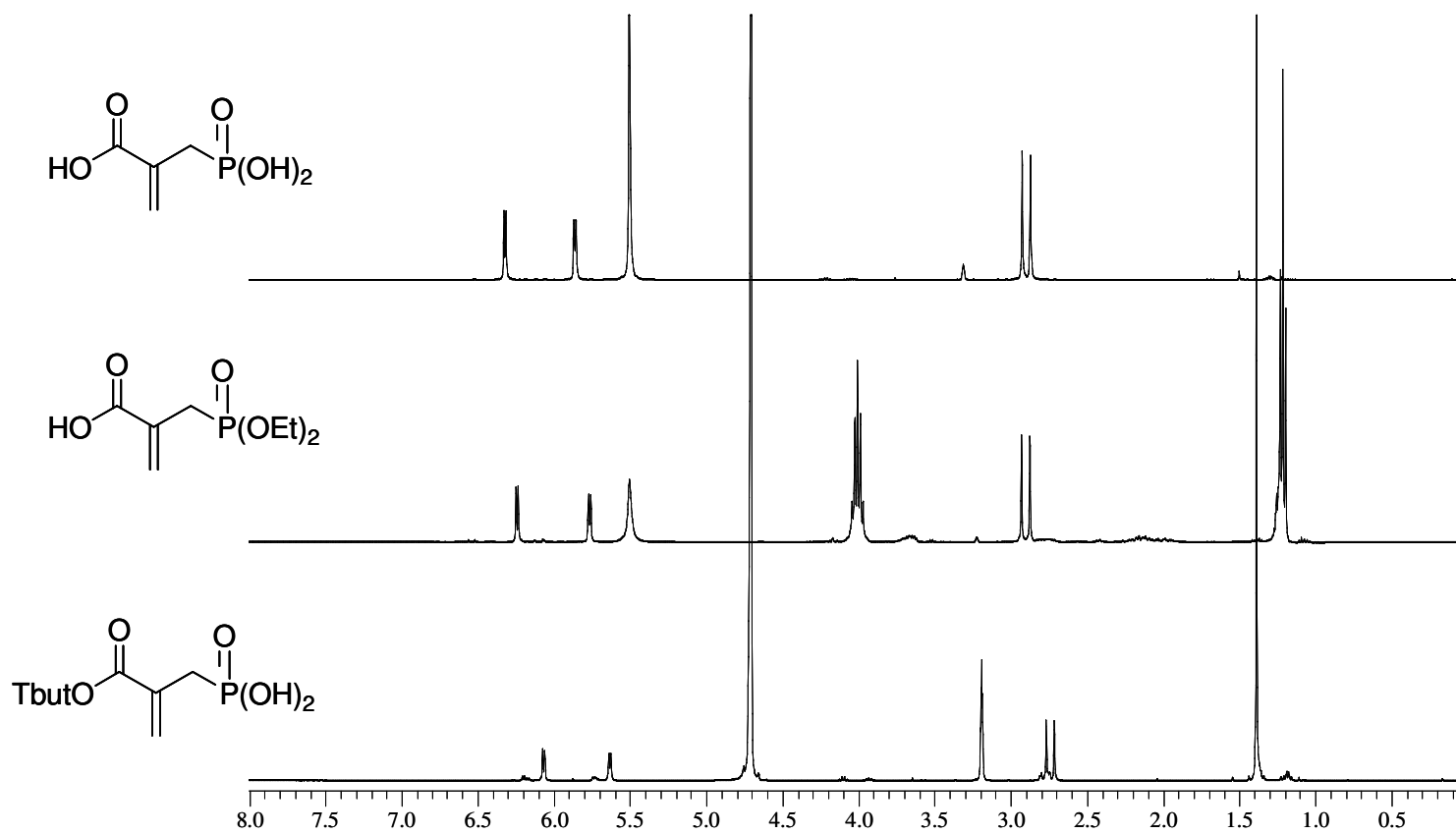


Figure 4.39. FT-IR spectrum of TBEP

The silylation of TBEP with TMSiBr, followed by methanolysis of the silyl derivative, gave TBPA as a colorless, viscous liquid in a 77 per cent yield. Both ^{13}C -NMR and ^1H -NMR spectra show a complete disappearance of the ethyl groups of the phosphonate ester (Figures 4.38 and 4.40).

The FT-IR spectrum showed a broad peak between 3500 and 2000 cm^{-1} due to phosphonic acid group (Figure 4.41).

This monomer was soluble in water, whereas TBEP was not.

Figure 4.40. $^1\text{H-NMR}$ spectra of TBPA, CAEP and CAPA

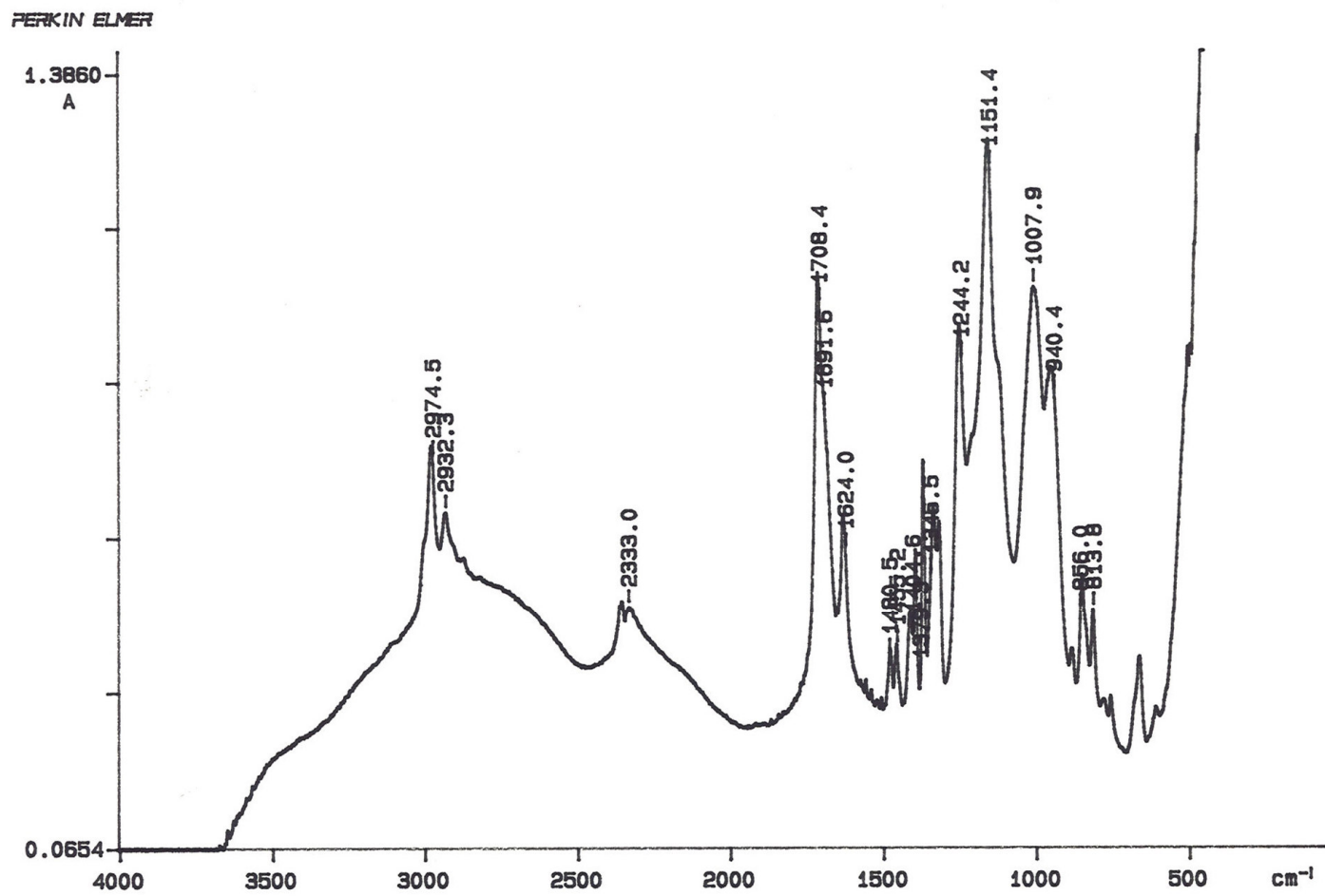


Figure 4.41. FT-IR spectrum of TBPA

A further derivative of TBPA can be obtained by its hydrolysis. Thus, the tert-butyl ester group of the TBPA was easily hydrolyzed by mixing with trifluoroacetic acid. CAPA containing both phosphonic acid and carboxylic acid functionalities was obtained as a white solid with a melting point of 157 °C in 59.3 per cent yield.

The ^{13}C -NMR spectrum of the monomer showed a complete disappearance of tert-butyl ester groups (Figure 4.38).

In the ^1H -NMR spectrum, methylene protons attached to phosphorus atom at 2.87 ppm and double bond protons at 5.86 and 6.32 ppm were characterized (Figure 4.40).

The FT-IR spectrum showed a broad peak between 3500 and 2000 cm^{-1} due to phosphonic and carboxylic acid groups, ester carbonyl at 1702 cm^{-1} , C=C stretching peak at 1628 cm^{-1} , and P=O vibrations at 1247 cm^{-1} (Figure 4.42).

The diacid CAPA was soluble both in water and ethanol which is important for dental applications.

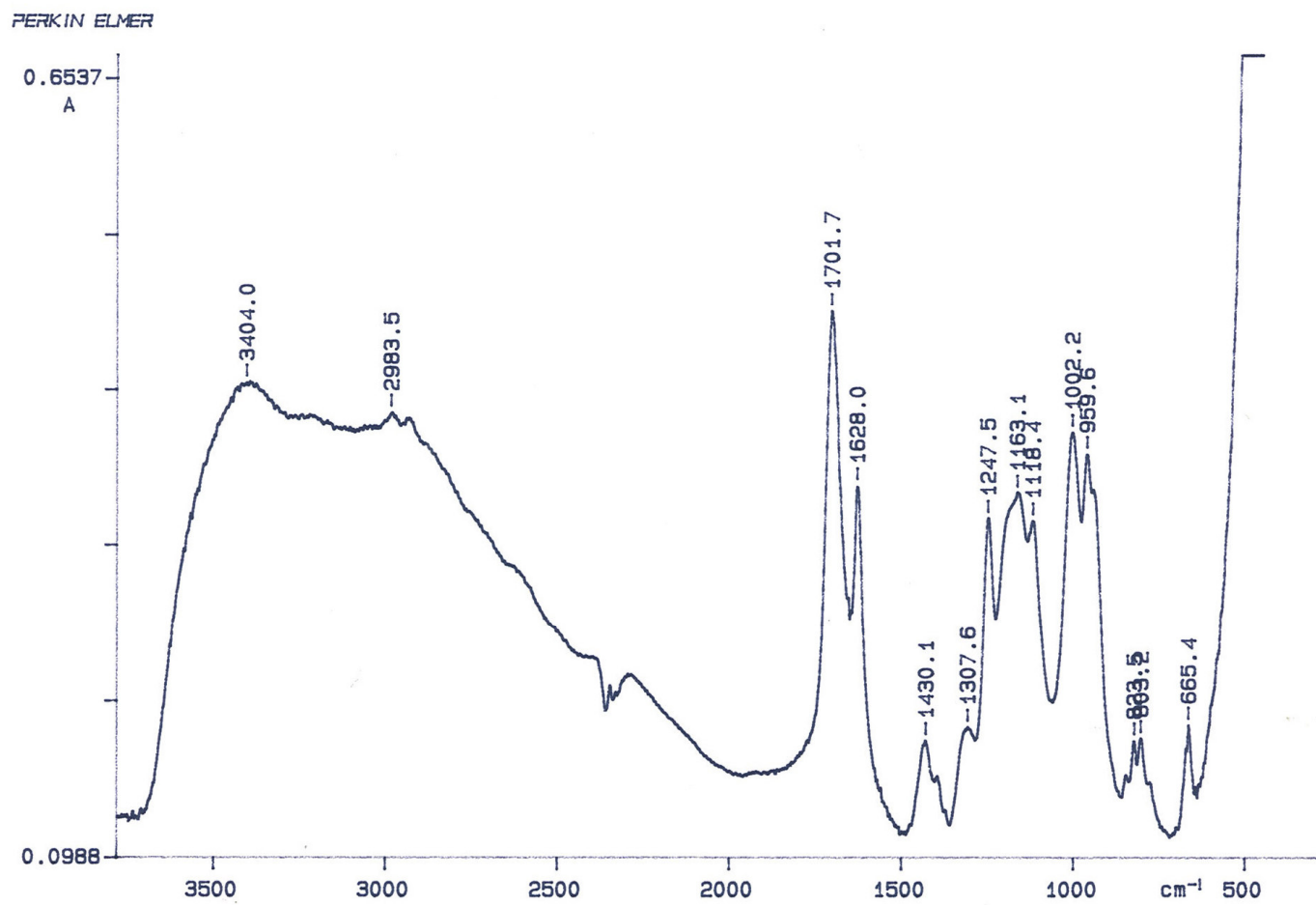


Figure 4.42. FT-IR spectrum of CAPA

Hydrolysis of tert-butyl groups of TBEP with CF_3COOH gave CAEP as a yellow viscous liquid.

The ^{13}C -NMR spectrum of this monomer showed characteristic peaks for a methyl carbon of the ethyl ester at 16.0 ppm, methylene carbon attached to phosphorus atom at 27.3 and 29.0 (doublet) ppm, methylene carbons of the ethyl ester at 62.7 ppm, double bond carbons at 128.3 and 132.2 ppm, and a carbonyl carbon at 167.5 ppm (Figure 4.38).

In the ^1H -NMR spectrum, methyl protons of the ethyl ester at 1.30 ppm, methylene protons attached to phosphorus atom at 2.96 and 3.02 ppm, methylene of ethyl ester at 4.09 ppm and double bond protons at 5.85 and 6.32 ppm were characterized (Figure 4.40).

The FT-IR spectrum showed characteristic peaks for carbonyl, double bond, $\text{P}=\text{O}$ and $\text{P}-\text{O}-\text{C}$ at 1713, 1631, 1238 and 1030 cm^{-1} . A broad peak between 3500 and 2000 cm^{-1} was due to carboxylic acid group (Figure 4.43).

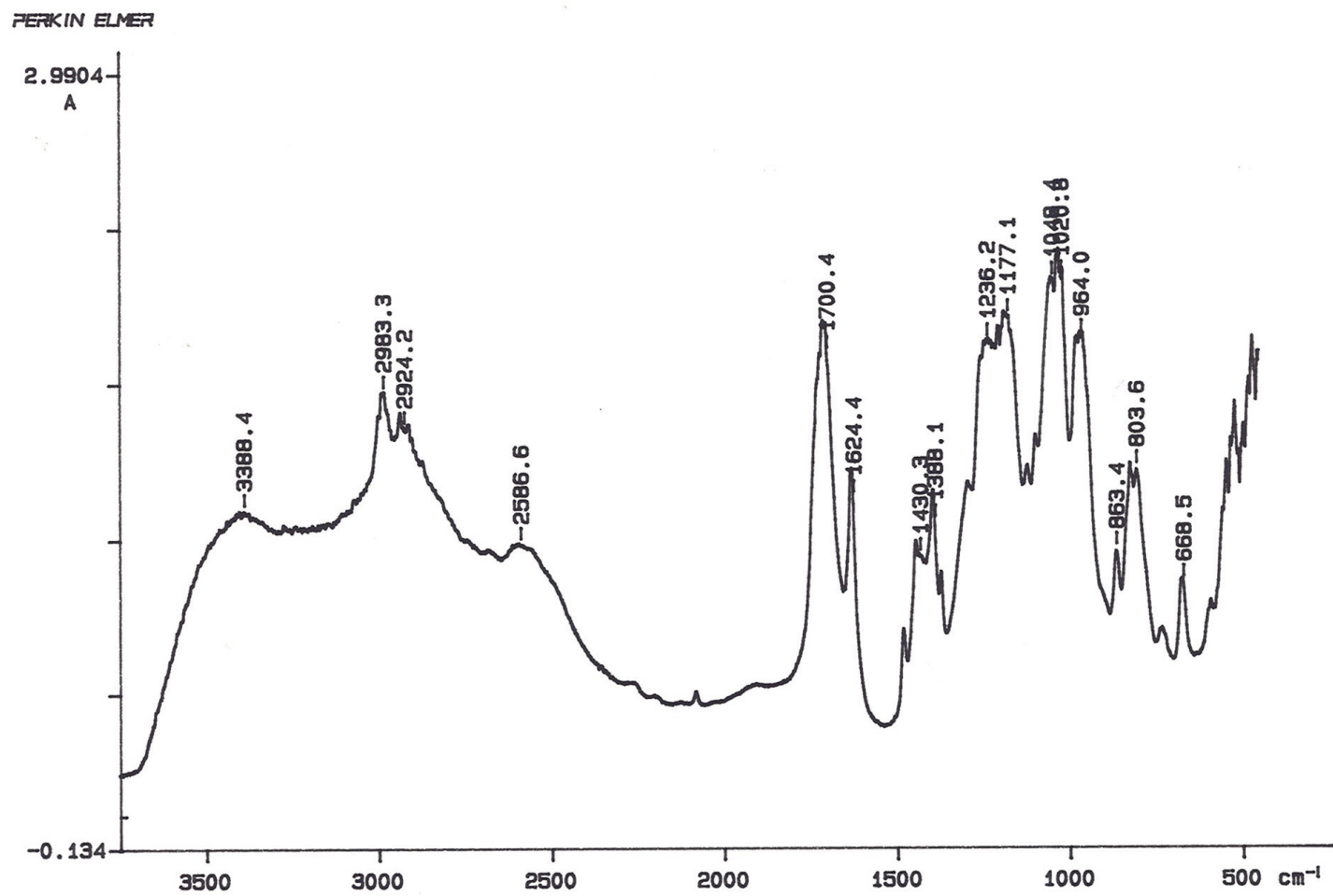


Figure 4.43. FT-IR spectrum of CAEP

4.3.2. Photopolymerizations

The reactivities of the synthesized monomers in photopolymerizations were investigated with photodifferential scanning calorimetry. All the polymerizations were performed under identical conditions; at temperature 40 °C with an initiator concentration of 2.0 mol per cent and UV light intensity of 15 mW/cm². Bulk photopolymerization of the solid CAPA was not possible at 40 °C due to its high melting point (157 °C). Therefore copolymerization of all the monomers with a commercial monomer (HEMA) widely used in dentistry was investigated. Figure 4.44 shows the exotherms recorded for the copolymerizations of TBEP, TBPA, CAPA and CAEP with HEMA. In all cases a shoulder appears on the rate curve prior to the maximum. The shoulder was probably due to the Trommsdorf effect for the early stages of polymerization where the termination mechanism becomes reaction diffusion limited as the mobility of the terminating radicals restricted. The rate of polymerization of HEMA was found to be higher than its comonomer mixtures (0.0328 s⁻¹) (Table 4.7). The incorporation of phosphorus containing monomers resulted in a decrease of polymerization rate. This may be due to steric effects of phosphorus groups in the propagation reaction. The reduction of the rate of the propagation by steric interference probably made the termination and chain transfer processes comparably more important and reduced the rate of polymerization. The maximum rate of polymerization for TBPA was found to be 1.32 times higher than TBEP. The maximum rates of polymerizations were found to be 0.0094 and 0.0124 s⁻¹ for TBEP and TBPA. This may be explained by the reduced steric effect due to hydrolysis of the ethyl groups of the phosphonate ester and increased hydrogen bonding capacity. Hydrolysis of the tert-butyl groups of TBPA also increased the rate with the rate of polymerizations of 0.0124 and 0.0173 s⁻¹ for TBPA and CAPA.

Hydrolysis of only tert-butyl ester groups of TBEP gave the highest maximum rate of polymerization of 0.0195 s⁻¹ (CAEP). The least sterically hindered CAPA did not show the highest rate of polymerization. This behavior may be explained due to very high melting point of CAPA (157 °C) compared to the polymerization temperature (40 °C) which lowers the degree of mobility leading to lower rate.

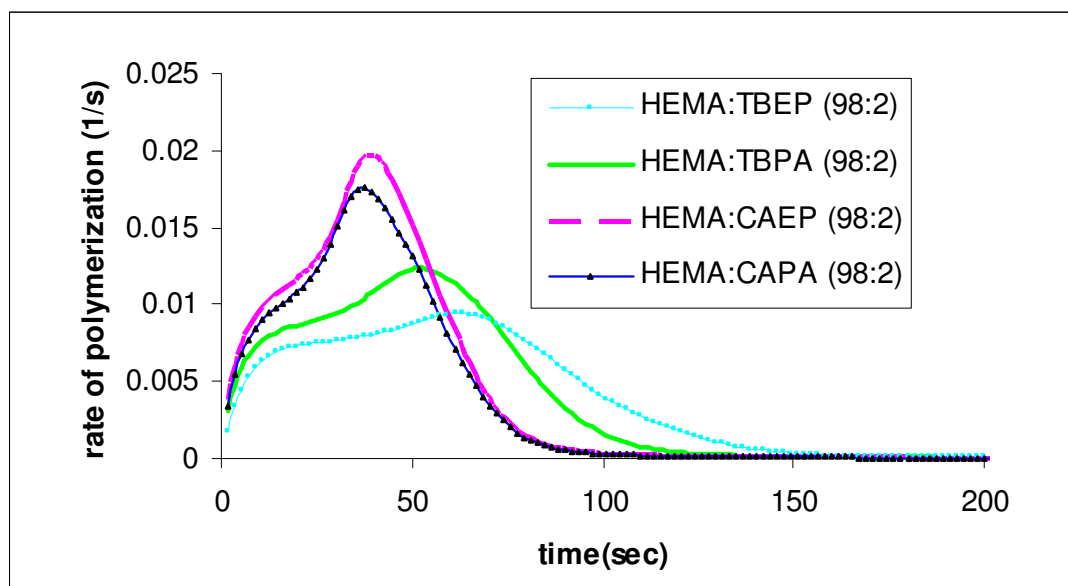


Figure 4.44. Rate of polymerization versus time graph for the copolymerizations of monomers

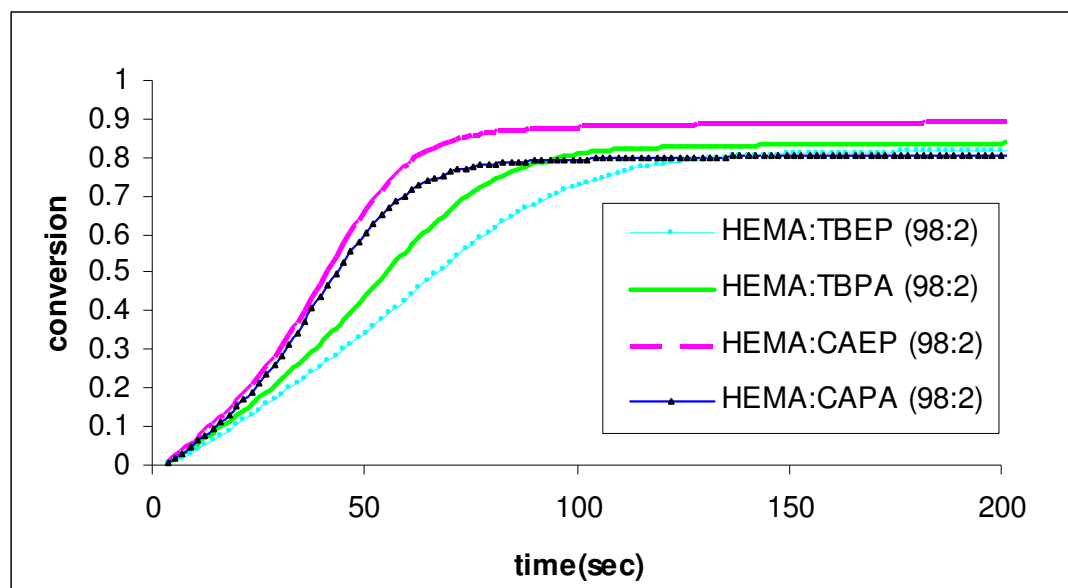


Figure 4.45. Conversion-time plots for the copolymerizations of monomers

Figure 4.45 shows the conversion-time plots of the monomers. Although the monomers have different chemical structures, they showed similar conversions of 80-90 per cent. CAPA with the higher polymerization rate did not give higher conversion than

other monomers. This may be again due to decreased mobility caused by high melting point of CAPA (157 °C) compared to the polymerization temperature (40 °C) and hydrogen bonding.

Table 4.7. Rate of polymerization and conversion data for the copolymerization of TBEP, TBPA, CAPA and CAEP with HEMA

Composition	R_p (s^{-1})	Conversion (%)
HEMA	0.0328	85.2
TBEP: HEMA (2:98)	0.0094	82.1
TBPA: HEMA (2:98)	0.0124	84.0
CAPA: HEMA (2:98)	0.0173	80.9
CAEP: HEMA (2:98)	0.0195	89.4

4.3.3. Computational Strategy

In this part of the study, the first three monomers polymerized under similar experimental conditions were modeled by Seyhan Salman. The propagation rate constant (k_p) was considered as a descriptor for the polymerizability behavior of the monomers. The effect of the chain-breaking reaction characterized by the chain transfer constant (k_{ct}) was computed.

She studied the potential energy profiles and the kinetics of chain propagation and the competing chain transfer reactions by considering the addition of the methyl radical to the double bond and the α -hydrogen abstraction as shown in Figure 4.46. Then calculated thermodynamic variables, such as the activation barriers and reaction enthalpies for methyl addition and hydrogen-abstraction reactions were evaluated and given in Table 4.8.

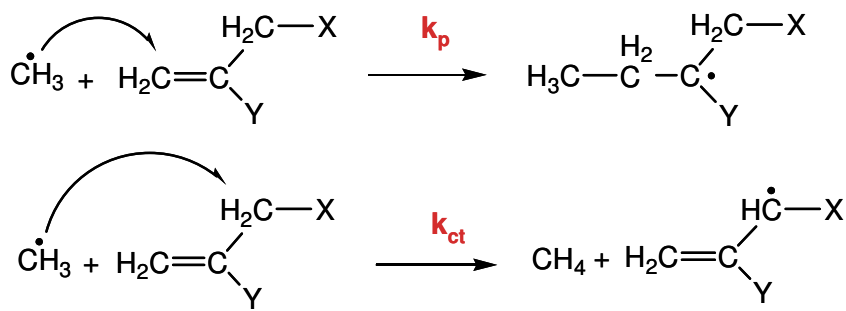


Figure 4.46. Model Propagation and Termination by Chain Transfer to Monomer Reactions (X represents the phosphonic acid derivatives and Y represents the carboxylic acid derivatives)

Table 4.8. Calculated activation barriers and reaction enthalpies (kcal/mol)

Monomer	Ea ₁	Ea ₂	ΔH ₁	ΔH ₂
TBEP	4.87	6.04	-31.85	-21.43
TBPA	1.18	9.85	-32.45	-18.73
CAPA	0.63	9.19	-32.77	-18.44

Ea = Addition barrier, Ea₂= H-abstraction barrier

ΔH₁= Reaction enthalpy for the methyl addition, ΔH₂= Reaction enthalpy for the hydrogen abstraction

The calculated activation barriers for the methyl addition to the monomers decrease as the rate of polymerization increases (see experimental rate of polymerization). The heat of polymerization for the methyl addition becomes more negative as the polymerization rate of the monomer increases. On the other hand, H-abstraction is less facile for TBPA and CAPA as compared to TBEP.

The hydrogen-abstraction barriers are higher in the case of TBPA and CAPA as compared to the activation barrier of TBEP (Table 4.8). The hydrogen bonds observed in the ground state geometries of TBPA and CAPA disappear at the transition state geometries. Since it costs energy to break the hydrogen bond interactions observed at the ground state, the hydrogen-abstraction barriers turn out to be higher than the one required for TBEP.

In the transition states (TS) of methyl addition to TBPA and CAPA, intramolecular hydrogen bonds form between the carboxylic groups and phosphonic acid groups. The addition transition states of TBPA and CAPA are stabilized via these intramolecular hydrogen bonds. Hydrogen bonds occurred in the ground state geometries of TBPA and CAPA in a similar manner between the carboxylic groups and phosphonic acid groups. Since the methyl radical was used to mimic the growing chain the effect of intermolecular hydrogen bonding between the growing chain and monomers added was not observed. Thus, the model takes into account only the steric effect of the monomer structure as well as the effect of intramolecular hydrogen bonding.

The rate constants for addition (k_p) and chain transfer by hydrogen-abstraction (k_{ct}) were evaluated and were given in Table 4.9.

Table 4.9. Rate constants for addition (k_p) and chain transfer by hydrogen-abstraction (k_{ct}) compared to experimental rate

Monomer	k_p	k_{ct}	Experimental Rate (s^{-1})
TBEP	$3.61 \cdot 10^3$	$2.22 \cdot 10^1$	0.0094
TBPA	$1.23 \cdot 10^5$	$3.46 \cdot 10^{-2}$	0.0124
CAPA	$5.15 \cdot 10^5$	$1.62 \cdot 10^{-1}$	0.0173

The k_p value increases as the experimentally reported rate of polymerization increases. Also, the k_p values for TBPA and CAPA were found to be higher than that of TBEP, resulting in higher R_p . The reason for the enhanced k_p is due to intra molecular H-bonding or/and reduced steric effect. The lower k_{ct} values in the case of TBPA and CAPA as compared to TBEP are due to the high hydrogen-abstraction activation barriers as discussed already.

Jansen et al. found that the monomers capable of forming intermolecular hydrogen bonds exhibit higher polymerization rates compared to their non-hydrogen bonding analogues. The high reactivities were suggested to be due to pre-organization via

hydrogen bonding to bring the double bonds close to each other and enhance the rate of polymerization [30].

In order to take into account the effect of intermolecular hydrogen bonding she modeled the interactions at the addition and hydrogen-abstraction transition states of CAPA by using $\cdot\text{CH}(\text{COOH})\text{CH}_2\text{PO}(\text{OH})_2$ type of attacking radical. It was observed that, the intermolecular hydrogen bonds at the addition transition state of CAPA stabilize the propagating radicals and enhance the propagation reaction. The hydrogen-abstraction transition state does not possess any stabilizing interactions which would facilitate the termination by chain transfer. Both behaviors complement each other to predict a higher polymerization rate for CAPA as experimentally observed.

4.4. Synthesis of Diethyliminodiacetate-Containing Monomers from AHM, EHMA, TBHMA and TBEED

The chemical adhesion of monomers to tooth can occur by ionic or covalent bonds generated by the reaction of adhesive groups and dental tissue. For example, ionic bonds are formed by the acid groups of the monomer with the inorganic component, which is hydroxyapatite. In addition, chelating groups such as iminodiacetic acid enable the formation of complexes with the calcium ions of dentin and enamel.

In this part, diethyliminodiacetate was used as a potential chelating as well as an adhesive group and it was introduced to alkyl α -hydroxymethyl acrylate derivatives via reactive secondary amine hydrogen. The reactivities of the synthesized monomers in photopolymerization were investigated with photo-DSC and the chelating ability of them with Ni(II) were measured with an ultraviolet-visible spectrophotometer.

4.4.1. Reaction of 3-Acryloyloxy-2-Hydroxypropylmethacrylate (AHM) with Diethyliminodiacetate

AHM is a mixed acrylate/methacrylate crosslinker containing a centered hydroxyl group. It shows faster photopolymerization rates than commercial dimethacrylate monomers, and it is almost as fast as typical diacrylates. Amine Michael addition to this monomer allows us to develop new monomers and crosslinkers with different reactivities which contain a variety of additional functional groups [122, 123]. Using the same approach, we planned to synthesize a new derivative via Micheal addition of diethyliminodiacetate to the acrylate group of AHM (Figure 4.47). This reaction was tried at room temperature with or without solvent (ethanol) using 1:1 mole ratio of AHM to diethyliminodiacetate. Unfortunately, no addition to acrylate double bond was observed. Then reactions were done at a higher temperature (65 °C) but crosslinked polymers were obtained. All attempted reactions were unsuccessful to give the desired Micheal adduct, confirmed by monitoring the reactions with ^{13}C -NMR spectroscopy. An explanation could be that diethyliminodiacetate group is too bulky so its addition to the double bond is sterically hindered. Therefore this method was given up in the course of thesis.



Figure 4.47. Micheal addition of diethyliminodiacetate to AHM

4.4.2. Synthesis of TBEED-IDA

Synthesis of the first diethyliminodiacetate-containing monomer involved three steps (Figure 4.48). At the first step ether dimer of tert-butyl α -hydroxymethyl acrylate (TBEED) was synthesized. Hydrolysis of the tert-butyl groups using excess CF_3COOH gave a dicarboxylic acid monomer (TBEED-acid). The last step involved the aminolysis of TBEED-acid with diethyliminodiacetate in the presence of 1,3-dicyclohexylcarbodiimid (DCC) and catalytic amount of DMAP in CH_2Cl_2 at room temperature. Then, the reaction mixture was diluted with chloroform, cooled and filtered to get rid off the reaction by-product, N,N'-dicyclohexylurea. It was also extracted with water. The product was obtained as a yellow, oily liquid in a 84.8 per cent yield. It was soluble in common organic solvents like methanol, ether, dichloromethane and chloroform but insoluble in hexane. Both the ^{13}C -NMR and ^1H -NMR spectra showed some impurities. Purification by column chromatography on a silica gel using dichloromethane initially and gradually changing to five per cent methanol eluent was not successful.

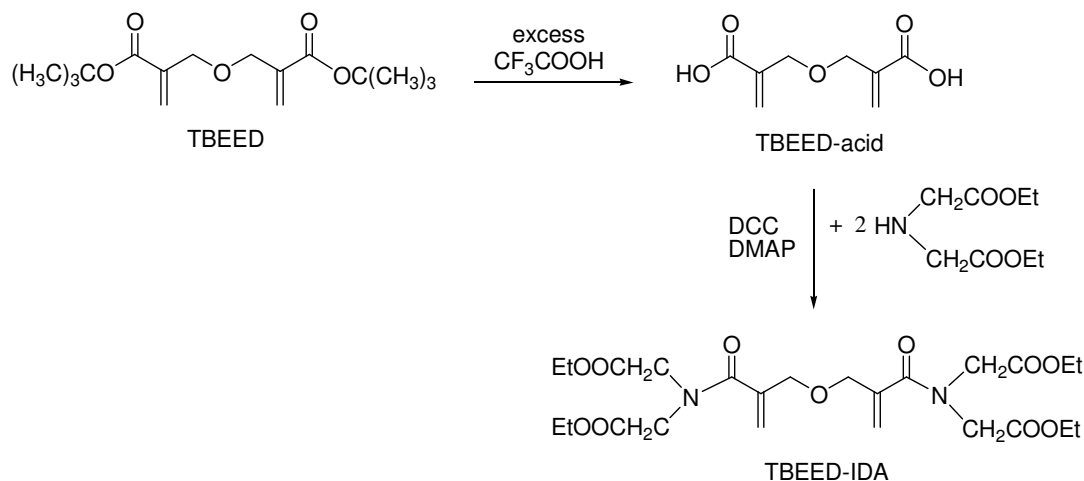
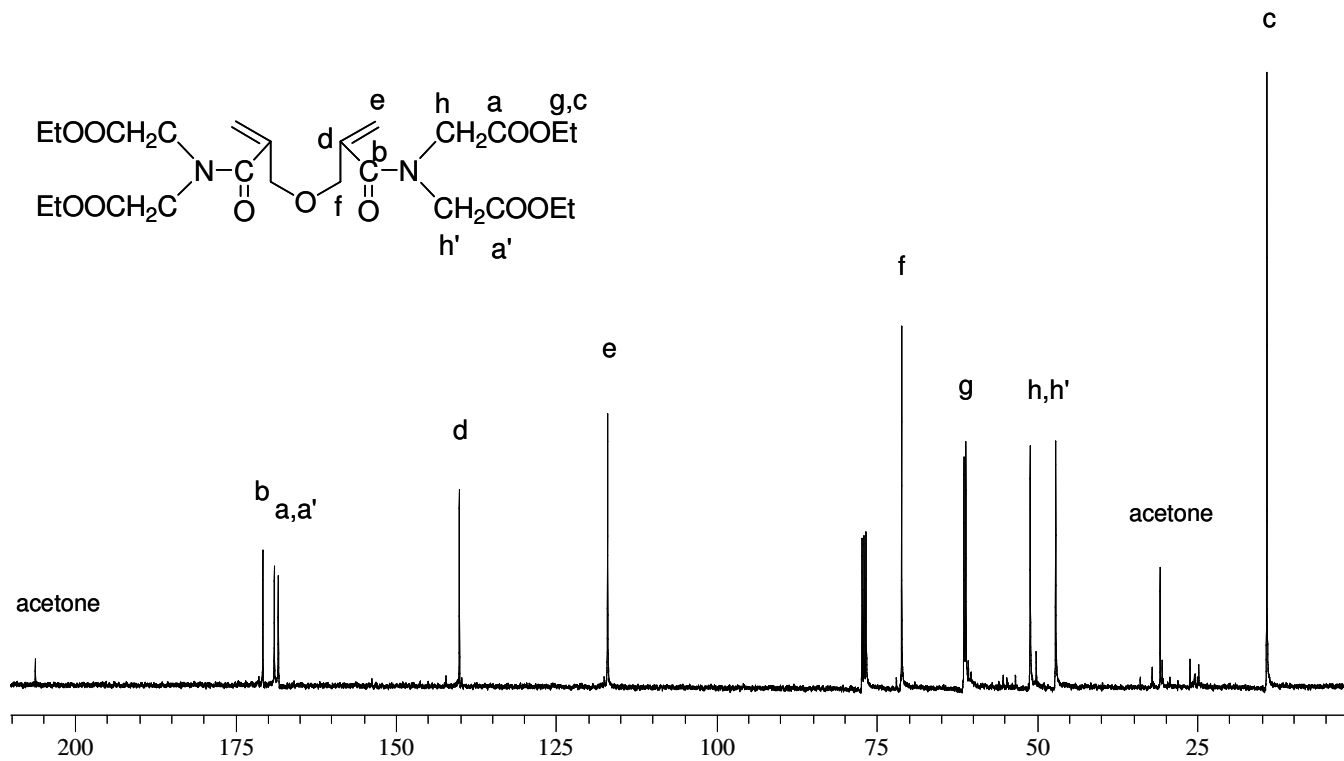


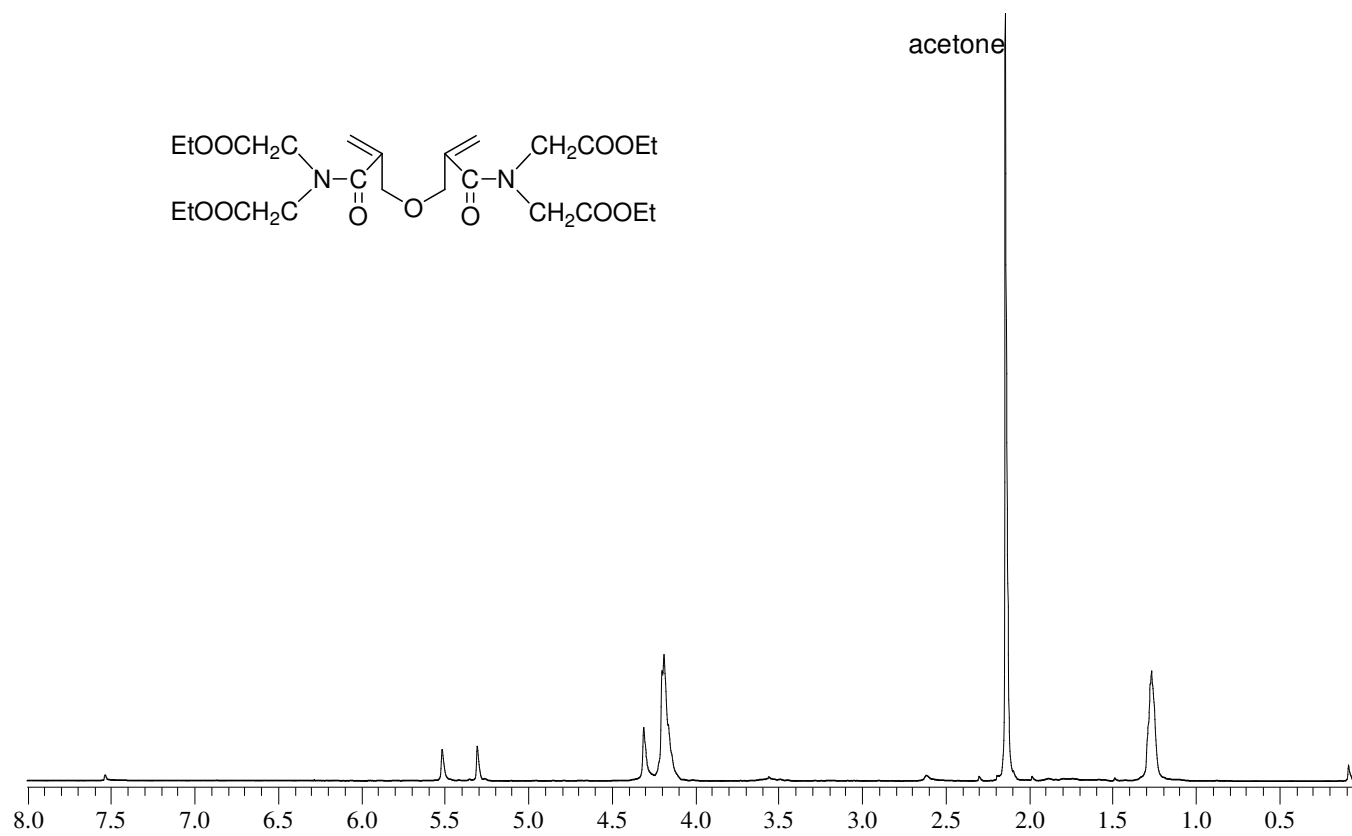
Figure 4.48. Synthesis of TBEED-IDA

The ^{13}C -NMR spectrum of the monomer showed characteristic peaks for methyl carbons at 14.24 ppm, methylene carbons attached to the nitrogen atom at 47.36 and 51.26 ppm (doublet), methylene carbons attached to oxygen at 60.97 and 61.72 ppm (doublet), methylene carbons attached to double bond carbons at 71.46 ppm and double bond carbons at 116.97 and 140.40 ppm, ester carbonyl carbons at 168.47 and 168.99 ppm (doublet) and amide carbonyl carbon at 171.2 ppm (Figure 4.49).

In the ^1H -NMR spectrum, methyl protons at 1.27 ppm, methylenes of ethyl ester and methylene protons attached to nitrogen atom overlap at 4.19 ppm, ether methylenes at 4.31 ppm and double bond protons at 5.31 and 5.51 ppm were characterized (Figure 4.50).

The FT-IR spectrum of this monomer showed characteristic peaks for carbonyl of ester, carbonyl of amide, double bond and C-O at 1745, 1654, 1629 and 1184 cm^{-1} respectively (Figure 4.51).

Figure 4.49. ^{13}C -NMR spectrum of TBEED-IDA

Figure 4.50. ¹H-NMR spectrum of TBEEED-IDA

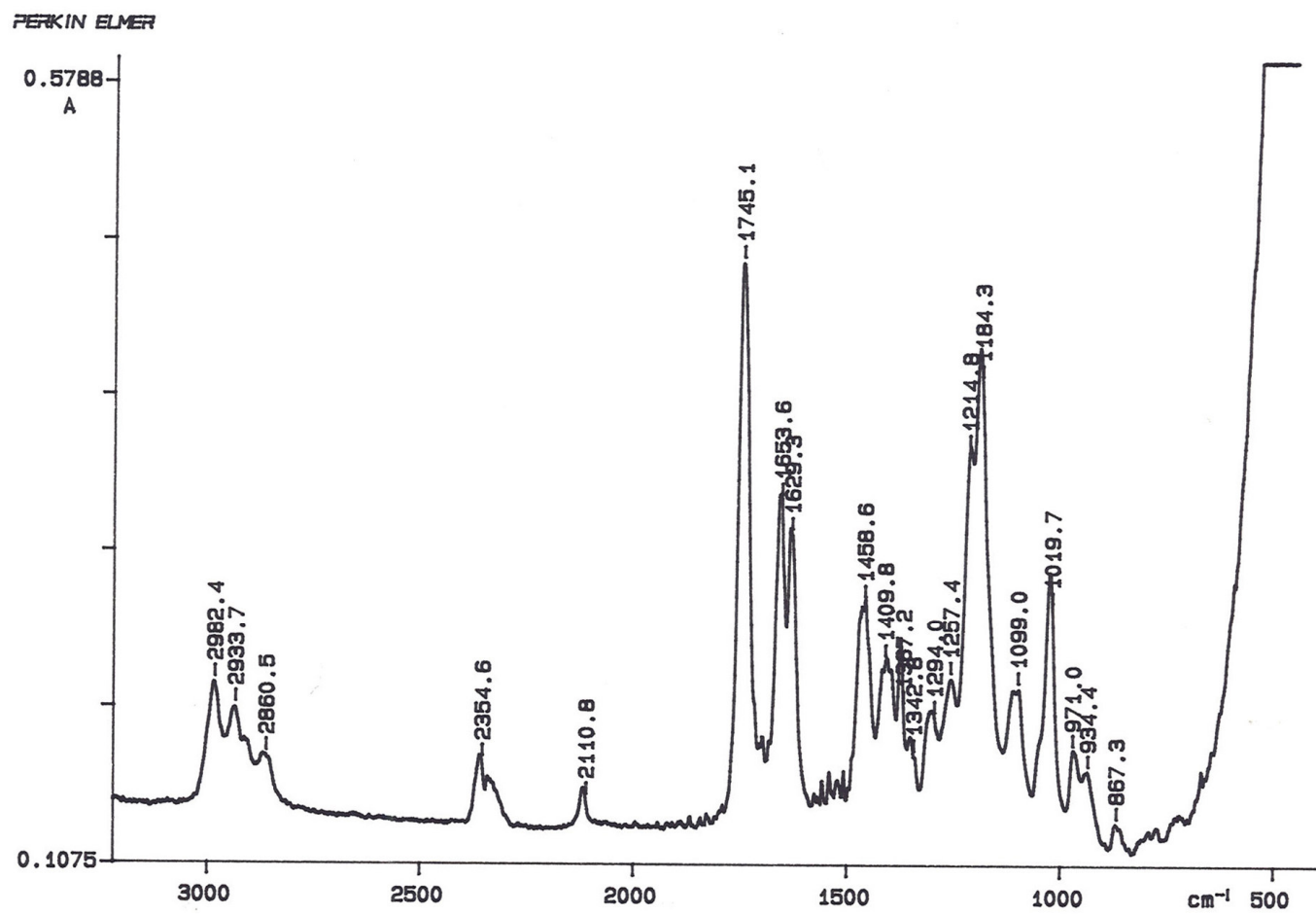


Figure 4.51. FT-IR spectrum of TBEED-IDA

This monomer contains two potential metal-chelating groups attached to the double bond through unhydrolyzable amide linkages. Hydrolysis of the ester groups of this monomer with equimolar amount KOH in water at room temperature was unsuccessful. Therefore, two different methods were used to synthesize the monomer containing potassium salt of iminodiacetate. In the first method, potassium salt of iminodiacetate was prepared and reacted with TBEED-acid in methanol. The second method, involved the reaction of potassium salt of iminodiacetate with diacid chloride derivative of TBEED in the presence of TEA in THF. ¹³C-NMR spectrum confirmed product formation. But the products obtained from both methods contained a residual impurity which could not be removed.

4.4.3. Synthesis of EBBr-IDA and EBBr-IDA-K⁺

The second monomer was prepared via a reactive allylic bromide reaction of EBMA with diethyliminodiacetate in the presence of TEA as catalyst in diethylether at room temperature (Figure 4.52). After the reaction was finished, it was extracted with one weight per cent of HCl to get rid off excess diethyliminodiacetate and TEA. The evaporation of solvent gave the product as a light yellow oil in a 90.8 per cent yield. The product was soluble in most common solvents like methanol, THF, diethyl ether, chloroform and hexane.

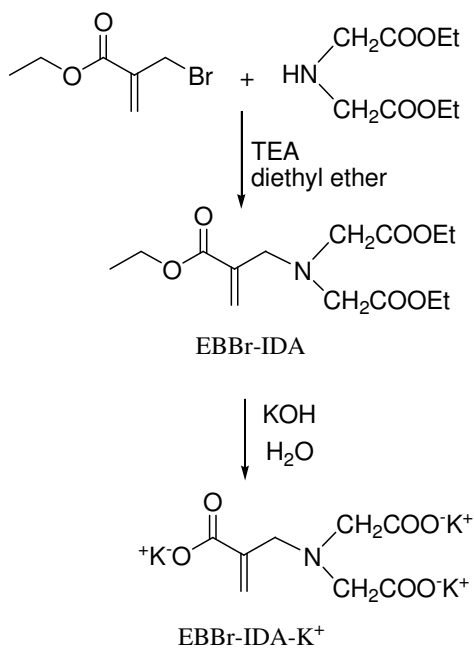
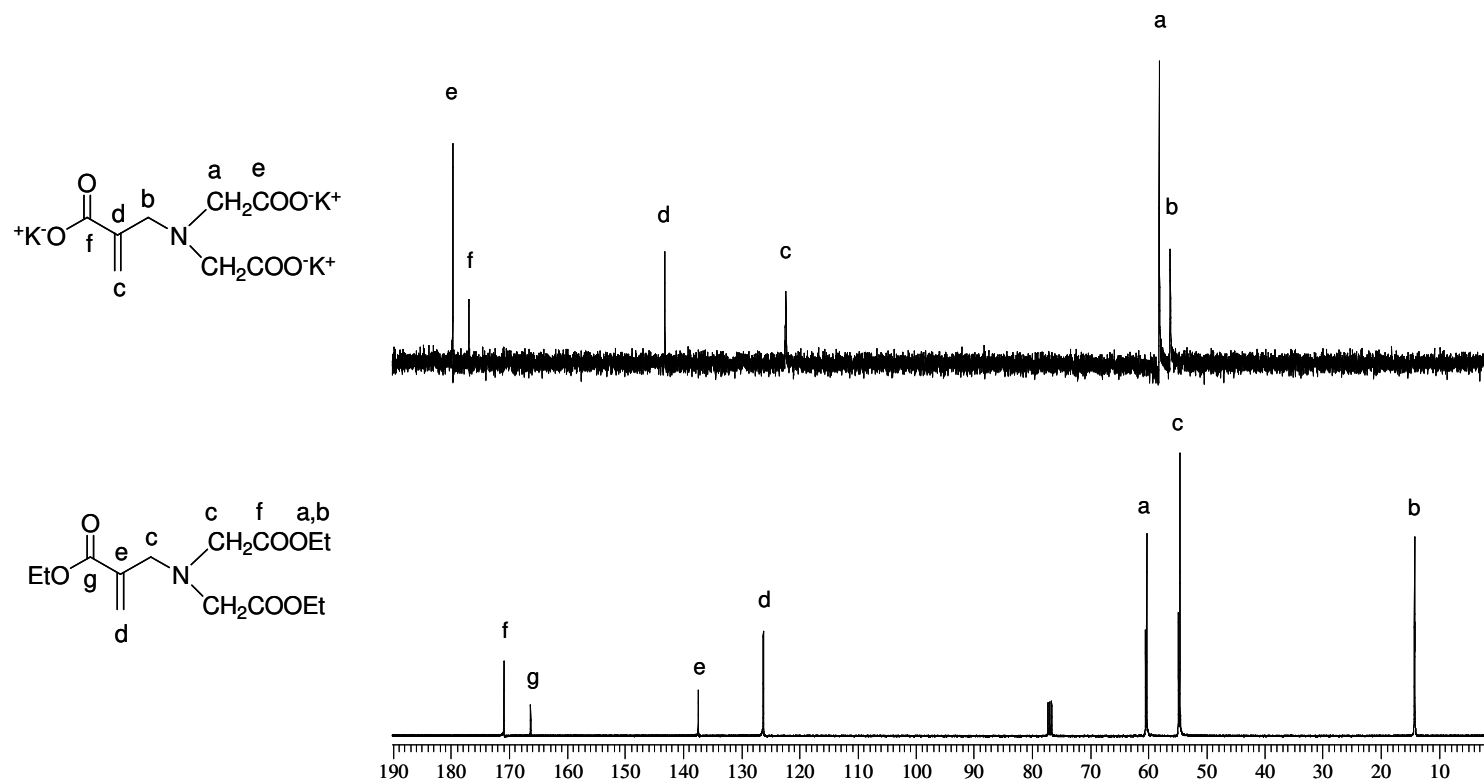


Figure 4.52. Synthesis of EBBr-IDA and EBBr-IDA-K⁺

In the ¹³C-NMR spectrum, the methyl carbons appear at 14.21 ppm, methylene carbons attached to the nitrogen atom show peaks at 54.82 ppm, methylene carbon attached to the oxygen atom is at 60.3 ppm. The double bond peaks appear at 126.52 and 137.53 ppm and carbonyl carbons are at 166.19 and 170.84 ppm (Figure 4.53).

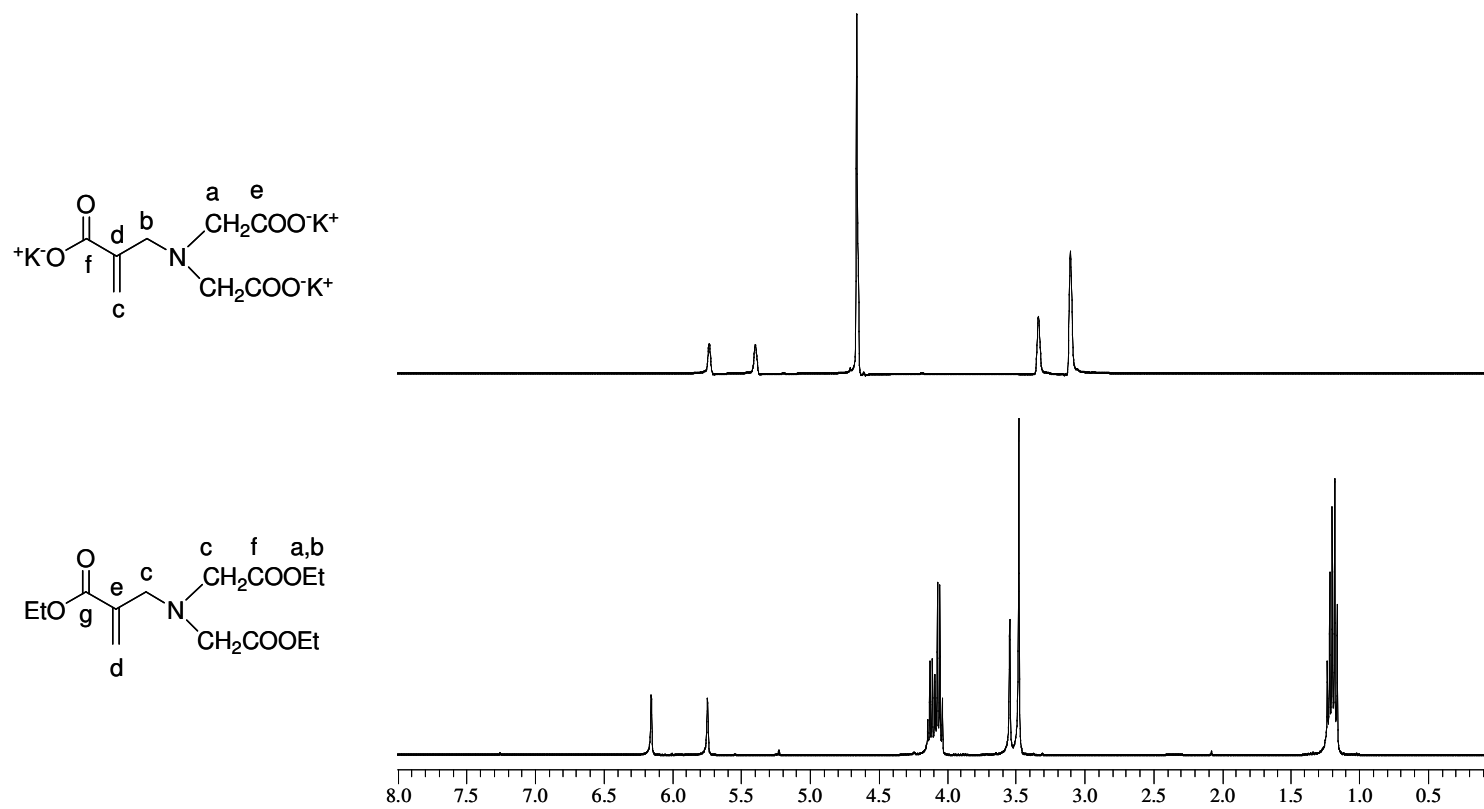
In the ¹H-NMR spectrum, methyl protons at 1.29 ppm, methylene protons attached to nitrogen atom at 3.56 ppm, methylenes attached to double bond carbon at 3.61 ppm, methylenes of ethyl ester at 4.17 ppm and double bond protons at 5.82 and 6.24 ppm were characterized (Figure 4.54).

In the FT-IR spectra the absorption band at 1739 cm⁻¹ is caused by stretching vibrations of the ester carbonyl groups. The bands at 1632 and 1189 cm⁻¹ are due to double bond and C-C(=O)-O stretching (Figure 4.55).



Figure

4.53. ^{13}C -NMR spectra of EBBr-IDA and EBBr-IDA- K^+

Figure 4.54. ¹H-NMR spectra of EBBr-IDA and EBBr-IDA-K⁺

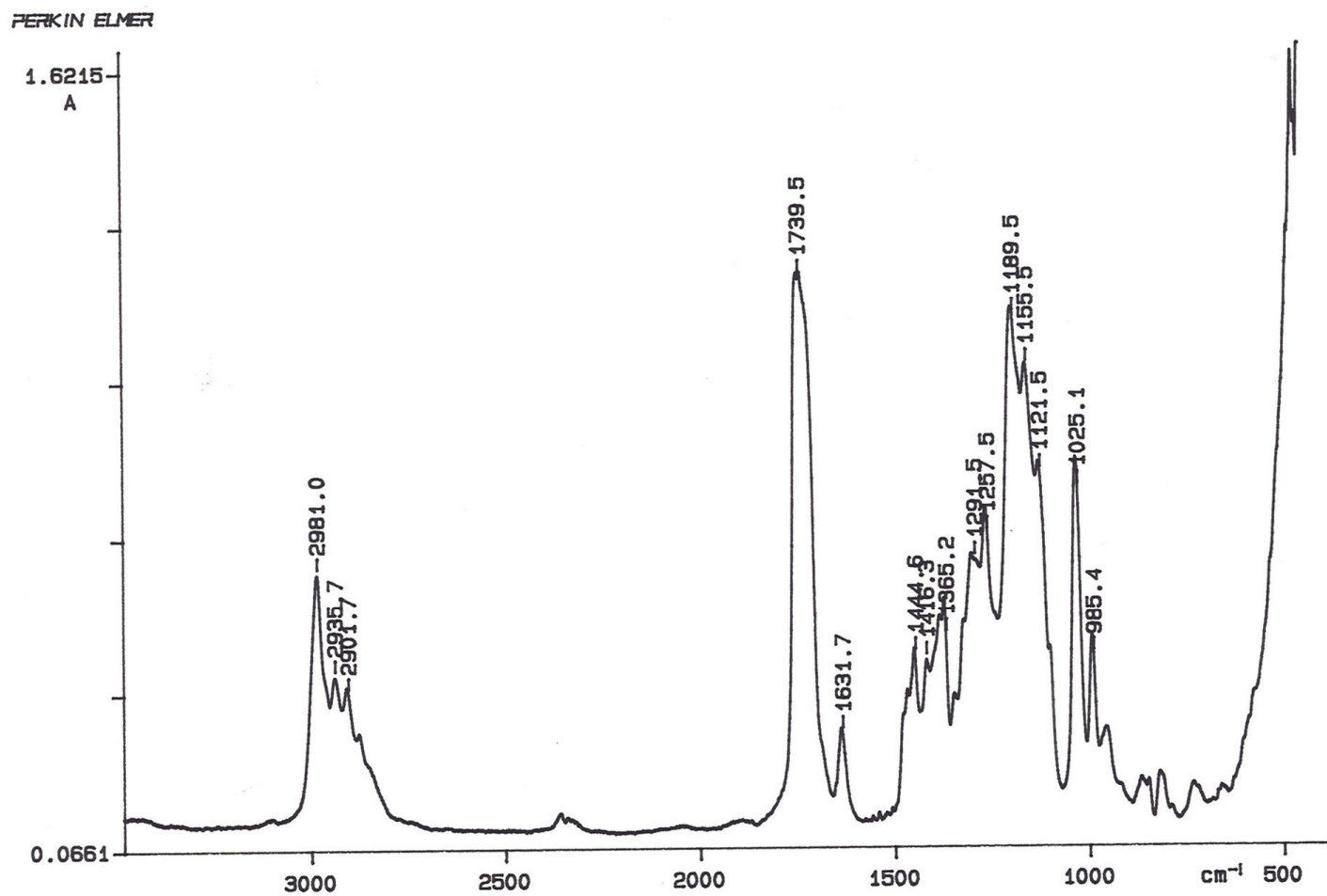
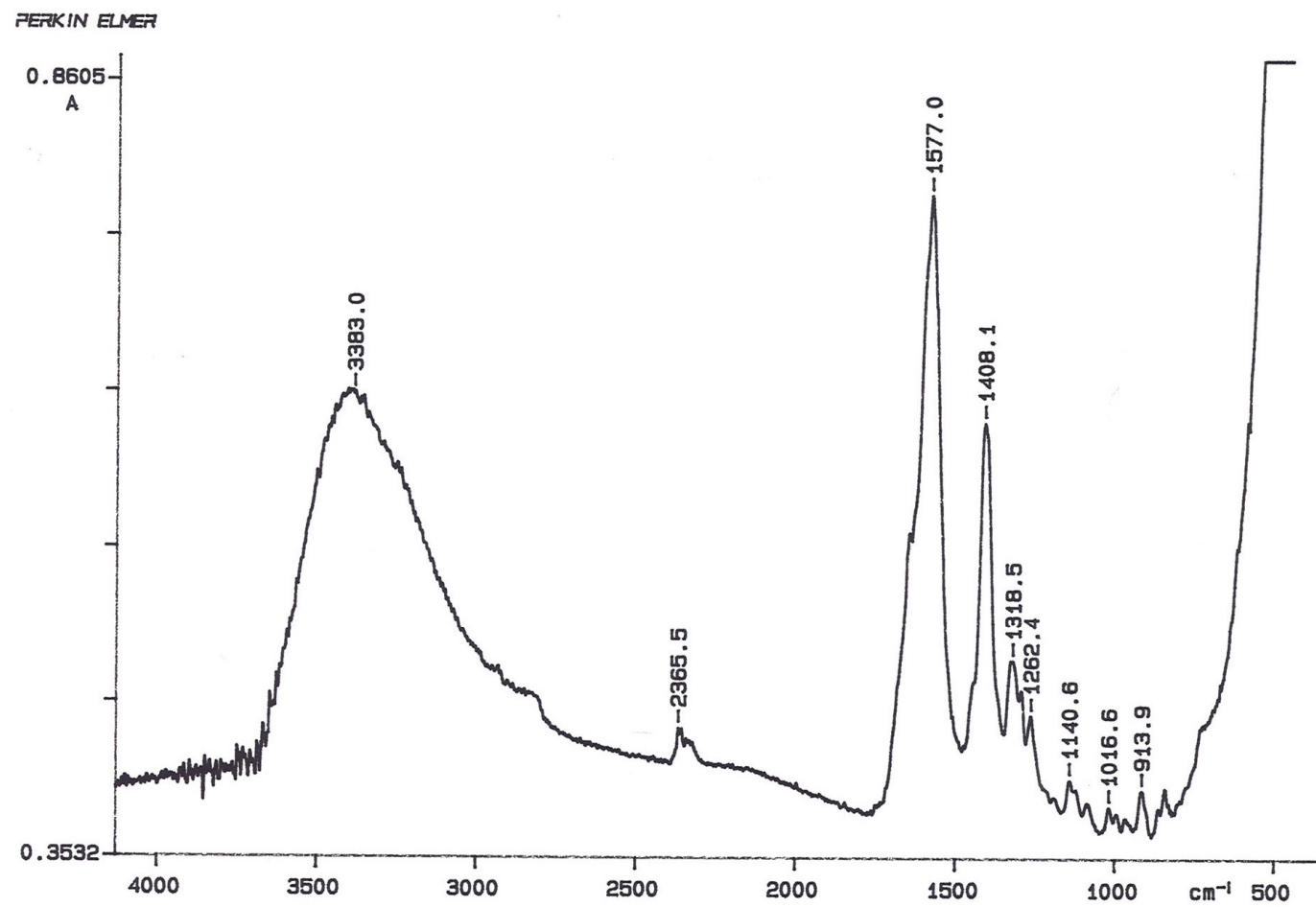


Figure 4.55. FT-IR spectrum of EBr-IDA

This monomer contains one potential metal chelating iminodiacetate functionality attached by an amine linkage. The hydrolysis of the ethyl groups of this monomer was conducted with an equimolar amount of aqueous KOH at room temperature. After sublimation of water, the product was purified by dissolving in warm methanol, filtering the solution to remove any KCl salt and then precipitating into acetone to give EBBr-IDA-K⁺ in 76.6 per cent yield. EBBr-IDA-K⁺ can act as a metal-chelate through iminodiacetate group and a metal-binder through carboxylate group.

Both ¹³C-NMR and ¹H-NMR spectra of EBBr-IDA-K⁺ showed a complete disappearance of ethyl ester groups of EBBr-IDA (Figures 4.53 and 4.54).

In the FT-IR spectra, a strong asymmetrical stretching band of carboxylate anion is at 1577 cm⁻¹ and a weaker, symmetrical stretching band of carboxylate anion is at 1408 cm⁻¹ (Figure 4.56).

Figure 4.56. FT-IR spectrum of EBBR-IDA- K^+

TBHMA was reacted with thionyl chloride to give CMAC which is the key intermediate in the synthesis of many reactions [86]. However, synthesis of CMAC does not work smoothly. The product is contaminated by HCl adduct which is difficult to separate from CMAC. Purification by distillation reduced the yield to 34.0 per cent and damaged the vacuum-pump.

CMAC-IDA, with identical amide and amine groups was synthesized by the reaction of CMAC with diethyliminodiacetate in the presence of TEA as an acid scavenger and catalyst in THF (Figure 4.57). After the reaction, the precipitate was filtered off and the solvent was evaporated. The residue was dissolved in dichloromethane and washed with water. Then, organic phase was dried, solvent was removed and the pure product was obtained as a yellow oil in 91.1 per cent yield.

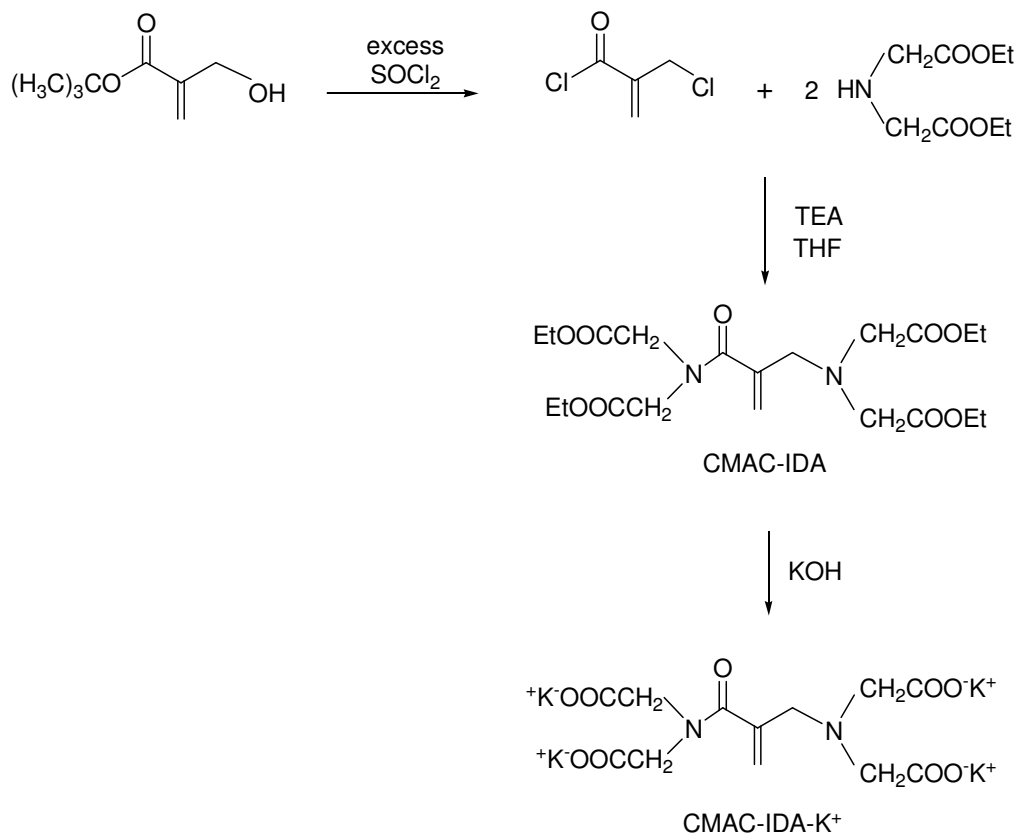


Figure 4.57. Synthesis of CMAC-IDA and CMAC-IDA-K⁺

The ¹³C-NMR spectrum of this monomer shows the peak for methyl carbons at 14.22 ppm. Methylene carbons attached to the amide nitrogen appear at 47.21 and 51.10 ppm (doublet), methylene carbons attached to the nitrogen atom show peak at 54.68 ppm, methylene carbon attached to double bond carbon is at 56.97 ppm and finally, methylene carbons attached to oxygen atoms are at 60.31, 61.05, 61.36 ppm. The double bond peaks appear at 116.78 and 140.71 ppm and amide carbonyl carbon is at 168.37, 168.95 and ester carbonyl carbons are at 170.64 ppm and 171.62 ppm (Figure 4.58).

In the ¹H-NMR spectrum, methyl protons at 1.28 ppm, methylene protons attached to nitrogen atom at 3.56 ppm, methylenes attached to double bond carbon at 3.59 ppm, methylenes of ethyl ester and methylenes attached to the amide nitrogen overlap at 4.12-4.29 ppm and double bond protons at 5.28 and 5.51 ppm were characterized (Figure 4.59).

The FT-IR spectrum of this monomer showed characteristic peaks for carbonyl of ester, carbonyl of amide, double bond and C-O at 1743, 1655, 1623 and 1186 cm^{-1} respectively (Figure 4.60).

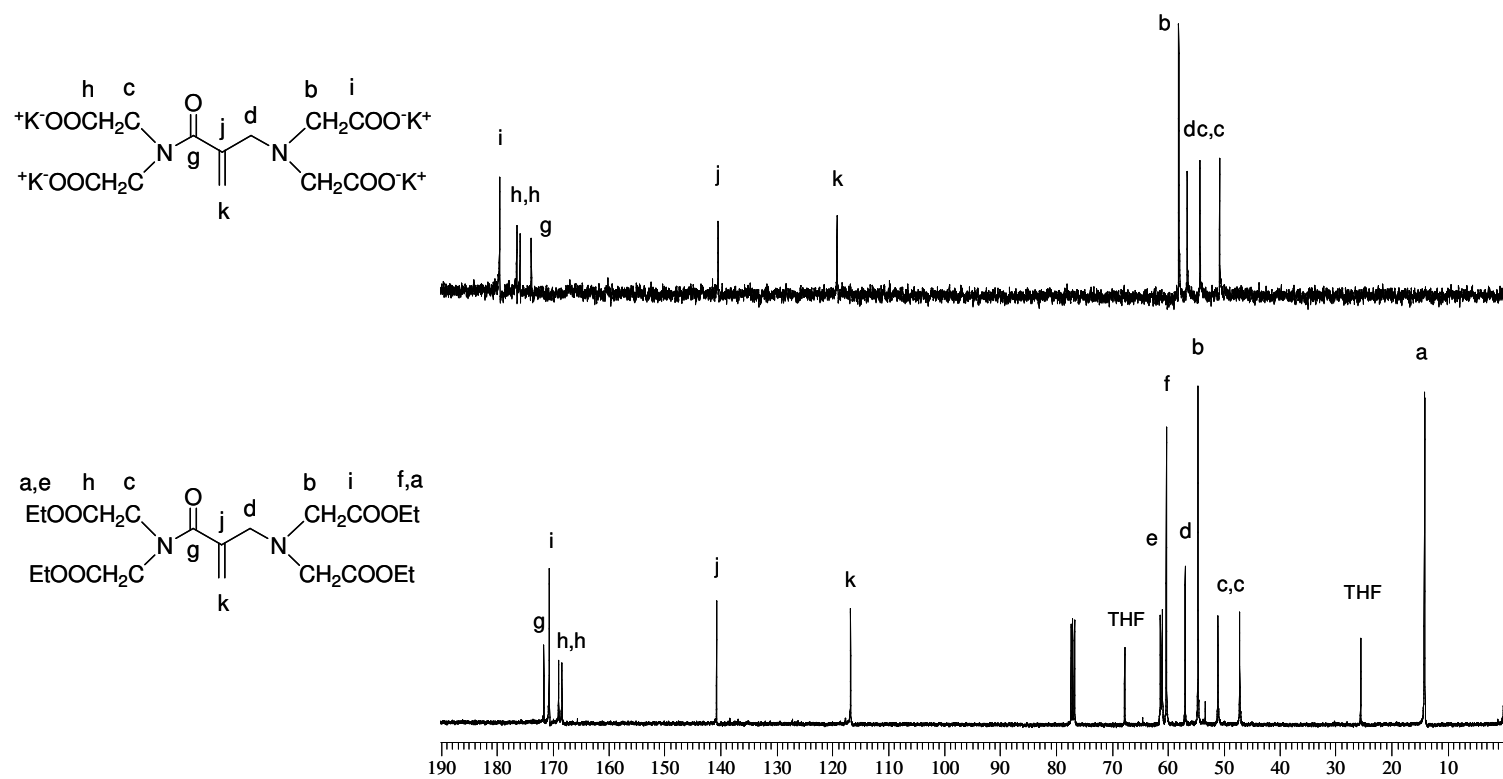
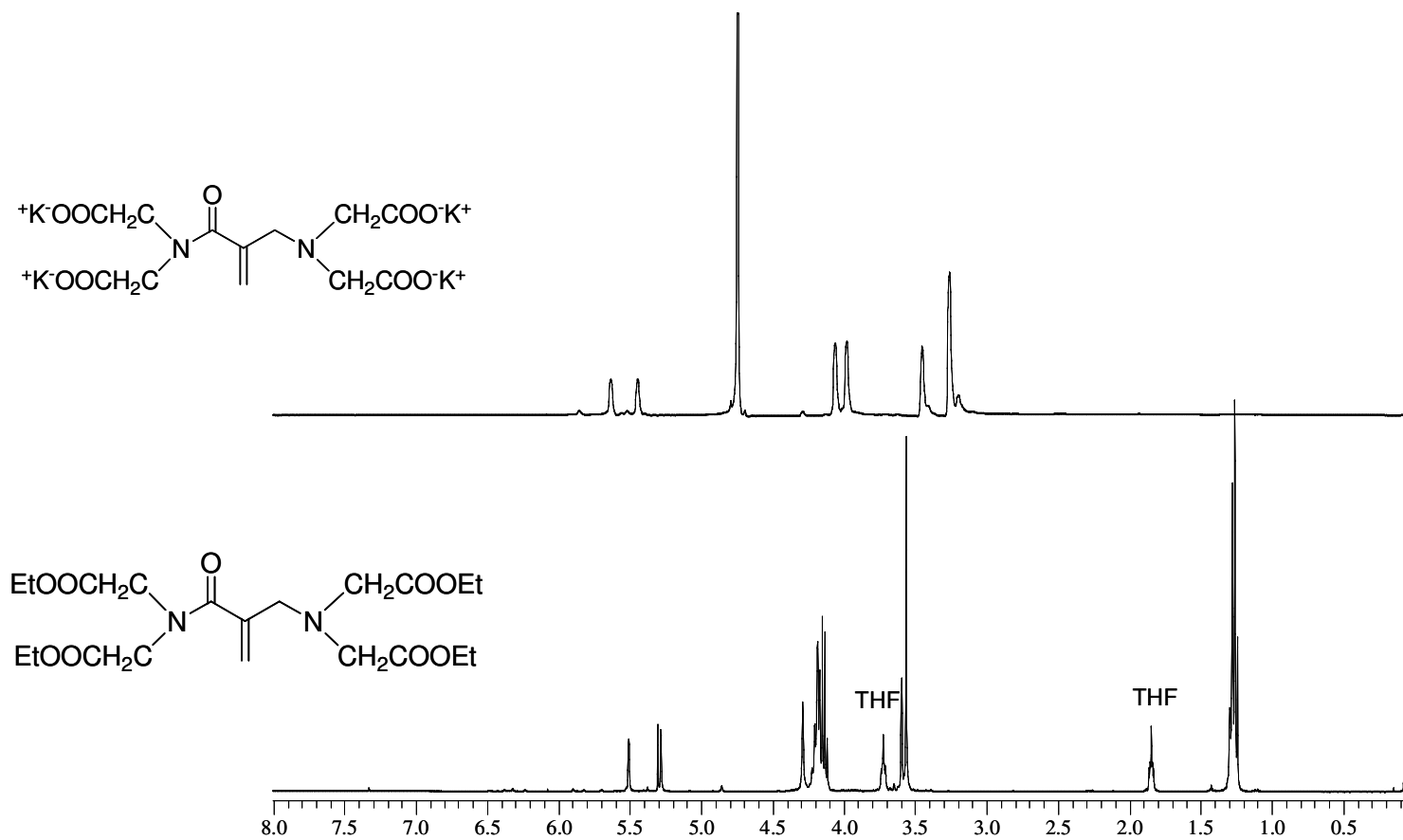


Figure 4.58. ^{13}C -NMR spectra of CMAC-IDA and CMAC-IDA-K⁺

Figure 4.59. ¹H-NMR spectra of CMAC-IDA and CMAC-IDA-K⁺

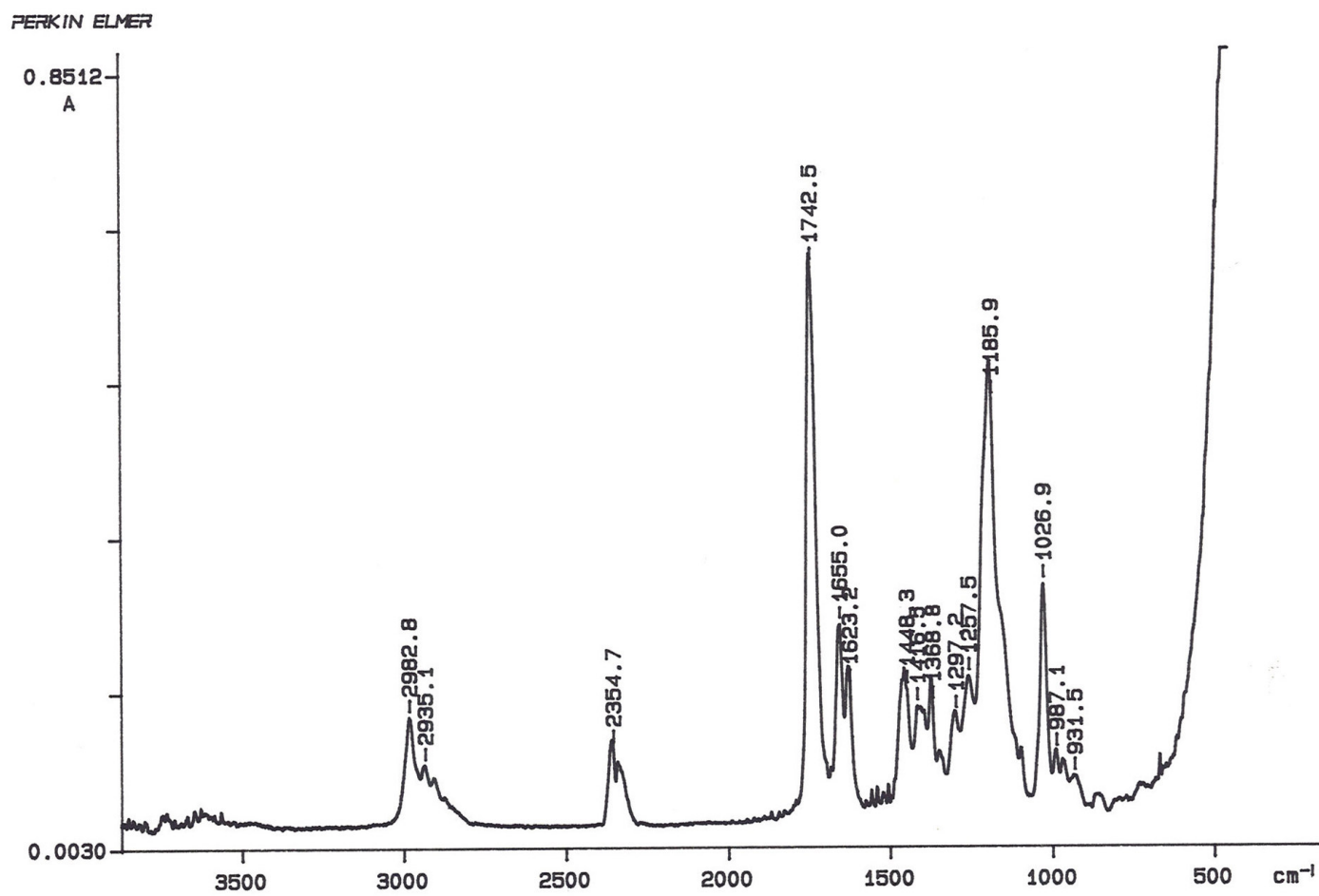
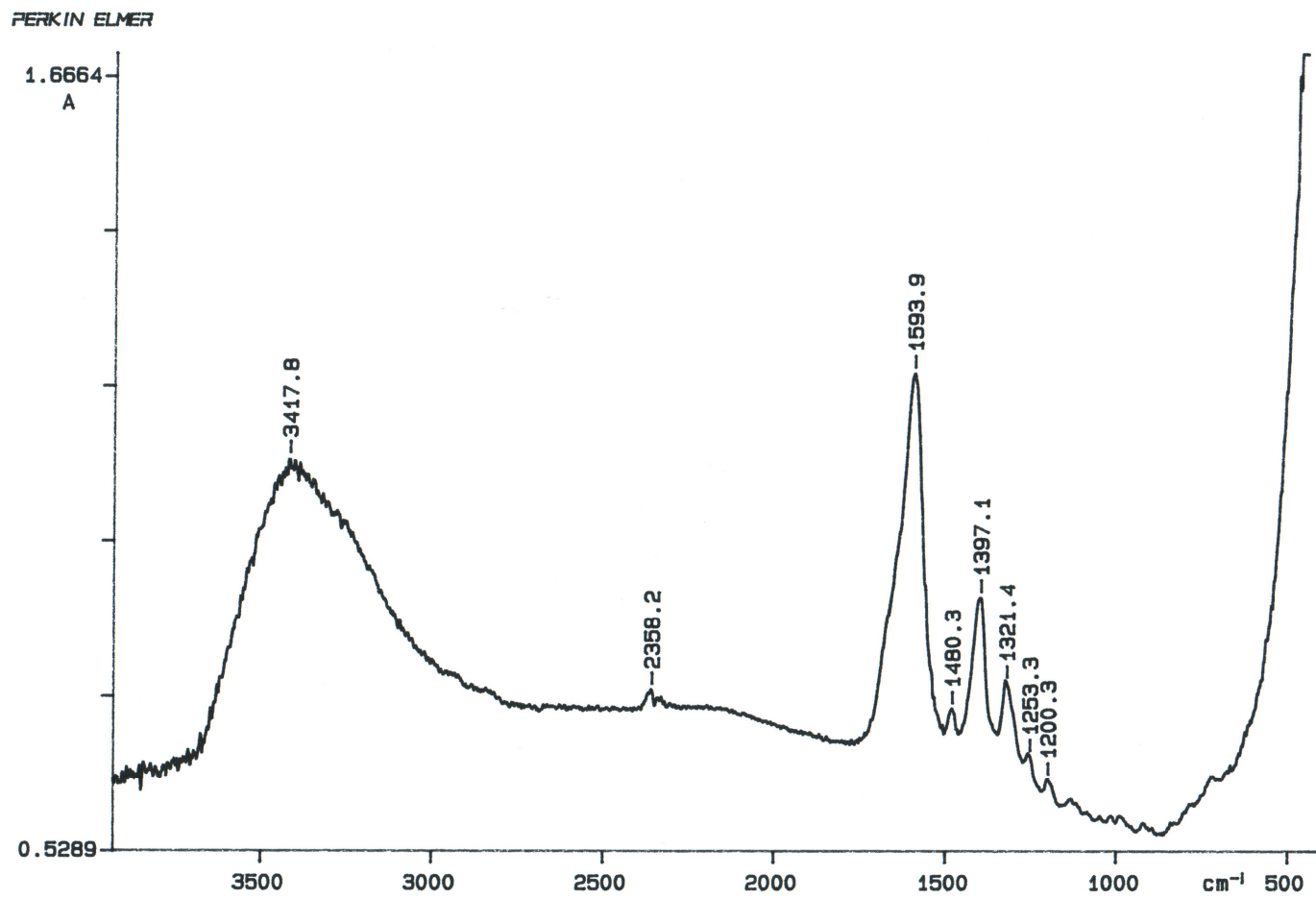


Figure 4.60. FT-IR spectrum of CMAC-IDA

CMAC-IDA was also hydrolyzed by equimolar amount of KOH at room temperature to give CMAC-IDA-K⁺. The product was obtained by sublimation of water and purified by dissolving in methanol, filtering to remove any KCl salt and then precipitating into acetone in 58.5 per cent yield. CMAC-IDA-K⁺ contains two metal-chelating functionality.

Both ¹³C-NMR and ¹H-NMR spectra of CMAC-IDA-K⁺ showed a complete disappearance of ethyl ester groups of CMAC-IDA (Figures 4.58 and 4.59).

In the FT-IR spectra, a strong asymmetrical stretching band of carboxylate anion is at 1594 cm⁻¹ and a weaker, symmetrical stretching band of carboxylate anion is at 1397 cm⁻¹ (Figure 4.61).

Figure 4.61. FT-IR spectrum of CMAC-IDA-K⁺

4.4.5. Photopolymerizations

The reactivities of the synthesized monomers in photopolymerization were investigated with photo-DSC. All the polymerizations were performed under identical conditions of initiator concentration (2.0 mol per cent), UV light intensity (15 mW/cm²) and temperature (40 °C). First, TBEED-IDA was homopolymerized and copolymerized with a highly reactive monomer TBEED. TBEED:monomer ratios were 95:5, 80:20, 50:50. Figure 4.62 shows the rate of polymerizations versus time plots. Conversion values were given in Table 4.10. TBEED-IDA showed very low polymerization rate and conversion (0.00093 s⁻¹, 17.8 per cent) compared to TBEED (0.032 s⁻¹, 80.8 per cent). Rate of copolymerization and conversion decreased with an increase in TBEED-IDA amount in the copolymer.

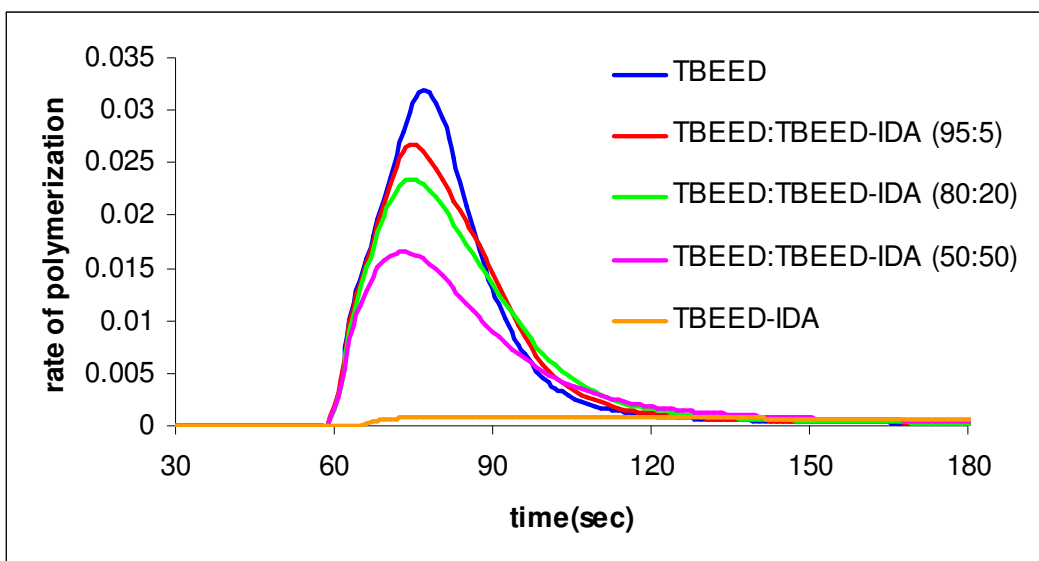


Figure 4.62. Rate of polymerization versus time graph of TBEED-IDA with TBEED

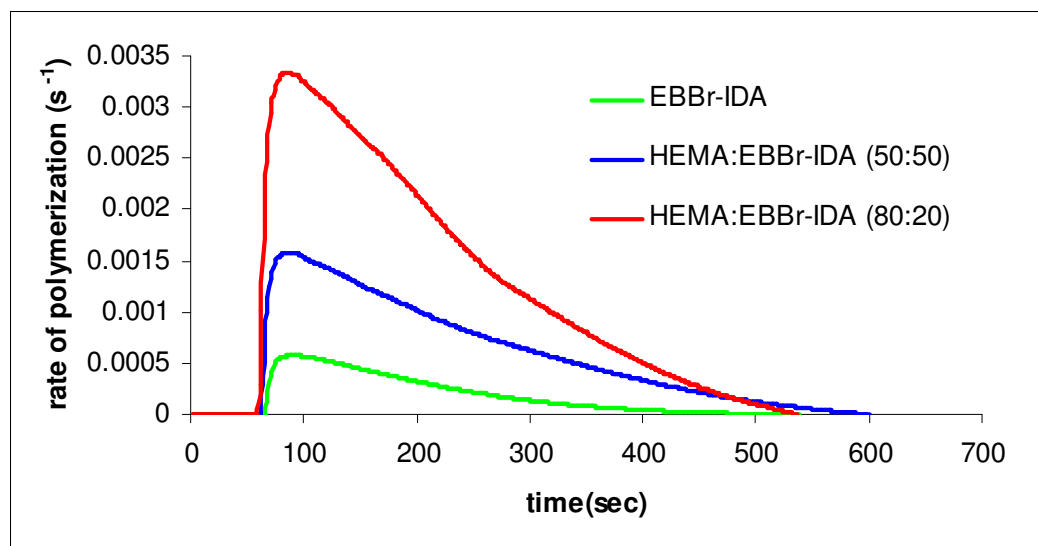


Figure 4.63. Rate of polymerization versus time graph of EBBr-IDA with HEMA

EBBr-IDA was homopolymerized and copolymerized with HEMA. Figure 4.63 and Table 4.10 show the rate of polymerizations and conversions. Rate of polymerization and conversion of EBBr-IDA (0.00057 s^{-1} , 9.4 per cent) were lower than HEMA (0.036 s^{-1} , 93.4 per cent). CMAC-IDA showed similar polymerization behaviour with the maximum rate of polymerization and conversion of 0.00028 s^{-1} , 6.5 per cent.

Table 4.10. Photopolymerization results

Composition	R_p (s^{-1})	Conversion (%)
TBEED	0.03199	80.8
TBEED:TBEED-IDA (95:5)	0.02672	77.8
TBEED:TBEED-IDA (80:20)	0.02347	74.1
TBEED:TBEED-IDA (50:50)	0.01653	60.4
TBEED-IDA	0.00093	17.8
HEMA	0.03598	93.4
HEMA:EBBr-IDA (80:20)	0.00333	65.3
HEMA:EBBr-IDA (50:50)	0.00157	33.4
EBBr-IDA	0.00057	9.4
CMAC-IDA	0.00028	6.5

As it was discussed before, the ^{13}C -NMR chemical shift differences ($\Delta\delta$) of the C=C double bonds of allyl monomers ($\text{C}_\beta\text{H}_2=\text{C}_\alpha$) were correlated with the radical polymerizability. Electron withdrawing substituents on the α -carbon cause downfield shifts of the β -carbon peak while the α -carbon is shifted upfield. The net result is a decrease in the chemical shift difference. The smaller the $\Delta\delta$ value is, the higher is the polymerizability of the monomer. Also, steric effects of the substituents reduced the conjugation between C=C and C=O and caused an increase in $\Delta\delta$ value and decreased polymerizability. It was shown in the literature that the conjugations between C=C and C=O double bonds of N,N-disubstituted methacrylamides are less effective than those of methyl methacrylate. So, the lower polymerization reactivity of N,N-disubstituted methacrylamides were explained by the twisted conformation between double bonds reducing conjugation and it appeared that methacryloyl groups of N,N-disubstituted methacrylamides are of a non-conjugative nature. The comparison of $\Delta\delta$ values of TBEED-IDA, EBBR-IDA and CMAC-IDA were listed in Table 4.11.

Table 4.11. ^{13}C -NMR chemical shifts of the two vinyl carbon peaks of the monomers

Monomers	$\text{C}_\alpha=$	$=\text{C}_\beta\text{H}_2$	$\Delta\delta$
TBEED-IDA	140.4	117.0	23.4
EBBR-IDA	137.5	126.5	11.0
CMAC-IDA	140.7	116.8	23.9
N,N-Dimethylmethacrylamide	140.8	115.4	25.4
MMA	136.3	125.5	10.8

It can be noticed from the $\Delta\delta$ values that, the extent of conjugation between C=C and C=O double bonds decreased for the N,N-disubstituted methacrylamide containing TBEED-IDA and CMAC-IDA which lead to lower homopolymerization tendency. On the other hand, the conjugative nature of EBBR-IDA is as effective as that of MMA but low rate of polymerization for EBBR-IDA was probably due to the presence of allylic group that can undergo degradative chain transfer. Among these three monomers, the lowest reactivity belongs to CMAC-IDA which has N,N-disubstituted methacrylamide as well as an allyl group and highest reactivity belongs to TBEED-IDA which has bulky

N,N-disubstituted methacrylamide groups that can increase the cyclization tendency of this dimer.

4.4.6. Solution Polymerizations in Water

The radical solution copolymerization of EBBr-IDA-K⁺ and CMAC-IDA-K⁺ with acrylamide (5:95 and 10:90) was carried out in water in the presence of V-50 at 65-67 °C to give a water soluble polymer (Figure 4.64). The total monomer and initiator concentrations were 8.33 M and 0.042 M respectively. The polymers were isolated by precipitation into acetone and purified by dialysis against water. ¹H-NMR spectra of the polymers showed no residual double bonds. The polymers were soluble in water and methanol, but were insoluble in acetone and ether. Polymer yields after dialysis with 6000-8000 molecular weight cutoff dialysis tubing were very low and decreased with increasing EBBr-IDA-K⁺ or CMAC-IDA-K⁺ in the feed (Table 4.12). This observation implies that polymers contained high fractions of short chains. The copolymer compositions were determined from the integrated ¹H-NMR spectra with the ratio of peak areas of backbone protons of the copolymer around 1.3 – 2.5 to the peak areas of methylene protons of EBBr-IDA-K⁺ or CMAC-IDA-K⁺ around 3.0 - 4.2 ppm.

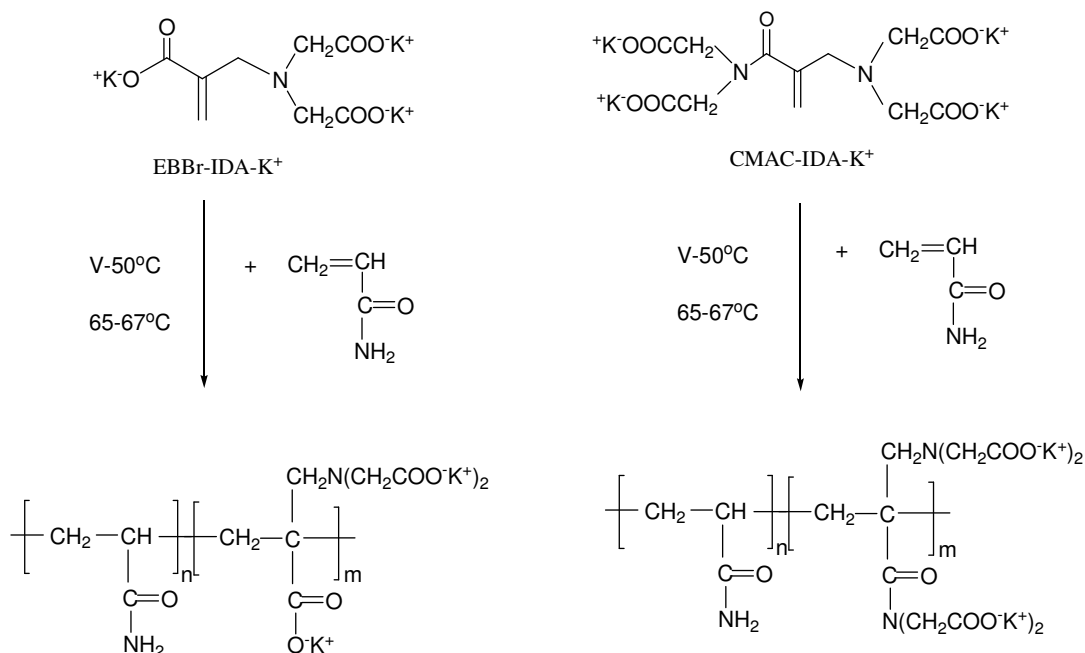


Figure 4.64. Copolymerizations of the chelating monomers with acrylamide

Table 4.12. Polymerization conditions and polymer characterization results

Monomer	[M]	[V-50]	Acrylamide in the feed	Monomer in the copolymer	Time (min)	Temp. (°C)	Yield (%)
Acrylamide:3	8.33	0.042	95	1.20	240	65-67	67.5 ^a , 11.4 ^b
Acrylamide:3	8.33	0.042	90	5.65	270	65-67	33.4 ^a , 6.6 ^b
Acrylamide:5	8.33	0.042	95	0.25	70	65-67	66.9 ^a , 17.6 ^b
Acrylamide:5	8.33	0.042	90	0.52	160	65-67	68.8 ^a , 11.3 ^b

^aafter first precipitation, ^bafter dialysis.

4.4.7. TGA Results

The thermal stabilities of the EBBr-IDA-K⁺ and CMAC-IDA-K⁺ and their copolymers were investigated by TGA. Figures 4.65 and 4.66 shows the TGA curves of the copolymers and monomers under nitrogen. The weight loss in the interval 0-200 °C may be attributed to the decomposition of carboxylate groups and to dehydration for both monomers and copolymers [124]. There was no weight loss in EBBr-IDA-K⁺ and CMAC-IDA-K⁺ between 200-300 °C, so, weight loss in the copolymers for this interval corresponds to the acrylamide segments. Final weight loss for EBBr-IDA-K⁺ and CMAC-IDA-K⁺ starts at 350 and 325 °C respectively and the major weight loss in the copolymers corresponds to the EBBr-IDA-K⁺ or CMAC-IDA-K⁺ segments as well as the rupture of the polymer chain.

The char residues increased on the incorporation of EBBr-IDA-K⁺ and CMAC-IDA-K⁺ in the copolymers. The copolymer acrylamide:EBBr-IDA-K⁺ (95:5) and (90:10) gave a char residue of 28.4 per cent and 34.3 per cent, whereas the char residues for the copolymer acrylamide:CMAC-IDA-K⁺ (95:5) and (90:10) were 23.3 per cent and 26.3 per cent respectively.

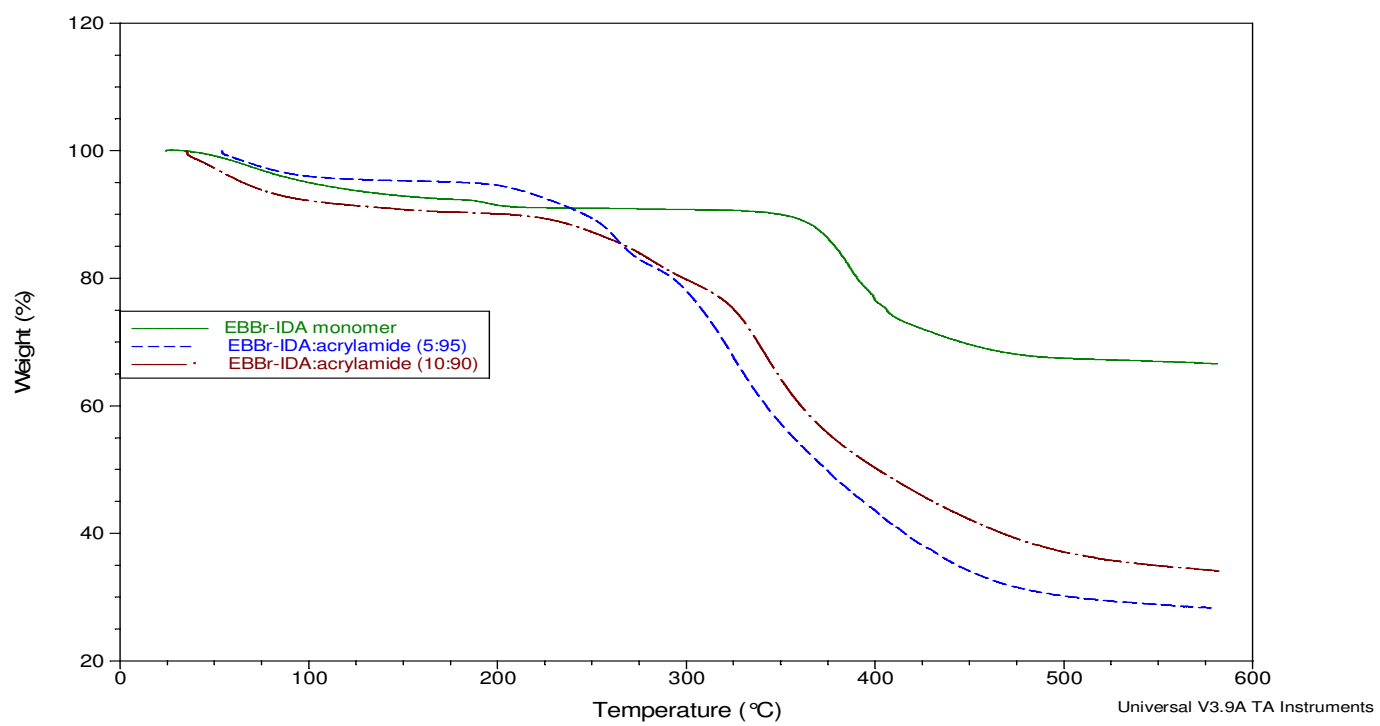


Figure 4.65.

curves of EBBr-IDA- K^+ and the copolymers, acrylamide:EBBr-IDA- K^+ (95:5), acrylamide:EBBr-IDA- K^+ (90:10)

TGA

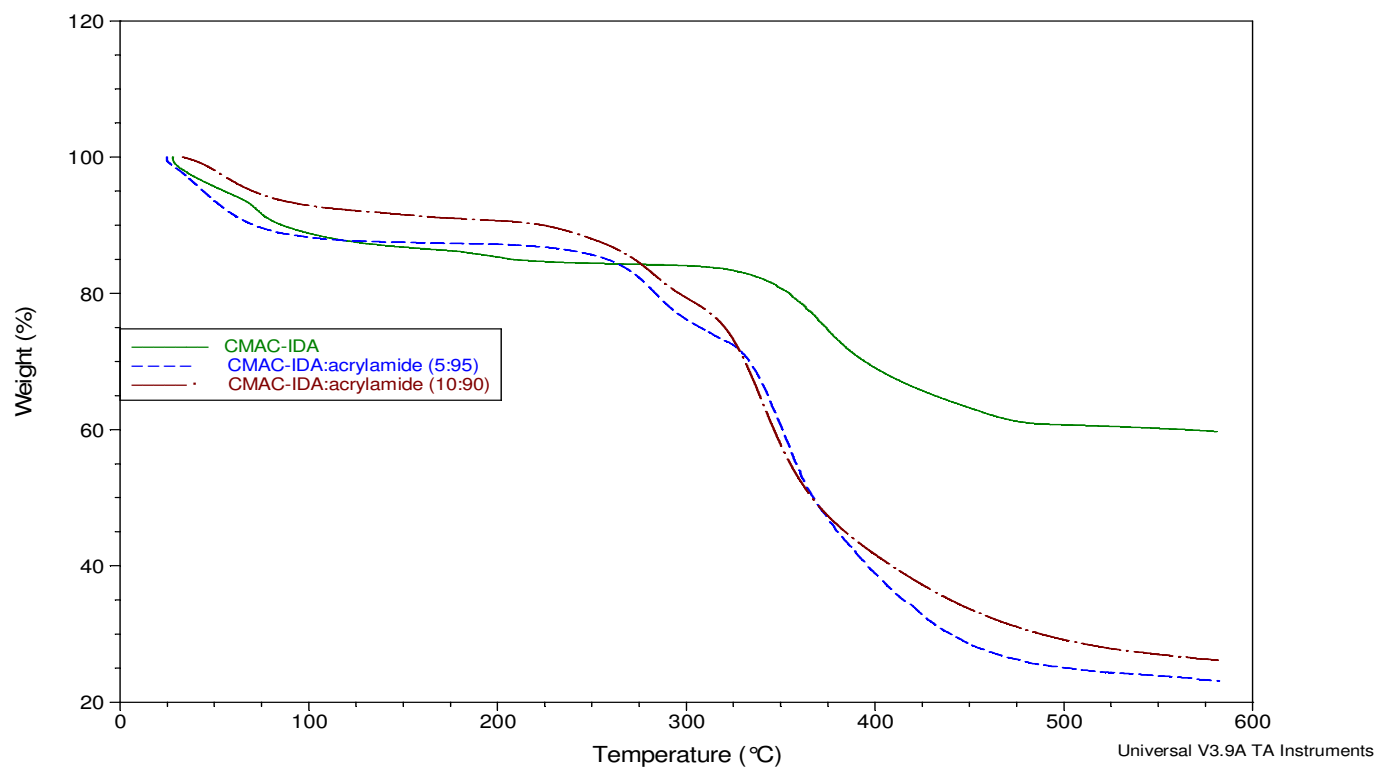


Figure 4.66. TGA curves of CMAC-IDA- K^+ and the copolymers, acrylamide:CMAC-IDA- K^+ (95:5), acrylamide:CMAC-IDA- K^+ (90:10)

As it was stated in the literature, decomposition activation energies for the metal complexes are higher than for the functionalized sodium salt, indicating the thermal stability gained on complexation with metal ions. The extra stability of the polymer-metal complexes arises from the formation of stable ring structures of the metal complexes. When we compared the thermal decomposition of acrylamide: EBBr-IDA- K^+ (90:10) copolymer with its Ni^{+2} complex from the derivative of weight with respect to temperature graph, we observed that the major decomposition for the acrylamide:EBBr-IDA- K^+ (90:10) copolymer was obtained at around 340 °C with a mass loss of 31.4 per cent and for the Ni^{+2} complex, major decomposition was obtained at around 361 °C with a mass loss of 35.8 per cent which indicated the thermal stability of acrylamide:EBBr-IDA- K^+ (90:10) copolymer increased on complexation with Ni^{+2} ions as expected (Figures 4.67 and 4.68).

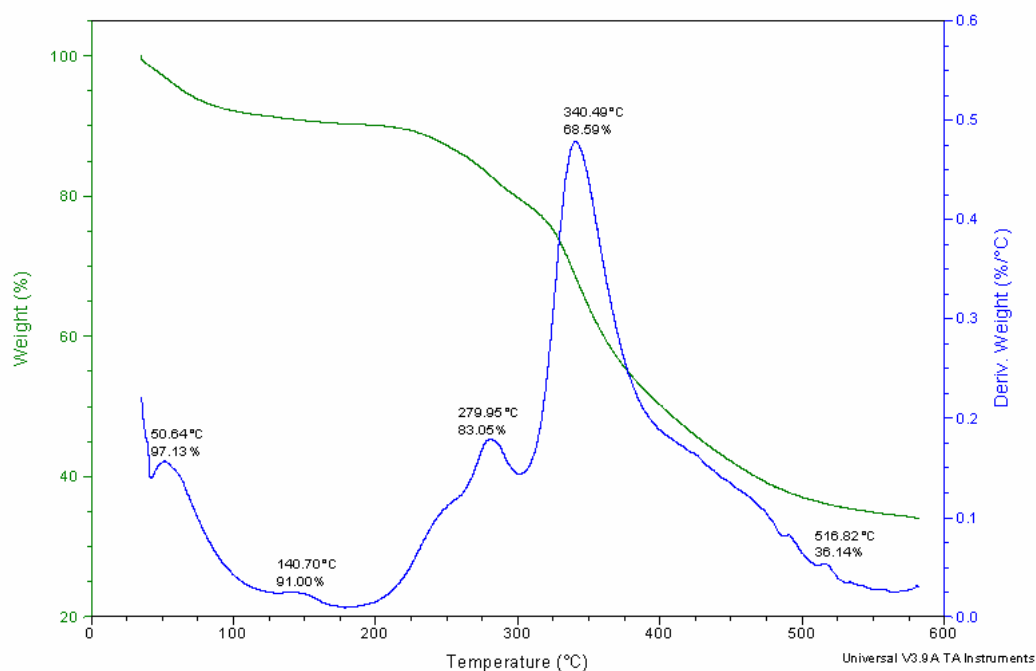


Figure 4.67. Weight loss and derivative of the weight loss curves with respect to temperature of acrylamide: EBBr-IDA- K^+ (90:10)

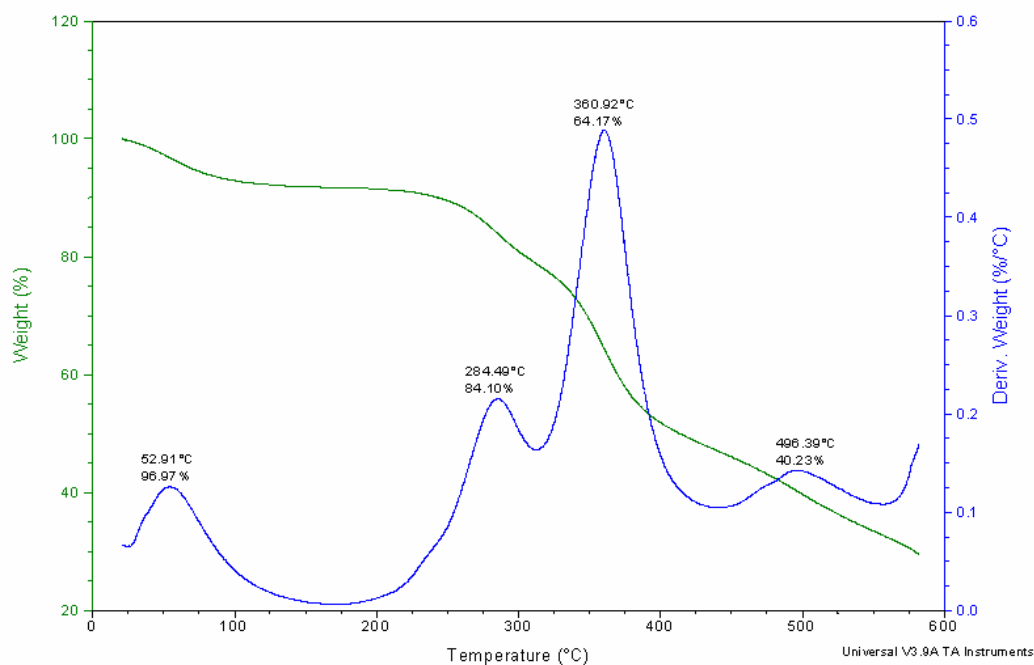


Figure 4.68. Weight loss and derivative of the weight loss curves with respect to temperature of acrylamide:EBBr-IDA-K⁺ (90:10) complexed with Ni²⁺

4.4.8. Ultraviolet-Visible Spectrophotometer Results

The chelating ability of EBBBr-IDA-K⁺ and CMAC-IDA-K⁺ was investigated using UV-visible spectroscopy at 500-900 nm where the monomers have no absorption. Maximum absorption value for Ni²⁺ was obtained at 717 nm. As EBBBr-IDA-K⁺ or CMAC-IDA-K⁺ was added to the Ni²⁺ solution, the maximum value shifted to shorter wavelengths (624 nm) with an increase in absorbance. This result confirms the Ni²⁺ chelating ability of EBBBr-IDA-K⁺ and CMAC-IDA-K⁺. Maximum absorption values and the corresponding wavelengths for different concentrations of EBBBr-IDA-K⁺ and CMAC-IDA-K⁺ were given in Table 4.13.

Table 4.13. Results of UV-visible spectrophotometer studies

[Concentrations] (*10⁻³ M)	Absorbance	λ_{\max} (nm)
Ni ⁺² [4.8]	0.013	717
Ni ⁺² [4.8] + EBBr-IDA-K ⁺ [1.2]	0.013	654
Ni ⁺² [4.8] + EBBr-IDA-K ⁺ [2.4]	0.025	639
Ni ⁺² [4.8] + EBBr-IDA-K ⁺ [3.6]	0.028	630
Ni ⁺² [4.8] + EBBr-IDA-K ⁺ [4.8]	0.053	624
Ni ⁺² [3.08]	0.008	717
Ni ⁺² [3.08] + CMAC-IDA-K ⁺ [0.77]	0.011	651
Ni ⁺² [3.08] + CMAC-IDA-K ⁺ [1.54]	0.014	639
Ni ⁺² [3.08] + CMAC-IDA-K ⁺ [2.31]	0.017	630
Ni ⁺² [3.08] + CMAC-IDA-K ⁺ [3.08]	0.025	624

5. CONCLUSIONS

In this study, new dental adhesive monomers based on alkyl α -hydroxymethyl acrylates and their derivatives were synthesized using simple synthetic methods. The monomers contained acidic groups such as phosphonic acid, carboxylic acid or chelating groups such as diethyliminodiacetate which can interact with the calcium ions in the tooth. We tried to investigate the monomers in terms of their homo- and copolymerizability, solubility, stability and interaction with the tooth component, HAP.

The cyclic monomers (1,6 heptadienes) displayed high cyclization tendencies and gave soluble polymers. The 2,6 disubstituted ether dimers, PHOSEED and PHOSEED-acid have the disadvantage of hydrolytic stability in water due to the presence of phosphonic groups via ester linkages. Also, molecular weights of the homopolymers and copolymers were low because of the chain transfer to monomers. On the other hand 4,4 disubstituted heptadienes are hydrolytically stable in water. Among them, phosphonic and carboxylic acid containing monomers showed reasonable polymerization reactivity, solubility in water and sufficient pH values so that they can be used as self-etching adhesive monomers.

A strong effect of the monomer structure on the rate of polymerization was observed. The polymerization reactivities of the monomers increased with decreasing steric hinderence and/or increasing electron withdrawing ability of the allyl substituents. The lower polymerization reactivity of N,N-disubstituted methacrylamides were explained by the twisted conformation between double bonds reducing conjugation eventhough amide linkage is very stable to hydrolytic stability and it is more biocompatible compared to acrylates.

Polymerizability of our monomers were correlated with the ^{13}C -NMR chemical shifts of their vinyl carbons. The smaller the chemical shift difference with electron-withdrawing substituents, the higher is the polymerizability of our monomers.

Conversion values were consistent with the T_g of our monomers such that as the monomeric T_g increased, flexibility of a monomer and conversion after polymerization decreased. One exception was due to carboxylic acid containing monomer CA-PA which had a limiting double bond conversion but higher polymerization rate. This can be explained by the hydrogen bonding capability between acid groups that could bring the double bonds close to each other and favored the polymerization.

Finally, the interaction of our most promising monomers, CA-PA and EC-PA with hydroxyapatite, as a model compound for dentin and enamel, was investigated using the ^{13}C -NMR technique. It was found out that, phosphonic acid group demineralized the calcium phosphate in the HAP in preference to the carboxylic acid. Both monomers were expected to enhance bonding of the resin to enamel but CA-PA could exhibit a priming capacity as well as an etching efficiency.

REFERENCES

1. *Tooth Anatomy*, [http://www.tooth.net/info/Anotomyof tooth.htm](http://www.tooth.net/info/Anotomyof%20tooth.htm), 2005.
2. *Structure of a Normal Tooth*, <http://www.mydr.com.au>, 2003.
3. Nicholson, J. W., “Adhesive Dental Materials-A Review”, *International Journal of Adhesion & Adhesives*, Vol. 18, pp. 229-236, 1998.
4. Ferracane, J. L., *Materials in Dentistry*, 2nd ed., Lippincott Williams & Wilkins, Baltimore, 2001.
5. Omura, I., J. Yamauchi, Y. Nagase and F. Uemuro, *Adhesive Composition*, US Pat, 1987; 4 650 847, Kuraray Co.
6. Beech, D. R., E. Rizzardo, W. D. Cook, and M. C. Smail, *Dental Restorative Material*, US Pat, 1988; 4 732 943, Commonwealth Scientific and Industrial Research Organization.
7. *The Various Categories of Adhesives*, <https://decs.nhgl.med.navy.mil/1QTR04/QA/dm1.htm>, 2005.
8. Itou, K., Y. Torii, Y. Nishitani, K. Ishikawa, K. Suzuki and K. Inoue, “Effect of Self-etching Primers Containing N-acryloyl Aspartic Acid on Dentin Adhesion”, *J Biomed Mater Res*, Vol. 51, pp. 569-574, 2000.
9. Hino, K., J. Yamauchi and K. Nishida, *Dental Compositions*, US Pat, 1994; 5 321 053, Kuraray Co.

10. Schulze, K. A., S. A. Oliveira, R. S. Wilson, S. A. Gansky, G. W. Marshall and S. J. Marshall, "Effect of Hydration Variability on Hybrid Layer Properties of a Self-etching versus an Acid-etching system", *Biomaterials*, Vol. 26, pp. 1011-1018, 2005.
11. Nishiyama, N., K. Fujita, T. Ikemi, T. Maeda, K. Suzuki and K. Nemoto, "Efficacy of Varying the NMEP Concentrations in the NMGLY-NMEP Self-etching Primer on the Resin-Tooth Bonding", *Biomaterials*, Vol. 26, pp. 2653-2661, 2005.
12. Peumans, M., P. Kanumilli, D. J. Munck, K. V. Landuyt, P. Lambrechts and B. V. Meerbeek, "Clinical Effectiveness of Contemporary Adhesives: A Systematic Review of Current Clinical Trials", *Dental Materials*, Vol. 21., pp. 864-881, 2005.
13. Moszner, N., U. Salz and J. Zimmermann, "Chemical Aspects of Self-etching Enamel-Dentin Adhesives: A Systematic Review", *Dental Materials*, Vol. 21., pp. 895-910, 2005.
14. Moszner, N., F. Zeuner, S. Pfeiffer, I. Schurte, V. Rheinberger and M. Drache, "Monomers For Adhesive Polymers, 3", *Macromol. Mater. Eng.*, Vol. 286, pp. 225-231, 2001.
15. Buonocore, G., W. Wileman and F. Brudevold, "A Report on a Resin Composition Capable of Bonding Human Dentin Surfaces", *J. Dental Research*, Vol. 35, pp. 846-851, 1956.
16. Omura, I., J. Yamauchi, Y. Nagase and F. Uemuro, *Phosphate Monoester Adhesive Composition*, US Pat, 1986; 4 612 384, Kuraray Co.
17. Avci, D. and L. J. Mathias, "Synthesis and Polymerization of Phosphorus-Containing Acrylates", *Journal of Polymer Science: Part A: Polymer Chemistry*, Vol. 40, pp. 3221-3231, 2002.

18. Avci, D. and L. J. Mathias, "Synthesis and Photopolymerizations of Phosphate-Containing Acrylate/(di)Methacrylate Monomers from 3-(acryloyloxy)-2-hydroxypropyl Methacrylate", *Polymer Bulletin*, Vol. 54, No. 1-2, pp.11, 2005.
19. Omura, I., J. Yamauchi, Y. Nagase and F. Uemuro, *Adhesive Composition*, US Pat, 1987; 4 650 847, Kuraray Co.
20. Klee, J. E., U. Lehmann and U. Walz, *One-Part Self-Etching, Self-Priming Dental Adhesive Composition*, EP, 2005; 1 548 021 A1, Dentsply Detrey GmbH.
21. Anbar, M. and E. P. Farley, "Potential Use of Organic Polyphosphonates as Adhesive in the Restoration of Teeth", *J. Dental Research*, Vol. 53, pp. 879-888, 1974.
22. Farley, E. P., R. L. Johnes and M. Anbar, "Improved Adhesion of Acrylic Restorative Materials to Dental Enamel by Pre-coating with Monomers Containing Phosphonate Groups", *J. Dental Research*, Vol. 56, pp. 943-952, 1977.
23. Tan, J., R. A. Gemeinhart, M. Ma and W. M. Saltzman, "Improved Cell Adhesion And Proliferation on the Synthetic Phosphonic Acid Containing Hydrogels", *Biomaterials*, Vol. 26, pp. 3663-3671, 2005.
24. Senhaji, O., J. J. Robin, M. Achchoubi and B. Boutevin, "Synthesis and Characterization of New Methacrylic Phosphonated Surface Active Monomer", *Macromol. Chem. Phys.*, Vol. 205, pp. 1039-1050, 2004.
25. Moszner, N., F. Zeuner, S. Pfeiffer, I. Schurte, V. Rheinberger and M. Drache, "Monomers For Adhesive Polymers, 2", *Macromol. Mater. Eng.*, Vol. 200, pp. 1062-1067, 1999.

26. Brondino, C. B., B. Boutevin, Y. Hervaud and M. Gaboyard, "Adhesive and Anticorrosive Properties of Poly(vinylidene fluoride) Powders Blended with Phosphonated Copolymers on Galvanized Steel Plates", *Journal of Applied Polymer Science*, Vol. 83, pp. 2227-2287, 2002.
27. Mou, L., G. Singh and J. W. Nicholson, "Synthesis of a Hydrophilic Phosphonic Acid Monomer for Dental Materials", *Chemical Communications*, pp. 345-346, 2000.
28. Avci, D. and A. Z. Albayrak, "Synthesis and Polymerization of Phosphorus-Containing Acrylates", *Journal of Polymer Science: Part A: Polymer Chemistry*, Vol. 41, pp. 2207-2217, 2003.
29. Moszner, N., F. Zeuner and V. Rheinberger, *Hydrolysis Stable and Polymerizable Acrylphosphonic Acids*, US Pat, 2001; 6 172 131 B1, Ivoclar A.G.
30. Moszner, N., "New Monomers for Dental Application", *Macromol. Symp.*, Vol. 217, pp. 63-75, 2004.
31. Finke, M., W. Rupp and E. Weiss, *2-Acrylamido- and 2-Methacrylamido-2-Methyl Propanephosphonic Acids and Their Salts, Process for the Preparation Thereof, and Use Thereof for the Manufacture of Copolymers*, US Pat, 1985; 4 526 728, Hoechst Aktiengesellschaft.
32. Erdmann, C., S. Ziegler, S. Neffgen, C. Bolln, W. Mühlbauer and R. Lück, *Dental Material Containing Phosphonic Acids*, US Pat, 2005; 6 902 608 B2, Ernst Mühlbauer GmbH & Co.
33. Sawada, K., W. Duan, M. Ono and K. Satoh, "Stability and Structure of Nitrilo (acetate-methylphosphonate) Complexes of the Alkaline-Earth and Divalent Transition Metal Ions in Aqueous Solution", *J Chem Soc., Dalton Trans.*, pp. 919-924, 2000.

34. Sawada, K., T. Miyagawa, T. Sakaguchi and K. Doi, "Structure and Thermodynamic Properties of Aminopolyphosphonate Complexes of the Alkaline-Earth Metal Ions", *J Chem Soc., Dalton Trans.*, pp. 3777-3784, 1993.
35. Duan, W., H. Oota and K. Sawada, "Stability and Structure of Ethylenedinitropoly(methylphosphonate) Complexes of the Alkaline-Earth Metal Ions in Aqueous Solution", *J Chem Soc., Dalton Trans.*, pp. 3075-3080, 1999.
36. Riedelsberger, K. and W. Jaeger, "Polymeric Aminomethylphosphonic Acids-1. Synthesis and Properties in Solution", *Designed Monomers and Polymers*, Vol. 1, pp. 387-407, 1998.
37. Riedelsberger, K., W. Jaeger and A. Friedrich, "Polymeric Aminomethylphosphonic Acids-2. Polychelatogenes for Separation of Transition Metal Ions By Membrane Filtration", *Designed Monomers and Polymers*, Vol. 3, pp. 35-53, 2000.
38. Alexandratos, S. D. and S. D. Smith, "Intraligand Cooperation in Metal Ion Binding by Immobilized Ligands: The Effect of Bifunctionality", *Journal of Applied Polymer Science*, Vol. 91, pp. 463-468, 2004.
39. Nishiyama, N., K. Suzuki, H. Yoshida, H. Teshima and K. Nemoto, "Hydrolytic Stability of Methacrylamide in Acidic Aqueous Solution", *Biomaterials*, Vol. 25, pp. 965-969, 2004.
40. Kitoh, S., K. Suzuki, T. Kiyohara and K. Kurita, "Adhesive Monomers to Dental Ceramics. III. Influence of Surface Treatment on Effective Adhesion of Calcium Metaphosphate Ceramic with N-(Vinylbenzyl)iminodiacetic Acid", *J Appl Polym Sci*, Vol. 60, pp. 1821-1825, 1996.
41. Xu, X., L. Ling, X. Ding and J. O. Burgess, "Synthesis and Characterization of a Novel Fluoride-Releasing Dimethacrylate Monomer and its Dental Composite", *J. Polym. Sci., Part A: Polymer Chemistry*, Vol. 42, pp. 985-998, 2004.

42. Xu, X., X. Ding, L. Ling and J. O. Burgess, "Synthesis and Characterization of a Novel Flouride-Releasing Monomers. II. Dimethacrylates Containing Bis(aminodiacetic Acid) and their Ternary Zirconium Flouride Complexes", *J. Polym. Sci., Part A: Polymer Chemistry*, Vol. 43, pp. 3153-3166, 2005.
43. Vanderlaan, D. G. and B. Susan, *Antibacterial, Insoluble, Metal-Chelating Polymers*, US Pat, 1996; 5 514 732, Johnson & Johnson Vision Products.
44. Chen, C. Y. and C. Y. Chen, "Stability Constants of Polymer Bound Iminodiacetate-Type Chelating Agents with Some Transition-Metal Ions", *J Appl Polym Sci*, Vol. 86, pp. 1986-1994, 2002.
45. Wang, C. C., C. Y. Chen and C. Y. Chang, "Synthesis and Chelating Resins with Iminodiacetic Acid and Its Wastewater Treatment Application", *J Appl Polym Sci*, Vol. 84, pp. 1353-1362, 2002.
46. Nishiyama, N., K. Suzuki, K. Komatsu, S. Yasuda and K. Nemoto, "A ^{13}C -NMR Study on the Adsorption Characteristics of HEMA to Dentinal Collagen", *J. Dental Research*, Vol. 81, pp. 469-471, 2002.
47. Nishiyama, N., K. Suzuki, A. Nagatsuka, I. Yokota and K. Nemoto, "Dissociation States of Collagen Functional Groups and their Effects on the Priming Efficacy of HEMA Bonded to Collagen", *J. Dental Research*, Vol. 82, pp. 257-261, 2003.
48. Sanares, A. M., A. Itthagarun, N. M. King, F. R. Tay and D. H. Pashley, "Adverse Surface Interactions between One-Bottle Light Cured and Chemical Cured Composites", *Dent. Mater.*, Vol. 17, pp. 542-546, 2001.
49. Tay, F. R., D. H. Pashley, C. K. Yiu, A. M. Sanares and S. H. Wei, "Factors Contributing to the Incompatibility between Simplified Step Adhesives and Chemically Cured or Dual Cured Composites. Part 1. Single Step Self-etching Adhesive", *J. Adhes. Dent.*, Vol. 5, pp. 27-40, 2003.

50. Tay, F. R., K. M. Moulding and D. H. Pashley, "Distribution of nanofillers from a simplified-step adhesive in acid-conditioned dentin" *J. Adhes. Dent.*, Vol. 1, pp. 103-117, 1999.
51. Matsunae, K. and A. Akahane, *Dental Adhesive Set*, US Pat, 2001; 6 217 644 B1, GC Corporation.
52. Atac, A. S., Z. C. Cehreli and B. Sener, "Antibacterial Activity of Fifth Generation Dentin Bonding Systems", *J. Endod.*, Vol. 27, pp. 730-733, 2001.
53. Imazato, S., T. Imai, R. B. Russell, M. Torii and S. Ebisu, "Antibacterial Activity of Cured Dental Resin Incorporating the Antibacterial Monomer MDPB and an Adhesion Promoting Monomer", *J. Biomed. Res.*, Vol. 39, pp. 511-515, 1998.
54. Yoshida, Y., B. V. Meerbeek, Y. Nakayama, M. Yoshioka, J. Snauwaery, Y. Abe, P. Lambrechts, G. Vanherle and M. Okazaki, "Adhesion to and Decalcification of Hydroxyapatite by Carboxylic Acids", *J. Dent. Res.*, Vol. 80, pp. 1565-1569, 2001.
55. Yoshida, Y., V. K. Nagakane, R. Fukuda, Y. Nakayama, M. Okazaki, H. Shintani, S. Inoue, Y. Tagawa, K. Suzuki, J. D. Munck and B. Meerbeek, "Comparative Study on Adhesive Performance of Functional Monomers", *J. Dent. Res.*, Vol. 83, pp. 454-458, 2004.
56. Nakabayashi, N., K. Kojima and E. Masuhara, "The Promotion of Adhesion by the Infiltration of Monomers into Tooth Substrates", *J. Biomed. Mater. Res.*, Vol. 16, pp. 265-273, 1982.
57. Yoshida, H. and N. Nishiyama, "Development of Self-etching Primer Comprised of Methacrylamide, N-methacryloyl Glycine", *Biomaterials*, Vol. 24, pp. 5203-5207, 2003.

58. Tay, F. R. and D. H. Pashley, "Aggressiveness of Contemporary Self-etching Systems. I: Depth of Penetration Beyond Dentin Smear Layers", *Dental Materials*, Vol. 17, pp. 296-308, 2001.
59. Nishiyama, N., K. Suzuki, T. Asakura, K. Komatsu and K. Nemato, "Adhesion of N-Methacryloyl- ω -Amino Acid Primers to Collagen Analyzed by ^{13}C -NMR", *J. Dent. Res.*, Vol. 80, pp. 855-859, 2001.
60. Nishiyama, N., T. Asakura, K. Suzuki, K. Komatsu and K. Nemato, "Bond Strength of Resin to Acid-etched Dentin Studied by ^{13}C -NMR: Interaction between N-Methacryloyl- ω -Amino Acid Primer to Dentinal Collagen", *J. Dent. Res.*, Vol. 79, pp. 806-811, 2000.
61. Nishiyama, N., T. Asakura, K. Suzuki, T. Sato and K. Nemato, "Adhesion Mechanism of Resin to Etched Dentin primed with N-methacryloyl Glycine Studied by ^{13}C -NMR", *J. Biomed. Mater. Res.*, Vol. 40, pp. 458-463, 1998.
62. Nakabayashi, N., K. Kojima and E. Masuhara, "The Promotion of Adhesion by the Infiltration of Monomers into Tooth Substrates", *J. Biomed. Mater. Res.*, Vol. 16, pp. 265-273, 1982.
63. Landuyt, K. L. V., P. Kanumilli, J. D. Munck, M. Peumans, P. Lambrechts and B. V. Meerbeek, "Bond Strength of a Mild Self-etch Adhesive with and without prior Acid-Etching", *Journal of Dentistry*, Vol. 34, pp.77-85, 2006.
64. Pashley, D. H. and F. R. Tay, "Aggressiveness of Contemporary Self-etching Systems. Part II: Etching Effects of Unground Enamel", *Dental Materials*, Vol. 17, pp. 430-444, 2001.
65. Koibuchi, H., N. Yasuda and N. Nakabayashi, "Bonding to Dentin with a Self-etching Primer: the Effects of Smear Layers", *Dental Materials*, Vol. 17, pp. 122-126, 2001.

66. Oliveira, S. S. A., M. K. Pugach, J. F. Hilton, L. G. Watanabe, S. J. Marshall and G. W. Marshall, "The Influence of the Dentin Smear Layer on Adhesion: a Self-etching Primer vs. a Total-etch system", *Dental Materials*, Vol. 19, pp. 758-767, 2003.
67. Hashimoto, M., S. Ito, F. R. Tay, N. R. Svizero, H. Sano, M. Kaga and D. H. Pashley, "Fluid Movement across the Resin-Dentin Interface during and after Bonding", *J. Dent. Res.*, Vol. 83, pp. 843-848, 2004.
68. Mathias, L. J., S. H. Kusefoglou, A. O. Kress, S. Lee, J. R. Wright, D. A. Culberson, S. C. Warren, R. M. Warren, S. Huang, D. R. Lopez, J. E. Ingram, C. W. Dickerson, M. Jenö, R. J. Halley, R. F. Colletti, G. Cei and C. C. Geiger, "Multifunctional Acrylate Monomers, Dimers and Oligomers: Applications from Contact Lenses to Wood-Polymer Composites", *Makromol. Chem., Macromol. Symp.*, Vol. 51, pp. 153-167, 1991.
69. Avci, D., L. J. Mathias and K. Thigpen, "Photopolymerization Studies of Alkyl and Aryl Ester Derivatives of Ethyl α -Hydroxymethylacrylate", *Journal of Polymer Science: Part A: Polymer Chemistry*, Vol. 34, pp. 3191-3201, 1996.
70. Thompson, R. D., T. B. Barclay, K. R. Basu and L. J. Mathias, "Facile Synthesis and Polymerization of Ether Substituted Methacrylates", *Polym. J.*, Vol. 27, No. 4, pp. 325-338, 1995.
71. Yu, C., B. Liu and L. Hu, "Efficient Baylis-Hillman Reaction Using Stoichiometric Base Catalyst and an Aqueous Medium", *J. Org. Chem.*, Vol. 66, pp. 5413-5418, 2001.
72. Huang, J. and M. Shi, "Polymer-Supported Lewis Bases for the Baylis-Hillman Reaction", *Adv. Synth. Catal.*, Vol. 345, pp. 953-958, 2003.
73. Brzezinski, L. J., S. Rafel and J. W. Leathy, "The Asymmetric Baylis-Hillman Reaction as a Template in Organic Synthesis", *Tetrahedron*, Vol. 53, pp. 6423-6434, 1997.

74. Aggerwal, V. K., D. K. Dean, A. Mereu and R. Williams, "Rate Acceleration of the Baylis-Hillman Reaction in Polar Solvents (Water and Formamide). Dominant Role of Hydrogen Bonding, Not Hydrophobic Effects, Is Implicated", *J. Org. Chem.*, Vol. 67, pp.510-514, 2002.
75. Aggerwall, V. K., A. Mereu, G. J. Tarver and R. McCague, "Metal- and Ligand-Accelerated Catalysis of the Baylis-Hillman Reactions", *J. Org. Chem.*, Vol. 63, pp.7183-7189, 1998.
76. Yang, K. S., W. D. Lee, J. F. Pan and K. Chen, "Chiral Lewis Acid-Catalyzed Asymmetric Baylis-Hillman Reactions", *J. Org. Chem.*, Vol. 68, pp.915-919, 2003.
77. Pereira, S. I., J. Adrio, A. M. S. Silva and J. C. Carretero, "Ferrocenylphosphines as New Catalysts for Baylis-Hillman Reactions", *J. Org. Chem.*, Vol. 70, pp. 10175-10177, 2005.
78. He, Z., X. Tang, Y. Chen and Z. He, "The First Air Stable and Efficient Nucleophilic Trialkylphosphine Organocatalyst for the Baylis-Hillman Reaction", *Adv. Synth. Catal.*, Vol. 348, pp. 413-417, 2006.
79. Caumul, P. and H. C. Hailes, "Baylis-Hillman Reactions in Aqueous Acidic Media", *Tetrahedron Letters*, Vol. 46, pp. 8125-8127, 2005.
80. Mathias, L. J. and S. H. Kusefoglou, "New Difunctional Methacrylate Ethers and Acetals: Readily Available Derivatives of α -Hydroxymethyl Acrylates", *Macromolecules*, Vol. 20, No. 8, pp.2039, 1987.
81. Mathias, L. J., S. H. Kusefoglou, A.O. Kress, S. Lee, C. W. Dickerson and S. F. Thames, "New Acrylate-Containing Dimers and Oligomers for Crosslinking Vinyl Polymers", *Polymer News*, Vol. 17, pp. 36-42, 1992.
82. Alkyl 2-(Hydroxymethyl)acrylate,
<http://www.shokubai.co.co.jp/english/main/>

[kaihatsu /echiru a/echiru.htm](#), 2004.

83. Ueda, M., T. Koyama, M. Mano and M. Yazawa, "Radical-Initiated Homopolymerization and Copolymerization of Ethyl α -Hydroxymethylacrylate", *Journal of Polymer Science, Part A*, Vol.27, pp.751-762, 1989.
84. Mathias, L. J., S. H. Kusefoglu and A. O. Kress, "A Simple One-Step Synthesis of Unsaturated Copolyesters", *Journal of Applied Polymer Science*, Vol. 38, pp.1037-1051, 1989.
85. Warren, S.C. and L. J. Mathias, "Synthesis and Polymerization of Ethyl α -Chloro methylacrylate and Related Derivatives", *Journal of Polymer Science: Part A:Polymer Chemistry*, Vol. 28, pp. 1637-1648, 1990.
86. Jariwala, C. P. and L. J. Mathias, "Synthesis, Polymerization, and Characterization of Novel Semifluorinated Methacrylates, Including Novel Liquid Crystalline Materials", *Macromolecules*, Vol. 26, pp. 5129-5136, 1993.
87. Avci, D., L. J. Mathias and K. Thigpen, "Photopolymerization Studies of Alkyl and Aryl Ester Derivatives of Ethyl α -Hydroxymethacrylate", *Journal of Polymer Science Part A:Polymer Chemistry*, Vol. 34, pp. 3191-3201, 1996.
88. Mathias, L. J., K. Thigpen and D. Avci, "Superfast Methacrylate Photomonomers: Ester Derivatives of Ethyl α -Hydroxymethacrylates", *Macromolecules*, Vol. 28, pp. 8872-8874, 1995.
89. Avci, D., S. H. Kusefoglu, R. D. Thompson and L. J. Mathias, "Ester Derivatives of α -Hydroxymethacrylates: Itaconate Isomers Giving High Molecular Weight Polymers", *Journal of Polymer Science: Part A:Polymer Chemistry*, Vol. 32, 2937-2945, 1994.
90. Yamada, B. and S. Kobatake, "Radical Polymerization, co-Polymerization, and Chain Transfer of α -Substituted Acrylic Esters", *Prog. Polym. Sci.*, Vol. 19, pp. 1089-1131, 1994.

91. Yamada, B., S. Kobatake and T. Otsu, "Control of Molecular Weight and End Group of Polymer by Addition-Fragmentation reaction with α -(Bromomethyl)acrylate and Allyl Bromide", *Polymer Journal*, Vol. 24, pp. 281-290, 1992.
92. Zetterlund P. B., K. Miyake, K. Goto and B. Yamada, "Addition-Fragmentation Chain Transfer: Molecular Weight Distribution and Retardation in the System Methyl Methacrylate/Methyl α -(Bromomethyl)acrylate", *Journal of Polymer Science, Part A: Polymer Chemistry*, Vol. 42, pp. 2640-2650, 2004.
93. Yamada, B., S. Kobatake and S. Aoki, "Polymerization and Copolymerization of Methyl 2-(Chloromethyl)acrylate in Competition with Addition-Fragmentation", *Macromolecules*, Vol. 26, pp. 5099-5104, 1993.
94. Yamada, B. and S. Kobatake, "Radical Polymerization, co-Polymerization, and Chain Transfer of α -Substituted Acrylic Esters", *Progress in Polymer Science*, Vol. 19 (6), pp. 1089, 1994.
95. Lee, S., S. F. Thames and L. J. Mathias, "In Situ Formation of New Crosslinking Agents from Acrylate Derivatives and Bisepoxides", *Journal of Polymer Science, Part A: Polymer Chemistry*, Vol. 28, pp. 525-549, 1990.
96. Avci, D. and L. J. Mathias, "Synthesis and Photopolymerizations of New Hydroxyl-Containing Dimethacrylate Crosslinkers", *Polymer*, Vol. 45, pp. 1763-1769, 2004.
97. Avci, D., J. Nobles and L. J. Mathias, "Synthesis and Photopolymerization Kinetics of New Flexible Diacrylate and Dimethacrylate Crosslinkers Based on C18 Diacid", *Polymer*, Vol. 44, pp. 963-968, 2003.
98. Fernandes-Monreal, M. C., R. Cuervo and E. L. Madruga, "Free-Radical Homopolymerization and Copolymerization of Ethyl α -Hydroxymethylacrylate in Tetrahydrofuran", *Journal of Polymer Science, Part A: Polymer Chemistry*, Vol. 30, pp. 2313-2319, 1992.

99. Smith, T. J., B. S. Shemper, J. S. Nobles, A. M. Casanova, C. Ott and L. J. Mathias, "Crosslinking Kinetics of Methyl and Ethyl (α -Hydroxymethyl) Acrylates: Effect of Crosslinker Type and Functionality", *Polymer*, Vol. 44, pp. 6211-6216, 2003.
100. Mathias, L. J., R. M. Warren and S. Huang, "tert-Butyl α -(Hydroxymethyl)acrylate and Its Ether Dimer: Multifunctional Monomers Giving Polymers with Easily Cleaved Ester Groups", *American Chemical Society J.*, Vol. 24, pp. 2036-2042, 1991.
101. Kodiara, T., "Structural Control During the Cyclopolymerization of Unconjugated Dienes", *Progress in Polymer Science*, Vol. 25, pp. 627-676, 2000.
102. Mathias L. J., R. W. Warren and S. Huang, "tert-Butyl α -(Hydroxymethyl)acrylate and Its Ether Dimer: Multifunctional Monomers Giving Polymers with Easily Cleaved Ester Groups", *Macromolecules*, Vol. 24, pp. 2036-2042, 1991.
103. Mathias L. J. and S. H. Kusefoglou, *Acrylate Ester Ether Derivatives*, US Pat, 1991; 4 999 410, University of Southern Mississippi, Hattiesburg, Miss.
104. Stansbury, J. W., "Difunctional and Multifunctional Monomers Capable of Cyclopolymerization", *Macromolecules*, Vol. 24, pp. 2029-2035, 1991.
105. Stansbury, J. W., *Synthetic Dental Compositions Formed From Cyclopolymerizable bis-Acrylate and Multi-functional Oligomer and Bonding Method*, US Pat, 1989; 5 145 374, The United States of America by the Secretary of Commerce, Washington D.C.
106. Mathias, L. J., "Cyclopolymerization Overview: Recent Developments Leading to Molecular Control of Cyclization Efficiency", *TRIP*, Vol. 4(10), pp. 330-336, 1996.

107. Tsuda, T. and L. J. Mathias, "Cyclopolymerization of Ether Dimers of α -(Hydroxymethyl) Acrylic Acid and its Alkyl Esters: Substituent Effect on Cyclization Efficiency and Microstructures", *Polymer*, Vol. 35(15), pp. 3317-3328, 1994.
108. Tsuda, T., R. D. Thompson and L. J. Mathias, "Cyclopolymerization of Diallyl Malononitrile and the Thioether Dimer of Ethyl α -Chloromethylacrylate", *Pure Applied Chemistry*, Vol. A31(11), pp.1867-1879, 1994.
109. Tsuda, T. and L. J. Mathias, "New Dicyano-Containing Cyclopolymers Having High Stereoregularity Derived from Dimethacrylmalononitrile", *Macromolecules*, Vol. 26, pp. 6359-6363, 1993.
110. Thang, S. H., E. Rizzado and G. Moad, *Cyclopolymerization Monomers and Polymers*, US Pat., 1998; 5 830 966, E. I: du Pont de Nemours and Company, Wemington, Del.; Commonwealth Scientific & Industrial research Organization, Campbell, Australia.
111. Avci, D., C. Haynes and L. J. Mathias, "Cyclopolymerization of Amine-Linked Diacrylate Monomers", *Journal of Polymer Science: Part A: Polymer Chemistry*, Vol. 35, pp. 2111-2121, 1997.
112. Avci, D., N. Osanyan and L. J. Mathias, "Synthesis and Quaternization of Amine-Linked Diacrylate Monomers", *Polymer Preprints*, Vol. 42(2), pp. 514-515, 2001.
113. Michalovic, M., D. Avci and L. J. Mathias, "Polymerization of α -(N-Vinylformamidomethyl)acrylates: cyclopolymers from non-symmetric monomers", *Designed Monomers and Polymers*, Vol. 2, No. 3, pp. 199-208, 1999.
114. Thompson, R. D. T., W. L. Jarret and L. J. Mathias, "Unusually Facile Cyclopolymerization of a New Allyl Ether Substituted Acrylate and Confirmation of Repeat Unit Structure by INADEQUATE NMR", *Macromolecules*, Vol. 25, pp. 6455-6459, 1992.

115. Avci, D., K. Lemopulo and L. J. Mathias, "Cyclocopolymerization of Allyl-Acrylate Quaternary Ammonium Salts with Diallylmethylammonium Chloride", *Journal of Polymer Science: Part A: Polymer Chemistry*, Vol. 39, pp. 640-649, 2001.
116. Avci, D. and L. J. Mathias, "Synthesis and Cyclopolymerization of Novel Allyl-Acrylate Quaternary Ammonium Salts", *Journal of Polymer Science: Part A: Polymer Chemistry*, Vol. 37, pp. 901-907, 1999.
117. Brandrup, J. and E. H. Immergut, *Polymer Handbook*, Wiley Interscience, New York, 1975.
118. Anseth, K. S., C. M. Wang and C. N. Bowman, "Kinetic Evidence of Reaction Diffusion during the Polymerization of Multi(methyl)acrylate Monomers", *Macromolecules*, Vol. 27, pp. 650, 1994.
119. Vaidya, R. A. and L. J. Mathias, "On Predicting Free Radical Polymerizability of Allyl Monomers", *J. Polym. Sci.: Polym. Symp.*, 74, 243, 1986.
120. Sideridou, I., V. Tserki and G. Papanastasiou, "Effect of Chemical Structure on Degree of Conversion in Light-Cured Dimethacrylate-Based Dental Resins", *Biomaterials*, Vol. 23, pp. 1819, 2002.
121. Anseth, K. S., L. M. Kline, T. A. Walker, K. J. Anderson and C. N. Bowman, "Reaction Kinetics and Volume Relaxation during Polymerizations of Multiethylene Glycol Dimethacrylates", *Macromolecules*, Vol. 28, pp. 2491, 1995.
122. Ayfer, B., B. Dizman, M. O. Elasri, L. J. Mathias and D. Avci, "Synthesis and Antibacterial Activities of New Quaternary Ammonium Monomers", *Designed Monomers and Polymers*, Vol. 8, No. 5, pp. 437, 2005.
123. Vilcu, R., I. I. Bujor, M. Olteanu and I. Demetrescu, "Thermal Stability of Copolymer Acrylamide-Maleic Anhydride", *Journal of Applied Polymer Science*, Vol. 33, No.7, pp. 2431, 1987